2008

Inhibition of the NF-KB Signaling Pathway and Its Effects on Apoptosis and Cancer

Joseph A. Lupica
Cleveland State University

INHIBITION OF THE NF-κB SIGNALING PATHWAY AND ITS EFFECTS ON APOPTOSIS AND CANCER

JOSEPH A. LUPICA

Bachelor of Sceince

Cleveland State University

June, 2000

Submitted in partial fulfillment of requirement for the degree

DOCTOR OF PHILOSOPHY IN CLINICAL-BIOANALYTICAL CHEMISTRY

at the

CLEVELAND STATE UNIVERSITY

May 2008

This dissertation has been approved for the Department of Chemistry and the College of Graduate Studies by

6/19/08

Dissertation Committee Co-Chairperson, **Joseph A. DiDonato, PhD.**

Department of Cell Biology, Cleveland Clinic

6/19/08

Dissertation Committee Co-Chairperson, **Lily Ng, PhD.**

Chair Department of Chemistry, Cleveland State University

6/19/08

Dissertation Committee Member, **Michael Kalafatis, PhD.**

Department of Chemistry, Cleveland State University

6/19/08

Dissertation Committee Member, **Aimin Zhou, PhD.**

Department of Chemistry, Cleveland State University

6/19/08

Dissertaion Committee Member, **Girish Shukla, PhD.**

Department of Biological, Geological, and Environmental Science

Cleveland State University

DEDICATIONS AND ACKNOWLEDGMENTS

I would like to thank and acknowledge those who have helped and encouraged me throughout work on my Ph.D. I am grateful to have had the opportunity to be involved in the Chemistry graduate program at Cleveland State University.

Most importantly, I would like to thank my wife, and best friend Kathy whose unwavering support, encouragement and love has given my life meaning and made this endeavor possible. Thank you to my family, who have never failed me, for their encouragement and interest in my work as well as for understanding the missed and shortened family gatherings due to the time commitment involved in pursuing my Ph.D.

Thank you especially to Dr. Joseph DiDonato my research advisor, mentor and friend, for his support in all aspects of my laboratory training, for his patient manner of teaching, as well as his positive introduction into the world of a professional scientist. Thank you to Dr. Thomas Tallant and Dr. Niladri Kar, for their patient and painstakingly thorough instruction in the Bioanalytical techniques necessary for success in the field of Molecular Biology, for the opportunity to work on the Toll 5 project and especially for making working in the laboratory environment more enjoyable.

Thank you to Dr. Lily Ng, my academic advisor, for her advice and help in navigating the halls of academia, serving on my Dissertation committee and for her initial encouragement to enter the Ph.D. program.

I Thank Dr. Michael Kalifatis for stressing the importance of a sound foundation in Biochemistry as well as serving on my dissertation committee.

I would like to thank Dr. Aimin Zhou, and Dr. Girish Shukla for there time in reviewing my Thesis and serving on my Dissertation committee.

I would like to thank Dr. Dan Lindner for his support and affording me the opportunity to work with his research group on several projects. I would like to thank Dr. Bei Morrison for unselfishly including me in the IHPK2 project and Rebecca Haney for her work in the mouse studies.

Very special thanks to Dr. Joseph Bauer for introducing me to Nitrosylcobalamin and for his benevolent sharing of time, reagents and ideas. I especially thank Dr. Bauer for including my work in his publications, and for the opportunity to work on both Nitrosylcobalamin potentiating manuscripts. I hope that his compound may one day help in alleviating the suffering and heartbreak endured by many individuals and families.

I would like to dedicate this thesis to my brother Pete Lupica and good friend Rick Zielinski. Pete always had faith and confidence in my abilities, even when my own confidence failed. He protected me and taught me much about life and family. He was a positive role model and hero, and demonstrated that success may be achieved through hard work and patience. Rick was a close friend and confidant and we shared many of life's joys and sadness. Rick worked full time while successfully attending and graduating from Law School, he showed me the way back to College. Pete and Rick's lives were cut short by Cancer. They faced death courageously and were positive role models to the end. They are missed by their family and friends more than they could ever imagine.

INHIBITION OF THE NF-κB SIGNALING PATHWAY AND ITS EFFECTS ON APOPTOSIS AND CANCER

JOSEPH A. LUPICA

ABSTRACT

The Rel/NF-κB family of inducible transcription factors are evolutionarily conserved structurally and functionally, from insects to humans. They are ubiquitously expressed in a number of mature cell types, playing a pivotal role regulating cell growth, differentiation and apoptosis. Under normal circumstances, the proliferation of new cells is tightly regulated, as is the programmed lifespan of most cells, occasionally however cells loose their responsiveness to growth control mechanisms, resulting in a tumor or neoplasm. Sustained or chronic inflammation has been linked to a number of pathological conditions that destroy tissue and facilitate neoplastic growth. NF-κB in part mediates the opposing signals of cell survival and cell death, associated with this response. We hypothesized that inhibition of NF-κB would inhibit tumor cell growth. A number of anti-neoplastic drugs like some pro-inflammatory cytokines can activate both the cellular apoptotic and pro-survival (via NF-κB) pathways. We demonstrate, *in vitro*, that the use of Nitric Oxide mitigates NF-κB activation and induces program cell death, when administered as an adjuvant with this subset of pro-inflammatory cytokines. Secondly, several front-line anti-cancer drugs activate NF-κB as a result of their mode of action, resulting in the survival of a resistant population of tumor cells. In order to

abrogate this beneficial activity for the tumor cell we explore, both *in vitro* and *in vivo*, the use of Nitric Oxide to inhibit NF-κB, augmenting the efficacy of the anti-neoplastic drugs. Thirdly, we identify that the intracellular signaling kinase, Inositol Hexkisphosphate Kinase2 (IHPK2) , binds to a key component in the NF-κB signaling pathway, inhibiting NF-κB activity promoting apoptosis in tumor cells. Lastly, an in depth study investigating the major initiator of pro-inflammatory signaling during bacterial infection of cells by *Salmonela sp.* was in fact due to recognition of the bacterial protein flagellin by the cell surface receptor Toll-like receptor 5 (TLR5) leading to the activation of NF-κB. Flagellin, the product of the bacterial fliC gene which encodes this protein is the major protein constituent of the bacterial flagellar apparatus. Inflammation is a double edged sword. Initially the inflammatory response acts to destroy invading organisms and limit infection while alternatively, inflammation provides the cellular signaling events and growth factors that promote tumor cell survival and growth. There exists a fine balance between the cellular survival and death signal transduction pathways. This dichotomy pinpoints the NF-κB signaling pathway at this fulcrum as a potential target in drug development for the treatment of inflammation and inflammatory-mediated disease.

TABLE OF CONTENTS

LIST OF TABLES

LIST OF FIGURES

LIST OF ABBREVIATIONS

AP-1, activator protein-1

Apo2L/TRAIL, tumor necrosis factor-related apoptosis-inducing ligand

BF, bright field

DN, dominant negative

EMSA, electrophoretic mobility shift assay

ERK, extracellular regulated kinase

FBS, fetal bovine serum

GAPDH, glyceraldehyde-3phosphate dehydrogenase

GST, glutathione *S*-transferase

GTN, glycerol trinitrate

Gu-HCl, guanidinium hydrochloride

IκB, inhibitor of NF-κB

IB, immunoblot

IEC, intestinal epithelial cell

IFN, interferon

IHPK2, inositol hexakisphosphate kinase 2

IKK, Ikappa B kinase

IKK, inhibitor κB kinase

IL-1, interlukin-1

IN, input; Ct, cycle time

IκB, Ikappa B

JNK, Jun N-terminal kinase

KA, kinase assay

MAPK, mitogen activated protein kinase

MCP1, macrophage chemoattractant protein 1

MEF, mouse embryo fibroblast

MEF, murine embryonic fibroblast

NF-κB, nuclear factor kappa B

NOC-18 (DETA NONOate, (*Z*)-1-[2-(2-aminoethyl)-*N*-(2-ammonioethyl)amino]diazen-1-ium-1,2-diolate

NO-Cbl, nitrosylcobalamin

NP-40, nonidet-40

NRS, normal rabbit serum

PAGE, polyacrylamide gel electrophoresis

PARP, poly (ADP-ribose) polymerase

PBS, phosphate-buffered saline

PCR, polymerase chain assay

PMA, phorbol 12-myristate 13 acetate

PNPP, para nitrophenyl phosphate

RT-PCR, reverse transcription polymerase chain assay

SAPK, stress-activated protein kinase

SDS, sodium dodecyl sulfate

Sip, *Salmonella* invasion protein

siRNA, small interfering RNA

siSCR, siRNA-scrambled

SNAP, S-nitroso-*N*-acetyl-MD,L-penicillamine

SNP, sodium nitroprusside;

SRB, sulforhodamine B

TAK1, transforming growth factor β-activated kinase 1

TK, thymidine kinase

TLR, toll-like receptor

TNFα, tumor necrosis factor α

TRAF, TNF receptor-associated factor

TTSS, type III secretion system

TUNEL, terminal deoxynucleotidyltransferase-mediated dUTP nick end-labeling

WCE, whole cell extract

XIAP, X-linked inhibitor of apoptosis

CHAPTER I

INTRODUCTION

1.1 NF-κB

NF-κB occupies a significant role in the transcriptional regulation of a number of genes involved in the immune and inflammatory responses(Hayden and Ghosh, 2004). There are five members in the mammalian NF-κB family of transcription factors. RelA (p65), RelB, c-Rel, p50/105 (NF-κB1), and p52/p100 (NF-κB2)(Rothwarf and Karin, 1999). All NF-kB family members share a common protein domain, the REL homology domain, which is functionally a DNA-binding / dimerization domain that contains a nuclear localization sequence(Pahl, 1999).

NF-κB subunits p52 and p50 are formed from the proteolytic processing of precursor proteins p100 and p105, respectively and lack a transactivation domain. These precursor proteins p105 and p100 contain multiple copies of ankyrin repeats, which mediate protein-protein interactions in the carboxy-terminal one-third of the protein(Hayden and Ghosh, 2004). The second type of NF-κB subunits c-Rel, RelB-B and RelA/p65 contain transactivation domains and form heterodimers with p50 and p52(Hayden and Ghosh, 2004). All family members are capable of forming both hetero- and homodimers, with

the exception of RelB which can only form heterodimers. REL-A and p50 form the most common heterodimers, and it is the primary NF-κB transcription factor of interest in this study (Hayden and Ghosh, 2004).

NF-κB transcription factors are held inactive in the cytoplasm, bound to a member of a family of ankyrin repeat containing inhibitory proteins called the Inhibitor of kappaB (IκB). There are three members in this inhibitory family IκB-α, IκB-β, IκB-ε(Hayden and Ghosh, 2004). When bound to its inhibitor, NF-κB is restricted to the cytoplasm by virtue of shielding the access of the NF-κB nuclear localization sequence, blocking recognition and nuclear import(Rothwarf and Karin, 1999). Activation of NF-κB is initiated in the cytoplasm, by phorsphorylation-induced degradation of the IκB. The immediate upstream kinase phosphorylating IκB is Inhibitor of kappaB kinase (IKK)(Karin, 1999). IKK exists in the cytoplasm as multi-component signalasome, containing three core subunits IKK-α, IKK-β and IKK-γ(Hacker and Karin, 2006).

IKK phosphorylates two conserved N-terminal serine residues, S32 and S36 of IκB-α, triggering its polyubiquitination and degradation via the 26S proteasome(Hacker and Karin, 2006). Once free of its inhibitor, NF-κB undergoes further modifications to make it a more effective transcriptional activator and is then translocated to the nucleus(Li and Stark, 2002).

NF-κB promotes the transcription of a number of target genes involved in the inflammatory and immune responses, thereby serving as a link between the innate and adaptive immune systems(Karin and Ben-Neriah, 2000). The NF- κB signal transduction pathway is activated by a number of disparate ligands acting upon similar

cell surface and intracellular receptors including , the cytokines (TNF-α, Il-1α/β and TRAIL)(Silverman and Maniatis, 2001); bacterial products (LPS, flagellin, and non-methylated dsDNA)(Byrd-Leifer et al., 2001); viral components (dsDNA, dsRNA and ssRNA)(Takeda et al., 2003); and DNA damaging agents (ionizing radiation or oxidative stress and chemotherapeutic drugs)(Bender et al., 1998; Huang et al., 2003). A majority of NF-κB activators are functionally related by either pathogenic cellular invasion or cellular insult that initiates an immune response.

Overall NF-κB is activated in parallel with other mitogenic pathways. The activation of NF-κB regulates cell survival and cell death, mostly through inhibition of apoptosis or programmed cell death(Karin and Lin, 2002). In most cases, the pro-survival signals dominate, however if IKK or NF-κB are inhibited, the apoptotic mechanisms will predominate the cellular response.

1.2 IKK

Stimulation of numerous cellular transduction pathways may lead to the activation of NF-κB(Hayden and Ghosh, 2004). The key convergent point of these pathways is the activation of its upstream regulatory activating kinase, the IκB kinase (IKK)(Hacker and Karin, 2006). The IKK complex consists of the two highly conserved kinase subunits, IKK-α and IKK-β along with a structural, non-catalytic regulatory subunit IKK-γ (NEMO)(Rothwarf and Karin, 1999). IKK-α (85kD) and IKK-β(87kD) are the catalytic subunits in the IKK signaling complex, they are highly homologous proteins with 50% protein sequence similarity(Kwak et al., 2000). They each contain the following protein domains in the following order from amino to carboxyl end, the kinase domain, a leucine

zipper domain, and helix loop helix(Rothwarf and Karin, 1999). IKKα and β form homo and heterodimers through their leucine zipper domain. IKK-β has proven to be the primary catalytic kinase in NF-κB activation(Hayden and Ghosh, 2004). All three subunits IKK exist as a large 600-900 kDa complex based upon gel permeation(Hayden and Ghosh, 2004).

IKK-γ (NEMO) is an essential regulatory subunit of the IKK signaling complex. It is a predominately helical 48kd scaffolding protein and has no catalytic function of its own. The carboxy- terminal domain (C-ter) contains two coiled-coiled motifs' a leucine zipper, a proline rich region and a terminal zinc finger motif. The C-terminal region is required for full IKK activation(Agou et al., 2004), with the two coiled-coiled domains and leucine zipper essential for activation of NF-κB by LPS and TNF-α(Makris et al., 2002), and the zinc finger domain necessary for activation of NF-κB by DNA damaging agents(Huang et al., 2002). It is this carboxy-terminal domain that links upstream signaling events into the IKK complex.

Mutations in the zinc finger domain of IKK-γ result in the primary immune deficiency that is characterized by hyper-IgM syndrome(Jain et al., 2001). This mutation does not effect NF-κB activation by TNF-α or LPS. DNA damaging agents require the zinc finger of IKK-γ for NF-κB activation(Huang et al., 2002); conversely LPS and TNF-α are still able to activate NF-κB in the absence of the IKK-γ zinc finger, efficiently(Jain et al., 2001). Zinc and RING finger domains are common DNA binding and protein/protein interaction motifs. Zinc coordinated complexes are redox sensitive, and it

has been demonstrated that Nitrosative stress may disrupt the zinc finger domain, resulting in disruption of protein-protein interaction(Kroncke, 2003; Kroncke, 2001).

1.3 NF-κB ACTIVATORS

1.3.1 Tumor Necrosis Factor (TNF)

The super family, Tumor-necrosis Factor (TNF) includes 19 distinct ligands mediating their cellular response through 29 receptors. TNF ligands can either be soluble or membrane bound(Aggarwal, 2003). The membrane bound ligands are classified as Type II transmembrane proteins(Aggarwal, 2003).

The TNF receptors (TNFR) are classified into to two broad groups those containing a death domain (DD) and those without(Aggarwal, 2003). The receptors containing the DD are known as Death Receptors and when stimulated, may result in apoptosis(Aggarwal, 2003). The extracellular domain of the TNFR contains a cysteine rich region which facilitates receptor trimer formation, within the cellular membrane(Aggarwal, 2003). The trimer formation acts to mediate and expedite cellular signal transduction.

TNF ligands are highly potent activators of NF-κB, and are expressed primarily by cells of the immune system(Aggarwal, 2003), and are Type II transmembrane proteins(Contassot et al., 2007). The TNFR, on the other hand, is expressed in a wide variety of cell types and are classified as Type I membrane receptors(Aggarwal, 2003). Apoptotic and anti-apoptotic signaling can be simultaneously activated depending on the TNF ligand(Aggarwal, 2003; Karin and Ben-Neriah, 2000).

The apoptotic signaling is regulated through the death receptors. Upon ligand binding the death receptors form an inter-cellular complex of accessory proteins, identified as the Death Inducing Signaling Complex (DISC)(Contassot et al., 2007). Anti-apoptotic signals are generally mediated via NF-κB, the simultaneous activation of these opposing pathways poses a balance between life and death of the cell(Karin and Lin, 2002). The dominant pathway is dependent on the cell type and the ligand/receptor combination occurring during the activation.

NF-κB is the transcription factor for a number of TNF-family ligands and once activated causes an increase in transcription of both ligand and receptor genes(Brasier, 2006). The export of soluble ligand may affect the cell and surrounding cells in an autocrin or a paracrine fashion, magnifying death or survival signaling depending on the intensity and length of NF-κB activation(Brasier, 2006). TNF family members are also involved in development of secondary lymphoid organs; and stimulating cytotoxic immune effector cells, to recognize and destroy virally infected cells, as well aberrant tumor cells(Aggarwal, 2003).

Typically, once the trimerized TNF ligand binds to its receptor, adapter proteins are sequentially recruited to the TNFR and form a signaling complex. Members of the singling complex include TNF receptor-associated death domain protein (TRADD), TNF receptor-associated factor protein (TRAF2), receptor-interacting protein (RIP), TGF-β activated protein kinase 1-binding protein 1 &2 (TAB1 and TAB2), TGF-β activated kinase (TAK1), and IKK (Brasier, 2006; Jackson-Bernitsas et al., 2007) **(Fig 1.1)**.

The adapter proteins are essential for the recruitment of caspases, ubiquitin ligases and kinases, necessary for downstream NF-κB activity as well as apoptotic signaling(Jackson-Bernitsas et al., 2007). For example: Upon TNF family ligand binding RIP is recruited to the complex and interacts via its DD. IKK-γ translocates to the complex recruiting IKK-α and β. TAK1 phosphorylates critical serine residues on IKK-β, causing autophosphorylation as well as cross phosphorylation between IKK-α and IKK-β(Hayden and Ghosh, 2004), further activating the complex resulting in NF-κB activation, as described previously.

FIGURE 1.1

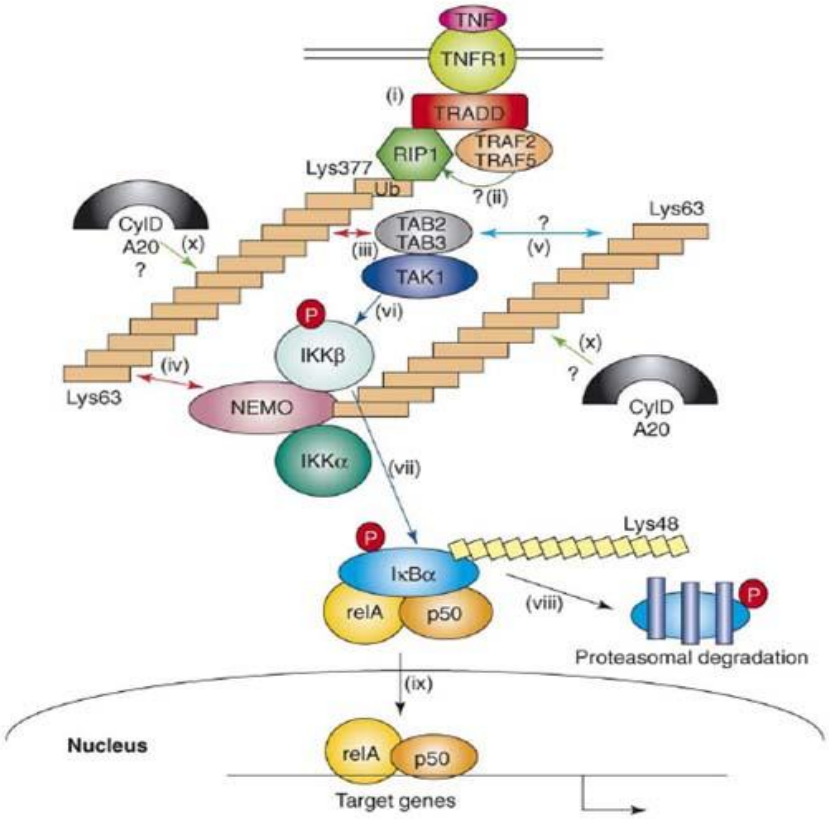

Figure 1.1: TNF-α mediated NF-κB activation involves recruitment of intermediate adapter proteins, as well as degradive and non-degradive Ubiquitination.

TNF-α ligand binding induces trimerization of its cognate receptor. This results in the recruitment of TRADD, the E3 ligase, TRAF2 and/or TRAF5 and the kinase RIP1. TRAF2 and/or TRAF5 Lys63 linked polyubiquitination of RIP1 results in the recruitment of TAK1-TAB1-(TAB2 or TAB3) to the complex. This results in the activation of the TAK1 kinase. The IKKα/β/γ is also recruited to the complex via an ubiquitin binding domain on NEMO, which has been Lys63 linked polyubiqitinated, facilitating recruitment to the complex. TAK1 then phosphorylates the IKKβ kinase subunit in its activation loop. IKKβ then phosphorylates IκB- α, NF-κB's inhibitory subunit, causing its to be Lys 48 linked polyubiquitinated and subsequently degraded by the proteasome. NF-κB is then translocated to the nucleus, activating its target genes. CYCLD and A20, two NF-κB target genes, encode specific Lys63 de-ubiquitinase, whose activity facilitates the complex disassembly. Illustrated by: (Israel, 2006)

1.3.2 Tumor necrosis factor related apoptosis inducing ligand (TRAIL/ Apo2L)

TRAIL, as a member of the TNF super family, is capable of inducing both survival and apoptotic pathways. It is expressed primarily by cells of the immune system (Falschlehner et al., 2007). The TRAIL ligand is normally membrane bound, but may be cleaved and become soluble (LeBlanc and Ashkenazi, 2003). It is associated with the killing of virally infected as well as neoplastic transformed cells. It is currently in clinical trials as a potential chemotherapeutic drug (Falschlehner et al., 2007).

Induction of the apoptotic pathway is mediated through the cytoplasmic formation of a DISC death signaling complex, resulting in direct activation of the extrinsic apoptotic pathway and indirect activation of the intrinsic pathway(Falschlehner et al., 2007). Activation of the survival pathway, although weak, is accomplished through induction of NF-κB (**Fig. 1.2)**.

There are currently five known TRAIL receptors, TRAIL- R1 (DR4) and TRAIL-R2 (DR-5) both of which posses an intracellular Death Domain (DD) and are capable of apoptotic signaling (LeBlanc and Ashkenazi, 2003). TRAIL-R3 (DcR1) and TRAIL-R4 (DcR2) are decoy receptors with no death signaling capabilities (LeBlanc and Ashkenazi, 2003). The fifth receptor is a soluble receptor osteoprotegerin (OPG). It has been suggested that increased expression of the decoy receptors, may act as a regulatory mechanism by sequestering the ligand from the complete signaling receptor.

The binding of Apo2L/TRAIL, to its cognate receptors, causes receptor trimerization and formation of the death-inducing signaling complex (DISC)(Contassot et al., 2007). Fas Associated Death Domain (FADD) is an essential adapter protein recruited to the

cytosolic tail of the TRAIL receptors. Upon arrival, it is able to interact via its DD to the DD on the cytoplasmic tails of the TRAIL receptors, priming formation of the DISC(Contassot et al., 2007). FADD then recruits pro-caspase 8 and pro-caspase 10 to the nascent DISC. The caspases are auto catalytically activated, inaugurating the protease cascade crucial for transmission of the apoptotic signal(Contassot et al., 2007).

The activation of caspase 8, by TRAIL, links the intrinsic and extrinsic apoptotic pathways. The activated initiator caspase, Caspase-8 has two preferred substrates, pro-caspase-3 and Bcl2 interacting protein (Bid)(Xiao-Ming Yin and Zheng Dong, 2003). Caspase-8 cleaves the Caspase-3 zymogen into a smaller catalytically active form. Pro-Caspase-3 is one of a number of effector caspases. The effector caspases, once catalytically activated, are directly or indirectly involved in the cleavage and degradation of several crucial cellular proteins(Xiao-Ming Yin and Zheng Dong, 2003).

Caspase-8 cleaves Bid into a truncated version, tBid. The protein tBid translocates to the mitochondria, activating other mitochondrial membrane proteins, resulting in the formation of channels in the outer mitochondrial membrane. The channels permeabilize the outer mitochondrial membrane, instigating the release of cytocrome c as well as other pro-apoptotic proteins(Falschlehner et al., 2007). One group of proteins, such as cytocrome c, initiates the activity of cellular pro-apoptotic caspases. The second group, are endonucleases that translocate to the nucleus and induce DNA degradation(Xiao-Ming Yin and Zheng Dong, 2003).

The key nexus to NF-κB activation by TRAIL relies on the recruitment of Receptor-interacting protein (RIP), to the signaling complex. RIP along with FADD, TRAF2 and

TRADD form a signaling complex that mitigates the activation of the IKK/NF-κB signaling cascade(Falschlehner et al., 2007). Not all of the TNF family members activate NF-κB with the same intensity (**Fig. 1.3**). Apo1/TRAIL induces apoptosis but is a weak activator of NF-κB. However this activation is sufficient to somewhat contradict the apoptotic effects of TRAIL. This weak inducer phenomenon may be exploited to combat neoplastic growth. If NF-κB can be simultaneously inhibited, as TRAIL induces apoptosis, the aberrant growth could be eliminated(Bauer et al., 2007).

FIGURE 1.2

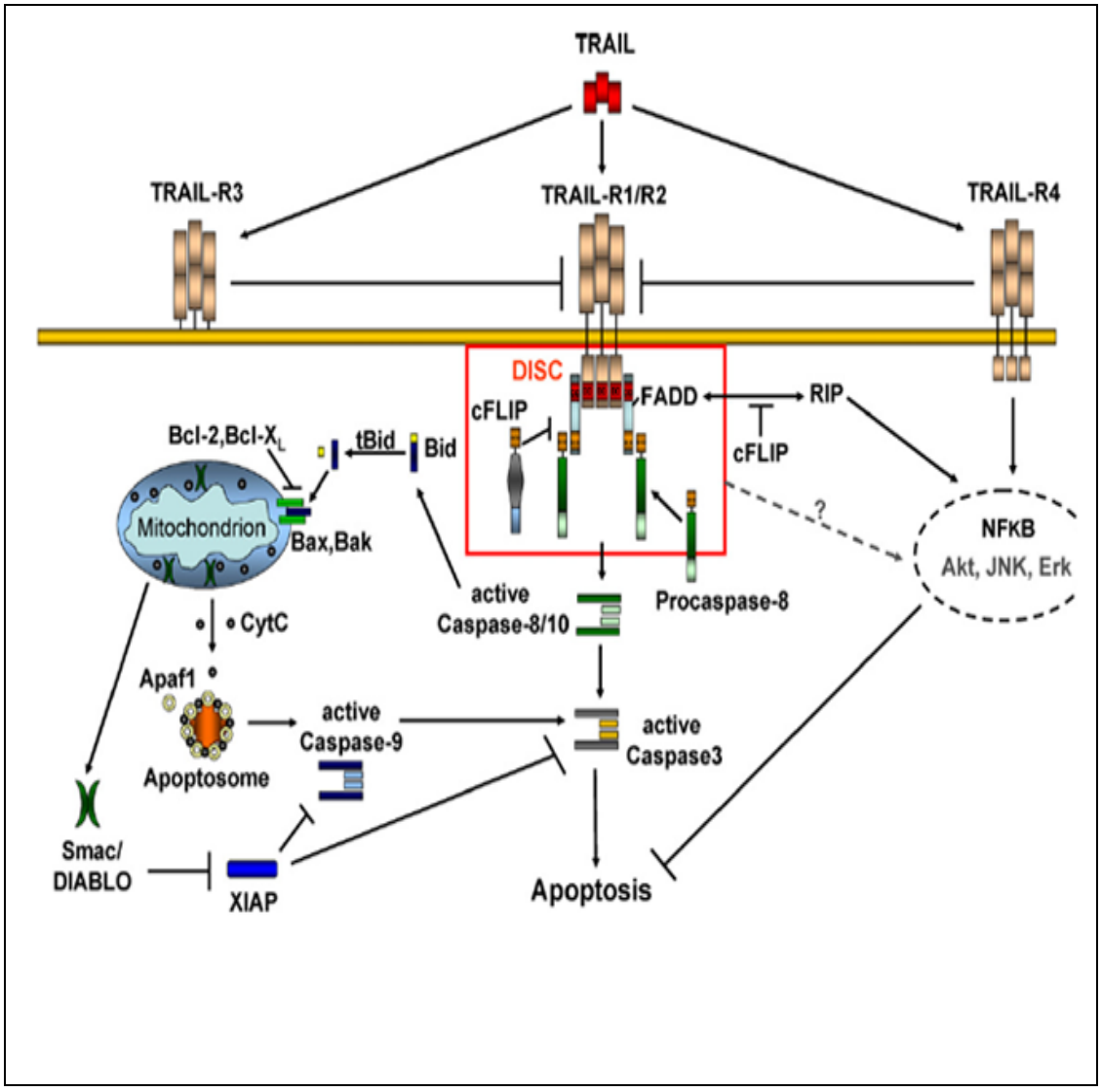

Figure 1.2: The TRAIL death pathway mediates cross talk between the "extrinsic and intrinsic" apoptotic pathways.

TRAIL/ApoL ligand binding, through formation of the death-inducing signaling complex (DISC), activates both the extrinsic and intrinsic apoptotic pathway, while additionally activating the pro-survival NF-κB transduction pathway abrogating and/or delaying the death signal. The adapter protein FADD plays a key dual role in the pathway. It recruits both receptors interacting protein (RIP) to the DISC resulting in eventual NF-κB activation and survival, as well as initiator pro-caspases 8/10 priming the death cascade. Illustrated by: (Falschlehner et al., 2007)

FIGURE 1.3

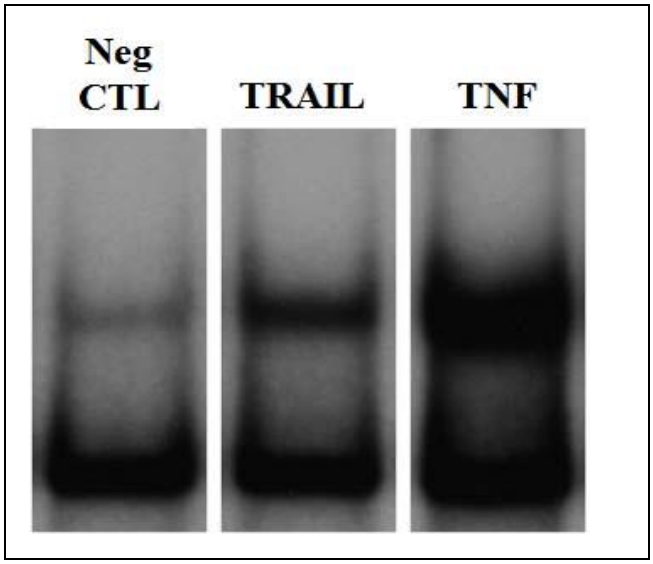

Fig 1.3: TNF family members exhibit differential NF-κB DNA binding activity.

TRAIL treated cells exhibit 75% less activation than TNF-α treated samples, as demonstrated by Electrophoretic mobility shift assay (EMSA). EMSA was performed using 25ug of A375 Whole cell Extract, as described in (Bauer et al., 2007)). The Cells were treated for 1 hour with TRAIL/ApoL1 (100ng/ml) or 15min with TNF-α (20ng/mL) The concentration of ligand(s) used were several fold in excess necessary to saturate available cellular receptors, in order to insure maximum NF-κB binding activity.

1.3.3 Pathogen Associated Molecular Patterns (PAMPS) and Toll-Like receptors (TLR)

The innate immune system recognizes broad molecular patterns, of conserved microbial components, that are characteristic of infection, or of microbial presence. These pattern specific ligands include bacterial cellular wall components, organelles, bacterial or viral DNA and viral RNAs(Dunne and O'Neill, 2005). These components are specific to specific classes of organisms and signal the immune system the type, and location of infection. These components are known as Pathogen Associated Molecular Patterns (PAMPS). PAMPS serve as ligands for Toll-Like receptors (TLR). TLR activation primes the adaptive immune system for induction, involving multiple cell types and tissues(Takeda et al., 2003).

TLRs are a Type I trans-membrane receptor, containing a cytoplasmic domain homologous to the IL-I receptor(Krishnan et al., 2007). Toll receptors are evolutionarily conserved from flies to man and are similar to receptors found throughout the animal and plant kingdoms(Takeda et al., 2003). The receptor was initially discovered and named Toll, in the fruit fly, Drosophila *melanogaster*. In Drosophila *it* is responsible for dorso-ventral pattern development in the embryo, and serves a role in protection against fungal invasion of the adult fly(Takeda et al., 2003). Thirteen TLR's have been identified in mammals, eleven in humans(Dunne and O'Neill, 2005). The mammalian Toll receptors have no apparent developmental pattern involvement, but function in the innate immune response only(Dunne and O'Neill, 2005).

Upon TLR ligand binding, the formation of a cytoplasmic signaling complex begins with the recruitment of MyD88, a scaffolding protein containing a Death

Domain(Beutler, 2004). MyD88 recruits IRAK-4 which then phosphorylates IRAK-1 and IRAK-2, which in turn recruits TRAF-6. TRAF-6 interacts with and ubiquitinase/activates TAK-1, an upstream activating kinase of IKK(Beutler, 2004). Subsequently, NF-κB, and MAPK-p38, via a parallel induction pathway, is activated leading to production of pro-inflammatory cytokines and further immune response (**Fig. 1.4)** (Beutler, 2004).

TLR 5, a typical MyD88-dependent TLR, is expressed in Monocytes/macrophages, Dendritic cells and mucosal epithelial cells of the respiratory and digestive tract. It is also expressed in microvascular endothelial cells. The gut epithelial cells express TLR-5 on their basolateral surface only(Takeda et al., 2003). Activation of TLR-5 by its ligand on this surface, signals a bacterial invasion of the gut epithelium from the lumen and breakthrough to the basal layer threatening a systemic infection.

Most enteric pathogens are flagellated. The flagella structure is relatively conserved throughout a number of diverse bacterial species. Human pathogens associated with the invasion of the alimentary canal or the respiratory tract, such as *Salmonella*, *Escherichia Coli, Pseudomonas and Legonella* utilize flagellum, for motility. Flagellin is the bacterial protein ligand responsible for activation of Toll like receptor 5 (Tallant et al., 2004). Throughout the course of microbial invasion the bacteria are constantly shedding flagellin protein, exposing the organism to flagellin monomers.

TLR's occupy the first line of cellular receptors in defense against microbial invasion. However the intensity of this response associated with chronic inflammation

has been implicated in immune and inflammatory diseases as well as cancer development(Coussens and Werb, 2002). Inappropriate activation and/or constitutive activation of NF-κB are commonly observed in many chronic inflammatory diseases including inflammatory bowel disease, arthritis and atherosclerosis, hepatitis, and *H.pylori* infection(Coussens and Werb, 2002; Killeen et al., 2006). A current belief is that in addition to the TLRs' ability to recognize exogenous pathogens and their products, they may also recognize modified endogenous proteins/products that initiate or are markers for a pathogenic condition(Cordon-Cardo and Prives, 1999).

Bacterial Lipopolysacharide (LPS) a bacterial cell wall component and TLR-4 ligand has been implicated in tumor metastasis of a murine breast carcinoma model(Killeen et al., 2006). Increased angiogenesis, vascular permeability and tumor cell invasion were all noted. TLR activation via LPS may favor tumor growth and metastasis directly through NF-κB activation(Coussens and Werb, 2002; Killeen et al., 2006). Activation of NF-κB is required for cells to undergo transformation and bypass the cellular death program. NF-κB activity also plays an important role in normal breast development and its activity is tightly controlled. In a majority of breast cancer tumors and cell lines derived from those tumors, NF-κB is chronically active(Aggarwal et al., 2006).

Lastly, we have discovered that an as yet undescribed NF-κB activation pathway exists in some breast cancer cells. This pathway involves the production of a factor(s) by some breast cancer cells that is recognized by a receptor protein that is a member of the Toll-like receptors. It is likely that in breast cancer cells, that produce these factors, the factor feeds back in an autocrine fashion and activates NF-κB in those cells via

recognition by the TLRs and provide for a growth, survival or metastatic advantage. Two of six BC cell lines, MDA-MB-468 and MDA-MB-231, actively produce a factor(s) that potently activate NF-κB specifically through a subset of TLRs. (**See Chapter VI)**.

We have examined the expression of many of the TLR family members in a number of established breast cancer cell lines and in a limited number of breast cancer tissues and normal breast tissue and discovered that various subsets of the TLRs were up regulated in expression in a majority of breast cancer tumors but not in normal breast tissue. **(See Chapter VI)**.

FIGURE 1.4

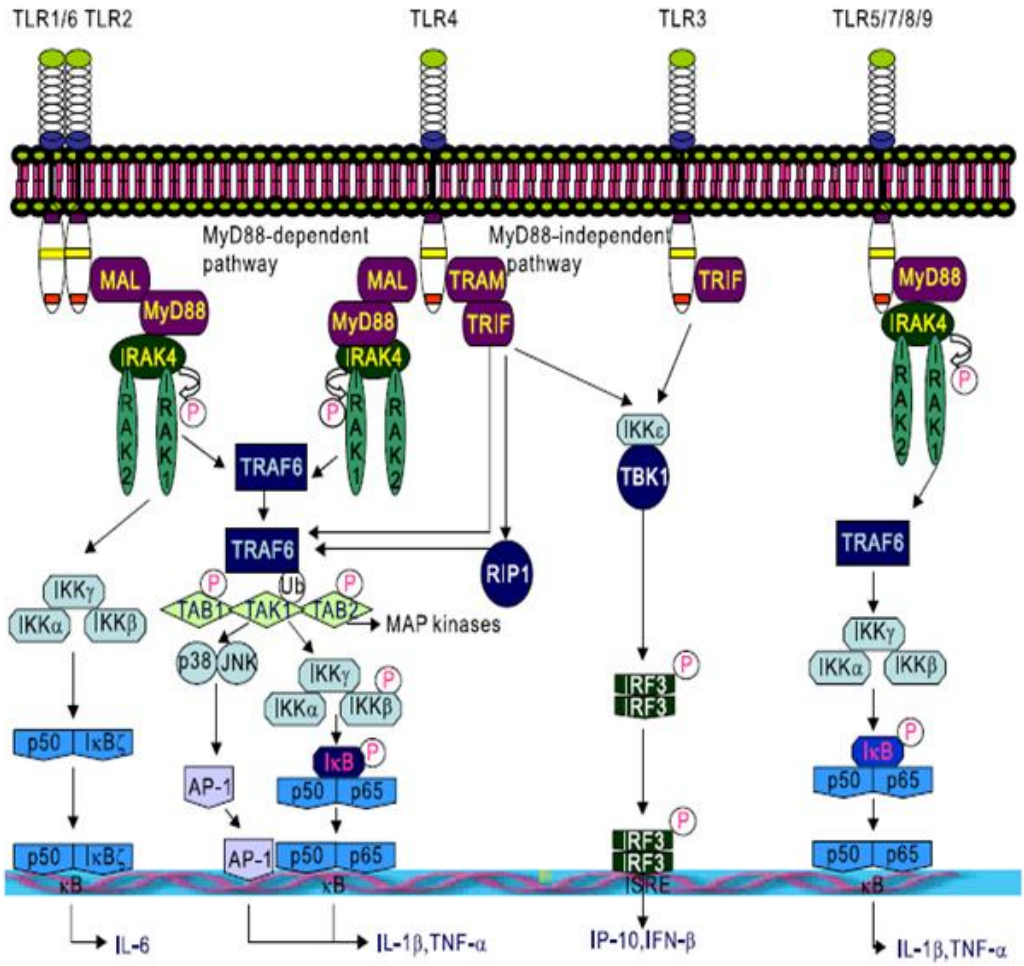

Figure 1.4: Toll Like Receptor (TLR) family members differentially utilizes adapter proteins and are broadly grouped into two signaling categories, MyD88 dependent and MyD88 independent pathways.

All TLRs utilize MyD88 with the exception of TLR3. MyD88 binds with the TIR domain of the receptor where it recruits and subsequently phosphorylates IRAK4. IRAK4 cross phosphorylates IRAK1. IRAK1 phosphorylates TRAF6 leading to the ubiquitination of TAK. TAK then activates the IKK signaling complex and NF-κB leading to an inflammatory response. Illustrated by: (Krishnan et al., 2007) with annotative modifications.

1.3.5 Activation of NF-κB due to Genotoxic Stress

Cells are continuously being bombarded with environmental stimuli, as well as bi- products of cellular respiration or activity, that may potentially damage its genetic material. In order to insure genetic stability, cells have developed a surveillance strategy to proofread the integrity of the genomic architecture(Ahn et al., 2004). These surveillance pathways or checkpoints, act as sentinels to alert the cell of defective or abnormal DNA. There are specific sensor proteins that are able to recognize the most lethal of DNA abnormalities Double Stranded Breaks (DSB)(Abraham, 2001).

In mammalian cells ATM (ataxia-telangiectasia mutated) and ATR (ATM and Rad 3-related) are two such checkpoint sensor proteins(Abraham, 2001). They are members of the phosphatidylinositol 3-kinase (PIKK) family and are multifunctional serine/threonine protein kinases(Kastan and Lim, 2000). The ATM gene was named after a genetic disorder called ataxia-telangiectasia (Kastan and Lim, 2000). Patients who exhibit a deletion of this gene are susceptible to inducers of double stranded breaks (DSB). ATM and ATR play prominent roles in sensing and signaling genomic instability.

ATM is activated by signaling that a DSB has occurred. It is considered a primary responder and mediates the activation of NF-κB, due to DSB(Habraken and Piette, 2006). The primary role of NF-κB is to protect the cell against the numerous apoptotic stimuli activated by the event(Habraken and Piette, 2006). Current research has strongly identified ATM as the primary mediating agent in NF-κB activation due to DSB, caused by genotoxic stress(Abraham, 2001). DNA damage caused by UV or ionizing radiation, and chemotherapeutic drugs such as cisplatin, doxorubicin, and etoposide are the most

characterized activators of NF-κB by ATM(Habraken and Piette, 2006).
Cells exhibiting a mutation in the ATM gene exhibit little or no NF-κB activation in response to DSB caused by genotoxic agents (Abraham, 2001).

Inactive nuclear ATM exists as a homodimer (Bakkenist and Kastan, 2003). Upon DNA damage recognition, ATM/ATR is recruited to the damaged site, and become activated. (Bakkenist and Kastan, 2003). ATM activation takes place quickly, and in the presence of a very small number of DSB or a disruption of the chromatin structure. A number of protein targets for activated ATM/ATR have been identified, including p53, Checkpoint kinase 2 (CHK2), and IKK-γ (NEMO) (Kastan and Lim, 2000)(**Fig. 1.5**).

NF-κB activation by ATM involves signaling from the nucleus to the cytoplasm through NEMO. This is accomplished via a series of phosphorylations, sumoylations and ubiquitinations (Mabb and Miyamoto, 2007; Ulrich, 2005; Wu et al., 2006).

Ubiquitin modification is primarily known for targeting a protein to the 26S proteasome. This involves the multi-branching of ubiquitin chains covalently linked on the target protein through a lysine 48 (K48) linkage of one ubiquitin unit, with the c terminal glycine (G76) of a second ubiquitin unit (Sun, 2006).

Each ubiquitin unit has multiple lysines, and each of the lysine attachment sites is unique and functionally diverse. For example, multi-branching of ubiquitin chains covalently linked through Lysine 63 of one unit, with the c terminal glycine G76 of a second ubiquitin unit (G76-K63) acts as signal transduction modification. Mono-ubiquitination may signal for membrane transport or transcriptional regulation (**Fig: 1.6)** (Sun, 2006).

FIGURE 1.5

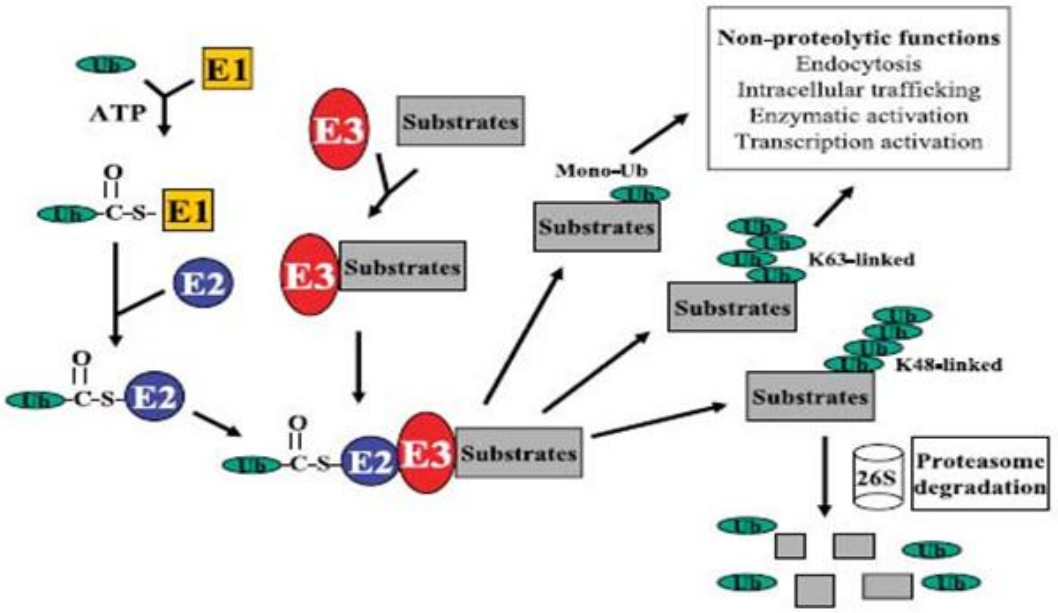

Figure 1.5: Post translational Ubiquitin linked modification of proteins plays a key role in the regulation of protein degradation, function and signal Transduction.

The addition of ubiquitin to a target protein takes place in a sequential three step process, involving three separate enzymes. Step1: Activation of ubiquitin by an activating enzyme (E1) that forms a thiol ester with the G76 carboxyl group of ubiquitin. Step 2: Conjugation, of the activated ubiquitin, to an intermediate protein (E2) that transiently carries the charged ubiquitin as a thiol ester. Step 3: The transfer of the activated ubiquitin from the E2 carrier protein, to a lysine on the final target by a ligase (E3). The E3 substrate can either be a free protein, or another ubiquitin molecule already bound to a target substrate. Illustrated by:(Sun, 2006)

FIGURE 1.6

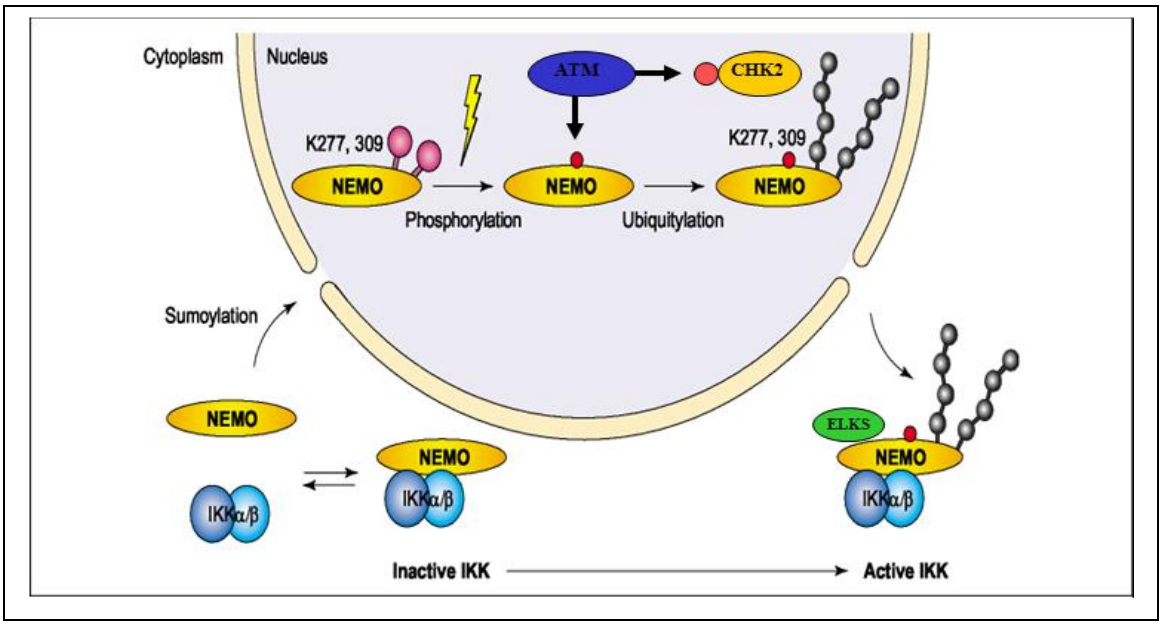

Figure 1.6: Sequential actions of SUMO and ubiquitin on NEMO.

The IKK regulatory subunit, NEMO, associates reversibly with the catalytic subunits IKKα and IKKβ. Sumoylation of NEMO causes its retention in the nucleus, where ATM-dependent signaling by DNA damage induces phosphorylation and subsequent ubiquitination of NEMO. The ubiquitinylated form can leave the nucleus and associate with ELKS and IKKα/β to yield an active kinase. Illustrated by (Ulrich, 2005), with modifications

A second post translational modification protein involved in NF- κB signaling is SUMO (small ubiquitin-like modifier) (Mabb and Miyamoto, 2007). SUMO utilizes a similar activating, conjugation, and ligation scheme as ubiquitin, with the exception that SUMO is generally thought to function as a monomer (Seeler and Dejean, 2001). SUMO substrates are mostly known to be nuclear proteins, indicating that sumoylation is part of a nuclear transport process (Seeler and Dejean, 2001). The first identified SUMO-modified protein, RanGAP, a small GTPase activating protein plays a role in nuclear import.

Crosstalk between SUMO and Ubiquitin may exist either in an antagonistic or co-operative manner(Ulrich, 2005). The apparent cooperative cross talk between the two conjugation systems of sumoylation and ubiquitination is demonstrated on their effects involved with the modification of NEMO(Ulrich, 2005).

The C-terminal zinc-finger domain of NEMO is essential for activation of IKK due to genotoxic stress caused by Ionizing Radiation, UV radiation or chemical DNA damaging agents such as Doxorubicin, Daunorubicin, and VP-16(Huang et al., 2002). Two zinc finger lysines, K277 and K309 of IKKγ are sumoylated upon cellular exposure to DNA damaging agents causing NEMO to accumulate in the nucleus(Ulrich, 2005).

In order to maintain homeostasis, sumoylation and ubiquitination of NEMO takes place constitutively(Mabb and Miyamoto, 2007). However, in response to DNA damage additional NEMO is sumoylated and sequestered in the nucleus(Ulrich, 2005). NEMO is then phosphorylated on Serine 85, by activated ATM. This is required for NEMO to become mono-ubiquitinated directing export of NEMO from the nucleus back to the

cytoplasm. Ubiquitinated NEMO is able to recruit additional protein components necessary for IKK activation(Ulrich, 2005).

The requirement for NEMO ubiquitination to activate IKK has been demonstrated in response to cytokine stimulation(Israel, 2006). This ubiquitin modification is cytoplasmic directed. Multi-branched (G76-K63) ubiquitination of NEMO, on lysine 399 of its zinc finger (Sebban et al., 2006), is necessary but not essential for the assembly and subsequent activation of the IKK complex(Huang et al., 2002; Makris et al., 2002). Mutations in the zinc finger diminishes but does not abrogate activation of NF-κB by stimulation with TNF-α or IL-1. In addition TNF-α is more sensitive to the mutations than IL-1 (Makris et al., 2002).

The signal event resulting in activating NF-κB, due to genotoxic stress, originates in the nucleus of the cell and is caused by check point surveillance mechanisms that sense the stalling of replication or transcription machinery due to double stranded DNA breaks(Ulrich, 2005). This inside out signal to activate IKK contains a temporal component that results in a slower kinetic activation of the transcription factor than would normally be observed during cytokine activation (Huang et al., 2002).

The slower kinetic activators use distinct portions of IKK-γ, concentrating on or in close proximity to the zinc finger(Huang et al., 2002). Disruption of the zinc finger abrogates IKK activation(Huang et al., 2002). The inside out signal has two activating components. The first component activates the apoptotic machinery of the cell, i.e. activation of p53 by ATM (Ulrich, 2005; Wu et al., 2006).

The second component activates the pro-survival cascade, spearheaded by NF-κB, retarding full activation of the apoptotic machinery, allowing the cell time to affect repair.

The use of ionizing radiation and drugs such as cisplatin, doxorubicin, and etoposide are commonly used in anti cancer therapy. However the activation of NF-κB counteracts the apoptotic effects of these treatments. The temporal lag time in NF-κB activation and necessity of the zinc finger for IKK activation, due to these chemotherapy treatments, makes IKK-γ an interesting target for drug intervention. Specifically, zinc fingers are redox sensitive (Kroncke and Carlberg, 2000), targeting the zinc finger for nitrosative modification by a Nitric Oxide donating compound, may abrogate IKK signaling due to functional loss of IKKγ's zinc finger.

1.4 NF-κB AND APOPTOSIS

Programmed cell death is a complicated cascade of cellular events, of which two major pathways predominate, Apoptosis and Necrosis (Ghobrial et al., 2005). Typical apoptotic characteristics include membrane blebbing, cellular collapse, nuclear and organelle condensation and compartmentalization, and lastly DNA degradation (Jin and El-Deiry, 2005).

In mammalian cells there are two major cellular apoptotic pathways extrinsic and intrinsic (**Fig. 1.7)**. The extrinsic pathway is ligand-specific and Death Receptor-mediated. The intrinsic pathway involves the mitochondria and a family of proteins known as Bcl-2 family members (Xiao-Ming Yin and Zheng Dong, 2003). The two apoptotic pathways generally depend on several members of a cysteine protease family known as caspases (Jin and El-Deiry, 2005).

The caspases are aspartate-specific, and act in an initiator - effector manner. They exist in the cytoplasm as an inactive pro-caspase. Early activated caspases are known as *initiator* caspases. Initiator caspases activate a second tier of proteases known as *effector* caspases (Ghobrial et al., 2005). The post-translational regulation of these proteins insures a rapid and irreversible activation cascade. The activation of these effector caspases is a clear indication that the cellular apoptotic pathway has been activated (Jin and El-Deiry, 2005).

Cells undergoing necrosis swell, resulting in loss of membrane integrity and eventually lyse (Jin and El-Deiry, 2005). This release of cellular contents results in a massive inflammatory response that could possibly result in shock, organ failure, limb

perfusion and death. The preferential strategy and cellular response to traditional cancer therapy is controlled cellular apoptosis rather than necrosis.

A poor inducer of apoptosis is not necessarily a result of its ability to adequately activate the cellular apoptotic machinery. It is just as likely to be a poor or weak inducer of apoptosis due to its inability to fully activate NF-κB, whose target genes; the cellular inhibitors of apoptosis (CIAPs) prevent programmed cell death (Ghobrial et al., 2005).

The activation of IKK and the subsequent activation of NF-κB leads to the induction of genes whose protein products, in most cases, results in the prevention of apoptosis and necrosis. Many of the NF-κB activating ligands, receptors, adapter proteins, and inhibitors of Apoptosis are target genes of NF-κB. TNF, TNF receptor, TRAF and X-linked inhibitor of Apoptosis are just a few (Ghobrial et al., 2005). Once activated NF-κB plays a major role in further providing key factors necessary for its further activation in an autocrine fashion.

FIGURE 1.7

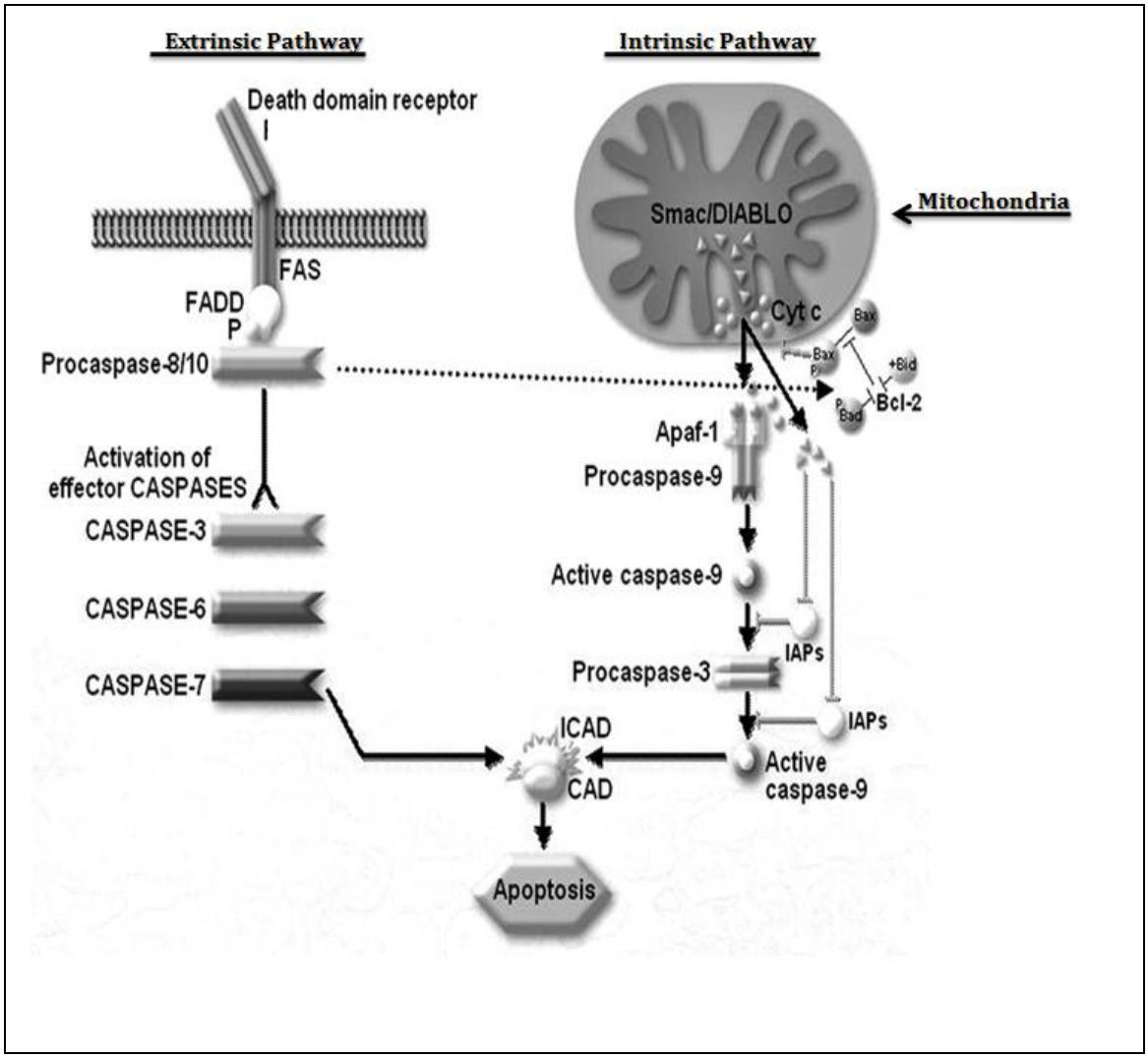

Figure 1.7: Apoptosis occurs through two main pathways.

The extrinsic pathway is triggered through death receptor activation and formation of DISC, leading to initiator pro-caspase congregation. Stimulation of the second pathway, the intrinsic pathway, results in the release of cytochrome-c from the mitochondria and activation of the death signal. The intrinsic and extrinsic pathways converge to form a final common pathway resulting in the activation of caspases that cleave regulatory and structural molecules effecting in the death of the cell. Illustrated by (Ghobrial et al., 2005), with modifications.

1.4.1 X-Linked Inhibitor of Apoptosis Protein (XIAP)

Inhibitors of apoptosis proteins are a family of proteins whose actions are known to inhibit apoptosis. It is thought that they accomplish this action, utilizing one of two mechanisms. Ubiquitinating apoptotic proteins thereby targeting them for degradation, or by sterically hindering the protein from engaging its cognate substrate (Eckelman et al., 2006). The most well known are cellular IAP-1, IAP-2 (cIAP-1 and cIAP-2 respectively) and XIAP. These inhibitors act upon the caspase proteins, specifically caspases 3-7-9. Inhibition of these caspases will subsequently block down stream activation of apoptosis (**Fig. 1.8)**.

The characterizing feature of the IAP family of proteins is a series of 70-80 amino acid Baculovirus IAP Repeat (BIR) domains (Xiao-Ming Yin and Zheng Dong, 2003). The domain is histidine and cysteine rich, and exists in a folded globular formation. Each of the BIR domains are functionally independent and chelate a zinc ion(Xiao-Ming Yin and Zheng Dong, 2003). The BIR domain is essential in allowing XIAP to associate with both initiator and effector caspases (Salvesen and Duckett, 2002). This association blocks activation of caspases, as previously described, thereby inhibiting apoptosis.

In addition, XIAP as well as other IAP's, contain an E3 Ubiquitin ligase domain at its C- terminus, containing a RING finger, a subset of the classical zinc finger domain (Mani and Gelmann, 2005). The E3 ligase recruits target proteins, including other IAP's for ubiquitination and subsequent degradation regulating the cellular apoptotic signaling. The ubiquitination and degradation of IAP's correspond to an advancement of the apoptotic signal (Salvesen and Duckett, 2002). It follows that inhibition of XIAP, either

transcriptionally through inhibition of NF-κB or by targeting its activitiy with a chemical inhibitor, will enhance the apoptotic effect on the cell (Schimmer et al., 2006).

FIGURE 1.8

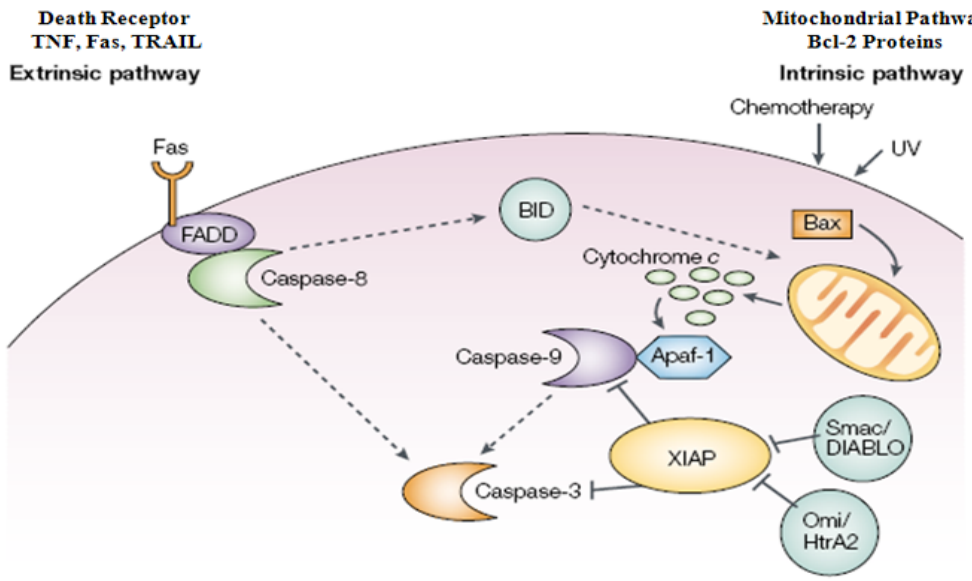

Figure 1.8: XIAP inhibits caspases in both the intrinsic and extrinsic apoptotic pathways.

XIAP directly inhibits key activated caspases, in both pathways. XIAP binds to the effector caspase-3 and caspase-9, via its BIR domain, hindering substrate engagement by the proteases. Illustrated by (Salvesen and Duckett, 2002), with modifications.

1.4.2 Akt

Akt is a family of serine threonine protein-kinases. It has been demonstrated that it may regulate cancer metastasis and chemotherapeutic resistance and has been found to be constitutively active in a number of cancers (Vivanco and Sawyers, 2002). The biological consequences of Akt activation effect cell survival, proliferation, and growth (Datta et al., 1999).

Akt contains an N-terminal, pleckstrin homology domain (PH), a central kinase domain, and a c-terminal regulatory domain (Vivanco and Sawyers, 2002). The PH domain mediates recruitment to the cellular membrane as well as protein-protein and/or protein-lipid interactions. Four activating phosphorylation sites have been identified on Akt; however the primary activation targets are threonine 308 and serine 473 (Datta et al., 1999). Several regulatory kinase complexes have been indentified that are capable of phosphorylating Akt but both primary activation sites are phosphorylated by the kinase complex, 3-phosphoinositide-dependant protein kinase (PDK1/PKR-2)(Datta et al., 1999).

Upon cellular growth factor or cytokine stimulation phosphatidylinositol 3-kinase (PI3K) activates the classical second messenger, phosphatidylinositol 3, 4, 5, triphosphate (PIP3) (Datta et al., 1999). PIP3 recruits Akt, via its PH domain, to the inner leaflet of cellular membrane. Upon membrane association it is targeted for phosphorylation and subsequent activation, upon activation Akt is released into the cytosol (Datta et al., 1999).

Activated Akt is involved in both pro-survival and apoptotic pathways. Akt has been shown to phosphorylate IKK-α triggering NF-κB activation and subsequent pro-survival signaling (**Fig. 1.9)** (Datta et al., 1999).

Two apoptotic proteins, examined in this study and affected by Akt are the B-cell lymphoma (Bcl) family of proteins and capasese-9. During apoptosis, following a series of cascading events, the mitochondrial membrane becomes increasingly more permeable (Ghobrial et al., 2005). This is accomplished through the formation of pores in the mitochondrial membrane, mediating the release of cytochrome-C into the cytoplasm, a hallmark signal of apoptosis (Xiao-Ming Yin and Zheng Dong, 2003). A member of the Bcl family of proteins, Bcl-X_L, mediates the inhibition of the formation of these pores.

A second member of this family BAD, is an in inhibitor of Bcl-X_L. Under homeostatic conditions, BAD is phosphorylated by Akt, and forms a dimer with a protein named 14-3-3 (so called due to characteristic migration patterns in electrophoretic gels), keeping it inactive (Kim and Chung, 2002). The non-phosphorylated species of BAD forms a dimer with Bcl-X_L, inhibiting its anti-apoptotic effects (Xiao-Ming Yin and Zheng Dong, 2003).

Caspase-9, an initiator caspase, exists in cytoplasm as a zymogen. Upon release of cytocrome-C pro-caspase-9 is incorporated into an apoptotic structure, named the apoptosome which facilities caspase-9 auto activation (Xiao-Ming Yin and Zheng Dong, 2003). Once activated caspase-9 is able to activate the executioner caspase, caspase-3 facilitating the apoptotic advance (Datta et al., 1999).

It has been demonstrated that Akt is able to phosphorylate caspase-9 causing its inactivation. This event takes places post -cytocrome C release from the mitochondria, demonstrating Akt has both pre and post Apoptotic regulatory roles (Datta et al., 1999).

A number of studies have shown that the cell death inducing effect of chemotherapy depends on induction of apoptosis and that disruption of the apoptosis signaling cascade may thus be an important cause for chemotherapy resistance (Debatin, 2004; Ziegler and Kung, 2008). Given the key role that Akt occupies in cell survival, it follows that inhibition of constitutively active Akt and/or Akt activated by cytokines or chemotherapeutic drugs, may increase the efficacy of the drug to destroy cancerous lesions.

FIGURE 1.9

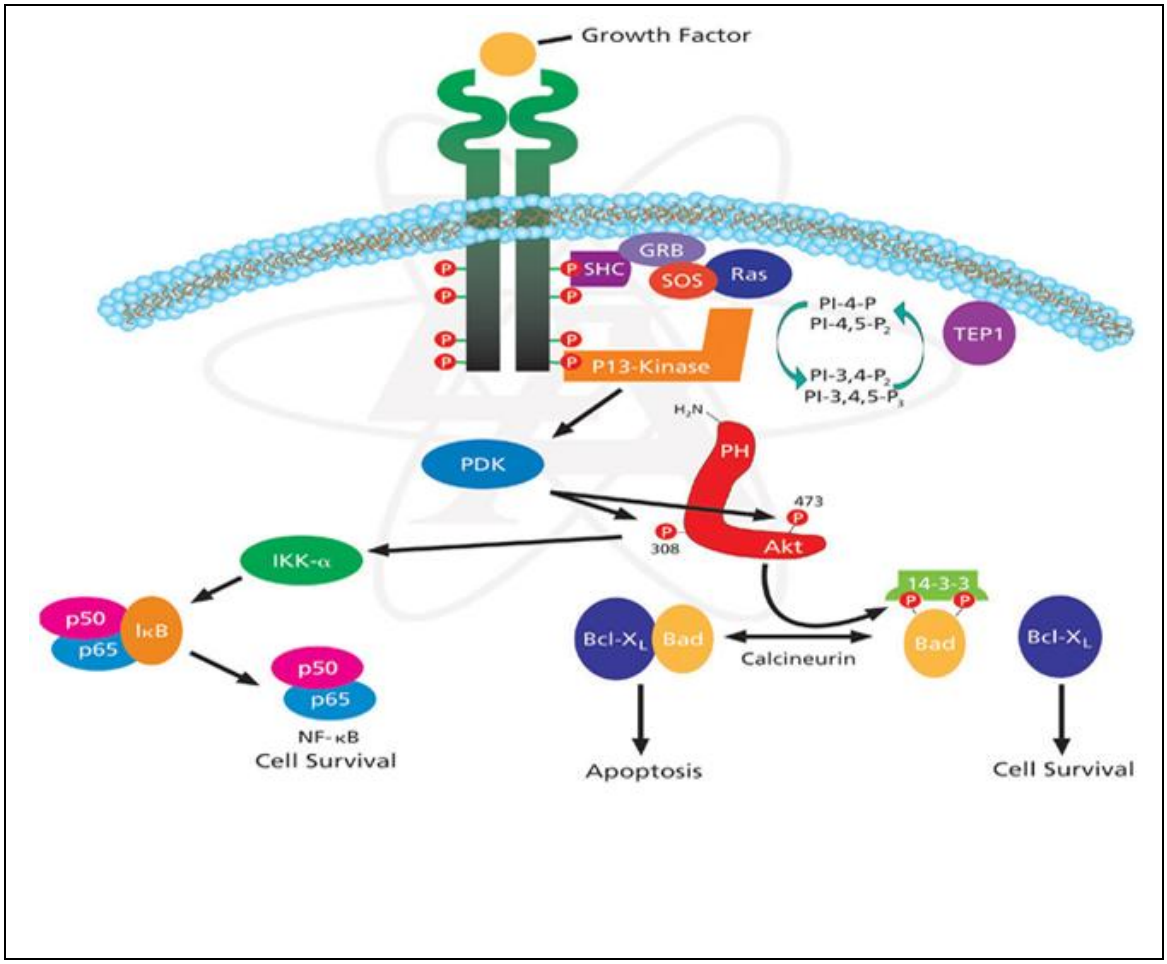

Figure 1.9: Activated Akt Signal Transduction effects the inhibition of Apoptosis through two distinct pathways.

The serine/threonine protein kinase Akt inhibits apoptosis by phosphorylating the Bad component of the Bad/Bcl-X_L complex. Bcl-X_L is an anti-apoptotic protein and it is inhibited by Bad. Phosphorylated Bad, binds to the 14-3-3 protein thereby blocking it from complexing with Bcl-X_L. BcL-X_L unencumbered by Bad is then able to promote cell survival. Secondly, Akt activates IKK-α which ultimately leads to NF-κB activation and cell survival. (Illustrated by SIGMA)

1.5 NITRIC OXIDE AND NF-κB

Nitric Oxide is a free radical that may affect a number of intracellular biological functions (Beckman and Koppenol, 1996). First identified and named Endothelium Derived Relaxation Factor (EDRF) (Mocellin et al., 2007), NO is rapidly diffusible in an aqueous medium and can freely cross cell membranes (Beckman and Koppenol, 1996). Within the aqueous milieu of the cell, Nitric Oxide can under go rapid auto-oxidation, resulting in the formation of a reactive nitrogen species that may engage a broad range of molecular targets (Beckman and Koppenol, 1996).

Endogenous NO is predominately produced by L-arginine catabolism to L-citrulline by a family of nitric oxide synthases (Korhonen et al., 2005). Cellular production, of nitric oxide, occurs in response to tissues damage and bacterial or viral infection (Mocellin et al., 2007). In addition, it has been identified as an inter- and intra-cellular messenger. Lastly, mounting evidence suggests that chronic nitric oxide production is responsible for inflammatory bowel disease, neurodegenerative disorders and cancer (Wink and Mitchell, 1998).

The wide range of targets presented to NO is due to its ability to participate in Redox Chemistry. The moieties of interest in protein chemistry that can be modified by nitric oxide are tyrosine residues to form 3-nitrotyrosine and cysteine residues to form S-nitrosothiols (Mikkelsen and Wardman, 2003; Squadrito and Pryor, 1998).

The formation of the S-nitrosothiols or 3-nitrotyrosine can disrupt the functionality of the protein if either of these residues are located in: the active site of an enzyme or areas involved in protein to protein or protein to DNA interaction (Marshall et al., 2000;

Squadrito and Pryor, 1998). For example, this inhibition can be in the form of blocking the active site of a kinase or changing the conformation of the protein and sterically hindering its ability to phosphorylate or to complex with another protein(Mikkelsen and Wardman, 2003).

The effects of NO are mediated mainly via three routes. NO can react specifically with transition metals (iron, copper, and zinc) (Hess et al., 2005). These metals are abundantly present in prosthetic groups of proteins. NO is a Lewis base forming a nitrosyl complex with the transition metal (Hess et al., 2005). This may trigger a conformational change in the protein affecting its activity. For example, soluble guanylate cyclase contains a heme group required for activation. Nitric Oxide is able to bind with the heme group modifying the porphyrin ring, activating the enzyme (Davis et al., 2001).

Secondly, NO reacting with the cysteine residues of proteins may form Nitrosothiols. This is commonly referred to as S-nitrosylation. As with phosphorylation, S-nitrosylation may effect the activity of the protein, and is reversible (Hess et al., 2005; Kroncke, 2003).

Thirdly, through the formation of peroxynitrite ($ONOO^-$), a powerful nitrating agent that is able to modify proteins (Mocellin et al., 2007). It is formed in a reaction between NO and superoxide ion. Peroxynitrite formation in excess, results in nitrated proteins, in particular tyrosine moieties (Radi, 2004). Tyrosine nitration is a protein modification that can be used as a marker for excess peroxynitrite formation. In addition Tyrosine nitration can significantly modify the function a protein (Radi, 2004).

Transcription factors commonly exhibit at least two functional domains, A DNA binding domain and an activation domain. The transcription factor binds to a specific sequence in the promoter or enhancer of a gene, thereby stimulating or blocking transcription of that gene. The activation domain mediates protein to protein interactions with other activators, co-activators and general transcription factors of the transcription mechanisms to facilitate transcription (Alberts et al., 1994). It has been demonstrated that treatment with exogenous NO donors can cause zinc finger domains to denature and thus become non-functional(Kroncke and Carlberg, 2000). The NO will complex with a critical cysteine in the zinc finger domain, the subsequent S-nitrosylation induces dissociation of the cysteine-Zn^{2+} linkage, causing the zinc finger to disassociate (Kroncke, 2001; Marshall et al., 2000).

It has been proposed that NO can regulate the activation of NF-κB through several modifications to the secondary structure. It has been demonstrated that S-nitrosylation of a cysteine in the activation loop of the IKK-β kinase, will limit its ability to autophosphorylate as well as phosphorylate IκB-α (Reynaert et al., 2004). S-nitrosylation of the p50 subunit of NF-κB will result in blocking NF-κB binding to its consensus sequence (Matthews et al., 1996) (Marshall and Stamler, 2001). Similarly, two tyrosine residues on the p65 subunit of NF-κB, (Tyr-66 and Tyr-152) may be nitrated hindering and or blocking the transactivation potential of the transcription factor (Park et al., 2005). Lastly, nitration of a tyrosine residues on IκB-α (Tyr-181), an inhibitor of NF-κB, by constitutive NO synthase activation, leads to diasociation of intact IκB-α from the p65-p50 dimer. This results in activating NF-κB in an IKK-β independent manner (Yakovlev et al., 2007).

1.6 NO DONORS

1.6.1 Nitrosylcobalamine (NO-Cbl)

NO-Cbl is a vitamin B12 analog, nitrosylated utilizing Nitric oxide gas. Once nitrosylated NO-Cbl may be used as a nitric oxide donor in a biological system. Under neutral or basic conditions NO-Cbl maintains a stable configuration. However, under acidic conditions the nitric oxide moiety is released.

Nitric Oxide, from NO-Cbl enters the cell in two ways. Release of nitric oxide from the B12 complex and diffusion through the cell membrane, as with other NO donors, this is considered a minor or secondary release mechanism. The second or primary mechanism is receptor mediated. The nitrosylated B12 molecule is a ligand for the B12 receptor and are absorbed into the cell via endocytosis. Once inside the endosome a reduction in the pH of the vesicle causes a release of the nitric oxide moieties and they diffuse throughout the cell.

1.6.2 DETA NONOate (NOC-18)

A nitric oxide donor also known as NOC-18. Half-life at pH 7.4 22^0 C of 56hrs. NOC-18 releases nitric oxide, in solution in a controlled manner allowing entry into the cell by natural diffusion.

1.6.3 Sodium Nitropruside (SNP)

Also know as Sodium Nitroferricyanide (III) Dihydrate (SNP) Half life at pH 7.4 22^0C is a few minutes. NO begins being released up dissolution in water.

1.7 TOPOISOMERASE POISINSAND NF-κB

The winding nature and close packing of double helix DNA within the nucleus leads to inter-tangling of individual chromosomes. This creates topological obstacles that must be overcome in order to allow for replication, transcription, recombination, condensation, and independent segregation. This obstacle is over come utilizing enzymes named Topoisomerses (Alberts et al., 1994).

Mammalian cells contain two broad classes of Topoisomerase, Topoisomerase type I and Topoisomerase type II, both types exist as several isoforms (Wang, 2002). Topoisomerase covalently links itself to a DNA phosphate creating a strand break (either a single for Topo I or a double break for Topo II in the DNA backbone (Alberts et al., 1994). The enzyme then passes the other strand through the breaks and then reseals the break and leaves the DNA. This breakage and reunion of the DNA strands facilitates the release of the torsional tension in the wound DNA double helix due to transcription or replication of the cellular DNA (Wang, 2002).

Topoisomerase type I enzymes introduce a single stranded break in the DNA double helix. Replication,or translation is able to proceed by simply unraveling a short length of DNA that is immediately ahead of the replication/translation fork (Wang, 2002).

Topoisomerase II is able to form covalent linkage with both strands of the DNA helix simultaneously. In this manner it is able to make transient double strand break or a gate within the backbone of the double helix. It then shepherds entangled DNA through the gate. Reseals the break and dissociates from the DNA (Wang, 2002).

In addition, during metaphase, an essential part of mitosis, chromosomes must be able to independently segregate, then migrate to opposite poles. By untangling intertwining DNA, Topoisomerase II facilitates this mechanism allowing cells to proceed through to cytokinesis (Alberts et al., 1994). Chromosomes of cells treated with Topoisomerase II poisons are extremely fragmented and stalled in G_2 phase (McClendon and Osheroff, 2007).

Standard anti- tumor therapy involves the use of Topoisomerase I and II poisons as anti-neoplastic agents, for many forms of cancer. The primary function of the drugs interferes with the ability of the enzyme to repair the single, or double stranded breaks in the DNA double helix (Li and Liu, 2001). This disabled repair mechanism result in permanent double stranded breaks, causing the cell to stall in either S_1 or G_2 triggering activation of the Apoptotic cell death pathway (Kaufmann, 1998).

The Topoisomerase enzymes occupy an important role in cellular growth and survival. They are especially critical in neoplastic malignancies due to their proliferative potential. The introduction of unrepairable DSB exploits the ability of the DSB sentinel mechanisms to stall cell propagation, guarding against further genomic instability.

Genomic instability in the form of double stranded breaks results in a concomitant activation of NF-κB and the cell survival pathway, a conundrum in application of these drugs as anti-neoplastic agents. Development of an adjuvant therapy that would eliminate or reduce the NF-κB activation could likely increase the efficacy of these poisons. We have demonstrated, *in vitro and in vivo*, that the use of nitric oxide donating compounds as an adjuvant with chemotherapeutic drugs, is able to inhibit NF-κB activity while simultaneously increasing apoptotic cytotoxicity.

CHAPTER II

SUPPRESSION OF NF-κB SURVIAL SIGNALING BY NITROSYLCOMBALAMINE SENSITIZES NEOPLASMS TO THE ANTI-TUMOR EFFECTS OF Apo2L/TRAIL

2.1 ABSTRACT

The anti-tumor activity of nitrosylcobalamin (NO-Cbl), an analog of vitamin B12 that delivers nitric oxide (NO) and increases the expression of tumor necrosis factor-related apoptosis-inducing ligand (Apo2L/TRAIL) and its receptors in human tumors, has been previously demonstrated. The specific aim of this study was to examine whether NO-Cbl could sensitize drug-resistant melanomas to Apo2L/TRAIL. Antiproliferative effects of NO-Cbl and Apo2L/TRAIL were assessed in malignant melanomas and non-tumorigenic melanocyte and fibroblast cell lines. Athymic nude mice bearing human melanoma A375 xenografts were treated with NO-Cbl and Apo2L/TRAIL. Apoptosis was measured by TUNEL and confirmed by examining levels and activity of key mediators of apoptosis. The activation status of NF-κB was established by assaying DNA binding, luciferase reporter activity, the phosphorylation status of IκBα, and *in vitro* IKK activity. NO-Cbl sensitized Apo2L/TRAIL-resistant melanoma cell lines to growth inhibition by Apo2L/TRAIL but had minimal effect on normal cell lines. NO-Cbl and Apo2L/TRAIL

exerted synergistic anti-tumor activity against A375 xenografts. Treatment with NO-Cbl followed by Apo2L/TRAIL induced apoptosis in Apo2L/TRAIL-resistant tumor cells, characterized by cleavage of caspase-3, caspase-8, and PARP. NO-Cbl inhibited IKK activation, characterized by decreased phosphorylation of IκBα and inhibition of NF-κB DNA binding activity. NO-Cbl suppressed Apo2L/TRAIL- and TNF-α-mediated activation of a transfected NF-κB-driven luciferase reporter. XIAP, an inhibitor of apoptosis, was inactivated by NO-Cbl. NO-Cbl treatment rendered Apo2L/TRAIL-resistant malignancies sensitive to the anti-tumor effects of Apo2L/TRAIL *in vitro* and *in vivo*. The use of NO-Cbl and Apo2L/TRAIL capitalizes on the tumor-specific properties of both agents and represents a promising anti-cancer combination.

2.2 INTODUCTION

Apoptosis is the rigorously controlled process of programmed cell death. Current trends in cancer drug design focus on selective targeting to activate the apoptotic signaling pathways within tumors while sparing normal cells (Reed, 2003). The tumor specific properties of tumor necrosis factor-related apoptosis-inducing ligand (Apo2L/TRAIL) have been widely reported (Ashkenazi, 2002; Pitti et al., 1996; Walczak et al., 1999; Wiley et al., 1995). Apo2L/TRAIL has been used as an anti-cancer agent alone and in combination with other agents (Ashkenazi et al., 1999; Frese et al., 2002; Gliniak and Le, 1999; Mizutani et al., 2002; Yamanaka et al., 2000) including ionizing radiation (Chinnaiyan et al., 2000; Di Pietro et al., 2001; Kim et al., 2001). Apo2L/TRAIL can initiate apoptosis in cells that overexpress the survival factors Bcl-2 and Bcl-X_L, and may represent a treatment strategy for tumors that have acquired resistance to chemotherapeutic drugs (Walczak et al., 2000).

Apo2L/TRAIL binds its cognate receptors and activates the caspase cascade utilizing adapter molecules such as FADD(Ashkenazi, 2002; Pan et al., 1997). TRAIL receptors, type II membrane-bound proteins, are members of the tumor necrosis factor (TNF) superfamily of receptors (Wiley et al., 1995). To date, five Apo2L/TRAIL receptors have been identified (Ashkenazi, 2002). Two receptors TRAIL-R1 (DR4) and TRAIL-R2 (DR5) mediate apoptotic signaling, and three non-functional receptors, DcR1, DcR2, and osteoprotegerin (OPG) may act as decoy receptors (Ashkenazi, 2002). Agents that increase expression of DR4 and DR5 may exhibit synergistic anti-tumor activity when combined with Apo2L/TRAIL (Gibson et al., 2000).

The anti-tumor effects of nitrosylcobalamin (NO-Cbl), an analogue of vitamin B12 (cobalamin, Cbl) coordinated with nitric oxide (NO) as a ligand, has been demonstrated (Bauer et al., 2002). Anti-tumor activity correlated with the expression of the transcobalamin II receptor (TCII-R) on the plasma membrane of tumor cells. NO-Cbl is an ideal candidate to be used in combination with Apo2L/TRAIL because NO-Cbl induced the mRNAs of DR4, DR5, and Apo2L/TRAIL in ovarian carcinoma cells (Bauer et al., 2002). Treatment of leukemia cells with Apo2L/TRAIL resulted in increased Apo2L/TRAIL mRNA and protein, suggesting autocrine regulation that can function in a positive feedback loop (Herr et al., 2000). Transfecting ovarian carcinoma cells with a non-functional, dominant negative DR5 receptor (DR5Δ) (Gong and Almasan, 2000) abrogated increases in DR4, DR5, and Apo2L/TRAIL when treated with NO-Cbl.[2] This suggested that a functional Apo2L/TRAIL receptor was necessary for the autoinduction of Apo2L/TRAIL, and that DR5Δ interfered with positive feedback signaling.

Cytokines of the TNF superfamily, upon receptor ligation, simultaneously induce an apoptotic signal (mediated via caspase-8) in addition to a survival signal (mediated by activation of NF-κB) (Bharti and Aggarwal, 2002). NF-κB is a transcription factor that generally functions to suppress apoptosis (Bharti and Aggarwal, 2002; Bours et al., 2000). Binding of TNF-α (DiDonato et al., 1997a) or Apo2L/TRAIL (Baetu et al., 2001) to their cognate receptors results in the phosphorylation and activation of the inhibitor of κB-kinase (IKK). In its quiescent state, NF-κB is complexed to the inhibitor of κB (IκB) in the cytoplasm (DiDonato et al., 1995b). Activated IKK phosphorylates serine 32 and serine 36 of IκB (DiDonato et al., 1996). Once phosphorylated, IκB is ubiquitinated and targeted for proteolysis as it remains complexed to NF-κB (DiDonato et al., 1995a). Within the proteosome IκB is degraded, while NF-κB is not, allowing NF-κB to translocate to the nucleus where it binds to NF-κB response elements, which activate transcription of target genes (DiDonato et al., 1997a; DiDonato et al., 1995b). NF-κB stimulates transcription of genes such as Bcl-X_L and cIAP that function as survival factors (Chen et al., 2000; LaCasse et al., 1998). Therefore, agents that inhibit NF-κB may have anti-tumor activity.

NO is a ubiquitous, multifaceted signaling molecule (Anggard, 1994; Gross and Wolin, 1995) that inhibits NF-κB DNA binding activity (DelaTorre et al., 1997) and suppresses the cell survival function of NF-κB (D'Acquisto et al., 2001; Kang et al., 2002). Sulfasalazine, an anti-inflammatory agent, inhibits NF-κB activity, enhancing Apo2L/TRAIL-induced apoptosis in human leukemia cells (Goke et al., 2000). Furthermore, Apo2L/TRAIL-induced apoptosis was increased in prostate carcinoma cells that were infected with a mutant IκB, supporting the role of NF-κB as a TRAIL-induced survival factor (Eid et al., 2002). The use of NO-Cbl to deliver nitric oxide and suppress the

survival arm of NF-κB is a promising strategy to enhance the anti-tumor effects of Apo2L/TRAIL in resistant tumors.

In this study we pretreated cells with NO-Cbl to inhibit NF-κB activity and enhance the apoptotic signal of Apo2L/TRAIL. Our specific aims were to: 1) measure the anti-tumor effects of NO-Cbl and Apo2L/TRAIL in Apo2L/TRAIL-resistant cell lines, and to 2) determine the mechanism by which NO-Cbl inhibits NF-κB activation.

2.3 MATERIAL AND METHODS

2.3.1 Synthesis of Nitrosylcobalamin

Nitrosylcobalamin was synthesized as previously described (Bauer, 1998; Bauer et al., 2002). Hydroxocobalamin (vitamin B12a) acetate (George Uhe Company, Paramus, NJ) was dissolved in dichloromethane (Burdick and Jackson, Muskegon, MI) and exposed to CP grade NO gas (Praxair, Wickliff, OH) at 150 psi. The reaction proceeds in a closed system within a high-pressure gas cylinder (Praxair, Cleveland, OH). The system was nitrogen-purged daily and evacuated prior to NO exposure. The NO gas was scrubbed prior to entering the system using a stainless steel cylinder (Swagelok, Abbott valve and fitting, Solon, OH) containing NaOH pellets. The solid NO-Cbl product was collected following rotary evaporation of the solvent and stored at –80 °C prior to use.

2.3.2 Cell Culture and Cytokine Treatments

Human melanoma tumor cell lines, WM9 and WM3211 (Wistar Institute, Philadelphia, PA), and A375(ATCC, Manassas, VA) were grown in Dulbecco's modified Eagle medium (DMEM; Invitrogen) supplemented with heat-inactivated 10% fetal bovine serum (FBS; HyClone, Logan, UT) and 1% Antibiotic-Antimycotic (Invitrogen). Cells were maintained in 5% CO_2 at 37 °C in a humidified tissue culture incubator. Primary non-tumorigenic melanoma cell lines (DMN-1 and CMN-1, A. Gudkov, CCF, Cleveland, OH), and human foreskin fibroblasts (HFF; CCF, Cleveland, OH) were cultured in DMEM-F12 medium supplemented with 10% fetal bovine serum. Cells were confirmed as mycoplasma free.

All experiments were performed using trimeric recombinant human Apo2L/TRAIL (Lawrence et al., 2001) (Genentech Inc., San Francisco, CA) and were independently

confirmed using recombinant Apo2L/TRAIL from another source (Peprotech Inc, NJ). Apo2L/TRAIL (Genentech Inc.), consisted of >99% trimeric protein with Zn^{+2}, which is necessary for optimal biologic activity of Apo2L/TRAIL (Lawrence et al., 2001).

2.3.2 Sulforhodamine B cell Growth Assay

Cells were harvested with 0.5% trypsin/0.53 mM EDTA, washed with phosphate-buffered saline and resuspended in media containing 10% fetal bovine serum. Cells were plated in 96-well plates in 0.2-ml aliquots containing 10,000 cells. Cells were allowed to adhere to the plate for 4 h and then NO-Cbl was added in different dilutions (25, 50 and 100 µM) to the assay plate. Replicates of four were performed for each treatment. After 16 h, recombinant human Apo2L/TRAIL was added at different concentrations (25–100 ng/ml). Growth was monitored by the sulforhodamine B (SRB; Sigma Chemical) colorimetric assay (Skehan et al., 1990). After 40 h growth, the medium was removed, and the cells were fixed with 10% trichloroacetic acid and stained with SRB. Bound dye was eluted from the cells with 10 mM Tris-HCl (pH 10.5) and absorbance was measured at 570 nm using Lab systems Multiskan RC 96-well plate reader (Lab Systems Multiscan RC, Thermo Lab Systems, Franklin, MA). To quantify the growth of the cells, the experimental absorbance values (A_{exp}) were compared with initial absorbance readings representing the starting cell numbers (A_{ini}). To determine the starting cell number, an additional 96-well plate was seeded with cells and fixed at the beginning of the experiment. The absorbances derived from the initial plate and from the untreated cells at the end of the growth period (A_{fin}) were defined as 0 and 100% growth, respectively. The percentage control growth ($100\% \times [A_{exp} - A_{ini}]/[A_{fin} - A_{ini}]$) is expressed as a percentage of untreated controls.

2.3.3 In Vivo Experiments

The Institutional Animal Care and Use Committee at the Cleveland Clinic Foundation approved all procedures for animal experimentation. 5-week-old NCR male athymic nude homozygous (*nu*/*nu*) mice (Taconic, Germantown, NY) were inoculated with A375 tumors. There were four experimental groups (untreated, single agents, and the combination) $n = 8$. Cultured tumor cells (4×10^6) were inoculated into flanks in the mid-axillary line. NO-Cbl was given twice daily (50 mg/kg s.c.) and recombinant trimeric Apo2L/TRAIL (50 mg/kg s.c.) (Skehan et al., 1990) was administered every other day, starting on day 2. Tumor volume was measured three times a week using the formula for a prolate spheroid: $(4/3)\ \pi ab^2$ where 2a = major axis, 2b = minor axis. Formalin-fixed sections were processed by the Cleveland Clinic Histology Core. Sections were stained with hematoxylin and eosin and evaluated for pathologic changes in a blinded fashion.

2.3.4 TUNEL Assay

A375 cells were cultured for 36 h and exposed to various treatments (control, NO-Cbl, Apo2L/TRAIL, and NO-Cbl + Apo2L/TRAIL). Apoptotic cells were detected by TUNEL (terminal deoxynucleotidyltransferase-mediated dUTP-biotin nick end-labeling) staining using a commercially available kit (APO-BRDU kit, BD PharMingen, San Diego, CA). Cells were processed according to the manufacturer's recommended protocol. The percentage of fluorescein isothiocyanate-positive cells was analyzed by fluorescent-activated cell scanning (FACS, Becton Dickinson, Facsvantage, and San Diego, CA).

2.3.5 Gel Electrophoresis and Immunoblot Analyses

Whole cell lysates were prepared in 1x lysis buffer (50 mM Tris-Cl, pH 8.0, 1% Triton X-100, 10% glycerol, 1 mM EDTA, 250 mM NaCl, 1 mM dithiothreitol, 1 mM phenylmethylsulfonyl fluoride, 10 µg/ml aprotinin, 10 µg/ml leupeptin, and 10 µg/ml pepstatin) for subsequent immunoblotting studies. SDS-PAGE was conducted by using the Laemmli buffer system and 12% polyacrylamide gels. Proteins were transferred onto polyvinylidene difluoride membranes by the semidry method (Trans Blot S.D., BioRad, Hercules, and CA). Binding of the primary and secondary antibodies was performed according to standard protocols (Chawla-Sarkar et al., 2002). Membranes were immunoblotted with pAb to caspase-3, caspase-8, XIAP (BD PharMingen), PARP (BioMOL), FLIP (Calbiochem), pIκBα, IκBα (Cell Signaling), cIAP-1, anti-IKKα/β (Santa Cruz Biotechnology) followed by incubation with horseradish peroxidase-conjugated secondary antibodies (Pierce). Immunoreactive bands were visualized by using enhanced chemiluminescence (PerkinElmer). Equal protein loading was confirmed by reprobing with monoclonal anti-actin antibody (Sigma Chemical Co.). All immunoblots in this study were repeated 3 times with reproducible results.

2.3.6 Electrophoretic Mobility Shift Assay (EMSA)

A375 cells were treated with NO donors (NO-Cbl, NOC-18, SNAP, 100 µM, 16 h), or with Apo2L/TRAIL (100 ng/ml) or TNF-α (20 ng/ml) for 15 min and 1 h, or with NO donors (16 h) followed by Apo2L/TRAIL or TNF-α (15 min and 1 h). Plates were washed twice with ice-cold phosphate-buffered saline. Cells were resuspended in cold 1x lysis buffer (20 mM HEPES, 20 mM NaF, 1 mM Na_3VO_4, 1 mM EDTA, 1 mM dithiothreitol, 100 mM NaCl, 10% glycerol, and protease inhibitors) as previously

described (Li et al., 2000) and incubated on ice for 30 min followed by centrifugation at 4 °C at 10,000 rpm for 10 min. Supernatants were transferred to fresh tubes and protein concentrations were assessed using the Bradford method (BioRAD protein assay, BioRad). The NF-κB consensus binding sequence (5'-AGTTGAGGGGACTTTCCCAGGC-3') from the IFN-β gene promoter was end-labeled with [γ-^{32}P]dATP (3000 Ci/mol) using T4 polynucleotide kinase. DNA binding reactions were performed in 20 µl reaction volumes for 20 min at 25 °C containing 10 µg of protein, 20 mM HEPES, 10 mM KCl, 0.1% Nonidet P-40, 0.5 mM dithiothreitol, and 10% glycerol. Complexes were separated from the free probe on 6% nondenaturing polyacrylamide gels in 0.5x TBE buffer at 200 V for 2 h. Gels were dried and exposed to film. To verify the identity of the band observed lysates from A375 cells stimulated for 15 min with TNF-α (20 ng/ml) were incubated with anti-NF-κB p50 or p65 antibodies (Santa Cruz Biotechnology).

2.3.7 Dual Luciferase NF-κB Reporter Assay

The NF-κB-luciferase (NF-κB-luc) reporter plasmid, containing a 2xNF-κB response element fused to luciferase, has been previously characterized (Elewaut et al., 1999). *Renilla* luciferase (pRL-TK, Promega, Madison, WI) was co-transfected to normalize for transfection efficiency. A375 cells were co-transfected with 20 µg of NF-κB-luc and 10 µg of pRL-TK using Lipofectamine plus (Invitrogen). After transfection cells were allowed to recover overnight and were plated in 6-well plates. Cells were pretreated with NO-Cbl (100 µM) for 16 h followed by TNF-α (10 ng/ml) or Apo2L/TRAIL (100 ng/ml) for 4 h. Cells were then harvested in 1x passive lysis buffer and luciferase activity was measured according to the manufacturer's protocol (Promega,

Madison, WI) using a Wallac 1420 multilabel counter (PerkinElmer). Fold induction of NF-κB-luciferase for each treatment was based on untreated values normalized to the fold induction of pRL-TK reporter values. The assays were performed in triplicate.

2.3.8 IκB kinase (IKK) assay

Whole cell extracts (300 µg) were supplemented with 150 µl of Buffer A (20 mM HEPES, pH 7.9, 20 mM β-glycerophosphate, 10 mM NaF, 0.1 mM orthovanadate, 5 mM *p*-nitrophenyl phosphate (pNPP), 10 mM 2-mercaptoethanol, 0.5 mM phenylmethylsulfonyl fluoride, and protease mixture), 2 µl of normal rabbit serum, and mixed by rotation at 4 °Cfor1has previously described (DiDonato, 2000). A 50% slurry of protein G-Sepharose (80 µl) (Amersham Biosciences) prepared in Buffer A (without mercaptoethanol or phenylmethylsulfonyl fluoride) was added and mixed by rotation at 4 °C for 1 h. Protein G-Sepharose was removed by centrifugation at 800 x *g* for 1 min and discarded. Anti-IKKα monoclonal antibody (0.5 µg, BD PharMingen), or anti-β-actin epitope antibody was added to the supernatant and mixed by rotation at 4 °C for 2 h. A 50% slurry of protein G-Sepharose (60 µl) prepared in Buffer C (Buffer A plus 50 mM NaCl and 10 mM $MgCl_2$, without mercaptoethanol and phenylmethylsulfonyl fluoride) was added and mixed by rotation in the cold for 30 min. Protein G immunopellets were collected by centrifugation at 800 x *g* for 30 s, washed three times with Buffer B (Buffer A plus 250 mM NaCl), and once with Buffer C (Buffer A plus 50 mM NaCl and 10 mM $MgCl_2$). Immunopellets were resuspended in 30 µl of kinase buffer with 0.1 mM orthovanadate, 50 µM unlabeled ATP, 5 µCi of [γ-^{32}P]ATP, 2 mM dithiothreitol, and 2 µg of recombinant GST-IκBα1–54 (DiDonato et al., 1997a) and incubated at 30 °C for 30 min. Reactions were stopped by the addition of 15 µl of 4x SDS-PAGE loading buffer

(200 mM Tris-HCl, pH 6.8, 8% SDS, 40% glycerol, 0.2% 2-mercaptoethanol), heated at 95 °C for 10 min, and resolved by SDS-PAGE on a 12% acrylamide gel by standard procedures. Gels were rinsed, stained with Bio-Safe Coomassie (BioRad) to visualize protein bands, rinsed, photographed, then dried and exposed to Kodak X-OMAT AR film (Eastman Kodak Co., Rochester, New York) to detect substrate phosphorylation. IKK activation was quantified by PhosphorImage analysis on a Storm-840 imager using Image Quant v 4.2 software (Molecular Dynamics, Amersham Biosciences).

2.3.9 Statistical Analysis

Median effect analysis was used to characterize the interaction between NO-Cbl and Apo2L/TRAIL (Chou and Talalay, 1984). A combination index (CI) >1 indicates antagonism, CI = 1 indicates additivity, and CI <1 indicates synergy. Differences in mean tumor volume between groups were compared using the unpaired two-tailed Student's *t* test, using a pooled estimator of variance to determine statistical significance.

2.4 RESULTS

2.4.1 Anti-tumor Effects of NO-Cbl, Apo2L/TRAIL Vitro and in Vivo

To test our hypothesis that NO-Cbl would enhance the anti-cellular effects of Apo2L/TRAIL against malignant Apo2L/TRAIL-resistant cell lines, we measured the antiproliferative effects of three melanoma lines A375, WM9, and WM3211 (previously shown to be resistant to Apo2L/TRAIL) (Chawla-Sarkar et al., 2002). Three non-malignant human cell lines CMN1 and DMN1 (normal melanocytes) and primary human foreskin fibroblasts (HFF) were examined to demonstrate the tumor-specific effects of NO-Cbl and Apo2L/TRAIL. We used the SRB antiproliferative assay, used by the National Cancer Institute (NCI) to evaluate new chemotherapeutic agents (Skehan et al.,

1990). Median effect analysis was used to characterize the interaction between NO-Cbl and Apo2L/TRAIL (Chou and Talalay, 1984). Cells were pretreated with NO-Cbl for 16 h followed by Apo2L/TRAIL for 24 h. Sequential drug treatment resulted in synergistic antiproliferative activity in all three malignant cell lines (**Fig. 2.1*a***). Non-malignant cells were resistant to the antiproliferative effects of NO-Cbl, Apo2L/TRAIL and the combination (**Fig. 2.1b**). This is consistent with the tumor-specific properties of both NO-Cbl and Apo2L/TRAIL (Bauer et al., 2002; Lawrence et al., 2001).

FIGURE 2.1

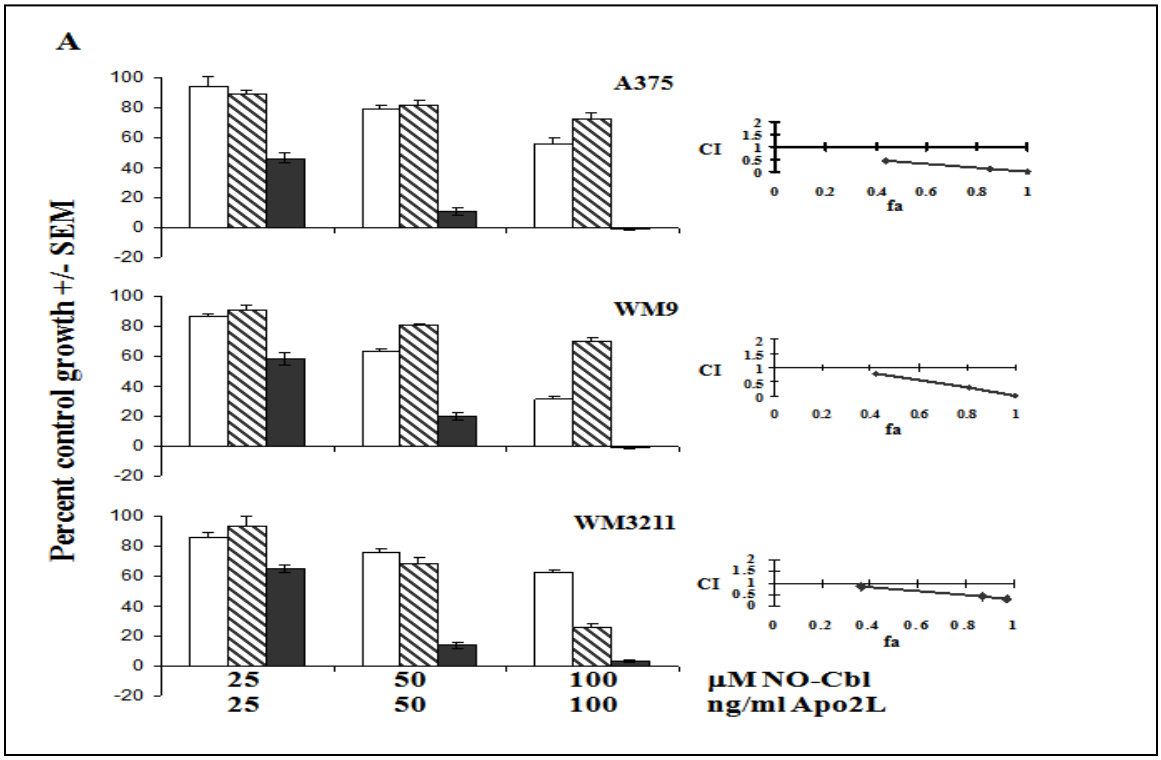
A
A375
WM9
WM3211
Percent control growth +/- SEM
CI
fa
25
25
50
50
100
100
µM NO-Cbl
ng/ml Apo2L

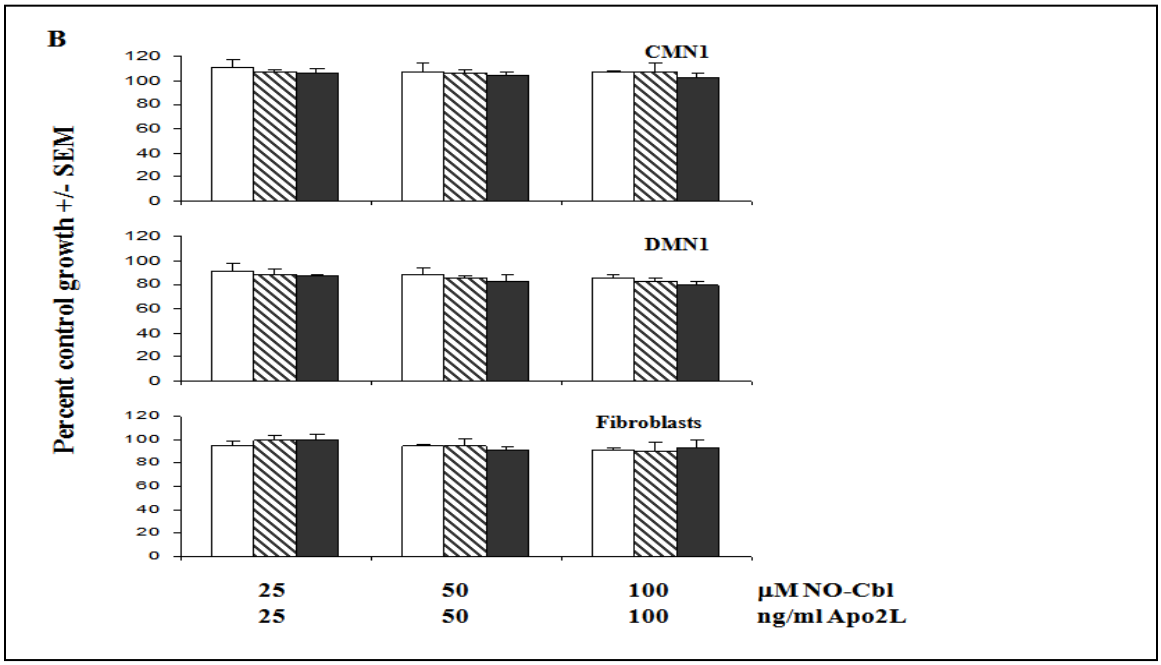
B
CMN1
DMN1
Fibroblasts
Percent control growth +/- SEM
25
25
50
50
100
100
µM NO-Cbl
ng/ml Apo2L

Figure 2.1: Effects of nitrosylcobalamin (NO-Cbl), Apo2L/TRAIL, and the combination on the proliferation of melanoma cell lines A375, WM9, and WM3211 and normal cell lines CMN1, DMN1, and primary HFF fibroblasts.

Left panels, cells were treated with NO-Cbl (**open bars**), Apo2L/TRAIL (**hatched bars**), or pretreated with NO-Cbl followed by Apo2L/TRAIL (**solid bars**) for 3 days, and growth was measured by the colorimetric sulforhodamine B assay (Skehan et al., 1990). Data points represent the mean of four replicates ± S.E. **Right panels**, synergy between NO-Cbl and Apo2L/TRAIL was determined by median effect analysis (Chou and Talalay, 1984; Rubinstein et al., 1990), (combination index >1 indicates antagonism, = 1 indicates additivity, and <1 indicates synergy). **a**, the sequential treatment of NO-Cbl and Apo2L/TRAIL induced synergistic antiproliferative activity in A375, WM9, and WM3211 cells at each combined dose. **b**, normal melanocyte CMN1 and DMN1 cell lines, and normal HFF fibroblasts were completely resistant to simultaneous exposure to NO-Cbl, Apo2L/TRAIL, or the pretreatment with NO-Cbl followed by Apo2L/TRAIL.

To test drug activity *in vivo*, subcutaneous A375 xenografts were established in nude mice. Daily drug treatments began on day 2 following implantation, at which time tumors were both visible and palpable (**Fig. 2.2**). After 21 days, the tumors in mice treated with single agent NO-Cbl or Apo2L/TRAIL were not significantly smaller than controls. However, the tumors in mice treated with the combination of NO-Cbl and Apo2L/TRAIL were 82.42% smaller than control tumors ($p \leq 0.00016$). The mice maintained their weight and activity and exhibited no adverse side effects due to single agents or the combination. Compared with the *in vitro* activity of Apo2L/TRAIL, the enhanced anti-tumor activity observed *in vivo* likely results from multiple biological effects. It has been confirmed that Apo2L/TRAIL up-regulates NK activity *in vivo* resulting in synergistic anti-tumor effects (Sato et al., 2001). Though athymic nude mice lack T-cells, they possess robust NK cell activity.

2.4.2 Mechanism of NO-Cbl/Apo2L/TRAIL-initiated Apoptosis

The A375 cell line has a defect in Apo2L/TRAIL gene induction (Chawla-Sarkar et al., 2001). Therefore, additive cellular responses from endogenous Apo2L/TRAIL were avoided. We performed TUNEL assays of A375 cells treated *in vitro* with NO-Cbl, Apo2L/TRAIL, or the combination. Treatment with NO-Cbl (100 µM) or Apo2L/TRAIL (100 ng/ml) for 36 h induced 6.2% and 5.4% TUNEL-positive cells, respectively (**Fig. 2.3**). The simultaneous co-treatment of A375 cells with NO-Cbl (100 µM) and Apo2L/TRAIL (100 ng/ml) for 36 h resulted in 28.2% TUNEL-positive cells. However, sequential pre-treatment of A375 cells with NO-Cbl (100 µM) for 12 h, followed by Apo2L/TRAIL (100 ng/ml) for an additional 24 h induced 98.4% TUNEL-positive cells, suggesting that

NO-Cbl primes cells to Apo2L/TRAIL-induced apoptosis. In contrast, pre-treatment with Apo2L/TRAIL followed by NO-Cbl did not enhance TUNEL staining.

FIGURE 2.2

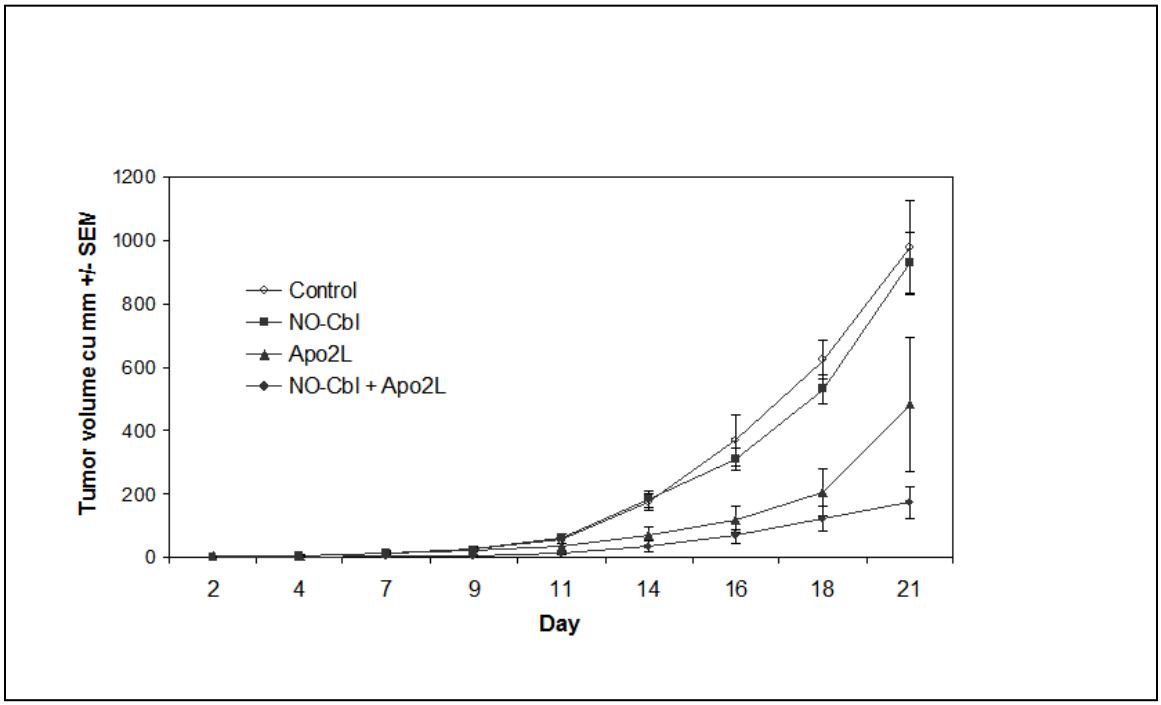

Figure 2.2: Effect of NO-Cbl, Apo2L/TRAIL and the combination on the growth of A375 melanoma Xenografts.

NCR male athymic nude (nu/nu) mice were injected subcutaneously with 4 x 10^6 A375 cells (n = 8 per group). Crug treatments began on day 2 after injection of tumor cells. NO-Cbl was administered twice daily for the duration of the study. Apo2L/TRAIL was administered every other day. Control mice received phosphate buffered saline. Tumor volume was measured three times per week. Data points represent volume (in cubic mm) +/- S.E.

FIGURE 2.3

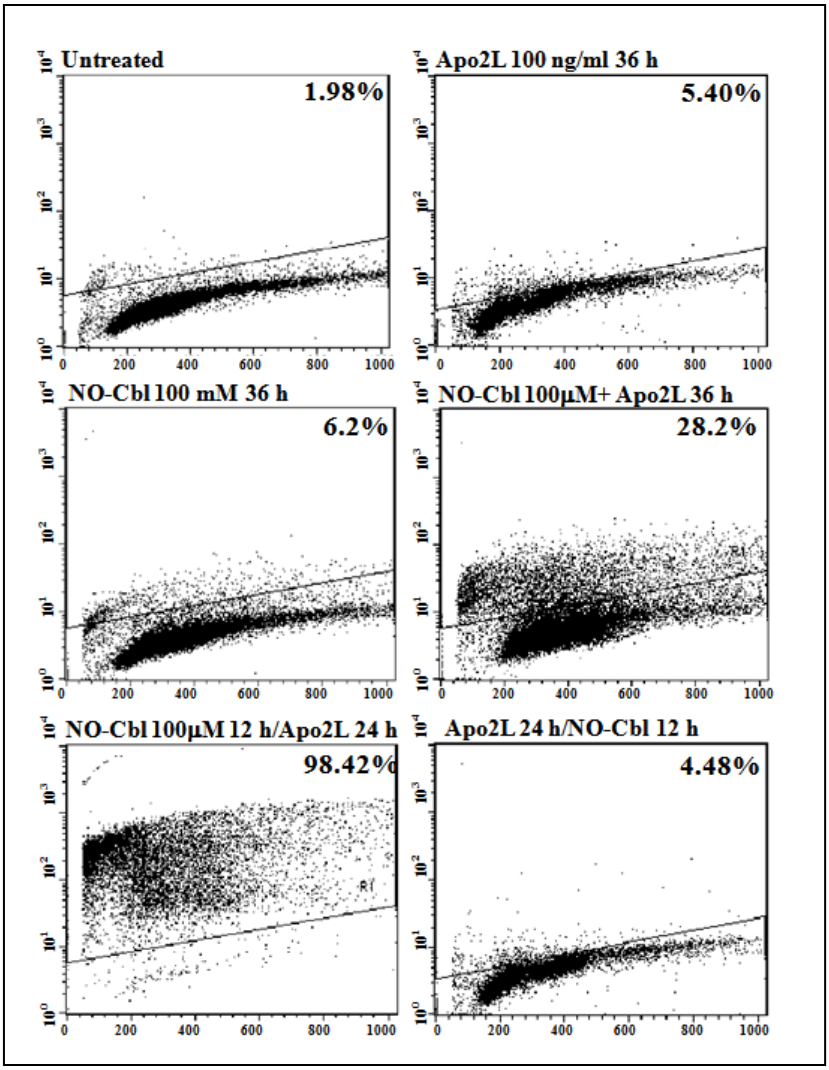

Figure 2.3: TUNEL apoptosis assay

A375 cells were treated with NO-Cbl and Apo2L/TRAIL alone, and in combination with NO-Cbl. NO-Cbl and Apo2L/TRAIL were minimally effective as agents but demonstrated greater apoptosis when administered concomitantly. The highest levels of apoptosis were observed when cells were pretreated with NO-Cbl for 12 h followed by Apo2L/TRAIL treatment for 24h. Conversely, the effect of Apo2L/TRAIL followed by NO-Cbl was no different than Apo2L/TRAIL alone.

To further examine apoptosis pathways, we performed immunoblot analysis using antibodies to various components of the apoptosis signaling cascade. A375 cells were treated with NO-Cbl (50–100 μM) for 16 h followed by Apo2L/TRAIL (100 ng/ml) treatment for 6–12 h. Whole cell lysates were probed for caspase-8, caspase-3, and PARP cleavage. Cells pre-treated with NO-Cbl followed by Apo2L/TRAIL demonstrated enhanced cleavage of caspase-8, caspase-3, and PARP, indicating activation of initiators and effectors of apoptosis (**Fig. 2.4a**). In addition, cleavage of the X-linked inhibitor of apoptosis (XIAP) was enhanced by NO-Cbl pre-treatment followed by Apo2L/TRAIL (**Fig. 2.4b**), indicating that NO-Cbl promoted degradation of an apoptosis inhibitor. Some melanomas have increased XIAP activity which may contribute to their resistance (Lillehoj et al., 2002). This effect was specific to XIAP, as there was no change in the levels of cIAP-1 or FLIP (**Fig. 2.4b**).

FIGURE 2.4

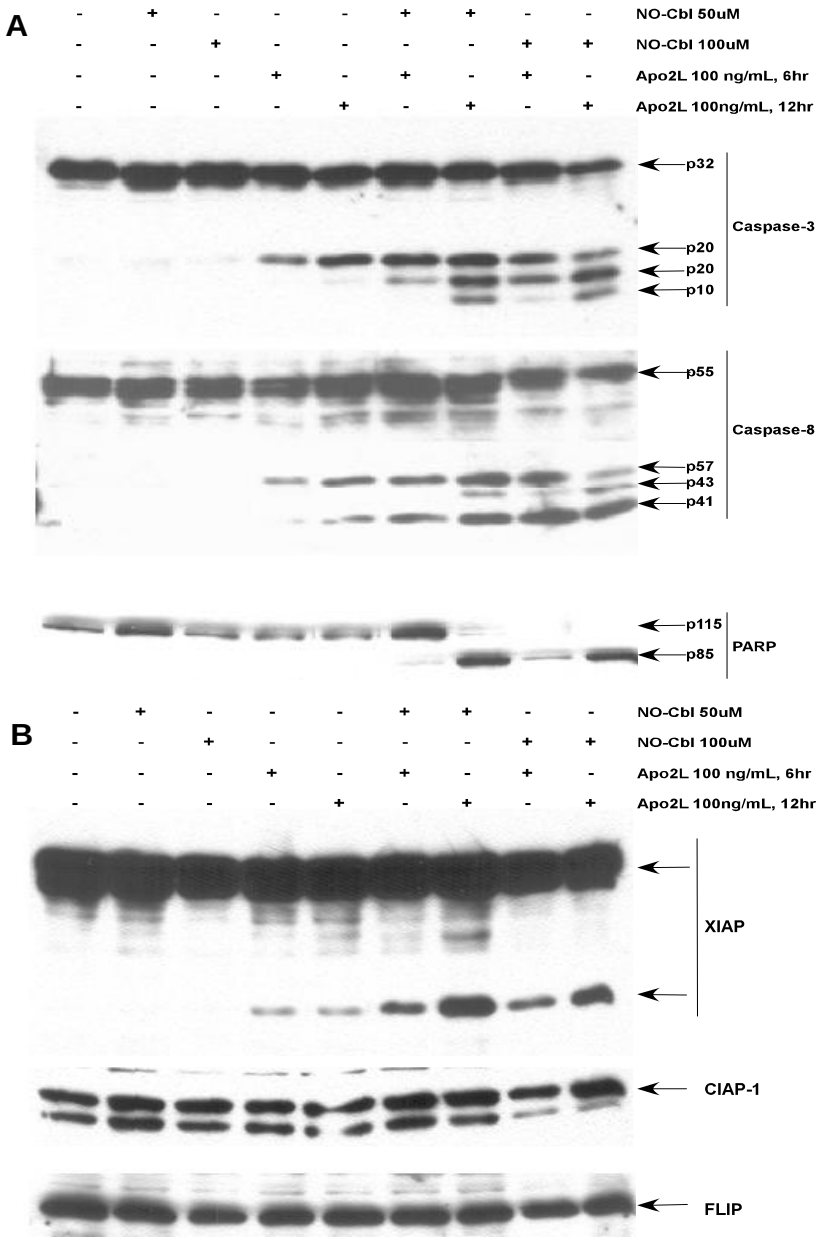

Figure 2.4: Western blot analysis of mediators of Apoptosis

a, A375 cells were pre-treated with NO-Cbl for 16h, followed by Apo2L/TRAIL for 6 or 12h, which resulted in cleavage of caspase-3, caspase-8 and PARP. **b**, sequential NO-Cbl and Apo2L/TRAIL treatment caused cleavage of XIAP but not cIAP or FLIP

2.4.3 Inhibition of NF-κB Survival Signaling by NO-Cbl

We next used EMSA to examine the effects of NO-Cbl on NF-κB activation. The NF-κB binding element from the IFN-β gene promoter was used as a probe to assess DNA binding activity. A375 cells were treated with TNF-α (20 ng/ml), Apo2L/TRAIL (100 ng/ml) or NO-Cbl (100 μM). Pretreatment with NO-Cbl (16 h) completely inhibited NF-κB DNA binding activity induced by 1 h stimulation with Apo2L/TRAIL (**Fig. 2.5a, lanes 4 and 6**). NO-Cbl only partially inhibited NF-κB DNA binding activity induced by TNF-α at 15 min and 1 h (Fig. 5a, compare lanes 7–10). Antibodies to NF-κB-p50 or p65 induced a supershift and confirmed the presence of the p50 and p65 components of the NF-κB complex. Compared with TNF-α, which strongly activates NF-κB after 15 min, Apo2L/TRAIL is a weaker activator of NF-κB; band shifts are not detectable 15-min poststimulation with Apo2L/TRAIL, but do appear by 1 h. This effect has previously been observed in renal cell carcinomas (Oya et al., 2001). Pretreatment with other NO donors including NOC-18 (100 μM) and SNAP (100 μM) also inhibited NF-κB DNA binding activity induced by Apo2L/TRAIL (**Fig. 2.5b**).

Transient transfection assays were performed to assess NF-κB transcriptional activity. A375 cells were co-transfected with a NF-κB-luciferase reporter (NF-κB-luc) and *Renilla* luciferase (to assess transfection efficiency). Cells were pretreated with NO-Cbl (100 μM) for 16 h followed by treatment with Apo2L/TRAIL (100 ng/ml) or TNF-α (10 ng/ml) for 4 h. NO-Cbl pretreatment caused a 34 and 51% inhibition of NF-κB activity in response to Apo2L/TRAIL and TNF-α, respectively (**Fig. 2.5c**).

FIGURE 2.5

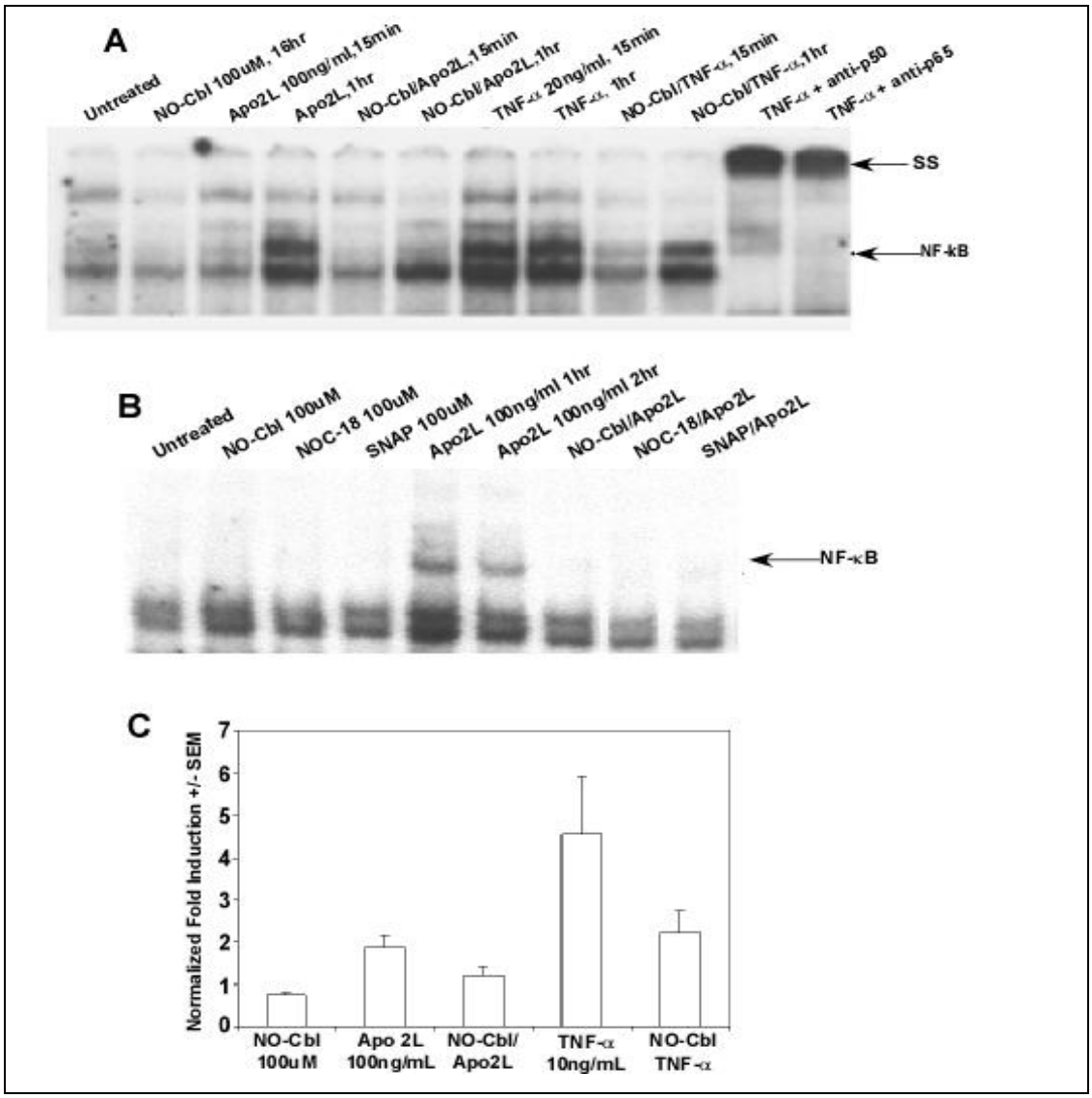

Figure 2.5: EMSA: NF-κB DNA Binding activity.

a, pretreatment of A375 cells with NO-Cbl (16h) inhibited the NF-κB DNA binding activity induced by Apo2L/TRAIL, or TNF-α. Incubation of lysates with anti-NF-κB p50 or anti-NF-κB p65 antibodies resulted in supershift (SS) of the NF-κB complex. **b**, pretreatment with NO donors, NOC-18 and SNAP for 16h also reduced Apo2L/TRAIL-induced NF-κB DNA binding. **c**, NF-κB-luc-transfected A375 cells were pretreated with NO-Cbl for 1h followed by Apo2L/TRAIL or TNF-α for 4h. *Renilla* luciferase was co-transfected to normalize samples for transfection efficiency. Cell lysates were analyzed for NF-κB-luc reporter activity. NO-Cbl pretreatment inhibited Apo2L/TRAIL and TNF-α induced activation of NF-κB luc reporter.

We next determined whether NO-Cbl treatment could affect the degradation of IκBα, the prototypic inhibitor of NF-κB (DiDonato et al., 1995b). After a 15-min stimulation with TNF-α (20 ng/ml) or Apo2L/TRAIL (100 ng/ml, 30 min), IκBα was almost completely degraded (**Fig. 2.6a**). However, NO-Cbl pretreatment for 16 h (100 µM) completely blocked IκBα degradation following stimulation with Apo2L/TRAIL. NO-Cbl was much less efficient at blocking IκBα degradation following TNF-α stimulation. Pretreatment with NO-Cbl for 16 h (100 µM) completely blocked IκBα phosphorylation induced by 1 h stimulation using Apo2L/TRAIL (100 ng/ml) and decreased that induced by TNF-α (20 ng/ml) (**Fig. 2.6b**). At 1 h following TNF-α stimulation, IKK remains activated, albeit at reduced levels compared to15 min (DiDonato et al., 1997b). Phosphorylation of IκBα (all of which has been newly synthesized by 1 h) is evident. After 1 h, total IκBα levels were comparable between treatment groups. Accordingly, phospho-IκBα migrates slower than IκBα (**Fig. 2.6b**, **compare lanes 3 and 4 to other lanes**). NOC-18 (100 µM) and SNAP (100 µM) also inhibited Apo2L/TRAIL induced phosphorylation of IκBα (**Fig. 2.6c**).

FIGURE 2.6

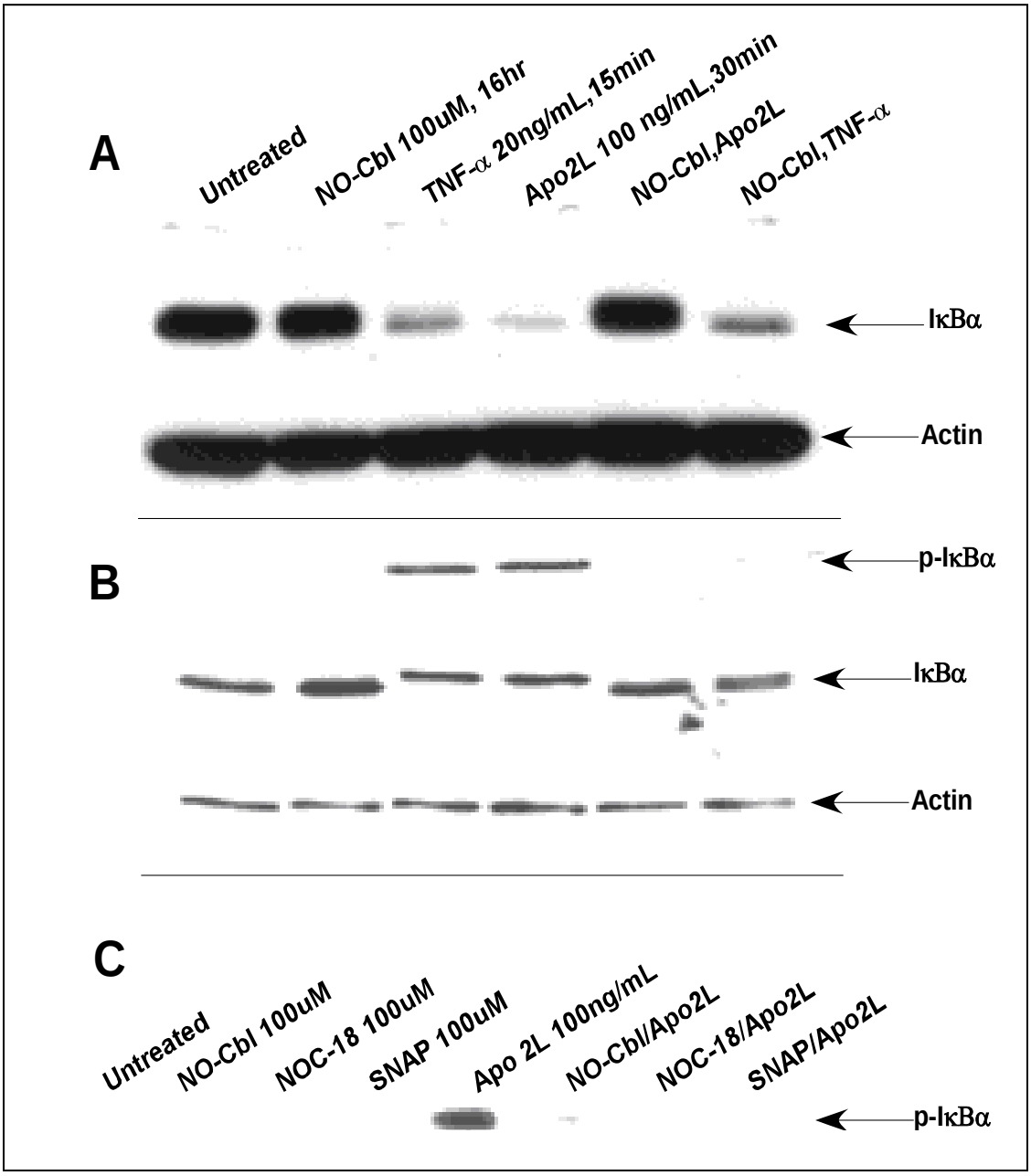
A
Untreated
NO-Cbl 100uM, 16hr
TNF-α 20ng/mL,15min
Apo2L 100 ng/mL,30min
NO-Cbl,Apo2L
NO-Cbl,TNF-α
IκBα
Actin
B
p-IκBα
IκBα
Actin
C
Untreated
NO-Cbl 100uM
NOC-18 100uM
SNAP 100uM
Apo 2L 100ng/mL
NO-Cbl/Apo2L
NOC-18/Apo2L
SNAP/Apo2L
p-IκBα

Figure 2.6: Western blot analysis of IκBα and phospho-IκBα.

A375 cells were pre-treated for 16 h with NO-Cbl followed by Apo2L/TRAIL or TNF-α stimulation. IκBα and phospho-IκBα protein levels were determined in A375 whole cell lysates. **a**, after stimulation with Apo2L/TRAIL (30 min) or TNF-α (15 min), IκBα was almost totally degraded. NO-Cbl efficiently blocked IκBα degradation following Apo2L/TRAIL, but only partially blocked IκBα degradation following TNF-α. **b,** after 1 h, cellular levels of IκBα are restored as a result of resynthesis. NO-Cbl blocks the phosphorylation of newly translated IκBα. Band retardation of IκBα is evident following Apo2L/TRAIL or TNF-α stimulation. Phospho-IκBα migrates slower than IκBα (**compare middle two lanes to other four lanes**). **c**, NO-Cbl, NOC-18, and SNAP pretreatment all inhibited Apo2L/TRAIL-induced IκBα phosphorylation.

2.4.4 Inactivation of IκB Kinase Activity by NO-Cbl

IκB kinase (IKK) is responsible for phosphorylation and activation of IκBα, therefore we examined the effect of NO-Cbl upon IKK activity. A375 cells were pretreated with NO-Cbl (100 µM) for 16 h followed by stimulation with Apo2L/TRAIL (100 ng/ml) or TNF-α (20 ng/ml) and whole cell extracts were prepared at 30 and 15 min after treatment, respectively. IKKα was immunoprecipitated from A375 whole cell extracts and IKK activity was assessed using recombinant GST-IκBα as a substrate (DiDonato et al., 1997a). NO-Cbl effectively inhibited IKK activity induced by TNF-α and Apo2L/TRAIL by 22 and 92%, respectively (**Fig. 2.7a**). Anti-β-actin antibody was used as an irrelevant antibody control for immunoprecipitation and yielded no signal. The kinase assay gel was stained with Coomassie Blue to visualize total protein and demonstrated equal loading of the substrate, GST-IκBα (**Fig. 2.7b**). The same cell extracts were probed for total IKK by immunoblot analysis and demonstrated equal loading of IKK (**Fig. 2.7c**).

FIGURE 2.7

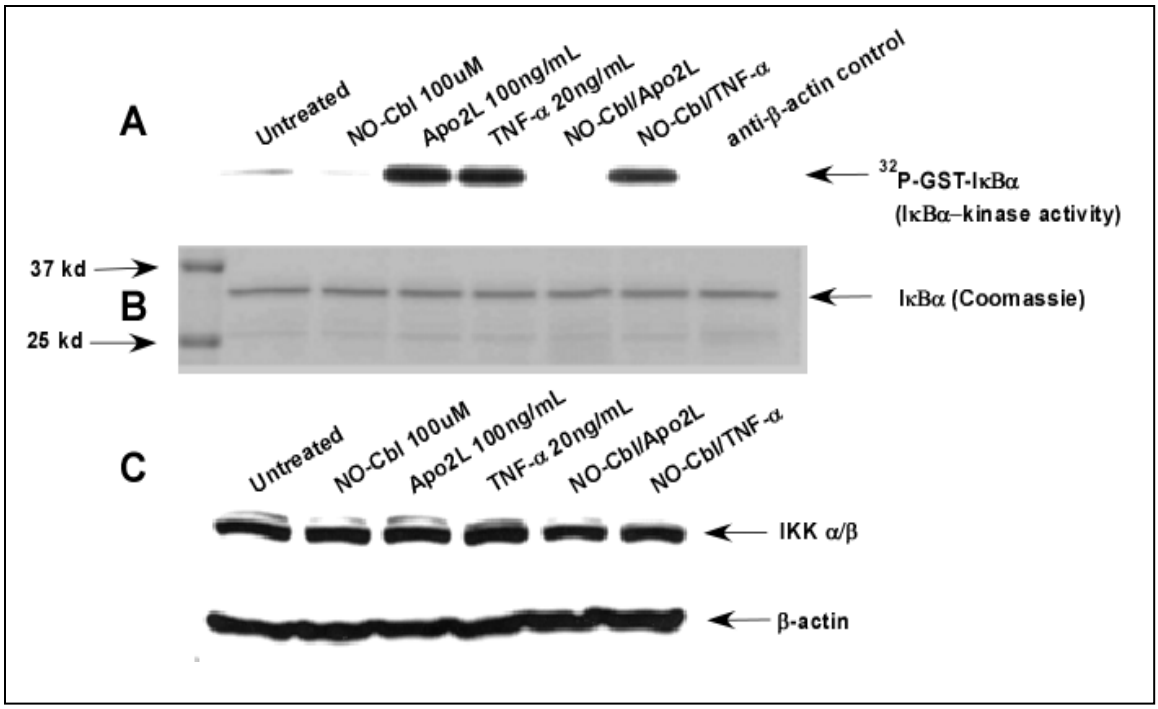

Figure 2.7: IκB kinase (IKK) activity

IKK activity was assessed using recombinant GST-IκBα-(1–54) and [γ-^{32}P]ATP as substrates. The phosphorylated GST fusion protein was detected by autoradiography. **a**, IKK activity was determined in A375 cells pretreated with NO-Cbl followed by Apo2L/TRAIL or TNF-α stimulation for 30 min and 15 min, respectively. NO-Cbl treatment inhibited IKK activity more effectively when Apo2L/TRAIL was the stimulus, compared with stimulation by TNF-α. Anti-β-actin antibody served as the irrelevant antibody with no phosphorylation of GST-IκBα-(1–54) observed. **b**, Coomassie Blue-stained gel shows equal loading of GST-IκBα-(1–54) substrate. **c**, immunoblot analysis shows the presence of equal amounts of total IKK in the lysates. β-actin was used as a loading control.

2.5 DISCUSSION

Induction of apoptosis by exogenous Apo2L/TRAIL requires effective activation of the Apo2L/TRAIL receptors and downstream signaling components. Apo2L/TRAIL as well as the DR4 and DR5 receptors are ubiquitously expressed in malignant cells. Moreover, sensitivity of melanoma cell lines to Apo2L/TRAIL correlated with levels of death receptor expression (Zhang et al., 1999). Cellular resistance to Apo2L/TRAIL may be due to defects in caspase signaling or caspase inhibition rather than over-expression of decoy receptors (Zhang et al., 1999). Defects in Apo2L/TRAIL gene induction as well as overexpression of inhibitors of apoptosis (such as XIAP) in melanoma cell lines which express Apo2L/TRAIL receptors, may account for resistance to Apo2L/TRAIL (Chawla-Sarkar et al., 2001; Chawla-Sarkar et al., 2002). Additionally, Apo2L/TRAIL resistance has been reported in nasopharyngeal carcinomas due to a homozygous deletion of DR4 (Ozoren et al., 2000). Conversely, enhanced survival signaling may also confer a growth advantage. Certain renal cell carcinomas may be resistant to Apo2L/TRAIL as a result of constitutively activated NF-κB (Oya et al., 2001). Also, constitutive activation of Akt/protein kinase B in melanomas increased basal NF-κB activity (Dhawan et al., 2002).

It has been demonstrated that IFN-β treatment increased expression of endogenous Apo2L/TRAIL and thus sensitized melanoma lines to the anti-tumor effects of exogenously administered recombinant Apo2L/TRAIL (Chawla-Sarkar et al., 2002). IFN-β did not alter the DNA binding activity of NF-κB in melanoma cells (Chawla-Sarkar et al., 2002). Previously it has been demonstrated that the anti-tumor effects of IFN-β and NO-Cbl were synergistic *in vitro* and *in vivo* (Bauer et al., 2002). Treatment with NO-Cbl

increased the expression of Apo2L/TRAIL, DR4, and DR5 mRNAs, and caspase-8 enzymatic activity, indicating activation of the extrinsic apoptotic pathway (Bauer et al., 2002). Thus, IFN-β mediates anti-growth effects in melanoma by enhancing Apo2L/TRAIL expression, rather than by inhibiting NF-κB activation.

In the current study we have shown that the anti-tumor activity of NO-Cbl was mediated in part by inhibition of NF-κB activation. NO-Cbl inhibited IKK enzymatic activity, preventing phosphorylation of IκB in response to Apo2L/TRAIL. Remarkably, NO-Cbl was more effective at inhibition of Apo2L/TRAIL-induced IKK activity compared with activation by TNF-α. We hypothesize that NO-Cbl may nitrosylate and deactivate a component of the Apo2L/TRAIL pathway that is absent from the TNF-α pathway. This functional divergence is under active investigation.

NO can inhibit NF-κB by nitrosylating critical cysteine residues (DelaTorre et al., 1997; Marshall and Stamler, 2001; Matthews et al., 1996). Interestingly, prostaglandins (PGA_1 and $15dPGJ_2$) can inhibit IKK by covalently modifying a critical cysteine residue (C179) within the activation loop (Rossi et al., 2000). In a similar manner, NO-Cbl may inhibit IKK, or an IKK-related kinase which is critical for Apo2L/TRAIL signaling, but is less important for TNF-α signaling.

Although SNAP and NOC-18 can inhibit NF-κB signaling, these NO donors release NO indiscriminately and completely lack any tumor specificity. High concentrations of the NO donor sodium nitroprusside (SNP, 1 mM) in combination with Apo2L/TRAIL was effective at killing human colorectal carcinoma cells (Lee et al., 2001). The combination of SNP and Apo2L/TRAIL activated caspase-8, caspase-3, and cytochrome *c* release, which were blocked by Bcl-2, suggesting that SNP-induced apoptosis was

mediated by the mitochondrial pathway. The combination of SNP and Apo2L/TRAIL is active against hematologic malignancies (Secchiero et al., 2001). Similarly, another NO donor, glycerol trinitrate (GTN) induced Apo2L/TRAIL mRNA in human leukemia cells and demonstrated antitumor activity (Chlichlia et al., 1998). However, most conventional NO donors, especially those with short half-lives such as GTN, SNP, and SNAP, induce significant toxicity to normal cells due to spontaneous NO release (Volk et al., 1995; Wink et al., 1996), a drawback to their use.

A major advantage of the pro-drug NO-Cbl is its tumor-specific accumulation. Cobalamin (Cbl) is avidly taken up by tumor cells relative to most normal tissues (Collins et al., 2000; Cooperman, 1960; Flodh and Ullberg, 1968). Unlike other nitric oxide donors, NO-Cbl releases NO inside the cell, and therefore minimizes systemic toxicity as a result of high plasma NO concentration. By taking advantage of the "Trojan Horse" properties of NO-Cbl, adverse side effects such as inappropriate vasodilation can be minimized. NO-Cbl is relatively tumor-specific due to higher transcobalamin receptor (TCII-R) expression in tumor cells compared with normal tissues. Fibroblasts and non-tumorigenic cell lines were quite resistant to NO-Cbl (ID_{50} of 85–250 μM) compared with tumor cell lines (ID_{50} as low as 2 μM) (Bauer et al., 2002). Drug schedule is a critical determinant of the anti-tumor activity of NO-Cbl. NO-Cbl pretreatment followed by Apo2L/TRAIL was most effective, whereas the converse treatment, or even simultaneous co-treatment, was less effective. NO-Cbl inhibits the NF-κB pro-survival arm of Apo2L/TRAIL signaling, allowing the apoptotic arm to proceed unopposed. We believe the combined tumor specific properties of NO-Cbl and Apo2L/TRAIL represent an improved targeted approach to anti-tumor therapy.

Published in: *The Journal of Biological Chemistry*, Vol. 278, No. 41, Issue of October 10, pp. 39461-39469, 2003.
Chawla-Sarkar M., Bauer J.A., Lupica J.A., Morrison B.H., Tang Z., Oates R.K., Almasan A., DiDonato J.A., Borden E.C., Lindner D.J.

CHAPTER III

NITROSYLCOBALAMIN POTENTIATES THE ANTI-NEOPLASTIC EFFECTS OF CHEMOTHERAPEUTIC AGENTS VIA SUPPRESSION OF SURVIAL SIGNALING

3.0 ABSTRACT

Nitrosylcobalamin (NO-Cbl) is a chemotherapeutic pro-drug derived from vitamin B12 that preferentially delivers nitric oxide (NO) to tumor cells, based upon increased receptor expression. NO-Cbl induces Apo2L/TRAIL-mediated apoptosis and inhibits survival signaling in a variety of malignant cell lines. Chemotherapeutic agents often simultaneously induce an apoptotic signal and activation of NF-κB, which has the undesired effect of promoting cell survival. The specific aims of this study were to 1) measure the anti-tumor effects of NO-Cbl alone and in combination with conventional chemotherapeutic agents, and to 2) examine the mechanism of action of NO-Cbl as a single agent and in combination therapy. Using anti-proliferative assays, electrophoretic mobility shift assay (EMSA), immunoblot analysis and kinase assays, we demonstrate an increase in the effectiveness of chemotherapeutic agents in combination with NO-Cbl as a result of suppressed NF-κB activation. Eighteen chemotherapeutic agents were tested in combination with NO-Cbl, in thirteen malignant cell lines, resulting in a synergistic anti-

proliferative effect in 78% of the combinations tested. NO-Cbl pre-treatment resulted in decreased NF-κB DNA binding activity, inhibition of IκB kinase (IKK) enzymatic activity, decreased AKT activation, increased caspase-8 and PARP cleavage, and decreased cellular XIAP protein levels. The use of NO-Cbl to inhibit survival signaling may enhance drug efficacy by preventing concomitant activation of NF-κB or AKT.

3.1 INTRODUCTION

A major obstacle to conventional chemotherapy is the unwanted activation of survival signaling which leads to acquired resistance and decreased therapeutic efficacy. Nuclear factor kappa-B (NF-κB) (Baldwin, 2001) and Akt (Kim and Chung, 2002) are critical mediators of cell survival that are activated following chemotherapy.

NF-κB is a family of heterodimers: NF-κB1 (p50/p105), NF-κB2 (p52/p100), REL, RELA (p65/NF-κB3) in mammals, Dorsal, Dif, and Relish in Drosophilia (Karin et al., 1999a). In its quiescent state, NF-κB is complexed to the inhibitor of κB (IκB) in the cytoplasm. Once phosphorylated , IκB is ubiquitinated and targeted for proteolysis as it remains complexed to NF-κB(DiDonato et al., 1995a). Within the proteosome IκB is degraded, while NF-κB is not, allowing NF-κB to translocate to the nucleus where it binds to NF-κB response elements which activate transcription of target genes (Karin et al., 1999b). NF-κB activation is mediated by kinase cascades that activate IκB kinase (IKK) which is comprised of the subunits IKKα, IKKβ, IKKγ and function to initiate the signal for degradation of IκB[3], (Wang et al., 1999).

Constitutive activation of NF-κB has been implicated in the development of chemo-resistance in several human carcinoma cell lines (Das and White, 1997; Wang et al., 1999; Weldon et al., 2001). Low dose doxorubicin can induce drug resistance in cervical

carcinoma cells(Yeh et al., 2003). Human breast cancer specimens contain high levels of NF-κB/RelA indicating constitutive NF-κB activation (Sovak et al., 1997). High levels of NF-κB and its downstream induced anti-apoptotic genes, bcl-2 and bax correlated with poor response in numerous breast cancer patients (Buchholz et al., 2005). Constitutive NF-κB activity is increased in colorectal cancer (Lind et al., 2001) and effective treatment is achieved by inhibiting NF-κB (Hochwald et al., 2003). Inhibitor of Kappa B Kinase (IKK), an activator of NF-κB, has been shown to be constitutively active in some prostate carcinoma cell lines (Gasparian et al., 2002). Inhibition of NF-κB increased the efficacy of a variety of chemotherapeutic agents including paclitaxel, etoposide, doxorubicin, cisplatin, 5-FU, irinotecan, CPT-11, and camptothecin (Arlt et al., 2001; Bava et al., 2005; Mabuchi et al., 2004a; Mabuchi et al., 2004b; Uetsuka et al., 2003) thereby potentiating apoptosis. Similarly, inhibition of AKT can enhance anti-tumor activity of paclitaxel against cervical carcinomas (Bava et al., 2005).

Akt, a serine/threonine kinase that mediates survival signaling, functions as an oncogene and is implicated in resistance to chemotherapy (Khwaja, 1999). AKT1 kinase was found to be elevated in the majority of primary prostate, breast and ovarian carcinomas examined and correlated with high grade and stage of disease (Sun et al., 2001). AKT2 was up-regulated in human ovarian (Cheng et al., 1992) and breast carcinomas (Yuan et al., 2003) and was associated with paclitaxel (Kim et al., 2007) and cisplatin resistance (Yuan et al., 2003). In addition, decreased activation of AKT via inhibition of phosphoinositide-3-kinase (PI3K) resulted in increased apoptosis of ovarian cancer cells (Yuan et al., 2000). AKT phosphorylates X-linked inhibitor of apoptosis (XIAP) thereby promoting cell survival (Dan et al., 2004). Thus, NF-κB and AKT-

mediated survival signaling limit the apoptotic-potential of chemotherapeutic agents suggesting that inhibitors of these pathways can suppress drug resistance and improve therapeutic efficacy.

We have previously demonstrated the anti-tumor activity of nitrosylcobalamin (NO-Cbl) as a single agent and in combination with biological therapies such as IFN-β (Bauer et al., 2002) and Apo2L/TRAIL (Chawla-Sarkar et al., 2003). NO-Cbl is a vitamin B12 based, nitric oxide donor, that functions as a biological "Trojan Horse" targeting cancer cells via vitamin B12 receptor (Transcobalamin II receptor, TCIIR) (Seetharam et al., 1999; Seetharam and Li, 2000) mediated uptake (Bauer et al., 2002) similar to clinical studies that target TCIIR in the detection of cancer (Collins and Hogenkamp, 1997; Collins et al., 2000).

We have previously shown that NO-Cbl suppressed Apo2L/TRAIL- and TNF-α-mediated IKK activation with subsequent decreased phosphorylation of IκBα and inhibition of NF-κB DNA binding activity(Chawla-Sarkar et al., 2003). NO-Cbl sensitized Apo2L/TRAIL-resistant cells to Apo2L/TRAIL-mediated cell death(Chawla-Sarkar et al., 2003). We have determined that NO-Cbl mediated apoptosis caused in part via activation of the death receptor 4 (DR4) by S-nitrosylation (Tang et al., 2006). DR4 mediated apoptosis is tumor specific because Apo2L/TRAIL is overexpressed on the surface of tumors but not on normal tissues such as liver or kidney (Ashkenazi et al., 1999). Thus, NO-Cbl is a promising candidate to promote apoptosis and minimize toxicity in combination chemotherapy. In the current study, we examined whether NO-Cbl pre-treatment could potentiate the anti-tumor effects of several chemotherapeutic agents.

3.2 MATERIALS AND METHODS

3.2.1 Synthesis of Nitrosylcobalamin

Nitrosylcobalamin was synthesized as previously described (Bauer, 1998). Hydroxocobalamin (vitamin B12a) acetate (Hebei Huarong Pharmaceutical Co, Hebei Province, China) was dissolved in dichloromethane (OmniSolv, EMD Chemicals, Gibbstown, NJ) and exposed to CP grade NO gas (Praxair, Wickliff, OH) at 75 psi. The reaction proceeds in a closed system within a high-pressure stainless steel reactor (Parr Instrument Co, Moline, IL). The system was purged daily and evacuated prior to NO exposure. The NO gas was scrubbed prior to entering the system using a stainless steel cylinder (Midwest Process Controls, Bay Village, OH) containing NaOH pellets. The solid NO-Cbl product was collected following rotary evaporation of the solvent and stored under argon at −80°C prior to use.

3.2.2 Cell Culture and Cytokine treatments

Human tumor cell lines (ATCC, Manassas, VA) were grown in RPMI 1640 and Dulbecco's modified Eagle medium as appropriate (DMEM, Cellgro, Mediatech Herndon, VA) supplemented with 10% fetal bovine serum (FBS, Mediatech) and 1% Antibiotic-Antimycotic (GIBCO BRL, Invitrogen, Carlsbad, CA) according to ATCC recommendations. Cells were maintained in 5% CO_2 at 37°C in a humidified incubator. Cells were confirmed as mycoplasma free using a commercially available kit (MycoAlert, Cambrex Corporation, East Rutherford, NJ).

3.2.3 Sulforhodamine B Cell Growth Assay

Cells were harvested with 0.5% trypsin/0.53 mM EDTA, washed with PBS and resuspended in media containing 10% FBS. Cells were plated in 96-well plates in 0.2 mL aliquots containing 2,000 cells. Cells were allowed to adhere to the plate for 4 h and then NO-Cbl was added in different dilutions to the assay plate. Replicates of eight were performed for each treatment. After 16 h, chemotherapeutic agents were added at different concentrations. Growth was monitored by the sulforhodamine B (SRB, Sigma Chemical, St. Louis, MO) colorimetric assay (Rubinstein et al., 1990; Skehan et al., 1990). After 80 h growth, the medium was removed, and cells were fixed with 10% trichloroacetic acid and stained with SRB. Bound dye was eluted from cells with 10 mM TRIS (pH 10.5) and absorbance was measured at 570 nm using a Lab Systems Multiskan RC 96-well plate reader (Lab Systems Multiscan RC, Thermo Lab Systems, Franklin, MA). To quantify growth of the cells, experimental absorbance values (A_{exp}) were compared with initial absorbance readings representing the starting cell numbers (A_{ini}).

To determine the starting cell number, an additional 96-well plate was seeded with cells and fixed at the beginning of the experiment. The absorbances derived from the initial plate and from the untreated cells at the end of the growth period (A_{fin}) were defined as 0% and 100% growth, respectively. The percentage control growth ($100\% \times [A_{exp} - A_{ini}]/[A_{fin} - A_{ini}]$) was expressed as a percentage of untreated controls.

3.2.4 *In vivo* experiments

Five week-old NCR male athymic nude homozygous *(nu/nu*) mice (Taconic, Germantown, NY) were inoculated with NIH-OVCAR-3 tumors. There were four experimental groups (untreated, single agents, and the combination), n = 10. Tumor cells (2×10^6) were inoculated into flanks in the mid-axillary line. NO-Cbl was given once daily (150 mg/kg, s.c.) and etoposide (2 mg/kg, s.c.) was administered once weekly, starting on day 2. Tumor volume was measured three times a week using the formula for a prolate spheroid: $(4/3)\ \pi ab^2$ where 2a = major axis, 2b = minor axis. Formalin-fixed sections were processed by the Cleveland Clinic Histology Core. Sections were stained with hematoxylin and eosin and evaluated for pathologic changes in a blinded fashion. For syngeneic studies, five week-old DBA/2 male mice (Taconic) were inoculated with P388 murine leukemia cells. There were four experimental groups (untreated, single agents, and the combination), n = 10. Tumor cells (10^5) were inoculated i.p.. NO-Cbl was given twice daily (165 mg/kg, i.p.) and doxorubicin (4 mg/kg, i.p.) was administered once weekly, starting on day 2. Animals were monitored for ninety days. The Institutional Animal Care and Use Committee at the Cleveland Clinic Foundation approved all procedures for animal experimentation.

3.2.5 Gel Electrophoresis and Immunoblot analyses

Cells were pre-treated with NO-Cbl (300 μM) for 16 h followed by doxorubicin (20 μM, 4 h), cisplatin (20 μM, 1 h), 5 flurouracil (5-FU, 100 μM, 5 h), etoposide (20 μM, 4 h), or paclitaxel (20 μM, 5 h). As a positive control for NF-κB induction, cells were treated with TNF-α (20 ng/mL, 15 min). Whole cell lysates were prepared in 1× high salt lysis buffer (20 mM HEPES, 400 mM NaCl, 25 mM β-glycerol phosphate, 25 mM NaF, 10 mM, para-nitrophenyl phosphate (PNPP), 10% glycerol, 0.5 mM NaOrthovanadate, 1mM PMSF, 0.5% NP40 and 1× protease inhibitor cocktail set I (Calbiochem) and 1× phosphatase inhibitor cocktail set II (Calbiochem) for subsequent immunoblotting studies. Total cell protein (80 μg per sample) was resolved by electrophoresis on a 10% Bis-TRIS gel (Criterion, Bio-Rad, Hercules, CA) resolved at 160 V for 1 hour and transferred to a PVDF membrane (Immobilon-P, Millipore, Bedford, MA) with the use of a wet transfer apparatus (Bio-Rad) for 30 min at 100 V . The membranes were incubated in blocking buffer (Starting Block T20, Pierce, Rockford, IL) for 1 h at room temperature and then incubated overnight with primary antibody [anti-phospho-AKT (Ser473) 1:1000, Cell Signaling, Boston, MA; anti-AKT 1:1000, Cell Signaling; anti-XIAP, 1:250-2000, BD Biosciences, San Jose CA; anti-Caspase-8 (1C12) 1:1000 Cell Signaling; anti-PARP 1:1000, Cell Signaling] diluted in Starting Block. After washing in 1× TBST (USB Corp, Cleveland, OH) membranes were incubated with horseradish peroxidase-conjugated goat secondary antibodies (Biorad) diluted in Starting Block for 1 h at room temperature. The protein bands were visualized by enhanced chemiluminescence (SuperSignal West Pico chemiluminescent substrate, Pierce). Antibodies against

glyceraldehyde-3-phosphate dehydrogenase (Trevigen, Gaithersburg, MD) were used to ensure equal loading.

3.2.6 Electrophoretic mobility shift assay (EMSA)

Cells were pre-treated with NO-Cbl (300 μM) for 16 h followed by doxorubicin (20 μM, 4 h) or cisplatin (20 μM, 1 h) or 5 flurouracil (5-FU, 100 μM, 5 h) or etoposide (20 μM, 4 h) or paclitaxel (20 μM, 5 h). As a positive control for NF-κB induction, cells were treated with TNF-α (20 ng/mL, 15 min). Plates were washed three times with ice-cold 1× DPBS (Cellgro, Mediatech). Cells were scraped from plates and resuspended in 1× high salt lysis buffer as above. The lysates were transferred to pre-chilled microcentrifuge tubes and incubated at 4°C using a vortex for 30 min followed by centrifugation at 20,000g for 15 min. Samples were snap frozen with liquid nitrogen and stored at −70°C until needed. Supernatants were transferred to fresh tubes and protein concentrations were assessed using the Bradford method (Bio-RAD protein assay, BioRad, Hercules, and CA). We used a commercially available consensus binding site for NFκB/c-Rel homodimeric and heterodimeric complexes as a probe to assess DNA binding activity. The NF-κB consensus binding sequence (5′AGTTGA**GGCGACTTTCCC**AGGC 3′) (sc-2505: Santa Cruz Biotechnology, Santa Cruz, CA) was end-labeled with γ^{32}P-dATP (3000 Ci/mol, Perkin Elmer, Boston MA), using T4 polynucleotide kinase (Roche, Indianapolis, IN). DNA binding reactions were performed in 28 μL reaction volume for 30 min on ice containing 20 μg protein, 100 mM HEPES, 3.0 mM EDTA, 50% glycerol, 3 mM DTT, 25 mM $MgCl_2$, 20 mM TRIS, pH 7.90, 5 ug Poly [d(I-C)] and labeled probe. Complexes were separated from the free probe on 6% non-denaturing polyacrylamide

gels in 0.5× TBE buffer at 195 V for 2 h. Gels were dried and exposed to film. To verify that the band shifts were comprised of NF-κB, lysates from cells that were stimulated by TNF-α (20 ng/mL, 15 min) were incubated with anti-NF-κB p65 antibody (100 ng/mL, Zymed, S. San Francisco, CA).

3.2.7 IκB kinase (IKK) assay

Whole cell extracts (200 µg) treated as above were supplemented with 150 µL of Buffer A (20 mM Hepes, pH 7.9, 20 mM beta-glycerophosphate, 10 mM NaF, 0.1 mM orthovanadate, 5 mM para-nitrophenyl phosphate (PNPP), 10 mM 2-mercaptoethanol (BME), 0.5 mM PMSF, and protease cocktail), 2 µL normal rabbit serum (NRS), and mixed by rotation at 4°C for 1 h as previously described (DiDonato and John, 2000). A 50% slurry of Protein G Sepharose (80 µL) (Amersham-Pharmacia, Piscataway, NJ) prepared in Buffer A (without BME or PMSF) was added and mixed by rotation at 4°C for 1 h. Protein G Sepharose was removed by centrifugation at 800g for 1 min and discarded. Anti-IKKα monoclonal antibody (0.5 µg, BD-Pharmingen, San Diego, CA), or anti-HA epitope antibody (Covance, Berkeley, CA) was added to the supernatant and mixed by rotation at 4°C for 2 h. A 50% slurry of Protein G Sepharose (60 µL) prepared in Buffer C (Buffer A plus 50 mM NaCl and 10 mM $MgCl_2$, without BME and PMSF) was added and mixed by rotation in the cold for 30 min. Protein G immunopellets were collected by centrifugation at 800 g for 30 sec, washed 3 times with Buffer B (Buffer A plus 250 mM NaCl), and once with Buffer C (Buffer A plus 50 mM NaCl and 10 mM $MgCl_2$). Immunopellets were re-suspended in 30 µL kinase buffer with 0.1 mM orthovanadate, 50 µM unlabeled ATP, 5 µCi γ^{32}P-ATP, 2 mM DTT, and 2 µg of

recombinant GST-IκBα1-54[39] and incubated at 30°C for 30 min. Reactions were stopped by the addition of 15 µL 4× SDS-PAGE loading buffer (200 mM Tris-HCl, pH 6.8, 8% SDS, 40% glycerol, 0.2% 2-mercaptoethanol), heated at 95°C for 10 min, and resolved by SDS-PAGE on a 12% acrylamide gel by standard procedures. Gels were rinsed, stained with Bio-Safe Coomassie (BioRad, Hercules, CA) to visualize protein bands, rinsed, photographed then dried and exposed to Kodak BioMax MR film (Eastman Kodak Co., Rochester, NY) to detect substrate phosphorylation. IKK activation was quantified by PhosphorImage analysis on a Storm-840 imager using Image Quant v 5.2 software (Molecular Dynamics, Amersham Biosciences, and Piscataway, NJ).

3.2.8 Statistical Analysis

Median effect analysis was used to characterize the interaction between NO-Cbl and various chemotherapeutic agents (Chou and Talalay, 1984). A combination index >1 indicates antagonism, = 1 indicates additivity, and <1 indicates synergy. Unless otherwise stated, results are expressed as means with 95% confidence intervals (95% CI). Differences in mean tumor volume between groups were compared using the unpaired two-tailed Student's *t* test, using a pooled estimator of variance, to determine statistical significance using Sigma Plot 10.0 (SPSS, Chicago, IL). The logrank test was used to calculate the significance of the Kaplan Meir survival curve. The experimental design utilized the same set of cell lysates for Figures 2-5, and the data was expressed as means (n = 3).

3.3 RESULTS

3.3.1 Anti-proliferative effects of NO-Cbl and chemotherapeutic agents *in vitro*

To test the hypothesis that NO-Cbl might potentiate the anti-neoplastic effects of various chemotherapeutic agents, we measured antiproliferative effects in thirteen cell lines using 18 chemotherapeutic agents (**Figure 3.1**). We used the SRB antiproliferative assay, which is utilized by the National Cancer Institute to evaluate new chemotherapeutic agents (Skehan et al., 1990). Median effect analysis characterized the interaction between NO-Cbl and the chemotherapeutic agents (Chou and Talalay, 1984). Cells were pre-treated with NO-Cbl for 16 h followed by the chemotherapeutic drugs for 80 h. Sequential treatment of tumor cell lines resulted in synergistic antiproliferative activity in 77.78% of the combinations tested, with a mean combination index of 0.44 (95% CI = 0.39 to 0.50). Antagonistic responses were observed in 22.22% of combinations, with an average combination index of 1.73 (95% CI = 1.33 to 2.12).

FIGURE 3.1

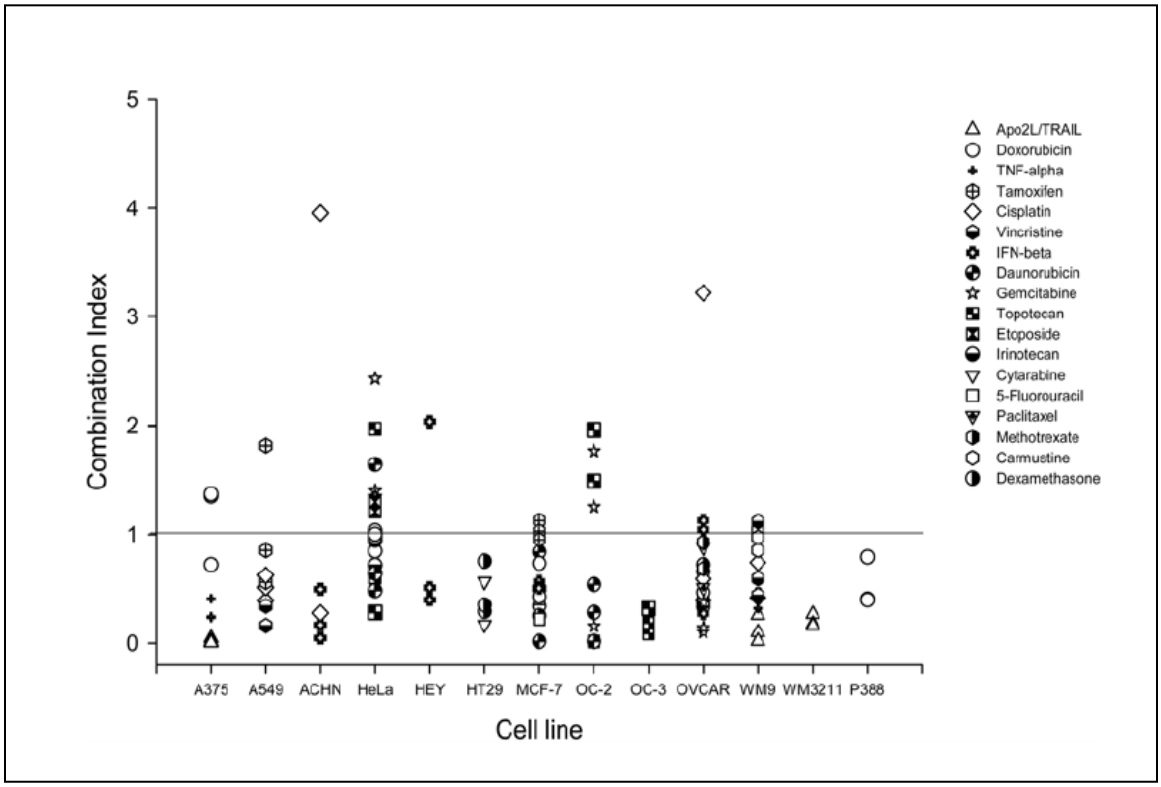

Figure 3.1. Effects of nitrosylcobalamin (NO-Cbl) and chemotherapeutic agents on the proliferation of A375 (melanoma), A549 (lung), ACHN (renal), HeLa (cervical) HEY (ovarian), HT29 (colon), MCF-7 (breast), OC-2 and OC-3 (platinum and paclitaxel refractory ovarian), OVCAR-3 (ovarian), WM9 and WM3211 (melanoma), and P388 (murine leukemia).

Cells were pre-treated with NO-Cbl for 16 h followed by addition of chemotherapeutic agents for five days, and growth was measured by the colorimetric sulforhodamine B assay (Skehan et al., 1990). Data points represent the combination index comparing low, medium, and high combinations of NO-Cbl and each chemotherapeutic agent (mean of eight replicates) to assess synergy. Synergy between NO-Cbl and various chemotherapeutic agents was determined by median effect analysis (Chou and Talalay, 1984), (combination index >1 indicates antagonism, = 1 indicates additivity, and <1 indicates synergy). The sequential treatment of NO-Cbl and chemotherapeutic drugs induced synergistic antiproliferative activity in 77.7% of the combinations examined.

3.3.2 NO-Cbl inhibits activation of NF-κB by chemotherapeutic agents

EMSA was utilized to examine the effects of NO-Cbl on NF-κB activation by chemotherapeutic agents (**Figure 3.2**). We examined four histologically distinct human tumor cell lines [A375 (melanoma), MCF-7 (breast carcinoma), SW480 (colon carcinoma), and OVCAR-3 (ovarian carcinoma)], assaying the effects of multiple chemotherapeutic drugs. TNF-α was used as a positive control for induction of NF-κB DNA binding activity. Specific antibodies to NF-κB-p65 induced a supershift and confirmed the presence of the p65/RelA component of NF-κB.

Doxorubicin treatment resulted in NF-κB activation in all four cell lines. NO-Cbl inhibited NF-κB DNA binding activity in A375 cells by 40.71% (95% CI = 40.52% to 40.87%), MCF-7 cells by 46.99% (95% CI = 46.41% to 47.64%), SW480 cells by 7.52% (95% CI = 5.71% to 9.14%), and OVCAR-3 cells by 40.13% (95% CI = 39.30% to 41.08%).

Cisplatin treatment resulted in low-level NF-κB activation in A375 cells. NO-Cbl inhibited cisplatin-induced activation by 41.54% (95% CI = 40.77% to 42.41%) in A375 cells. Cisplatin did not activate NF-κB in OVCAR-3 cells.

5-FU activated NF-κB in each cell line treated. NO-Cbl inhibited NF-κB activation in A375 cells by 6.89% (95% CI = 6.43% to 7.28%), SW480 cells by 38.14% (95% CI = 34.91% to 40.69%), and OVCAR-3 cells by 18.34% (95% CI = 17.90% to 18.72%).

Etoposide activated NF-κB in A375 and OVCAR-3 cells. Pre-treatment with NO-Cbl inhibited NF-κB DNA binding activity by 29.70% (95% CI = 28.79% to 30.69%) in A375 cells, and 30.37% (95% CI = 30.00% to 30.67%) in OVCAR-3 cells.

Paclitaxel treatment of MCF-7 and OVCAR-3 cells induced NF-κB activation in both cell lines. NO-Cbl inhibited paclitaxel-induced activation by 47.28% (95% CI = 46.23% to 48.43%) and 43.40% (95% CI = 42.48% to 44.47%) respectively, in MCF-7 and OVCAR-3 cells.

FIGURE 3.2

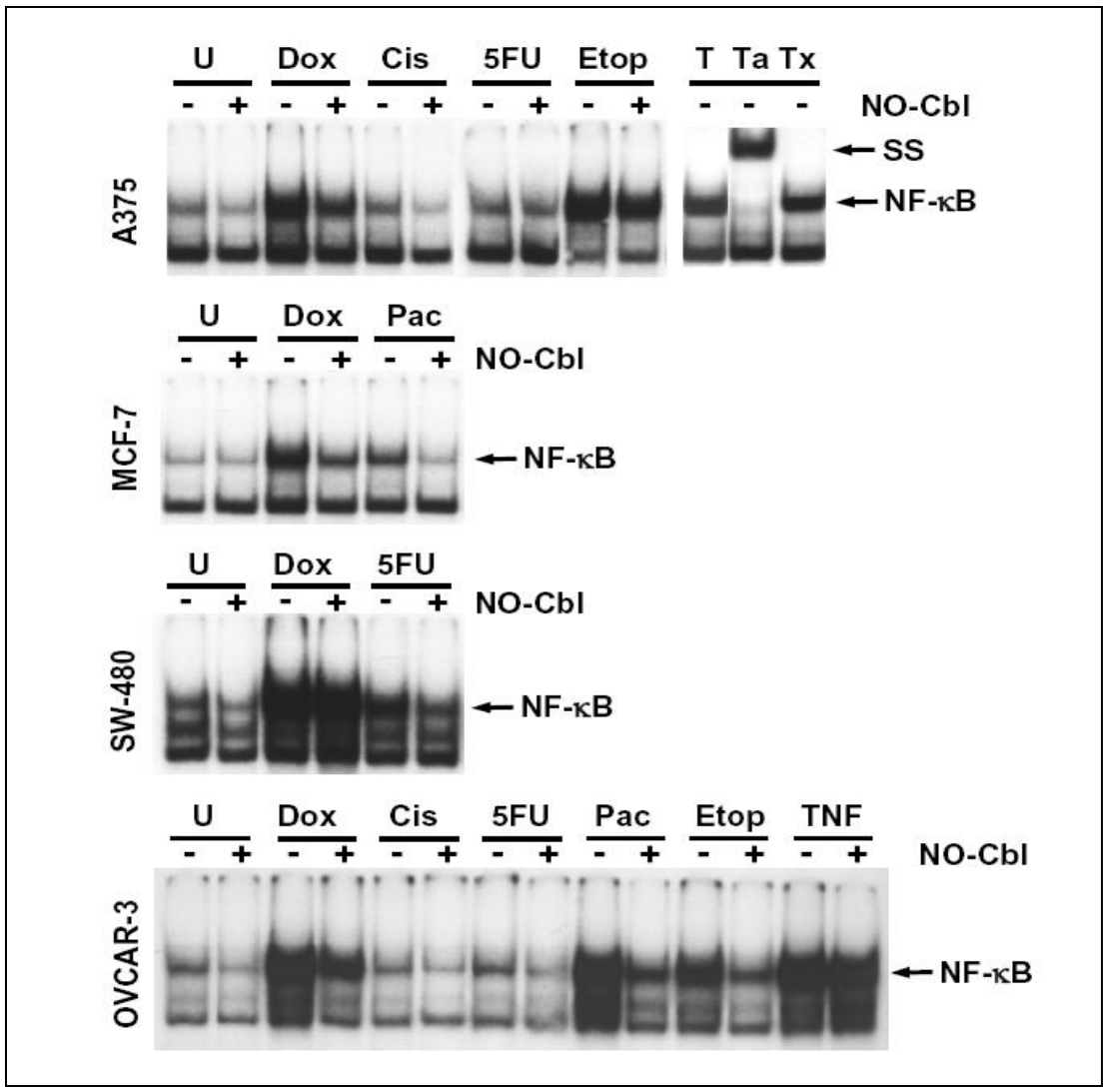

Figure 3.2: Electrophoretic Mobility Shift Assay (EMSA): NF-κB DNA binding activity.

Pretreatment of A375 (melanoma), MCF-7 (breast carcinoma), SW480 (colon carcinoma) and OVCAR-3 (ovarian carcinoma) cells with NO-Cbl (300 µM, 16 h) inhibited the NF-κB DNA binding activity induced by doxorubicin (20 µM, 4 h) or cisplatin (20 µM, 1 h) or 5 flurouracil (5-FU, 100 µM, 5 h) or etoposide (20 µM, 4 h) or paclitaxel (20 µM, 5 h). TNF-α (15 min) stimulation served as a positive control of NF-κB activation (T). Incubation of TNF-α treated lysates with anti-NF-κB p65 antibody resulted in supershift (SS) of the NF-κB complex (Ta). An irrelevant antibody was incubated with TNF-α treated lysates which did not result in a supershift (Tx).

3.3.3 NO-Cbl affects IκB kinase activity

IκB kinase (IKK) mediates phosphorylation of IκBα, marking it for eventual polyubiquitination and proteolysis thereby resulting in NF-κB activation (DiDonato et al., 1997a). Hence, we examined the effect of NO-Cbl upon IKK activity (**Figure 3.3**) using the same lysates used to assess NF-κB DNA binding activity. NO-Cbl treatment reduced basal IKK activity in all treatments, although IKK activity was not noticeably increased in A375 cells following treatment with any of the chemotherapeutic agents.

Doxorubicin activated IKK in MCF-7, SW480 and OVCAR-3 cells. NO-Cbl decreased IKK activity in MCF-7, SW480 and OVCAR-3 cells by 41.70% (95% CI = 39.65% to 44.47%), 45.22% (95% CI = 41.43% to 50.07%) and 50.69% (95% CI = 48.39% to 53.57%), respectively.

Cisplatin treatment resulted in minor activation of IKK only in OVCAR-3 cells. NO-Cbl was effective at inhibiting this activation by 17.06% (95% CI = 15.48% to 19.06%). 5-FU treatment resulted in IKK activation in SW480 and OVCAR-3 cells. NO-Cbl inhibited 5-FU induced IKK activation in SW480 cells by 18.85% (95% CI = 17.20% to 21.05%), and OVCAR-3 cells by 34.12% (95% CI = 31.21% to 37.74%). Paclitaxel did not activate IKK in MCF-7 or OVCAR-3 cells. Treatment of OVCAR-3 cells with etoposide resulted in IKK activation which was inhibited by NO-Cbl by 71% (95% CI = 70.22% to 71.96%).

FIGURE 3.3

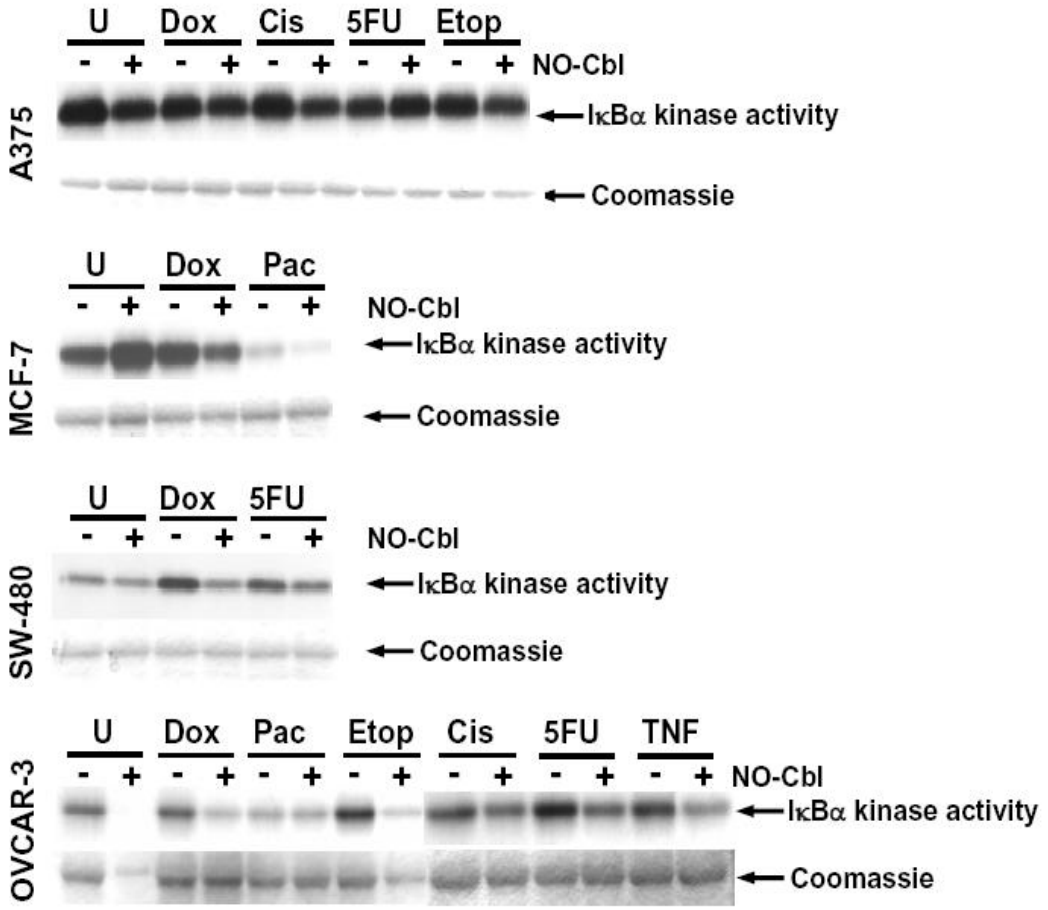

Figure 3.3: IκB kinase (IKK) activity. IKK activity was assessed using recombinant GST-IκBα(1-54) and γ^{32}P-ATP as substrates.

The phosphorylated GST fusion protein was detected by autoradiography. IKK activity was determined in cells that were pre-treated with NO-Cbl (300 µM, 16 h) followed by doxorubicin (20 µM, 4 h) or cisplatin (20 µM, 1 h) or 5 flurouracil (5-FU, 100 µM, 5 h) or etoposide (20 µM, 4 h) or paclitaxel (20 µM, 5 h). Anti-β-actin antibody was used as an irrelevant antibody control for immunoprecipitation and yielded no signal. After exposure to film, the gel was stained with Coomassie blue to visualize total protein and demonstrated equal loading of the GST-IκBα(1-54) substrate. The same cell extracts were probed for total IKK by immunoblot analysis and demonstrated equal loading of IKK.

3.3.4 Inhibition of AKT activation by NO-Cbl

Next we examined the role of the pro-survival protein AKT and the effects of NO-Cbl on its activation (**Figure 3.4**), using the same lysates utilized in the previous two experiments. In A375 cells, phosphorylation of AKT was enhanced following treatment by cisplatin, 5-FU and etoposide. NO-Cbl inhibited AKT activation following cisplatin treatment by 51.24% (95% CI = 50.73% to 51.73%), 5-FU by 42.82% (95% CI = 39.84% to 47.26%), and with etoposide by 46.85% (95% CI = 44.00% to 49.32%).

Doxorubicin increased the phosphorylation of AKT in MCF-7 and SW480 cells which was inhibited by NO-Cbl by 83.77% (95% CI = 81.43% to 86.21%) and 52.60% (95% CI = 49.62% to 55.04%), respectively. Treatment of MCF-7 cells with paclitaxel resulted in increased phosphorylation of AKT which was inhibited by 43.74% (95% CI = 42.01% to 45.00%) following NO-Cbl. Treatment of SW480 cells with 5-FU increased AKT activation which was inhibited by NO-Cbl by 32.50% (95% CI = 31.28% to 33.61%). Although increased phosphorylation of AKT did not occur with any of the chemotherapeutic agents in OVCAR-3 cells, which exhibited a high basal level of phosphorylated AKT, NO-Cbl reduced the high basal AKT phosphorylation levels.

FIGURE 3.4

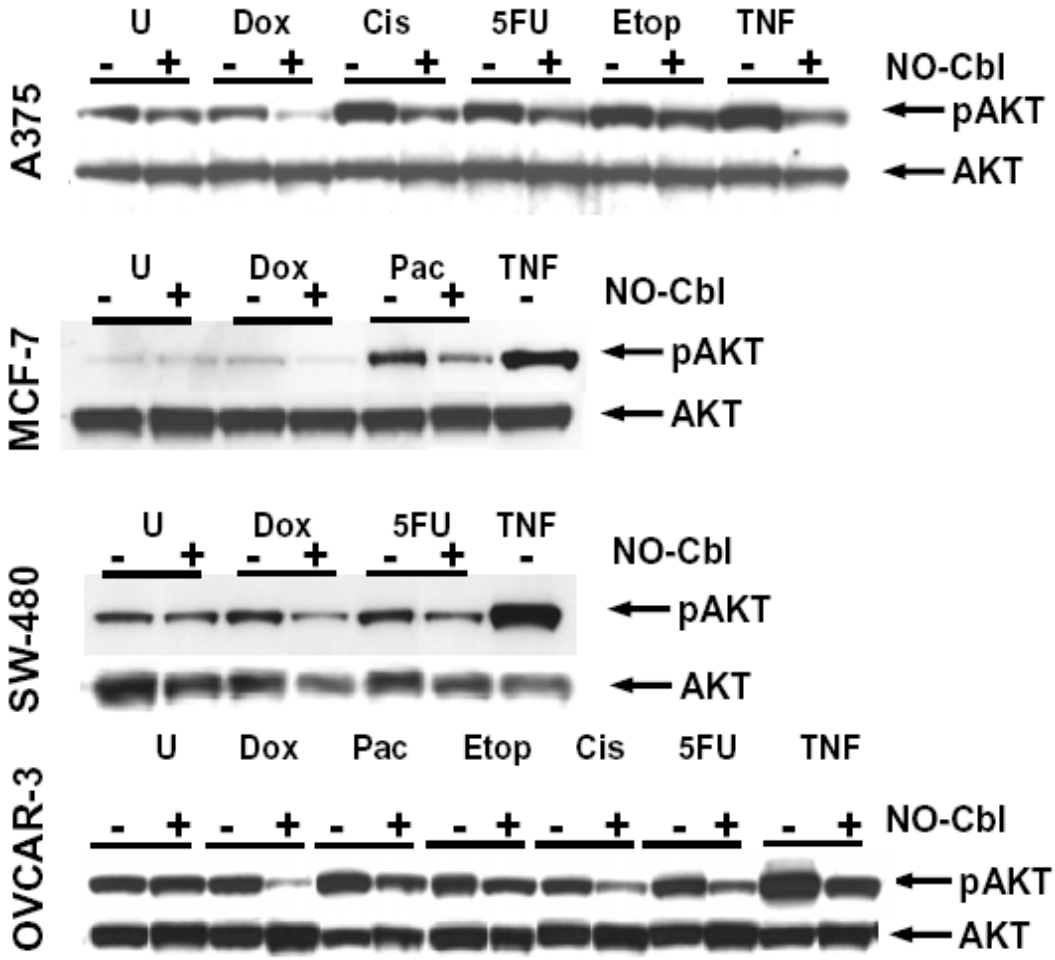

Figure 3.4: Western blot analysis of phospho-AKT.

Cells were pre-treated with NO-Cbl (300 µM, 16 h) followed by doxorubicin (20 µM, 4 h) or cisplatin (20 µM, 1 h) or 5 flurouracil (5-FU, 100 µM, 5 h) or etoposide (20 µM, 4 h) or paclitaxel (20 µM, 5 h). Whole cell lysates were probed with anti-phospho-AKT and then re-probed with anti-AKT (unphosphorylated) which served as a loading control.

3.3.5 XIAP expression is decreased with NO-Cbl treatment

X-linked mammalian inhibitor of apoptosis (XIAP), one of the most potent inhibitors of apoptosis, is a NF-κB-induced gene (Salvesen and Duckett, 2002).

Hence we examined effects of NO-Cbl upon downstream gene products induced by NF-κB (**Figure 3.5**).

Consistent with AKT phosphorylation in A375 cells, XIAP protein expression was enhanced following doxorubicin, cisplatin, 5-FU, and etoposide treatment. NO-Cbl blunted XIAP expression by 20.12% (95% CI = 14.64% to 23.79%) with doxorubicin, 19.40% (95% CI = 17.06% to 22.00%) with cisplatin, 21.12% (95% CI = 20.89% to 21.31%) with 5-FU, and 18.62% (95% CI = 17.57% to 20.09%) with etoposide.

In addition, doxorubicin increased XIAP expression in MCF-7, SW480, and OVCAR-3 cells; expression was inhibited with NO-Cbl treatment by 44.96% (95% CI = 39.66% to 47.85%), 12.16% (95% CI = 10.57% to 13.79%), and 64.90% (95% CI = 60.46% to 66.85%), respectively. 5-FU treatment increased XIAP expression in SW480 cells which was inhibited with NO-Cbl by 13.66% (95% CI = 11.87% to 15.75%). NO-Cbl treatment inhibited basal XIAP expression when combined with every chemotherapeutic agent in all cell lines examined.

FIGURE 3.5

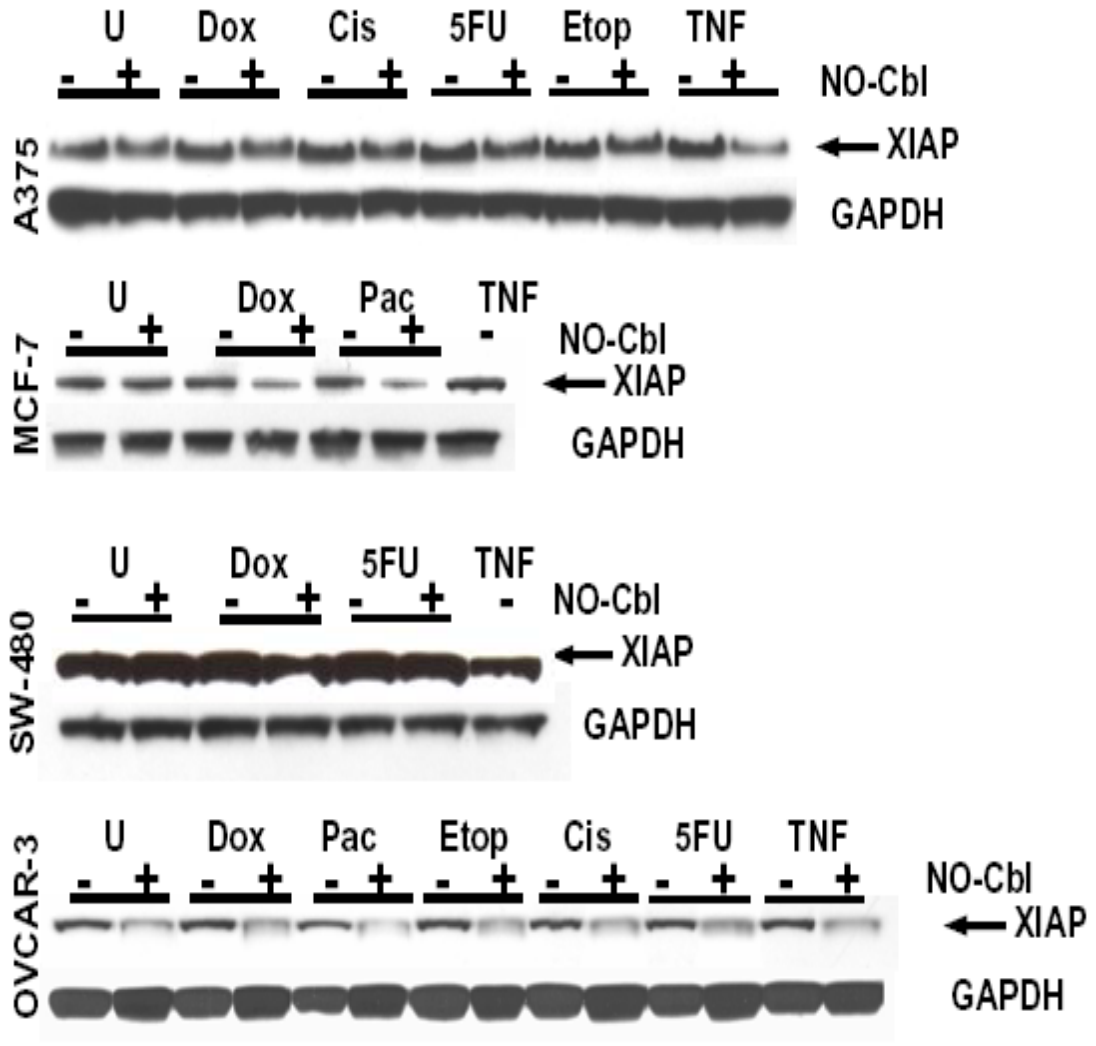

Figure 3.5: Western blot analysis of XIAP.

Cells were pre-treated with NO-Cbl (300 µM, 16 h) followed by doxorubicin (20 µM, 4 h) or cisplatin (20 µM, 1 h) or 5 flurouracil (5-FU, 100 µM, 5 h) or etoposide (20 µM, 4 h) or paclitaxel (20 µM, 5 h). XIAP protein levels were determined in whole cell lysates. GAPDH was used as a loading control.

3.3.6 Effect of NO-Cbl on mediators of apoptosis

A375 cells were stimulated with doxorubicin, followed by assessment of AKT phosphorylation, XIAP expression, and caspase-8 and PARP cleavage. (**Figure 3.6a**). NO-Cbl inhibited doxorubicin-mediated AKT activation at all time points, resulting in reduction of 85.73% (95% CI = 85.26% to 86.24%) at 8 h, 94.05% (95% CI = 92.44% to 96.02%) at 12 h, 60.94% (95% CI = 58.93% to 63.73%) at 16 h, and completely abrogated the signal at 24 h. In addition, degradation of XIAP was enhanced when NO-Cbl was combined with doxorubicin; this inhibition was 82.94% (95% CI = 81.27% to 84.14%) at 8 h, 49.36% (95% CI = 41.51% to 58.74%) at 12 h, 64.67% (95% CI = 60.68% to 67.69%) at 16 h, and 35.81% (95% CI = 33.93% to 36.54%) at 24 h.

Concordantly, caspase-8 activity was enhanced when NO-Cbl was combined with doxorubicin at 8, 12, 16 and 24 h by 41.39% (95% CI = 27.98% to 47.95%), 36.82% (95% CI = 32.79% to 39.87%), 17.54% (95% CI = 12.22% to 23.98%), and 25.28% (95% CI = 7.88% to 34.92%), respectively. PARP cleavage was increased at all time points following treatment with NO-Cbl and doxorubicin. NO-Cbl enhanced the cleavage of PARP by 82.94% (95% CI = 81.27% to 84.14%) at 8 h, 49.36% (95% CI = 41.51% to 58.74%) at 12 h, 64.67% (95% CI = 60.68% to 67.69%) at 16 h, and by 35.81% (95% CI = 33.93% to 36.54%) at 24 h.

Next, we examined the expression of XIAP in OVCAR-3 cells treated with etoposide and NO-Cbl (**Figure 3.6b**). Expression of XIAP protein, normally induced by etoposide, was reduced by NO-Cbl at 8, 12, and 16 h by 92.82% (95% CI = 89.60% to 97.78%), 8.57% (95% CI = 70.12% to 89.26%), and 98.59% (95% CI = 96.71% to 100%), respectively. After 24 h of NO-Cbl treatment, XIAP protein was undetectable.

FIGURE 3.6

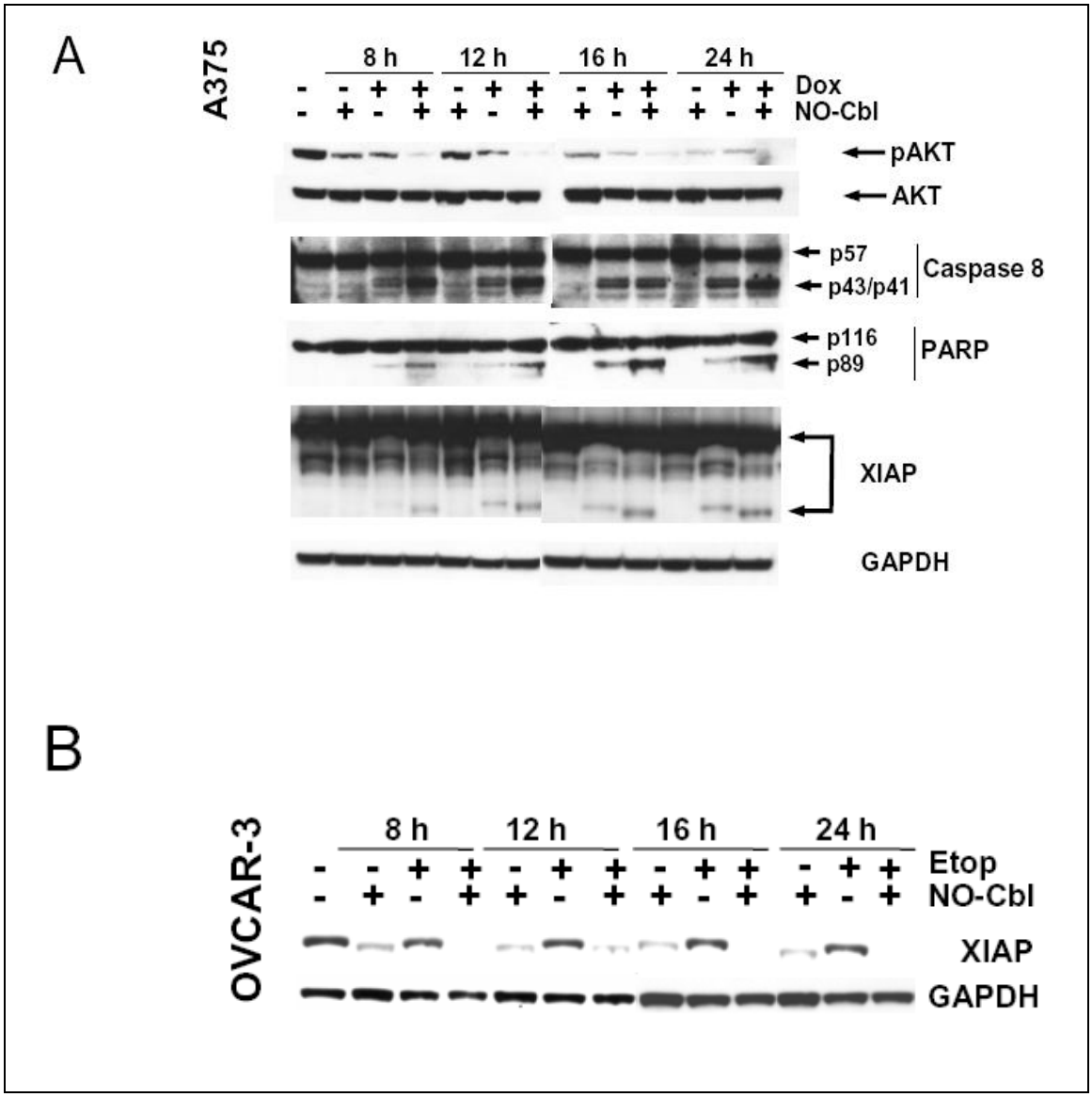

Figure 3.6: Western blot analysis of mediators of apoptosis.

a, Time course analysis of A375 cells pre-treated with NO-Cbl (300 µM, 16 h) followed by doxorubicin (20 µM, 4 h). Phospho-AKT, XIAP, caspase-8 and PARP immunoblots were performed on whole cell lysates. Note that caspase-8 and PARP cleavage were maximal with combination treatment at all time points. Degradation of XIAP was increased following combination treatment at all time points. **b**, OVCAR-3 cells were pre-treated with NO-Cbl (300 µM, 16 h) followed by etoposide (20 µM, 4 h). XIAP protein levels were determined. GAPDH was used as a loading control.

3.3.7 Anti-tumor effects of NO-Cbl and chemotherapeutic agents *in vivo*

In vitro combination therapy with NO-Cbl on tumor cells in culture exhibited positive effects in inhibiting cell proliferation and decreasing cell survival signaling (**Figs. 3.1–3.6**). To test drug combinations *in vivo*, subcutaneous NIH-OVCAR-3 xenografts were established in athymic nude mice. Daily drug treatments began on day 2 after cell inoculation, at which time tumors were both visible and palpable (**Figure 3.7a**). After 25 days, the tumors from mice treated with NO-Cbl were reduced in volume by 66.94% (95% CI = 60.90% to 69.81%; $P = 0.00068$) compared to controls. Tumors from mice treated with etoposide were smaller by 27.30% (95% CI = 19.70% to 30.90%; $P = 0.14099$) compared to control tumors. Mice receiving the combination of NO-Cbl and etoposide displayed tumors that were inhibited by 99.01% (95% CI = 98.48% to 100.12%; $P = .000012$) compared to controls. In two mice, tumors disappeared completely and did not recur 60 days after treatment cessation.

In a syngeneic P388 murine leukemia model, cells were inoculated into the peritoneal cavities of DBA/2 mice. Daily drug treatments began on day 2 following inoculation (**Figure 3.7b**). Untreated animals died by day 14. NO-Cbl treated animals survived until day 21. Doxorubicin treated animals survived until day 33. Combination drug treatment was discontinued on day 40 and resulted in 60% survival, monitored through day 90. Logrank analysis determined $P<0.001$ comparing Kaplan Meier survival curves.

FIGURE 3.7

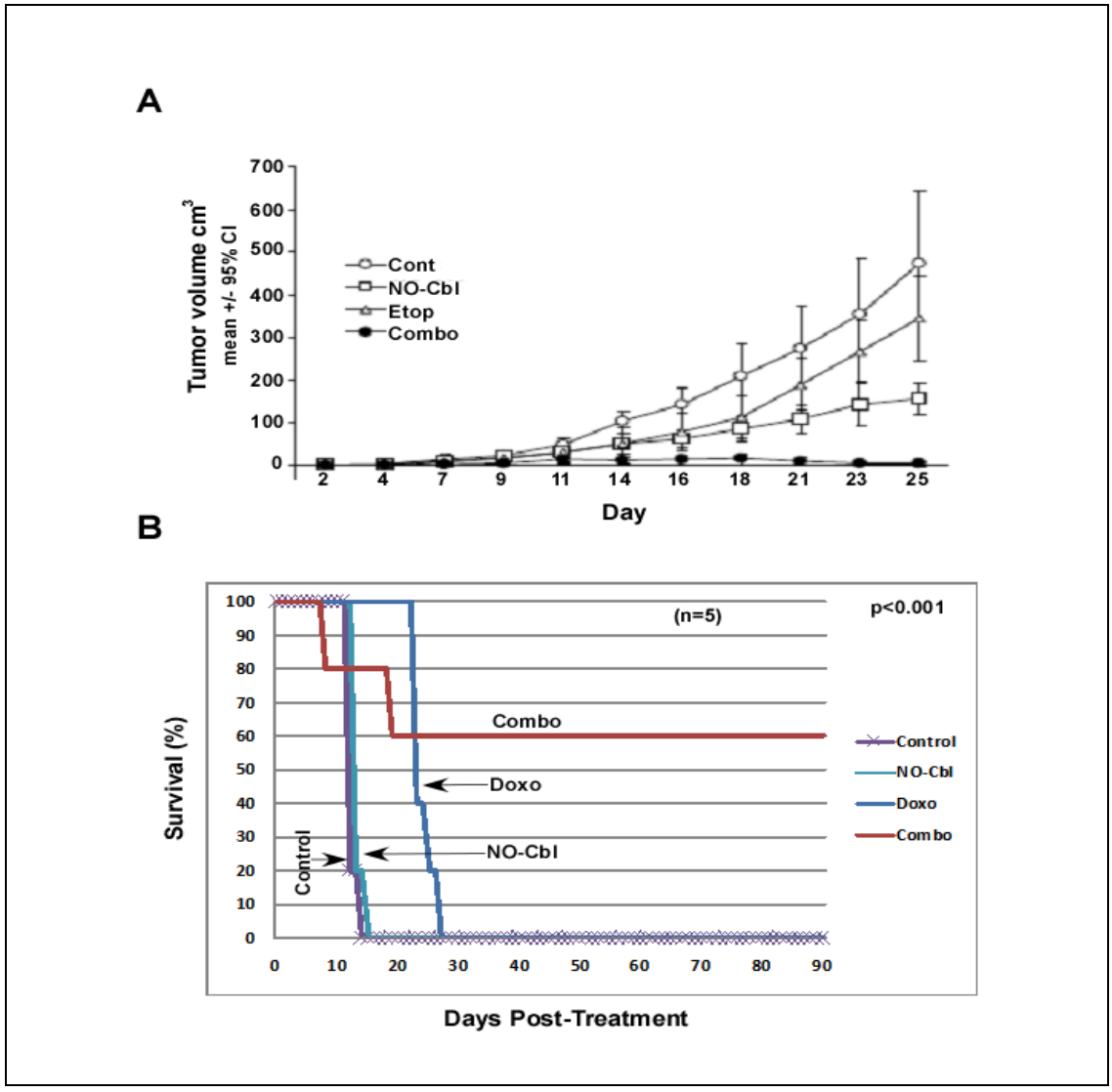

Figure 3.7: Effects of NO-Cbl and chemotherapeutic agents *in vivo.*

a, NCR male athymic nude (nu/nu) mice (*n* = 10 per group) were injected subcutaneously (s.c.) with 2×10^6 NIH-OVCAR-3 cells. Daily drug treatments of control (PBS), NO-Cbl (150 mg/kg, s.c.), etoposide (2 mg/kg, s.c.), and the combination began on day 2 following inoculation. Tumor volume was measured every other day. Points represent the mean tumor volume±95% CI. **b**, Kaplan-Meir survival curve. DBA/2 male mice (n = 5) were inoculated intraperitoneally (i.p.) with 10^5 P388 murine leukemia cells. NO-Cbl was given twice daily (165 mg/kg, i.p.) and doxorubicin (4 mg/kg, i.p.) was administered once weekly, starting on day 2. Treatment in the combination group ceased on day 40 and the animals continued to be monitored for ninety days. Significance comparing the survival of groups was calculated using the logrank test.

3.4 DISCUSSION

Nitric oxide (NO) is a ubiquitous multi-faceted signaling molecule critical to many physiological and pathological processes (Ray et al., 2007). A comprehensive review by Mocellin et al. details the use of NO donors to induce apoptosis (Mocellin et al., 2007). The connection between NO donors and apoptosis often seems paradoxic and depends upon cell type, site of delivery, and NO concentration. However, it is widely accepted that high levels of NO (>1 μM) can activate the extrinsic pathway of programmed cell death via protein nitrosylation (Mannick and Schonhoff, 2004; Tang et al., 2006) and can also activate the intrinsic pathway via oxidative stress and cytochrome c release (Murphy, 1999). Most conventional NO donors, especially those with short half-lives such as GTN, SNP and SNAP, induce significant toxicity to normal cells due to rapid NO release in biological fluids (Volk et al., 1995; Wink et al., 1996) a drawback to their use.

A major advantage of the pro-drug NO-Cbl is its tumor-specific accumulation due to higher transcobalamin receptor (TCII-R) expression in tumor cells compared to normal tissues (Bauer et al., 2002). Cobalamin (Cbl) is avidly taken up by tumor cells relative to most normal tissues (Collins et al., 2000; Cooperman, 1960; Flodh and Ullberg, 1968) Unlike other donors, NO-Cbl preferentially releases NO inside the cell, and therefore minimizes systemic toxicity due to high plasma NO concentration. By taking advantage of the "Trojan Horse" properties of NO-Cbl, side effects such as vasodilation can be minimized. We have not observed hypotension, bone marrow suppression or abnormal liver or kidney function in our rodent or canine studies following acute or chronic NO-Cbl administration (data not shown).

NO inhibits survival signaling via inhibition of NF-κB (Marshall and Stamler, 2001; Matthews et al., 1996) and AKT (Storling et al., 2005), both well characterized mediators of cell survival. A recent review by Nakanishi and Toi implicates NF-κB activation as a major contributor to lowering the apoptotic efficacy of chemotherapeutic agents and increasing drug resistance (Nakanishi and Toi, 2005).

The activation of NF-κB is a highly complex process. There are cell type-specific variations in NF-κB activation that differ between cell lines as well as activation differences among known NF-κB-activators. Taxol treatment of pancreatic cancer cell lines induces formation of several different NF-κB/IκB complexes, suggesting the presence of multiple up-stream activators of NF-κB (Dong et al., 2002). UV-induced DNA damage in HeLa cells is characterized by IKK-independent activation of NF-κB at early time points (30 min) and IKK-dependent activation at later times (15–20 h) (Bender et al., 1998). Doxorubicin initiates phosphoinositide-3-kinase (PI3K)-mediated degradation of IκB that is independent of the IKK signalosome (Tergaonkar et al., 2003). Conversely, both PI3K and AKT can mediate NF-κB activation via phosphorylation of threonine 23 of IKKα, leading to NF-κB activation (Ozes et al., 1999). In comparison, AKT required IKK in order to activate NF-κB (Madrid et al., 2000), specifically IKKβ (Madrid et al., 2001). In addition, AKT potentiates the effects of gemcitabine and paclitaxel in pancreatic cancer possibly via NF-κB activation (Fahy et al., 2004). Similarly, AKT can transiently bind and activate IKK following stimulation with platelet-derived growth factor (PDGF) (Romashkova and Makarov, 1999). In melanoma, AKT may activate NF-κB in an IKK-independent fashion (Dhawan et al., 2002) possibly

mediated by MAPK (Dhawan and Richmond, 2002). Undoubtedly, the complex nature of NF-κB activation can be as paradoxic as the cellular actions of NO.

Our data demonstrates consistent inhibition of NF-κB by NO-Cbl, irrespective of the survival pathways induced by a variety of chemotherapeutic agents. We demonstrate increased NF-κB DNA binding induced by almost every chemotherapeutic agent across all cell lines. Doxorubicin, etoposide, and paclitaxel induced NF-κB activation in all cell lines examined (**Figure 3.2**). Interestingly, A375 cells had greater constitutive IKK activation compared to MCF-7, SW480, and OVCAR-3 cells, and IKK activity in A375 cells was not noticeably enhanced by any chemotherapeutic agent (**Figure 3.3**). Yet, treatment of A375 cells with NO-Cbl reduced basal IKK activity. The absence of increased IKK activity in A375 cells following chemotherapeutic drug treatment may be attributed to: 1) differences in the kinetics of activation of IKK vs. NF-κB, and 2) preferential phosphorylation of the GST-IκBα(1-54) substrate by IKK-β rather than IKK-α (Zandi et al., 1998). These factors may result in understated IKK-α contributions to activation using the current kinase assay. Admittedly, IKK-α may play a more dominant role in NF-κB activation as compared to IKK-β mediated NF-κB activation in A375 cells, but this topic is ancillary to the conclusion of this study. The key observation is that where NF-κB is activated, NO-Cbl inhibits the activation and furthermore, in activation pathways that clearly utilize IKK to trigger NF-κB activation, NO-Cbl treatment inhibits IKK activity.

Conversely, AKT was activated by cisplatin, 5-FU, and etoposide in A375 cells. NO-Cbl markedly reduced AKT phosphorylation following all treatments (**Figure 3.4**). Thus, AKT may be involved in NF-κB activation, independent of IKK, as previously reported

(Dhawan et al., 2002). This may also explain activation of NF-κB in MCF-7 cells following treatment by paclitaxel, accompanied by AKT activation in the absence of IKK activation (**Figure 3.4**). Alternatively, AKT and IKK may act in concert to activate NF-κB (Romashkova and Makarov, 1999). In OVCAR-3 cells, AKT was not activated by any chemotherapeutic agent whereas IKK activation was induced by doxorubicin, etoposide, cisplatin, and 5-FU, suggesting IKK-dependent activation in these cells (**Figure 3.4**). Our results with paclitaxel are in agreement with results obtained by others in ovarian cancer cells using paclitaxel (Huang and Fan, 2002). Clearly, NF-κB signaling is a complex process involving several pathways that provide diverse control points resulting in a balance between apoptosis and survival.

NO-Cbl inhibited expression of a NF-κB-induced survival factor, namely X-linked inhibitor of apoptosis (XIAP) (**Figure 3.5**), consistent with other studies in which S-nitrosoglutathione (GSNO) inhibited XIAP expression (Manderscheid et al., 2001). Our data suggest that the inhibitory effects of NO-Cbl on XIAP are post-translational as well as transcriptional (**Figure 3.5**). The increase in caspase-8 activation, PARP cleavage and XIAP degradation are consistent with the synergistic anti-proliferative effects of NO-Cbl (**Figure 3.6**) and provide further evidence as to the chemopotentiating effects of NO-Cbl. Elimination of OVCAR-3 and P388 tumors *in vivo* (**Figure 3.7**) is consistent with the antiproliferative synergy observed *in vitro*.

We are continuing to study the mechanism by which NO-Cbl inhibits NF-κB activation. This likely involves S-nitrosylation (Stamler et al., 2001). Prostaglandins (PGA_1 and $15dPGJ_2$) inhibit IKK by covalently modifying a critical cysteine residue (C179) within the activation loop (Rossi et al., 2000). S-nitrosylation of IKK-β leads to

its inactivation (Reynaert et al., 2004). In addition, the NO donor SNAP has been shown to inhibit IKK-β (Waldow et al., 2006) as well as suppress AKT activation (Storling et al., 2005). Also, inactivation of AKT can result from S-nitrosylation and may be involved in insulin resistance (Yasukawa et al., 2005). Alternatively or in addition, both IKK-γ and XIAP contain zinc fingers which are known targets for nitrosylation (Kroncke and Carlberg, 2000). Others have shown that NO can inhibit NF-κB by direct S-nitrosylation of the DNA binding subunits (DelaTorre et al., 1997; Marshall and Stamler, 2001; Matthews et al., 1996) or tyrosine nitration (Park et al., 2005).

Therefore, NO-Cbl likely nitrosylates redox-sensitive residues in its target proteins, causing inhibition of NF-κB-mediated survival signaling and this appears to also be the case with AKT-mediated survival signaling. We have shown that NO-Cbl maximizes the anti-tumor effectiveness of primary chemotherapeutic agents. The use of NO-Cbl to inhibit survival signaling may prevent drug resistance, a common occurrence in multiple cycle chemotherapy, and may improve response rates and enhance drug efficacy.

Published in: *PLoS ONE* 2007 Dec. 12; 2(12): e1313
*Bauer J.A., *Lupica J.A., Schmidt H., Haney R.M., Masci R.K., Lee R.M., DiDonato J.A., Lindner D.J.
*Contributed equally to this work.

CHAPTER IV

EFFECTS OF INOSITOL HEXAKISPHOSPHATE KINASE 2 ON TRANSFORMINGGROWTH FACTOR β-ACTIVATED KINASE 1 AND NF-κB ACTIVATION

4.1 ABSTRACT

It has been previously shown that inositol hexakisphosphate kinase 2 (IHPK2) functions as a growth-suppressive and apoptosis-enhancing kinase during cell stress. Overexpression of IHPK2 sensitized ovarian carcinoma cell lines to the growth-suppressive and apoptotic effects of interferon β(IFN-β), IFN-α2, and γ-irradiation. Expression of a kinase-dead mutant abrogated 50% of the apoptosis induced by IFN-β. Because the kinase-dead mutant retained significant response to cell stressors, we hypothesized that a portion of the death-promoting function of IHPK2 was independent of its kinase activity. We now demonstrate that IHPK2 binds to tumor necrosis factor (TNF) receptor-associated factor (TRAF) 2 and interferes with phosphorylation of transforming growth factor β-activated kinase 1 (TAK1), thereby inhibiting NF-κB signaling. IHPK2 contains two sites required for TRAF2 binding, Ser-347 and Ser-359. Compared with wild type IHPK2-transfected cells, cells expressing S347A and S359A mutations displayed 3.5-fold greater TAK1 activation following TNF-α. This mutant demonstrated a 6–10-fold increase in NF-κB DNA binding following TNF-α compared with wild type IHPK2-expressing cells in which NF-κB DNA binding was inhibited.

Cells transfected with wild type IHPK2 or IHPK2 mutants that lacked S347A and S359A mutations displayed enhanced terminal deoxynucleotidyltransferase-mediated dUTP nick end-labeling staining following TNF-α. We believe that IHPK2-TRAF2 binding leads to attenuation of TAK1- and NF-κB-mediated signaling and is partially responsible for the apoptotic activity of IHPK2.

4.2 INTRODUCTION

Inositol polyphosphates play diverse biologic roles, including regulation of endocytic trafficking (Saiardi et al., 2002), protein phosphorylation (Saiardi et al., 2004), chemotaxis (Luo et al., 2003), regulation of non-homologous end joining (Abraham, 2001; Hanakahi et al., 2000; Ma and Lieber, 2002), and apoptosis (Morrison et al., 2001; Nagata et al., 2005). Inositol hexakisphosphate kinase 2 (IHPK2) is a kinase that catalyzes the synthesis of diphosphoinositol pentakisphosphate and bis-diphosphoinositol tetrakisphosphate. Overexpression of IHPK2 sensitizes ovarian carcinoma cell lines to the growth-suppressive and apoptotic effects of IFN-β, IFN-α2 treatment, and ionizing radiation(Morrison et al., 2002). Snyder and co-workers (Nagata et al., 2005) recently demonstrated that IHPK2 enhanced the cytotoxic actions of several different cell stressors.

By co-immunoprecipitation, we found that IHPK2 associated with TRAF2. The tumor necrosis factor (TNF) receptor-associated factor (TRAF) family of proteins serve as adapter proteins for the TNF-R and interleukin-1 receptor superfamilies (Arch et al., 1998; Kopp and Medzhitov, 1999). The role of TRAF2 in mediating the TNF-α response is controversial. Early studies with TRAF2 and TRAF5 knock-out mice or dominant negative (DN) TRAF2 mice suggested that these proteins were not essential or played

redundant roles in TNF-induced NF-κB activation (Lee et al., 1997; Nakano et al., 1999; Yeh et al., 1997). TRAF2$^{-/-}$ fibroblasts are severely impaired in their ability to activate c-Jun N-terminal kinase in response to TNF-α (Nakano et al., 1999). Subsequent studies suggested that TRAF2$^{-/-}$ fibroblasts (Devin et al., 2000) or TRAF2/TRAF5 double knock-out murine fibroblasts (Tada et al., 2001) were impaired in their ability to activate NF-κB in response to TNF-α. Most recently, Aggarwal and co-workers (Jackson-Bernitsas et al., 2007) have shown that NF-κB activation in carcinomas could be disrupted by expression of DN-TRAF2 but not by DN-TRAF5, suggesting that TRAF2 plays a critical role in TNF-α-induced NF-κB activation.

Within the trimeric signaling complex TRAF2 serves to recruit IκB kinase (IKK) and RIP1 to the TNF-R1 (Devin et al., 2001; Song et al., 1997). Transforming growth factor β -activated kinase (TAK1) is a critical component of this cascade, functioning downstream of RIP1 and TRAF2 to activate IKKβ (Shim et al., 2005). We hypothesized that the binding of IHPK2 to TRAF2 might disrupt TNF-α signaling. The aims of this study were to identify motifs in IHPK2 required for TRAF2 binding and to determine whether disruption of IHPK2-TRAF2 binding would affect TNF-α signaling.

4.3 EXPERIMENTAL PROCEDURES

Materials—Human IFN-β (Serono, Rockland, MA)-specific activity, 2.7×10^8 units/mg, was used in these studies.

4.3.1 Construction of IHPK2 SXXE Mutants

IHPK2 was cloned into the pCXN2myc mammalian expression vector (Kinoshita et al., 1998). Using PCR, point mutations were made in IHPK2. The serine residues in S*XX*E were changed to A*XX*E. Thus, the wild type sequences (in bold) S*XX*E1, VDIVDN**S**DCEPKS; S*XX*E2, LLENLT**S**RYEVPC; S*XX*E3, PEVVLD**S**DAEDLE; and S*XX*E4, EDLSEE**S**ADESAG were changed to S*XX*E1, VDIVDN**A**DCEPKS; S*XX*E2, LLENLT**A**RYEVPC; S*XX*E3, PEVVLD**A**DAEDLE; and S*XX*E4, EDLSEE**A**ADESAG. This was done using primers 5'-pGTGGACATTGTAGATAATGCAGACTGTGAACCAAAAAGT-3' and 5'-pACTTTTTGGTTCACAGTCTGCATTATCTACAATGTCCAC-3' for S*XX*E1, 5'-pTTACTGGAAAACCTGACTGCCCGCTATGAGGTGCCTTGT-3' and 5'-pACAAGGCACCTCATAGCGGGCAGTCAGGTTTTCCAGTAA-3' for S*XX*E2, 5'-pCCCGAAGTGGTCCTGGACGCAGATGCTGAGGATTTGGAG-3' and 5'-pCTCCAAATCCTCAGCATCTGCGTCCAGGACCACTTCGGG-3' for S*XX*E3, and 5'-pGAGGACCTGTCAGAGGAAGCAGCTGATGAGTCTGCTGGT-3' and 5'-pACCAGCAGACTCATCAGCTGCTTCCTCTGACAGGTCCTC-3' for S*XX*E4 (p indicates phosphorylated 5'-nucleotide). The PCR product was digested with EcoRI and XhoI and cloned into pCXN2myc. Mutations were confirmed by sequencing. TRAF2 cDNA was cloned into pCXN2myc in a similar manner. Constructs were transfected into NIH-OVCAR-3 cells by nucleofection with Cell Line Nucleofector kit T (Amaxa, Koeln,

Germany). For transient transfection studies, cells were utilized after 48 h. In other co-immunoprecipitation studies, transfectants were selected with G418 for 4 weeks of selection, and clones were pooled. Expression of mutants was monitored by immunoblotting.

4.3.2 siRNA Target Sequence

The IHPK2 target sequence consisted of a 29-mer oligonucleotide representing the 21-nucleotide sequence starting at nucleotide 181 (AAAUUCACUCCCCAGUACAAA) and contained an 8-nucleotide sequence at the 3'-end complementary to the T7 promoter primer provided in the Silencer siRNA construction kit (Ambion, Austin, TX). Complementary oligonucleotides were annealed, and double-stranded RNA was prepared by *in vitro* transcription. The resulting double-stranded RNA was then treated with RNase A and DNase I to generate the final siRNA product. An oligonucleotide sequence that does not silence any mammalian gene (siRNA-scrambled, siSCR) was utilized as a negative control. Nucleofection was used to transiently transfect siRNAs into cells at a concentration of 40 nM.

4.3.3 Immunopercipitation

Mouse monoclonal antibody (15 µg) made in our laboratory was incubated with Protein A-Sepharose beads (Amersham Biosciences) in cell lysis buffer (0.1% Nonidet P-40, 50 mM Tris, pH 8.0, 0.1 mM EDTA, 0.5 mM dithiothreitol, 75 mM NaCl, 10% glycerol, and protease inhibitors). For *in vitro* interaction studies, recombinant purified IHPK2 and TRAF2 (50 µg), encoded in pET32a and expressed in BL21-DE3 bacteria, were incubated in 20 mM Hepes, pH 7.9, 150 mM NaCl, 10 mM EDTA, 0.1% Nonidet P-40 (v/v), 10% glycerol, 1 mM dithiothreitol, 1 mM phenylmethanesulfonyl fluoride, 20 µg/ml leupeptin. For *in vivo* interaction studies, total cell protein (100 µg) was immunoprecipitated with IHPK2 monoclonal antibody. Precipitate was subjected to electrophoresis, transferred to polyvinylidene difluoride membrane, and immunoblotted with rabbit anti-mouse TRAF2 polyclonal antibody (Leinco Technologies, St. Louis,

MO). Membranes were incubated with anti-mouse IgG antibody conjugated to horseradish peroxidase and developed using ECL reagents (Pierce). Converse experiments were performed by immunoprecipitating with anti-TRAF2 and probing with anti-IHPK2. Lysates were also immunoprecipitated with anti-NF-κB p50 antibody (Zymed Laboratories Inc., San Francisco, CA), anti-TAK1 (Cell Signaling Technology, Danvers, MA), or anti-DR4 (Genetex, San Antonio, TX) and probed for IHPK2.

4.3.4 Immunoblot Analysis

Total cell protein (50 µg) was separated on 10% SDS-polyacrylamide gels and transferred to polyvinylidene difluoride membrane. Membranes were incubated with antibody raised against TAK1, or phospho-TAK1, or phospho-AKT or AKT (Cell Signaling Technology), or human XIAP (BD Transduction Laboratories, San Jose, CA), or GAPDH (Trevigen, Inc., Gaithersburg, MD). After washing, membranes were incubated with appropriate secondary antibody conjugated to horseradish peroxidase and developed using ECL reagents (Pierce). Band intensity was quantitated using densitometry (FluorChem SP imaging station; Alpha Innotech, San Leandro, CA). -Fold induction was expressed as the ratio of normalized band intensities: (TNF-treated)/(PBS-treated).

4.3.5 Electrophoretic Mobility Shift Assay (EMSA)

As a positive control for NF-κB induction, cells were treated with TNF-α (20 ng/ml) for 15 min. Plates were washed with cold Dulbecco's phosphate-buffered saline (Sigma). Cells were scraped from plates and resuspended in cold CellLytic M lysis reagent (Sigma) with phosphatase and protease inhibitors (Calbiochem). Lysates were incubated (4 °C, 30 min) followed by centrifugation (20,000 x *g* for 15 min). Supernatant protein concentrations were assessed using the Bradford method (Bio-Rad protein assay). The NF-κB consensus binding sequence oligonucleotide (5'-AGTTGA**GGCGACTTTCCC**AGGC-3') (Santa Cruz Biotechnology, Santa Cruz, CA) was end-labeled with [γ^{32}-P]dATP (PerkinElmer Life Sciences), using T4 polynucleotide kinase (Roche Applied Science). DNA binding reactions were performed (30 min, 4 °C, 20 µg of protein) in 100 mM HEPES, 3.0 mM EDTA, 50% glycerol, 5 mM dithiothreitol,

25 mM $MgCl_2$, 20 mM Tris, pH 7.90, 5 µg of poly d(I-C), and labeled probe. Complexes were resolved on 6% non-denaturing polyacrylamide gels. Gels were dried and exposed to film. To verify that band shifts were comprised of NF-κB, lysates were stimulated for 15 min with TNF-α (20 ng/ml) and incubated with 1 µg of anti-NF-κB p50 antibody (Zymed Laboratories Inc., San Francisco, CA). Band intensity was quantitated by phosphor image analysis on a Storm-840 imager using Image Quant v 5.1 software (Amersham Biosciences). -Fold induction was expressed as the ratio of normalized band intensities: (TNF-treated)/(PBS-treated).

4.3.6 IKK Assay

Whole cell extracts (300 µg of protein) were supplemented with 150 µl of Buffer A (20 mM Hepes, pH 7.9, 20 mM β-glycerophosphate, 10 mM NaF, 0.1 mM orthovanadate, 5 mM para-nitrophenyl phosphate, 10 mM 2-mercaptoethanol, 0.5 mM phenylmethylsulfonyl fluoride, and protease mixture) and 2 µl of normal rabbit serum and mixed by rotation (4 °C, 1 h) (DiDonato, 2000). A 50% slurry of Protein G-Sepharose (80 µl) (Amersham Biosciences) in Buffer A (without β-mercaptoethanol or phenylmethylsulfonyl fluoride) was added and mixed by rotation at 4 °C, 1 h. Protein G-Sepharose was removed by centrifugation (800 x *g*, 1 min) and discarded. Anti-IKKα monoclonal antibody (0.5 µg; BD Biosciences) or anti-β-actin antibody was added to the supernatant and mixed by rotation (4 °C, 2 h). A 50% slurry of Protein G-Sepharose (60 µl) prepared in Buffer C (Buffer A plus 50 mM NaCl and 10 mM $MgCl_2$, without β-mercaptoethanol and phenylmethylsulfonyl fluoride) was added and mixed by rotation (4 °C, 30 min). Protein G immunopellets were collected by centrifugation (800 x *g*, 30 s) and washed three times with Buffer B (Buffer A plus 250 mM NaCl) and once with

Buffer C (Buffer A plus 50 mM NaCl and 10 mM $MgCl_2$). Immunopellets were resuspended in 30 µl of kinase buffer with 0.1 mM orthovanadate, 50 µM unlabeled ATP, 5 µCi of [γ-^{32}P]ATP, 2 mM dithiothreitol, and 2 µg of recombinant GST-IκBα-(1–54) and incubated (30 °C, 30 min). Reactions were stopped with 15 µl of 4x SDS-PAGE loading buffer (200 mM Tris-HCl, pH 6.8, 8% SDS, 40% glycerol, 0.2% 2-mercaptoethanol), heated (95 °C, 10 min), and resolved by SDS-PAGE on 12% acrylamide gels. Gels were rinsed, stained with Bio-Safe Coomassie (Bio-Rad) to visualize protein bands, rinsed, photographed, dried, and exposed to Kodak X-OMAT AR film (Eastman Kodak Co., Rochester, NY) to detect substrate phosphorylation. IKK activation was quantified by phosphor image analysis (GE Healthcare).

4.3.7 Antiproliferative Assays

Cells were treated with IFN-β during growth in RPMI 1640 (Mediatech Inc., Herndon, VA) and 5% fetal bovine serum (HyClone, Logan, UT). Cells were confirmed mycoplasma-free by PCR. Growth was monitored using a colorimetric assay (Skehan et al., 1990). Each treatment group contained 8 replicates. Cells were fixed and stained with sulforhodamine B after 4 days. Bound dye was eluted from cells, and absorbance (A_{exp}) was measured at 570 nm. One plate was fixed 8 h after plating to determine the absorbance representing starting cell number (A_{ini}). Absorbance with this plate and that obtained with untreated cells at the end of the growth period (A_{fin}) were taken as 0 and 100% growth, respectively. Thus, Percent Control Growth = 00%*($A_{exp} - A_{ini}$)/$A_{fin} - A_{ini}$). Expressed as a percent of untreated controls, a decrease in cell number (relative to starting cell number) is a negative number on the *y*-axis.

4.3.8 TUNEL Assay

NIH-OVCAR-3 cells were exposed to TNF-α (10 ng/ml) for 16 h. Apoptotic cells were detected by TUNEL (terminal deoxynucleotidyltransferase-mediated dUTP-biotin nick end-labeling) staining using a kit (APO-BRDU kit; BD Biosciences). Cells were processed according to the manufacturer's protocol. The percentage of fluorescein isothiocyanate-positive cells was analyzed by fluorescent-activated cell scanning (Facsvantage; BD Biosciences).

4.4 RESULTS

4.4.1 IHPK2 Binds TRAF2

Bacterially translated proteins were co-immunoprecipitated with antibody specific for IHPK2 (**Fig. 4.1a, top lane**), whereas antibody to the DR4 death receptor did not precipitate TRAF2 (**Fig. 4.1a, bottom lane**). Untransfected NIH-OVCAR-3 cells were treated with PBS or IFN-β (100 units/ml, 24 h); lysates were immunoprecipitated (IP) with anti-IHPK2 followed by immunoblot (IB) with anti-TRAF2 antibody (**Fig. 4.1b, top lane**). IFN-β increased the interaction of IHPK2 with TRAF2. The converse experiment (IP with anti-TRAF2 and IB with IHPK2) gave similar results (**Fig. 4.1b, second lane**). Immunoprecipitation with irrelevant antibodies (p50 and TAK1) yielded no signal.

4.4.2 IHPK2 Knock Down Induces IFN-β Resistance

It has been previously shown that IFN-β induced IHPK2 in a post-transcriptional manner (Morrison et al., 2001). This induction could be detected after IFN-β (100 units/ml, 24 h, **Fig. 4.1c, top lane**). Transient transfection with siRNA against IHPK2 (siIHPK2) efficiently suppressed IHPK2 expression, whereas scrambled siRNA (siSCR) did not. Because siRNA can potentially induce an IFN response, we examined effects of

siRNA transfection on activation and phosphorylation of the transcription factor STAT1. Treatment of untransfected cells with IFN-β induced phosphorylation of STAT1 after 30 min, which was no longer detectable after 24 h. Similar activation of STAT1 was detected in siIHPK2- and siSCR-expressing cells, suggesting that down-regulation of IHPK2 did not affect IFN signaling. The expression of STAT1, an IFN-stimulated gene, was increased in untransfected, siIHPK2-transfected, and siSCR-transfected cells (**Fig. 4.1c, third lane**).

Transiently transfected NIH-OVCAR-3 cells were subjected to TUNEL analysis (**Fig. 4.1d**). Following IFN-β, cells expressing scrambled siRNA (siSCR) displayed 2-fold greater TUNEL staining (55%) compared with cells expressing siIHPK2 (23%). Similarly, siIHPK2 reduced the level of apoptosis following TNF-α from 67 to 32%. Hence, knock down of IHPK2 mRNA conferred resistance to apoptosis induced by IFN-β and by TNF-α. Inhibition of apoptosis correlated with enhanced proliferation. Anti-proliferative assays (**Fig. 4.11e**) revealed a 2-fold increase in ID_{50} for IFN-β in siIHPK2 cells compared with siSCR cells: 16 and 8 units/ml, respectively.

4.4.3 IHPK2 Mutation Inhibits IHPK2-TRAF2 Binding

Ligation of death receptors such as Fas, TNFR1, DR4, and DR5 activates the external apoptotic pathway. TNF-α binds TNFR1, inducing clustering of TRADD and receptor-interacting protein (RIP1), which leads to caspase activation. However, ligation of TNFR1 generates not only a death signal but an additional survival signal mediated by NF-κB. Apo2L/TRAIL triggers apoptosis via binding to death receptors DR4 and DR5. Immunoprecipitation of NIH-OVCAR-3 cell lysates with IHPK2 monoclonal antibody showed that there was no association between IHPK2 and DR4 or DR5 (not shown).

Treatment with IFN-β enhanced binding of IHPK2 to TRAF2 (**Fig. 4.1b**). The interaction was even stronger when TRAF2 and IHPK2 were co-transfected (**Fig. 4.2a**). When cells are transfected with only one construct (either IHPK2 or TRAF2, **Fig. 4.2, a and b, lanes 1–2**) less TRAF2 is immunoprecipitated when compared with co-transfection. IHPK2 contains four S*XX*E motifs, putative binding sites for TRAF2 (Park et al., 1999). For brevity, we named these sites S1 (S102), S2 (S211), S3 (S347), and S4 (S359). The four S*XX*E sites were point mutated (serine to alanine) singly and in combination. NIH-OVCAR-3 cells were stably co-transfected with IHPK2 mutants and TRAF2. Cell lysates were immunoprecipitated with IHPK2 monoclonal antibody. Immunoblot analysis demonstrated that two of the S*XX*E mutations (S3 and S4) in combination (but not singly) reduced TRAF2 binding activity (**Fig. 4.2a**). Protein levels of IHPK2 and TRAF2 were comparable in transfected cells (**Fig. 4.2b**).

FIGURE 4.1

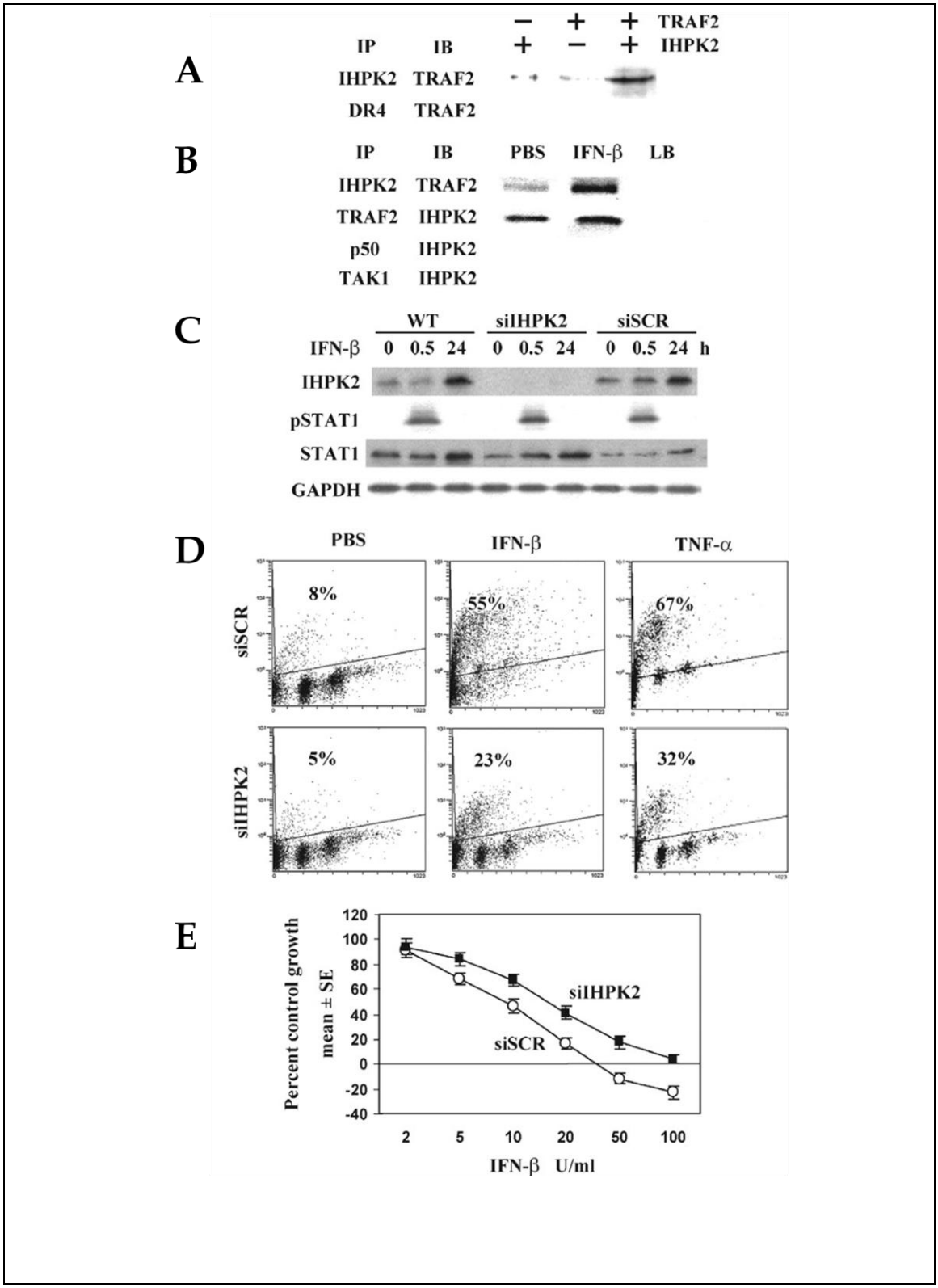
A
IP
IB
TRAF2
IHPK2
IHPK2 TRAF2
DR4 TRAF2
B
IP
IB
PBS
IFN-β
LB
IHPK2 TRAF2
TRAF2 IHPK2
p50 IHPK2
TAK1 IHPK2
C
WT
siIHPK2
siSCR
IFN-β 0 0.5 24 0 0.5 24 0 0.5 24 h
IHPK2
pSTAT1
STAT1
GAPDH
D
PBS
IFN-β
TNF-α
siSCR
siIHPK2
8%
55%
67%
5%
23%
32%
E
Percent control growth
mean ± SE
siIHPK2
siSCR
IFN-β U/ml

Figure 4.1: IHPK2-TRAF2 interaction.

a, interaction of recombinant proteins *in vitro*. Presence and absence of proteins indicated by + and–, respectively. The reaction was subject to immunoprecipitation (*IP*) followed by immunoblot (*IB*) with the indicated antibodies. **b**, wild type NIH-OVCAR-3 cells were treated with IFN-β (100 units/ml x 24 h). Lysates were subject to immunoprecipitation followed by immunoblot with the indicated antibodies. Anti-p50 NF-κB and anti-TAK1 were included as negative controls. As additional controls, lysis buffer (*LB*) alone, without cell lysate, was immunoprecipitated. **c**, untransfected (*WT*) cells were treated with PBS (*0h*) or IFN-β as above and harvested at 0.5 and 24 h. Immunoblots indicate induction of IHPK2 and STAT1 (at 24 h) and induction of pSTAT1 (at 30 min). Cells were transiently transfected with siRNA directed against IHPK2 (*siIHPK2*) or scrambled siRNA (*siSCR*) by nucleofection. Two days later cells were treated with PBS or IFN-β (*0.5* and *24 h*) and subjected to immunoblot analysis. **d**, transiently transfected cells were treated with PBS, IFN-β (100 units/ml), or TNF-α (10 ng/ml) for 24 h and subjected to TUNEL staining. **e**, transiently transfected cells were grown in the presence of IFN-β (0–100 units/ml). After 4 days of growth, cells were fixed and stained, and cell number (proportional to intensity of retained SRB dye) was expressed as a percentage of PBS-treated control cells (n = 8 replicates/data point).

FIGURE 4.2

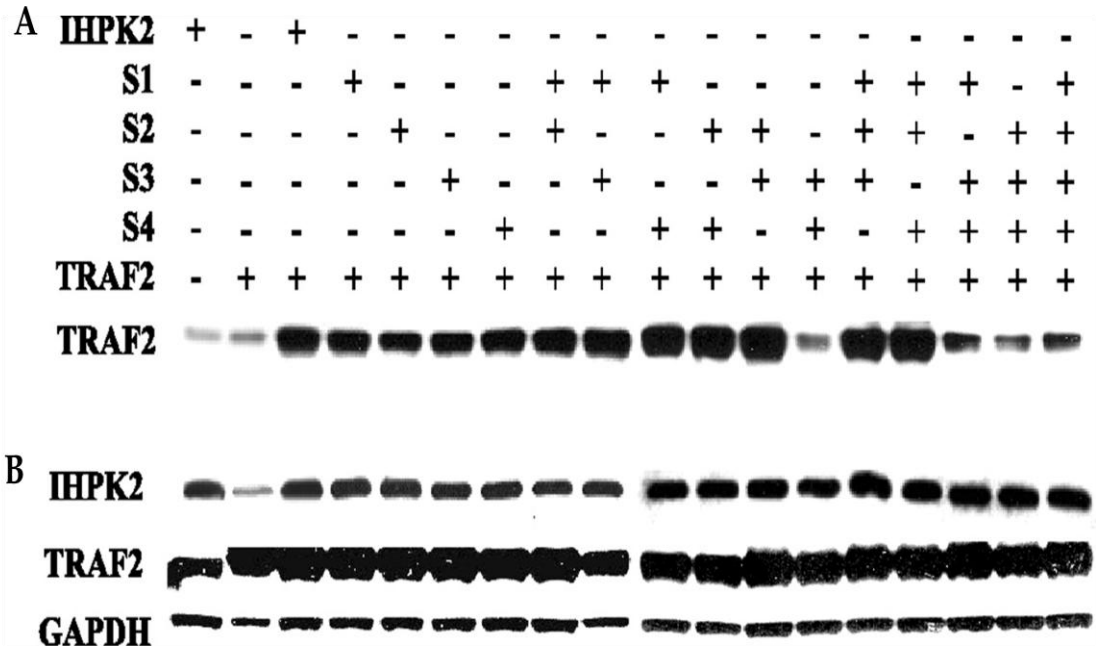

Figure 4.2: Effect of IHPK2 mutation on binding of IHPK2 to TRAF2.

a, NIH-OVCAR-3 cells were co-transfected with IHPK2 and TRAF2 by nucleofection. *Pluses* and *minuses* indicate the presence or absence of indicated construct, respectively. Total cell protein (100 µg) from each transfected cell line was immunoprecipitated with IHPK2 mouse monoclonal antibody. Precipitate was subjected to immunoblot analysis with TRAF2 polyclonal antibody (*bottom row*). Immunoblot analysis demonstrated that the IHPK2 S3&4 mutations in combination (but not single mutations) caused reduced TRAF2 binding when compared with the interaction of wild type IHPK2 and all other IHPK2 mutations. **b**, immunoblot to demonstrate protein levels of IHPK2, TRAF2, and GAPDH in lysates of transfected cells. The experiment was performed three times with similar results.

4.4.4 Effect of IHPK2 Mutation on TAK1 Phosphorylation

Because TAK1 plays an important role in the TNFR-mediated cascade and functions immediately downstream of TRAF2 (Shim et al., 2005), we determined whether IHPK2 mutation had any effect on phosphorylation of TAK1. Wild type untransfected and vector-transfected cells displayed a 2.5- to 3-fold induction of phospho-TAK1 (pTAK1) in response to TNF-α (**Fig. 4.3a**). TNF-α failed to activate TAK1 above base line in cells expressing IHPK2 or the S3 or S4 single mutants (<1.5-fold induction of pAKT). However, phosphorylation of TAK1 following TNF-α was restored in cells containing S3&S4 double mutants (3- to 3.5-fold induction). Hence, the S3&S4 double mutant had diminished TRAF2 binding and no longer inhibited TAK1 phosphorylation.

4.4.5 Effect of IHPK2 Mutation on AKT Phosphorylation

Because AKT may also contribute to NF-κB activation, mainly through phosphorylation of IKKα (Ozes et al., 1999), we determined whether IHPK2 mutation had any effect on activation of AKT. Wild type untransfected and vector-transfected cells displayed a 6-fold induction of phospho-AKT (pAKT) in response to TNF-α (**Fig. 4.3b**). The TNF-α response of cells expressing IHPK2 or the S3 or S4 single mutants was suppressed (1- to 1.5-fold induction of pAKT). However, the TNF-α response was restored in cells containing S3&S4 double mutants; they displayed 5- to 17-fold induction of pAKT (**Fig. 4.3b, bars 6–9**). Hence, the S3&S4 double mutant lost the ability to inhibit pAKT activation.

FIGURE 4.3

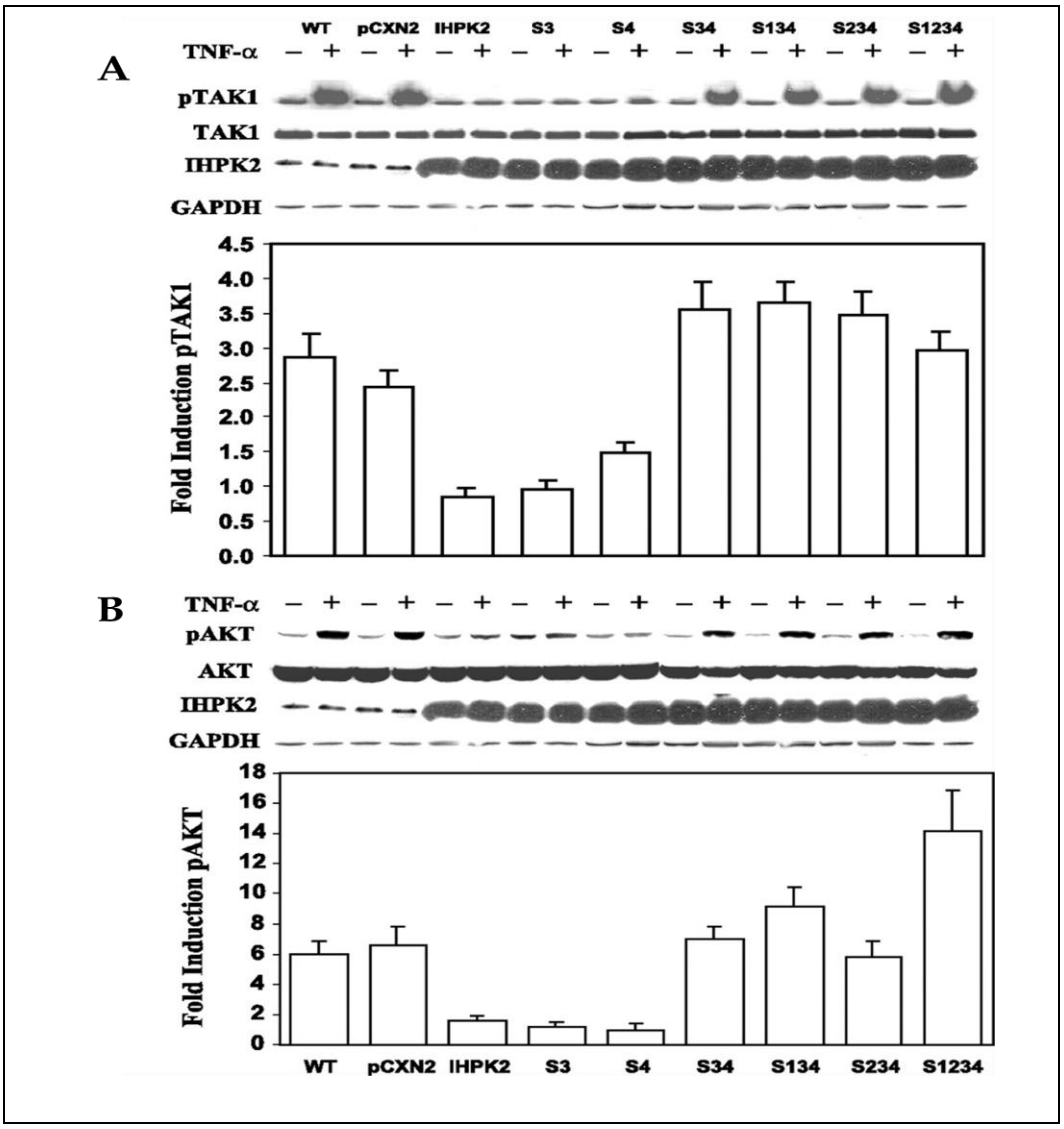

Figure 4.3: Effect of IHPK2 mutation on phosphorylation of TAK1 and AKT.

a, untransfected (*WT*), vector-transfected (*pCXN2*), and mutant-transfected cells were treated with PBS (–) or TNF-α, 15 ng/ml (+) for 1 h. Lysates were subjected to immunoblot with anti-phospho-TAK1 followed by stripping and reprobing with anti-TAK1. Expression of IHPK2 transgene is indicated, and GAPDH served as loading control. Bands were quantitated by densitometry, and -fold induction was calculated (n = 3). **b**, using the same lysates, similar studies were performed with anti-phospho-AKT and anti-AKT.

4.4.6 Effect of IHPK2 Mutation on IκBα Kinase Activity

The IKK complex, consisting of α, β, and γsubunits, is responsible for phosphorylation of IκB, leading to IκB degradation, and subsequent nuclear translocation of NF-κB. TAK1 phosphorylates IKKβ, the main catalytic subunit, whereas AKT phosphorylates IKKα. We examined IKK enzymatic activity in lysates of cells stably transfected with IHPK2 mutants. IKK was immunoprecipitated from cell extracts using anti-IKKα antibody, and kinase activity was assessed using recombinant GST-IκBα-(1–54) as a substrate. TNF-α induced IKKα activity in wild type untransfected cells, vector-transfected cells, and all transfectants (**Fig. 4.4**). Cells expressing IHPK2 S3&4 double mutants displayed similar kinase activity as wild type cells or other transfectants. Therefore, the S3&4 mutant did not appear to modulate IKK enzymatic activity *in vitro*.

FIGURE 4.4

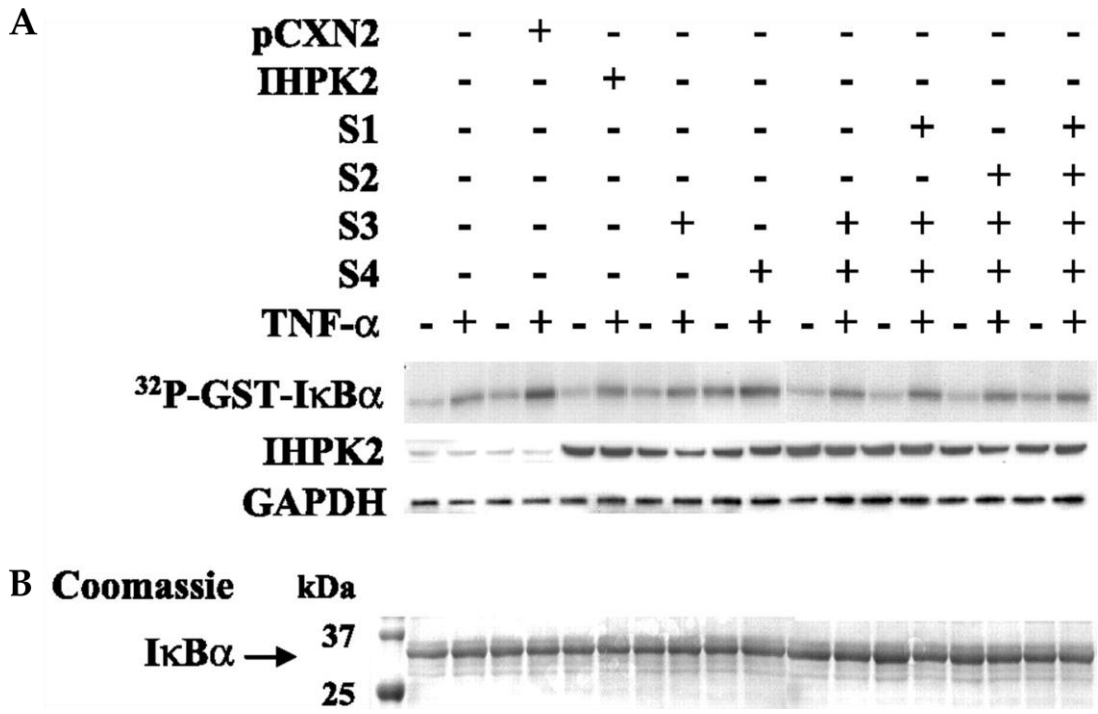

Figure 4.4: IKK activity.

IKK activity was assessed using recombinant GST-I$_\kappa$B$_\alpha$-(1–54) and [γ-^{32}P]ATP as substrates. The phosphorylated GST fusion protein was detected by autoradiography. **a**, IKK activity was determined in NIH-OVCAR-3 cells co-transfected with IHPK2 (wild type or mutants) and TRAF2, followed by TNF-α stimulation for 15 min. Cells expressing the double mutant did not show significant differences in IKK activity compared with cells expressing wild type IHPK2. Untreated cells typically exhibit 5–10% the activity of stimulated cells (DiDonato et al., 1997a). Expression of IHPK2 transgene is indicated, and GAPDH served as loading control. The experiment was performed three times with similar results. **b**, Coomassie blue-stained gel demonstrated equal loading of GST-I$_\kappa$B$_\alpha$-(1–54) substrate utilized in the kinase assay.

4.4.7 Effect of IHPK2 Mutation upon NF-κB DNA Binding

We next determined whether IHPK2-TRAF2 binding and inhibition of TAK1 phosphorylation disrupted NF-κB signaling. In untransfected wild type NIH-OVCAR-3 cells, treatment with TNF-α resulted in robust NF-κB activation as demonstrated by EMSA (**Fig. 4.5a**). Supershift (ss) with anti-p50 confirmed the identity of NF-κB. Transfection with IHPK2 reduced the intensity of DNA binding activity in response to TNF-α (**Fig. 4.5b, compare lanes 3–6**). Quantitation of the band shift indicated a 3-fold reduction (**Fig. 4.5b, bars 2 and 3**). Hence, overexpression of IHPK2 blunted NF-κB DNA binding activity in response to TNF-α. Cells expressing two IHPK2 mutations (S3&4) demonstrated 7- to 11-fold activation of NF-κB compared with cells co-transfected with wild type IHPK2. The other IHPK2 mutants that lacked S3&4 mutations had blunted NF-κB activation (1-fold induction).

4.4.8 Effect of IHPK2 Mutation on XIAP

Activated NF-κB translocates to the nucleus and induces transcription of target genes such as inhibitor of apoptosis proteins (IAPs). The X-linked mammalian inhibitor of apoptosis protein (XIAP) binds to caspase 3, caspase 9, DIABLO/Smac, HtrA2/Omi, and TAB1 (Auphan et al., 1995). Cells expressing IHPK2 mutants S3&4 displayed up to a 2.4-fold increase in XIAP. The IHPK2 single mutants (S3 and S4) acted like wild type IHPK2, resulting in suppressed XIAP expression (fold increase 0.1–0.9) (**Fig. 4.6**). Thus, effects of IHPK2 mutation upon XIAP induction correlated with changes in NF-κB DNA binding activity.

FIGURE 4.5

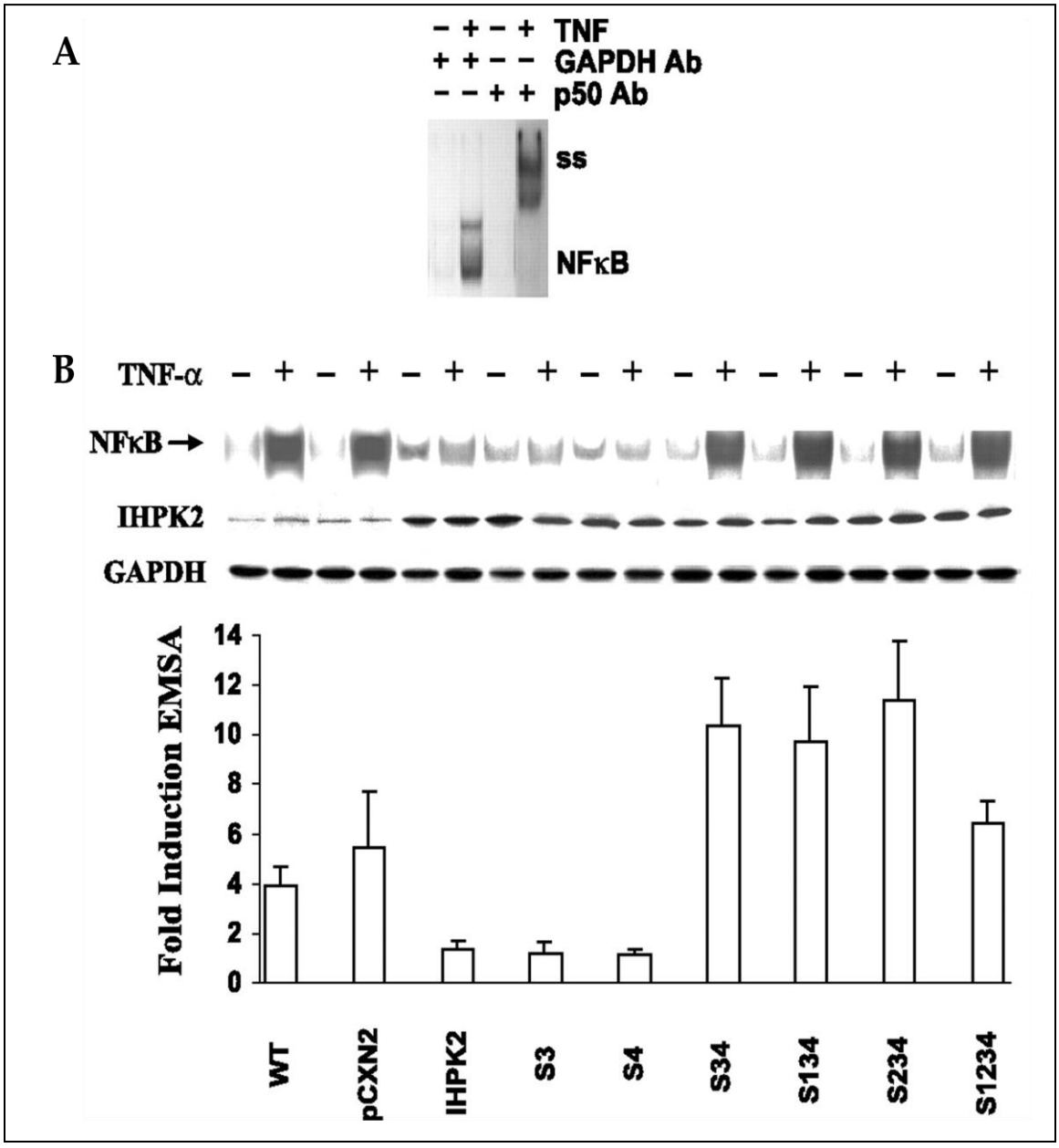
A
− + − + TNF
+ + − − GAPDH Ab
− − + + p50 Ab
ss
NFκB
B
TNF-α − + − + − + − + − + − + − + − + − +
NFκB →
IHPK2
GAPDH
Fold Induction EMSA
14
12
10
8
6
4
2
0
WT
pCXN2
IHPK2
S3
S4
S34
S134
S234
S1234

Figure 4.5: Effect of IHPK2 mutation upon NF-κB DNA binding activity.

a, wild type untransfected NIH-OVCAR-3 cells were treated with TNF-α, and EMSA was performed. Lysates were incubated with anti-GAPDH or anti-NF-κB(*p50*) prior to EMSA to demonstrate supershift (*ss*). **b**, cells transfected with IHPK2 S3&4 mutations (S347A and S359A) displayed enhanced NF-κB DNA binding activity induced by TNF-α. Cells transfected with wild type IHPK2 or IHPK2 mutants that lacked S3&4 mutations had suppressed NF-κB DNA binding activity. Cells were stimulated with TNF-α (20 ng/ml) for 15 min. Expression of IHPK2 transgene is indicated, and GAPDH served as loading control. EMSA band intensities were quantified with a Phosphorimager, and -fold induction was calculated. Cells expressing IHPK2 mutants S3&4, S1&3&4, S2&3&4, and S1&2&3&4 were 7- to 11-fold more effective at activation of NF-κB compared with cells transfected with wild type IHPK2, whereas cells expressing IHPK2 and single mutants had <2-fold induction. Data are expressed as mean ± S.E. of three separate experiments.

FIGURE 4.6

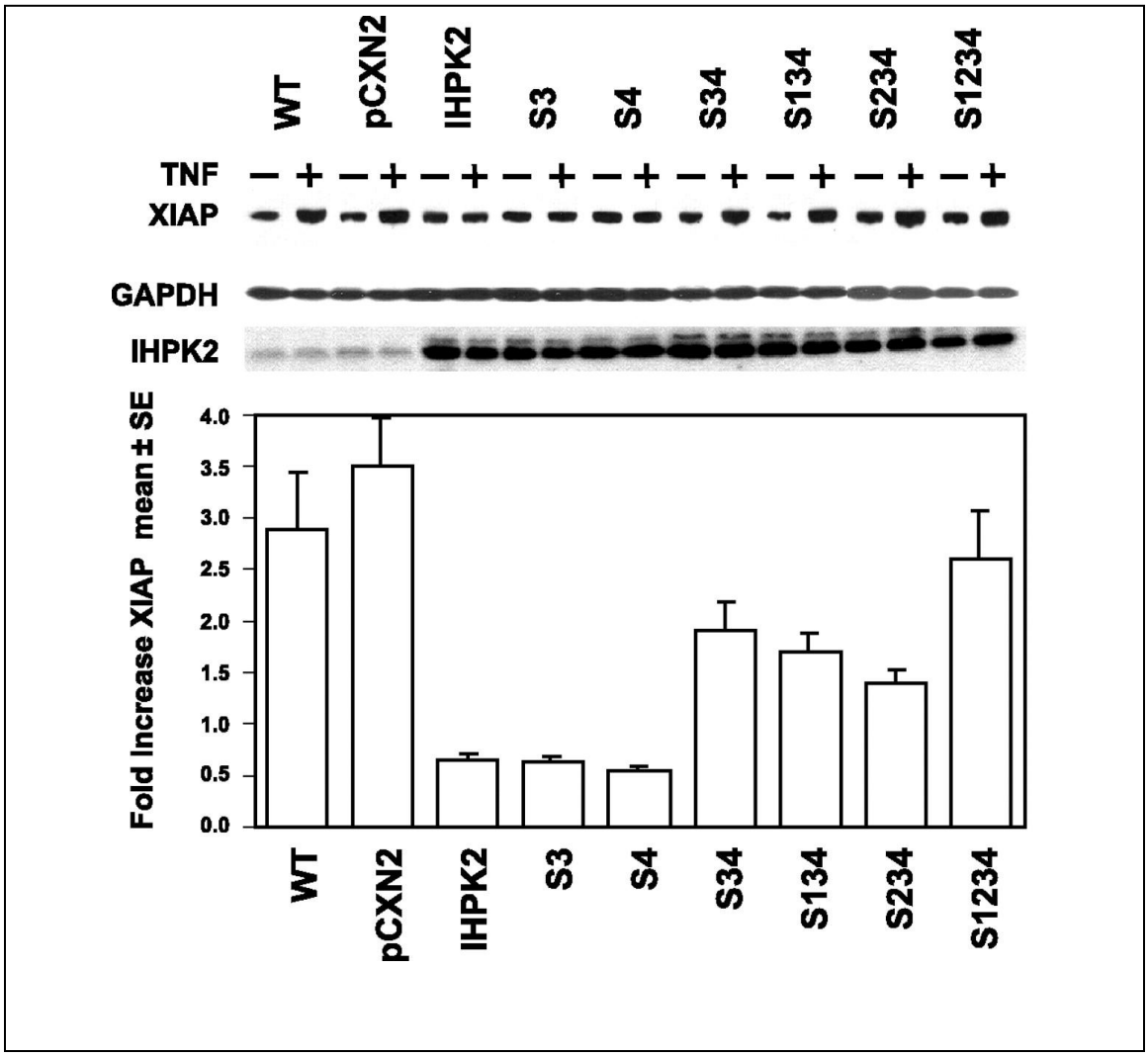

Figure 4.6: Effect of IHPK2 mutation on XIAP levels.

Immunoblotting for XIAP was performed with lysates harvested 24 h after TNF-α (15 ng/ml). Expression of IHPK2 transgene is indicated, and GAPDH served as loading control. Cells expressing IHPK2 mutations S3&4 had up to 2.4-fold increase in XIAP. XIAP was not induced in cells expressing IHPK2, or IHPK2 single mutations, demonstrating -fold increases of -0.1 to -0.9. -Fold increase <1.0 corresponds to decreased XIAP expression following TNF-α (n = 3).

4.4.9 IHPK2 Mutants Inhibit TNF-α-induced Apoptosis

The effects of IHPK2 mutation on TNF-α-induced apoptosis were analyzed by TUNEL (**Fig. 4.7**). Untransfected wild type and vector-transfected cells displayed 40 and 26% TUNEL positivity following TNF-α, respectively. Cells expressing IHPK2 or S3 or S4 single point mutations had enhanced TUNEL staining, 64, 51, 52%, respectively. Cells expressing the S3&S4 double mutation were 33% TUNEL-positive, a response that was similar to untransfected or vector-transfected cells. Therefore, the double mutant was defective in enhancing TNF-α-induced apoptosis.

4.4.10 IHPK2 Mutants Affect Growth-suppressive Activities of IFN-β

The biological relevance of the IHPK2 mutations was determined in antiproliferative assays using pools of stable transfectants. Overexpression of IHPK2 sensitized cells to IFN-β, as the IC_{50} value fell from 15 to 6 units/ml in vector-transfected and IHPK2-transfected cells, respectively (**Fig. 4.8**). Constructs containing the S3&4 mutations conferred resistance to IFN-β, as the IC_{50} value increased from 15 units/ml in vector-transfected cells to 20–75 units/ml in double mutant-transfected cells, respectively. Cells expressing irrelevant IHPK2 mutations (IRREL, constructs lacking S3&4 mutations) displayed sensitivity to IFN-β between that of vector- and IHPK2-transfected cells. Therefore, overexpression of IHPK2 sensitized cells to IFN-β, and the S3&4 double mutation conferred resistance to IFN-β.

FIGURE 4.7

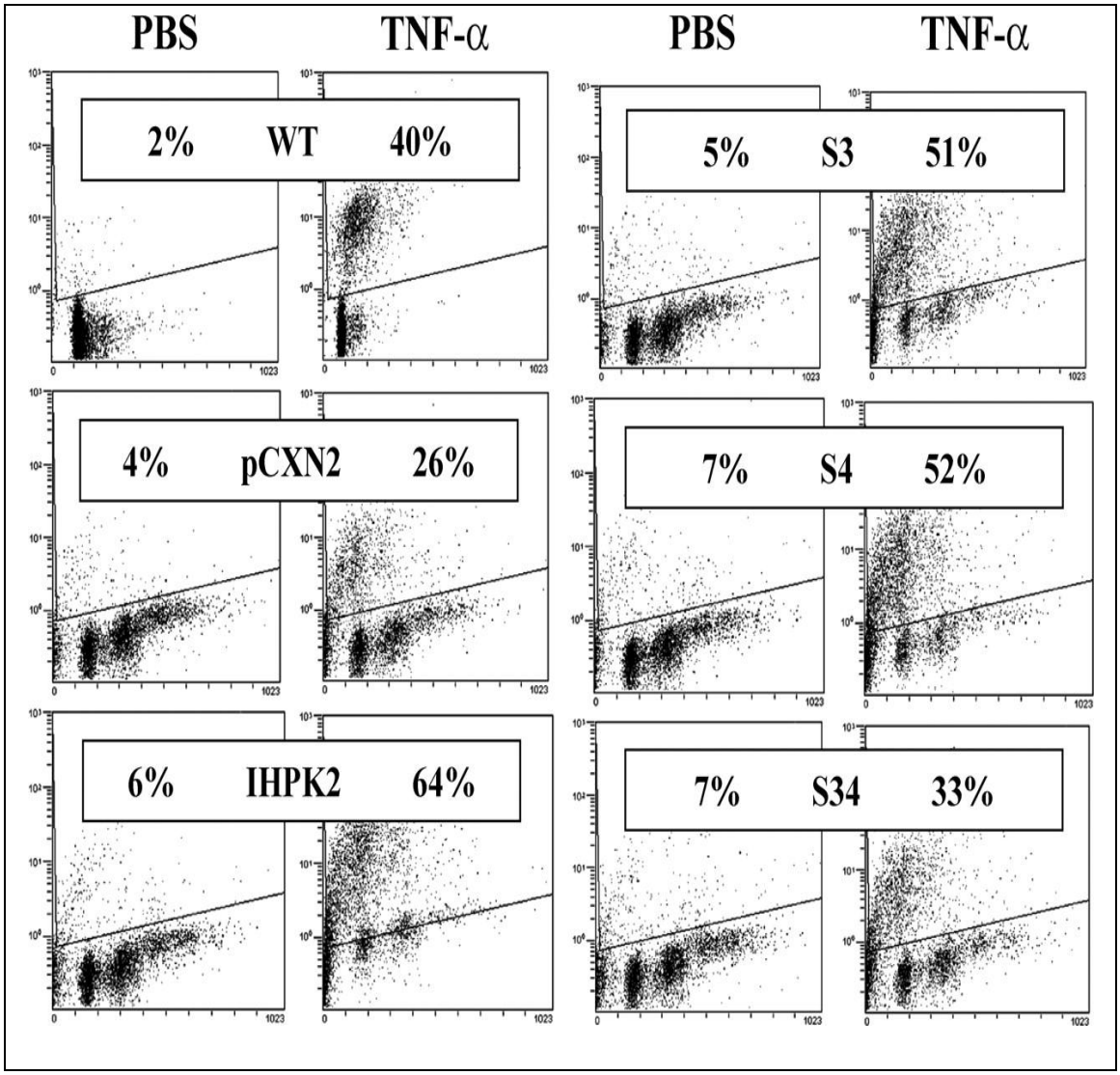

Figure 4.7: Effect of IHPK2 mutation on apoptosis induction by TNF-α.

Untransfected (*WT*), vector-transfected (*pCXN2*), and mutant-transfected cells were treated with PBS or TNF-α, 15 ng/ml for 16 h. Induction of apoptosis was determined by TUNEL staining.

FIGURE 4.8

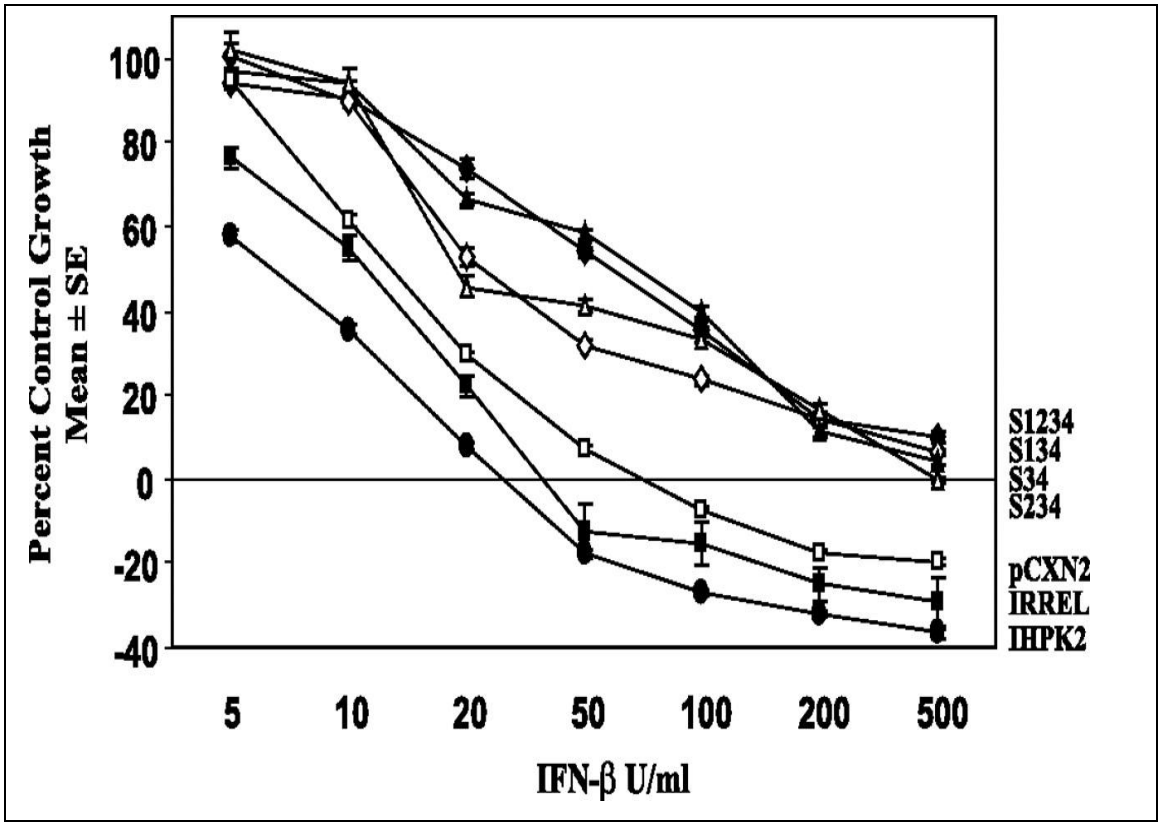

Figure 4.8: Effect of IHPK2 mutation on IFN-β antiproliferative activity.

NIH-OVCAR-3 cells were stably transfected with IHPK2 constructs and grown in the presence of 5–500 units/ml IFN-β. After 4 days, cells were fixed and stained with sulforhodamine B. Absorbance of bound dye was expressed as percent of untreated controls (n = 8, each data point). Overexpression of IHPK2 sensitized cells to IFN-β. Cells expressing IHPK2 mutations S3&4 in combination conferred relative resistance to IFN-β. The dose response curve of cells expressing irrelevant IHPK2 mutations (S1, S2, S3, S4, S1&2, S1&3, S1&4, S2&3, S2&4, S1&2&3, S1&2&4) lay in a narrow band between pCXN2 (vector) and IHPK2 and is represented as a single curve (*IRREL*).

4.5 DISCUSSION

In previous studies, overexpression of the kinase-dead IHPK2 mutant suppressed IFN-induced cell death, but the magnitude of suppression was 50%, even though transfection efficiency was 90%. Snyder and co-workers (Nagata et al., 2005) recently demonstrated that transfection of IHPK2 augmented the apoptotic activities of several cell stressors. Although transfection of all three subtypes of IHPK increased cell death, suppression of IHPK2, but not IHPK1 or IHPK3, abrogated apoptosis.

Our study and those of Snyder and co-workers suggest that kinase activity is not the sole determinant of the apoptotic activity of IHPK2. The present study provides evidence that IHPK2 is a TRAF2-interacting protein that suppresses TAK1 phosphorylation and inhibits NF-κB activation. In the absence of cell stressors such as IFN-β or TNF-α, IHPK2-TRAF2 interaction is still detected at low levels (**Fig. 4.1b**). This may be responsible for the ~10% constitutive levels of apoptosis observed in NIH-OVCAR-3 cells. Immunoprecipitation analysis confirmed that the S*XX*E mutations (S347A and S359A) in combination inhibited TRAF2 binding. Therefore, these residues are important for IHPK2-TRAF2 association. Cells expressing these IHPK2 mutations were more effective at phosphorylation of TAK1 and activation of NF-κB compared with cells expressing wild type IHPK2. Similarly, the double mutants were more effective at XIAP induction and more resistant to the apoptotic effects of IFN-β.

The NF-κB pathway is activated following degradation of IκB (Senftleben et al., 2001). This pathway depends on the IKK complex, which contains three subunits, IKKα, IKKβ, and IKKγ. TRAF2 functions to recruit IKKα and IKKβ to the TNF-R1 receptor (Devin et al., 2001). Although initial studies utilizing TRAF2 knock-out MEFs suggested

that TRAF2 did not play a role in activation of NF-κB by TNF-α (Yeh et al., 1997), later studies indicated that TRAF2 was indeed required for NF-κB activation. Nakano and co-workers (Tada et al., 2001) showed that TRAF2/TRAF5 double knock-out MEFs were severely impaired in NF-κB activation following TNF-α, suggesting that TRAF2 and TRAF5 function may be redundant. In squamous carcinoma, expression of DN-TRAF2 strongly inhibited transcription of an NF-κB reporter plasmid, whereas DN-TRAF5 had no effect on NF-κB activation (Jackson-Bernitsas et al., 2007). Hence, in some carcinomas TRAF2 and TRAF5 function is not redundant.

A model for this signaling cascade is: TNFR1-(RIP1/TRAF2)-TAK1-IKKβ-NF-κB. Knock-out MEFs that lack TAK1 cannot activate NF-κB in response to TNF-α and are highly sensitive to TNF-α-induced apoptosis, indicating that the survival pathway is severely inhibited in these cells (Shim et al., 2005). Phosphorylation of IKKα, mediated by NF-κB-inducing kinase, appears to be intact in TAK1 knock-out MEFs (Shim et al., 2005). Thus, TAK1 phosphorylates IKKβ but does not appear to phosphorylate IKKα. Immunoprecipitation experiments with recombinant proteins demonstrated that IKKβ is the main catalytic subunit of the IKK complex (Zandi et al., 1998).

The GST-IκBα-(1–54) fusion protein, containing glutathione and the first 54 residues of IκBα, is phosphorylated by IKK in the kinase assay. Antibodies directed against IKKβ disrupt IKK activity; therefore, antibodies against IKKα or IKKγ are generally utilized to precipitate the complex. Other proteins such as Cdc37 and Hsp90 may be required for optimal activity of the IKK complex (Chen et al., 2002). If such auxiliary proteins are not pulled down efficiently, the assay may not reflect the full extent of IκBα phosphorylation *in vivo*.

Mutation of IHPK2 clearly affected TAK1 phosphorylation (**Fig. 4.3a**) but did not affect IKK kinase activity *in vitro* (**Fig. 4.4a**). There is also cross-talk between TRAF2 and AKT in NIH-OVCAR-3 cells, as overexpression of IHPK2 inhibited AKT activation (**Fig. 4.3b**). CD40, a TNF receptor superfamily member, requires TRAF2 to activate AKT. In TRAF2 knock-out MEFs, and carcinoma cells that received siRNA-TRAF2, AKT phosphorylation was severely impaired (Davies et al., 2005). Our studies suggest that following binding to TRAF2, IHPK2 functions to inhibit TAK1 phosphorylation, AKT phosphorylation, and subsequent NF-κB activation.

Published in *The Journal of Biological Chemistry* Vol. 282, No. 21, pp 15349-15356
May 25, 2007.
Morrison B.H., Bauer J.A., Lupica J.A., Tang Z., Schmidt H., DiDonato J.A.,
Lindner D.J.

CHAPTER V

FLAGELLIN ACTING VIA TLR5 IS THE MAJOR ACTIVATOR OF KEY SIGNALING PATHWAYS LEADING TO NF-κB AND PROINFLAMMATORY GENE PROGRAM ACTIVATION IN INTESTINAL EPITHELIAL CELLS

5.1 ABSTRACT

Infection of intestinal epithelial cells by pathogenic *Salmonella* leads to activation of signaling cascades that ultimately initiate the proinflammatory gene program. The transcription factor NF-κB is a key regulator/activator of this gene program and is potently activated. We explored the mechanism by which *Salmonella* activates NF-κB during infection of cultured intestinal epithelial cells and found that flagellin produced by the bacteria and contained on them leads to NF-κB activation in all the cells; invasion of cells by the bacteria is not required to activate NF-κB. Purified flagellin activated the mitogen activated protein kinase (MAPK), stress-activated protein kinase (SAPK) and Ikappa B kinase (IKK) signaling pathways that lead to expression of the proinflammatory gene program in a temporal fashion nearly identical to that of infection of intestinal epithelial cells by *Salmonella*. Flagellin expression was required for *Salmonella* invasion of host cells and it activated NF-κB via toll-like receptor 5 (TLR5). Surprisingly, a

number of cell lines found to be unresponsive to flagellin express TLR5 and expression of exogenous TLR5 in these cells induces NF-κB activity in response to flagellin challenge although not robustly. Conversely, overexpression of dominant-negative TLR5 alleles only partially blocks NF-κB activation by flagellin. These observations are consistent with the possibility of either a very stable TLR5 signaling complex, the existence of a low abundance flagellin co-receptor or required adapter, or both. These collective results provide the evidence that flagellin acts as the main determinant of *Salmonella* mediated NF-κB and proinflammatory signaling and gene activation by this flagellated pathogen. In addition, expression of the *fli C* gene appears to play an important role in the proper functioning of the TTSS since mutants that fail to express *fli C* are defective in expressing a subset of Sip proteins and fail to invade host cells. Flagellin added in *trans* cannot restore the ability of the *fli C* mutant bacteria to invade intestinal epithelial cells. Lastly, TLR5 expression in weak and non-responding cells indicates that additional factors may be required for efficient signal propagation in response to flagellin recognition.

5.2 INTRODUCTION

Intestinal epithelial cells serve as a barrier between the luminal microflora and the body and as such are perfectly positioned to monitor the approach/invasion of pathogens. These intestinal epithelial cells (IECs) serve as innate immune sentinels and monitor their environment and constantly give out innate host defense instruction to local immune effector cells (Eckmann et al., 1995; Kagnoff and Eckmann, 1997). Pathogens such as *Salmonella* and other enteroinvasive pathogenic bacteria such as enteroinvasive *E. Coli*, *Shigella* and *Yersinia* upon infection of IECs leads to the up-regulation of the expression

of host genes, the products of which activate mucosal inflammatory and immune responses and alter epithelial cell functions (Eckmann et al., 1997; Elewaut et al., 1999; Jung et al., 1995; Witthoft et al., 1998). Previously we and others demonstrated that IKK via NF-κB and the SAPK signaling pathways via Jun N-terminal kinase (JNK) and p38 kinase were key regulators of the up-regulation of the proinflammatory gene program (Chen et al., 1996; Elewaut et al., 1999; Hardt et al., 1998; Hobbie et al., 1997), with NF-κB appearing to be the most critical (Elewaut et al., 1999). Typically *Salmonella* infects thirty-forty percent of IECs in culture models of infection (Valdivia et al., 1996), however, we and others have found that *Salmonella* infection activates NF-κB DNA binding activity to levels equivalent to that of TNFα which activates NF-κB in all of the cells (Elewaut et al., 1999). Previous studies examining NF-κB activation by *Salmonella* in HT29 colonic intestinal epithelial cells, which serve as model colonic epithelial cells in culture, indicated that delivery of *Salmonella* proteins into the host cell via its type III secretion system (TTSS), such as SopE and SopE2, the bacterially encoded exchange factors for the Rho-family members Rac1 and CdC42, result in exchange factor activation, cytoskeletal rearrangements and activation of the MAPK, SAPK and NF-κB signaling pathways (Bakshi et al., 2000; Galan, 2001; Galan and Collmer, 1999; Hardt et al., 1998; Hobbie et al., 1997; Kubori and Galan, 2002; Wood et al., 1996). Recent observations that utilized *Salmonella* strains that were defective in invasion and delivery of invasion proteins by the TTSS but not attachment indicated that additional factors other than those delivered by the TTSS could lead to NF-κB activation (Eaves-Pyles et al., 1999). Presently it is not clear what protein(s) dictate the activation of key signaling pathways that lead to the temporal expression of the proinflammatory gene program,

although the SopE proteins have been given extreme attention recently (Hardt et al., 1998; Hobbie et al., 1997; Wood et al., 1996).

In searching for additional *Salmonella* proteins that could activate the proinflammatory gene expression program, bacterial flagellin was recently found to be such a protein (Eaves-Pyles et al., 1999; Gewirtz et al., 2001b; McDermott et al., 2000) and had been shown previously to activate IL-8 expression in monocytes (Ciacci-Woolwine et al., 1998; McDermott et al., 2000; Moors et al., 2001). Flagellin was found to activate NF-κB in polarized epithelial cells only when flagellin was present on their basolateral surface (Gewirtz et al., 2001a) consistent with the idea that a cell surface receptor was present there and could recognize it. The toll-like receptors (TLRs) have been found to recognize pathogen associated molecular patterns (PAMPs) reviewed in (Akira, 2001; Akira and Hemmi, 2003; Medzhitov and Janeway, 2000; O'Neill, 2001). TLR2 interacts with TLR1 and TLR6 to recognize bacterial lipopeptides and zymosan respectively (Hajjar et al., 2001; Ozinsky et al., 2000). TLR4 recognizes LPS only when associated with its co-receptor MD2 and CD14 (Backhed et al., 2002; da Silva Correia et al., 2001; Kawasaki et al., 2001; Nagai et al., 2002). Recently, flagellin was demonstrated to be recognized by TLR5 and activate an innate host response (Gewirtz et al., 2001a; Hayashi et al., 2001). However, little was known or demonstrated about the endogenous levels of TLR5 in cells used in those studies and why those cells failed to respond to flagellin. Here we have identified flagellin as the primary initiator and temporal regulator of not only the major signaling pathways activated during *Salmonella* infection but also of key target genes of the proinflammatory gene program too. We have also found flagellin expression to be required for *Salmonella* bacterial invasion. Independently we

found TLR5 recognizes flagellin but its signaling activity toward this PAMP is consistent with either the aid of another flagellin-recognizing co-receptor (as TLR4 utilizes for LPS) or the use of another adapter protein, perhaps similar to MyD88, that is absent or present at low levels in flagellin non-or low-responding cells.

5.3 MATERIALS AND METHODS

5.3.1 Materials

Human tumor necrosis factor alpha (TNFα) and human IL-1 were purchased from R&D Systems (Minneapolis, MN). Tris [hydroxymethyl]aminomethane (Tris) was purchased from Fisher Scientific (Fairlawn, NJ). Fetal calf serum was purchased from US Biotechnologies Inc. (Parkerford, PA). Para-nitro-phenylphosphate (PNPP) was purchased from Aldrich Chemical (Milwaukee, WI). The Polyacrylamide gel electrophoresis (PAGE) supplies: acrylamide, bis-acrylamide, sodium dodecyl sulfate (SDS), TEMED, and ammonium persulfate were purchased from Bio-Rad Laboratories (Hercules, CA). Dulbecco's modified essential medium (DMEM), DMEM:F12, phosphate buffered saline (PBS), glutamine, penicillin G, streptomycin, amphotericin B, and Grace's Insect medium were purchased from Invitrogen (Carlsbad, CA). Luria Broth (LB) was purchased from Becton Dickson and Co (Sparks, MD). The protease inhibitors: aprotinin, bestatin, leupeptin, pepstatin A, and phenylmethylsulfonyl fluoride (PMSF) were purchased from Cal Biochem (La Jolla, CA). Protease inhibitor cocktail contained 10 μg/ml aprotinin, 2.5 μg/ml leupeptin, 8.3 μg/ml bestatin, and 1.7 μg/ml pepstatin A. Phorbol 12-myristate 13 acetate (PMA), N-[2-hydroxyethyl]piperazine-N'-[2-ethanesulfonic acid] (Hepes), anisomycin, and 2-[N-morpholino]ethanesulfonic acid (MES) were purchased from Sigma Chemical (St. Louis, MO).

5.3.2 Cell culture

HT29 human intestinal (colorectal adenocarcinoma) epithelial cells (ATCC HTB-38), HeLa cervical epithelial adenocarcinoma cells (ATCC CCL-2), 293T kidney cells (CRL-11268), A549 lung carcinoma cells (ATCC-185), and T98G glioblastoma cells (ATCC CRL-1690) were cultured in DMEM with 2 mM glutamine, 10% Fetal Calf Serum, 100 Units/ml Penicillin G, and 100 μg/ml Streptomycin at 37°C in a humidified 5% CO_2 atmosphere. T84 colorectal carcinoma cells (ATCC CCL-248) were cultured in DMEM:F12 with 2 mM glutamine, 5% Fetal Calf Serum, 100 Units/ml Penicillin G, and 100 μg/ml Streptomycin at 37°C in a humidified 5% CO_2 atmosphere. H5 insect cells (Invitrogen) were cultured in Grace's medium with 2 mM glutamine, 10% Fetal Calf Serum, 100 Units/ml Penicillin G, 100 μg/ml Streptomycin, and 0.25 μg/ml amphotericin B at 28°C. MyD88$^{-/-}$ & TLR2$^{-/-}$/TLR4$^{-/-}$ double knockout cells were obtained from Shizuo Akira and Osamu Takeuchi (Univ. of Osaka, Japan) and grown in DMEM with 2 mM glutamine, 10% Fetal Calf Serum, 100 Units/ml Penicillin G, and 100 μg/ml Streptomycin at 37°C in a humidified 5% CO_2 atmosphere.

5.3.3 Bacterial strains

Salmonella typhimurium strain SJW1103 (FliC, phase 1 flagellin, stabilized) (Yamaguchi et al., 1984) is a wild-type *Salmonella typhimurium* and can only express the Phase I fliC flagellin, SJW86 (SJW1103 FliC::TN10), and SJW134 (SJW1103 FliC and FljB deletions) were obtained from Robert Macnab (Yale Univ., Conn) and have been described (Williams et al., 1996). *Salmonella* serovar dublin strain 2229, strain SE1 (2229 SopE mutant), strain SB2 (2229 SopB mutant), and SE1SB2 (2229 SopE and SopB mutant) were obtained from Edward Galyov (Compton Laboratory, Berkshire, UK) and

have been described (Bakshi et al., 2000; Wood et al., 1996). *Salmonella* strains for stimulation were grown in LB at 37°C without agitation for 16 hours, centrifuged at 6,000 × g for 1 minute, gently washed with PBS, and gently suspended in DMEM to maintain cells with attached flagella.

Plasmid pFM10.1 (ampicillin resistance), encodes a green fluorescent protein (GFP) expressed after the *Salmonella* host is internalized by mammalian cells, obtained from Stanley Falkow (Stanford Univ., Stanford, CA) (Valdivia and Falkow, 1997; Valdivia et al., 1996) and was transformed into strains SJW1103 and SJW134 by electroporation. Strains containing pFM10.1 were designated SJW1103G and SJW134G.

5.3.4 Preparation and analysis of Salmonella cell free culture supernatant

Native flagellin was harvested from *S. dublin* 2229 or *S. typhimurium* SJW1103. Starter cultures were grown in Luria broth (LB) for 18 hours at 37°C with aeration, diluted 1:5000 in fresh LB, and grown for 12 hours under the same conditions. All subsequent procedures were performed at 4°C. Cells were removed from the medium by centrifugation at 10,000 × g for 5 min and discarded. The supernatant containing flagellin was filtered through a 0.8 micron filter (Millipore, Bedford, MA) to remove residual cells. Supernatant was concentrated 100 fold using an Amicon 100 kiloDalton (kDa) cutoff membrane (Millipore). Initial studies used concentrated culture supernatant from *S. dublin* strain 2229 that was treated with DNase, RNase, Protease K, boiled for 20 min or 100 mM DTT at 37°C for 2 hours and used for stimulation of cultured cells.

Concentrated *S. typhimurium* 1103 bacterial culture supernatant was washed 4 times by 1:10 dilution with 50 mM MES, pH 6.0, 50 mM NaCl and re-concentrated. Material not retained by the 100 kDa membrane was discarded. Washed culture supernatant was fractionated by gel permeation or anion exchange chromatography for analysis. For long-term storage, washed culture supernatant was supplemented with protease cocktail and stored at -20°C.

Fractionation by gel permeation chromatography was performed with a Superose 12HR column (Pharmacia) on a Bio-Logic system (Bio-Rad). One-half mililiter of 100× washed supernatant (equivalent of 50 ml original culture supernatant) was separated on the column at 0.4 ml/minute in 50 mM Hepes, pH 7.4, 200 mM NaCl. Fractions (0.5 ml) were collected, and 50 µl was fractionated by SDS-PAGE and stained with Bio-Safe Coomassie (Bio-Rad). Thirty microliters of each fraction was used for stimulation of

HT29 cells (60 mm dishes) for 45 min and NF-κB DNA binding activity in the resulting whole cell extracts were assayed by EMSA. The column was standardized with catalase (232 kDa), aldolase (158 kDa), albumin (67 kDa), ovalbumin (43 kDa), and Chymotripsinogen A (25 kDa), all obtained from Amersham-Pharmacia.

Fractionation by anion exchange chromatography was performed with Poros HQ matrix (2 ml column, PerSeptive Biosystems, Farmingham, MA) on a Bio-Logic system. Five mililiters of 100× washed supernatant (equivalent of 500 ml original culture supernatant) was separated at 1 ml/minute in 50 mM Hepes, pH 7.4, and a NaCl gradient from 50–500 mM. Fractions were collected and 5 µl of each fraction was examined by 10% SDS-PAGE. Proteins were fractionated on duplicate 10% SDS-PAGE precast gels (BioRad). One gel was stained with Bio-Safe Coomassie (Bio-Rad) and the protein bands were isolated for Mass Spectroscopy analysis (CCF Mass spectroscopy core facility) from the other identical non-stained gel, by electro-elution with a whole gel eluter (Bio-Rad) and SDS was removed with SDS-Out (Pierce, Rockland, IL) per the manufacturer's directions. Proteins isolated from bands B1 to B6 were acetone precipitated by addition of 20 µg Aprotinin and 5 µg of BSA to each eluted fraction, ice-cold acetone (-20°C) was added to 80%, mixed well and precipitated overnight at -20°C. Proteins were pelleted by centrifugation at 14,000 × g in the cold for 30 min, acetone/liquid was removed and the pellets washed 2× with 1 ml acetone (-20°C). After removal of the acetone, protein pellets were air dried and then resuspended and denatured in 5 µl of 6 M guanidinium hydrochloride (Gu-HCl) at room temperature for 30 min. Resuspended proteins were two-fold serially diluted in DMEM to a final Gu-HCl concentration of 55 mM to renature the proteins. Two hundred fifty microliters of individual renatured proteins/DMEM were

added per ml to HT29 cells (60 mm dishes) and whole cell extracts were prepared 45 min after stimulation and were assayed for NF-κB DNA binding activity by EMSA.

5.3.5 Purification of flagellin (purified flagellin)

The washed and concentrated culture supernatant from *S. typhimurium* 1103 containing flagellin was boiled for 20 minutes and precipitants removed by centrifugation at 15,000 × g. The supernatant containing flagellin was diluted 1:2 with 50 mM MES, pH 6.0, 50 mM NaCl and mixed with 2 ml Poros SP cation exchange matrix (PerSeptive Biosystems) per 1 liter of original culture. The Poros SP matrix was prepared as a 50% slurry and equilibrated with 50 mM MES, pH 6.0. The flagellin preparation and matrix were mixed on a roller at 12 to 14 RPM for 2 hours. The matrix along with bound contaminants was removed by filtration through a 0.85 micron filter and discarded, flagellin failed to bind to the cation exchange matrix at pH 6.0 and eluted in the flowthrough and was collected.

The pH of the flowthrough was adjusted by five-fold dilution of the sample with 50 mM Hepes, pH 7.8, 50 mM NaCl, and loaded onto a Poros HQ anion exchange column (2 ml column, PerSeptive Biosystems) equilibrated with 50 mM Hepes, pH 7.4, 50 mM NaCl. The column was washed with 2 volumes 50 mM Hepes, pH, 7.4, 50 mM NaCl, and eluted with a 10 column volume linear gradient of 50–500 mM NaCl in 50 mM Hepes, pH 7.4. Flagellin eluted from the column between 200–275 mM NaCl. Fractions containing flagellin were pooled and concentrated. The preparation was determined to be pure by electrophoresis of 5 μg protein by SDS-PAGE and stained with Bio-Safe Coomassie (Bio-Rad). Samples were stored at -80°C in 50 mM Hepes, pH 7.4, approx

225 mM NaCl, 10% glycerol and protease cocktail. A 4 liter preparation of culture supernatant yielded 2 mg purified flagellin.

5.3.6 In-gel tryptic digestion and protein identification by LC-MS

Gels were fixed and stained (Bio-Safe Blue, BioRad). All of the following procedures were performed by the CCF Mass spectroscopy core facility. Excised gel bands were reduced (100 mM DTT), and alkylated (100 mM iodoacetamide). Proteins in the gel bands were digested with modified trypsin (Promega, 20 μg/mL) with an overnight incubation at 37°C. Tryptic peptides were extracted from the gel with 50% acetonitrile, 0.1% acetic acid, concentrated in a SpeedVac (Thermo Savant) to remove acetonitrile, and reconstituted to 20 uL with 0.1% acetic acid. Extracted peptides were subjected to reversed phase (50 uM ID packed with Phenomenex Jupiter C18, 6 cm capillary column) liquid chromatography (2%–70% solvent B; Solvent A, 50 mM acetic acid, aqueous, Solvent B acetonitrile), coupled to a Finnigan LCQ DECA ion trap mass spectrometer for peptide sequencing, as described (DiDonato et al., 1997a).

5.3.7 Preparation of GST-IκBa1-54 and GST-cJUN1-79 kinase substrates

IκBα amino acids 1 to 54 fused to GST or cJUN amino acids 1–79 fused to GST were prepared as previously described (DiDonato, 2000; DiDonato et al., 1997a; Hibi et al., 1993) and stored in kinase buffer (20 mM Hepes, pH 7.6, 10 MM MgCl2, 10 mM NaCl, 2 mM beta-glycerophosphate, 10 mM PNPP).

5.3.8 Preparation of cells for microscopy

HT29 cells for microscopic examination were grown in 6 well plates on sterile cover slips to a density of 50–75%. Cells were stimulated as described above. After stimulation,

cover slips with HT29 cells were washed 2 times with ice cold PBS and fixed with 4% w/v formalin at room temperature for 20 minutes. Cells were washed 4 times with PBS prior to mounting for visualization of *Salmonella* invasion. Cover slips were mounted with Vectashield mounting medium with DAPI (Vector Laboratories, Burlingame, CA), and cover slips sealed to slides.

Cells for antibody staining were treated with absolute methanol for 20 minutes following formalin fixation, then washed 3 times with PBS supplemented with 0.1% BSA (PBSB) and used directly or stored in the cold after azide was added to 0.02%. For p65(RelA) localization, cells on coverslips were blocked for 1 h at 37°C with PBS supplemented with 1% BSA. The PBSB was removed, washed once with PBSB and coverslips were placed cell-side down onto 150 µl of p65 antibody (Zymed, South San Francisco, CA) diluted 1:1500 in PBSB on a square of parafilm and placed in a humidified chamber at 37°C for 1.5 h. Coverslips were removed and placed cell-side up in 6-well dishes and washed 3 × 5 min with PBSB. Coverslips were then removed and placed cell-side down onto 150 µl of FITC-labeled donkey anti-rabbit secondary antibody (Jackson Immunoresearch Laboratories, West Grove, PA) (1:300 in PBSB) on a square of parafilm and placed in a humidified chamber at 37°C for 1.5 h. Coverslips were removed and placed cell-side up in 6-well dishes and washed 5 × 5 min with PBSB, removed and placed cell-side down onto slides mounted with Vectashield (Vector Laboratories, Burlingame, CA) with DAPI and then sealed. NF-κB localization was determined by indirect immunofluorescence. Samples were observed on a Leica DMR upright microscope (Leica Microsystems Inc., Heidelberg, Germany) at 400× with oil immersion and equipped with FITC and UV filters. Images were collected with a MicroMax RS

camera (Princeton Instruments Inc., Princeton, NJ), and Image Pro plus, version 4.5, software (Media Cybermetics Inc., Carlsbad, CA). Color enhancements were performed with Image Pro plus software. Visible light plus color overlays for (**Fig. 5.1 and Fig. 5.5b**) were performed with MetaMorph Software (Universal Imaging Corp., Downington, PA).

5.3.9 Bacterial infection and cell stimulation

Mouse embryo fibroblasts (MEFs) or HT29 cells were grown in DMEM as above to a density of 90% prior to stimulation. All cells were washed with warm PBS and supplemented with DMEM without serum or antibiotics in preparation for stimulation. Cells were stimulated with; 10 ng/ml TNFα, 1 μg/ml flagellin unless specified otherwise, 20 μg/ml Anisomycin, 12.5 ng/ml PMA, or 10^8 *Salmonella*/ml at 37°C for desired times and extracts prepared as below. Cells harvested beyond one hour were washed with warm PBS and supplemented with warm DMEM, 2 mM glutamine, and 200 ug/ml gentamycin after 1 hour and returned to 37°C until extract preparation desired.

5.3.10 Whole cell extract preparation

Cells were washed with ice-cold PBS and all subsequent steps carried out at 4°C or on ice. Cells were scraped from the dish in ice-cold PBS, and collected by centrifugation at 1000 × g for 1 minute. Cells were lysed by suspension in 50 mM Tris-HCl, pH 7.6, 400 mM NaCl, 25 mM beta-glycerol phosphate, 25 mM NaF, 10 mM PNPP, 10 % glycerol, 0.5 mM sodium orthovanadate, 0.5% nonidet-40 (NP-40), 5 mM benzamidine, 2.5 mM metabisulfite, 1 mM PMSF, 1 mM DTT and protease inhibitor cocktail as described (Elewaut et al., 1999).

5.3.11 Electromobility shift assays (EMSA)

NF-κB DNA binding assays were carried out as previously described (DiDonato et al., 1997a; DiDonato et al., 1995a; Elewaut et al., 1999). Anti-p65 antibody (Zymed, South San Francisco), anti-p50 antibody (Santa Cruz Biotechnologies, Santa Cruz, CA), and anti-STAT3 antibody (Santa Cruz) were used for EMSA supershifts.

5.3.12 Invasion assay

HT29 cells, 90–95% confluent in 35 mm round dishes, were prepared for stimulation as above and treated with a 1 ml suspension of Salmonella SJW1103 or SJW134 or left untreated in triplicate as above. After one hour, HT29 cells were washed 4× with warm PBS, supplemented with warm DMEM, 2 mM glutamine, and 200 μg/ml gentamycin, and incubated at 37°C for 4 hours. Cells were then harvested as above and lysed by suspension in 1 ml sterile distilled water. Ten-fold serial dilutions were prepared in PBS and 100 μl of each dilution was plated on LB agar plates and grown at 37°C for 20 hours. Colonies were counted and averaged.

5.3.13 Kinase assays

Whole cell extracts (250 μg) were supplemented with 150 μl of Buffer A (20 mM Hepes, pH 7.9, 20 mM beta-glycerophosphate, 10 mM NaF, 0.1 mM orthovanadate, 5 mM PNPP, 10 mM 2-mercaptoethanol, 0.5 mM PMSF, and protease inhibitor cocktail), and immuno precipitation kinase assays carried out as described (Elewaut et al., 1999) using either IKKα monoclonal antibody (PharMingen – Becton Dickson), anti-JNK1 (Santa Cruz Biotechnologies, Santa Cruz, CA), or anti-hemagglutinin (HA) epitope antibody (Covence Antibodies, Princeton, NJ) as indicated. Protein G immunopellets were collected by centrifugation at 500 × g for 30 sec, washed 3 times with Buffer B

(Buffer A plus 250 mM NaCl), and one time with Buffer C (Buffer A plus 50 mM NaCl and 10 mM $MgCl_2$). Immunopellets were resuspended in 30 µl Kinase buffer with 0.1 mM orthovanadate, 50 µM "cold" ATP, 5 µCi γ-^{32}P-ATP, 2 mM DTT, and 2 µg of soluble GST-IκBα1–54 or GST-cJUN1-79, and incubated at 30°C for 30 minutes. Reactions were stopped by the addition of 15 µl 4× SDS-PAGE loading buffer, heated at 95°C for 5 minutes, and resolved on 10% SDS-PAGE gels by standard procedures. Gels were rinsed, stained with Bio-Safe Coomassie (Bio-Rad) to visualize protein bands, rinsed, photographed then dried and exposed to Kodak X-OMAT AR film (Eastman Kodak Co., Rochester, NY) to detect substrate phosphorylation.

5.3.14 Immunoblotting

Protein samples (40 µg) were resolved by SDS-PAGE on a 10% acrylamide gels by standard procedures, and proteins transferred to PVDF membrane (Millipore) and probed with antibodies as described (Elewaut et al., 1999). Membranes were washed 3× briefly with TBST, incubated with a 1:1000 dilution (1:800 for anti-TLR5) of the primary antibody in TBST, 1% non-fat milk for 1 hour, washed 3 × 5 min with TBST, and then incubated with a 1:2000 dilution of the appropriate HRP-conjugated secondary antibody in TBST, 0.5% non-fat milk for 1 hour. Primary antibodies used were: anti-IKKα/β (H-470, Santa Cruz), anti-JNK1, anti-ERK2 (K-23, Santa Cruz), anti-phospho-ERK (E-4, Santa Cruz), anti-p38MAPK (Cell Signaling Technologies, Beverly, MA), anti-phosopho-p38MAPK (Cell Signaling), anti-TLR5 (H-127, Santa Cruz), anti-muc1 (H-295, Santa Cruz) and anti-actin (C-11, Santa Cruz). Secondary antibodies used were: anti-mouse IgG HRP conjugate (Amersham-Pharmacia), anti-rabbit IgG HRP conjugate (Amersham-Pharmacia), anti-goat IgG-HRP conjugate (Santa Cruz). HRP activity was

detected by ECL (Amersham-Pharmacia) as per manufacturer's instructions, on Kodak X-OMAT AR film.

5.3.15 Construction of dominant-negative TLRs

All DN-TLRs were constructed using PCR. The universal 5' primer consisted of a 5'KPN I restriction site followed by sequences encoding the kozak sequence, translational start site, and preprotrypsin leader sequence of pCMV-1 (Sigma) that all the wild-type TLRs were initially cloned into. The 3' anti-sense (AS) primers were human TLRgene-specific primers (sequences available upon request) that created a stop codon immediately after a conserved tryptophan in Box 9 of the TLR TIR homology domain according to Bazan (Rock et al., 1998), thus creating carboxy terminus deletions. The 5' end of the AS primer contained a number of convenient restriction sites to allow directional cloning. PCR was performed with turbo-Pfu polymerase (Stratagene, La Jolla, CA) using standard procedures on individual wild-type TLR pCMV-1 plasmid DNAs (5 ng each, kind gifts of R. Medzhitov, Yale Univ. and R. Ulevitch, TSRI) (Alexopoulou et al., 2001; Chuang and Ulevitch, 2000) with the 150 ng each of the universal 5' sense primer and individual gene-specific TLR 3' primers. PCR products were cleaned-up with PCR cleanup kit (Qiagen, Germany) digested with appropriate restriction enzymes, gel purified and then ligated into the mammalian expression vector pCDNA3.1 (Invitrogen). Positive clones were sequenced to verify the mutations and tested for expression in transient expression assays and detected on immunoblots by probing with anti-FLAG M2 monoclonal antibody (Sigma). All wild-type and DN-TLR alleles are amino terminus FLAG epitope-tagged.

5.3.16 Transfections

HT29 cells were transfected with Lipofectamine Plus (Invitrogen) as previously described (Elewaut et al., 1999). In transfections monitoring reporter gene expression, transfections were performed at least three times in 6 well dishes in triplicate with the total DNA mass kept constant at 4 μg (2 μg effector plasmid DNA, 100 ng 2× NF-κB Luc reporter gene, 50 ng pRL-TK, a thymidine kinase promoter driven *Renilla* luciferase normalization reporter and 1.85 μg pCDNA3.1 plasmid DNA as bulk filler DNA) and fire-fly luciferase expression was normalized to *Renilla* luciferase expression using the dual-luciferase assay (Promega, Madison, WI). Fold inductions were calculated and values between experiments did not vary more than 15%, a representative experiment is presented. Transfection of 293T cells was performed with lipofectamine 2000 (Invitrogen) in 6-well dishes in triplicate as per the manufacture's protocol. TLR expression plasmids were added at 2 μg/well, and NF-κB and normalization control plasmids were as above with HT29 cells and pCDNA3.1 plasmid DNA as bulk filler DNA to a final DNA mass of 4 μg/well. Fold inductions were calculated and values between experiments (N of 3) did not vary more than 10%, a representative experiment is presented.

5.3.17 Real Reverse Transcription and Real Time PCR (RT^2PCR)

Cells (N = 3) were stimulated 3 hours at 37°C with TNFα or FliC or left untreated and harvested for total RNA isolation. Total cellular RNA was extracted from cells with Trizol reagent (Invitrogen) (Elewaut et al., 1999) and reverse transcribed with ReactionReady first strand cDNA synthesis kit (SuperArray Bioscience Corp., Fredrick, MD). RNA (2.5 ug per 20 ul reaction) was reverse transcribed using random primers and

Moloney murine leukemia virus reverse transcriptase per manufacturer specified conditions. Controls without reverse transcriptase (minus RT) was also generated for each RNA sample. RT^2PCR was performed with an iCycler (Bio-Rad) to quantify TLR1 through TLR10 mRNA, 18S rRNA, and GAPDH mRNA. RT^2PCR (25 ul reaction volume) was performed with the appropriate primers (SuperArray) per manufacturers instructions in triplicate with HotStart Taq DNA polymerase (SuperArray) at 95°C for 15 min to activate Taq and amplified for 40 cycles (95°C, 30 sec, 55°C, 30 sec, 72°C, 30 sec). RT^2PCR was performed on the minus RT controls with TLR5 primers to detect DNA contamination. Real-time PCR analysis was performed using SYBR-green (Perkin-Elmer) according to manufacture's instructions with the specific primer pairs indicated above and primer pairs for 18S ribosomal RNA as reference RNA (Classic 18S primer pairs – Ambion Inc). Cycle time (Ct) was measured using the iCycler™ and its associated software (Bio-Rad). Relative transcript quantities were calculated by the ΔΔCt method using 18S ribosomal RNA as a reference amplified from samples using the Classic 18S primer pairs from Ambion, Inc (Austin, TX). Normalized samples were then expressed relative to the average ΔCt value for untreated controls to obtain relative fold-change in expression levels. Fold change in mRNA expression was expressed as $2^{\Delta\Delta Ct}$. ΔCt is the difference in threshold cycles for the TLR mRNAs and 18S rRNA. ΔΔCt is the difference between ΔCt non-simulated control and ΔCt stimulated sample. Values for fold-induction varied less than 5% among replicates.

5.4 RESULTS

5.4.1 Salmonella infection leads to a minority of cells invaded but activates NF-κB in nearly all cells

Previously, we have noted that pathogenic *Salmonella sp*. infection leads to potent IKK and NF-κB activation and activation of the proinflammatory gene program (Elewaut et al., 1999). Previous studies suggest that about thirty-forty percent of the intestinal epithelial cells are infected during a typical *Salmonella* infection in cultured intestinal epithelial cells (Valdivia et al., 1996). We wished to address the question of how bacterial infection of about thirty percent of the host cells could give rise to NF-κB DNA binding activity equivalent to activation of NF-κB in nearly all of the host cells as TNFα treatment of the cells does. To examine this phenomenon in detail HT29 cells either mock-infected or infected at a MOI of fifty for one-hour with wild-type *S. typhimurium* that had been transformed with the plasmid pFM10.1, that encodes green fluorescent protein (GFP) under the control of the *Salmonella* ssaH promoter and only functions once the bacteria has invaded the host cell (Valdivia and Falkow, 1997). As can be seen in (**Fig. 5.1a**), GFP expression occurs in about thirty to forty percent of the cells. We next examined the localization of the NF-κB subunit p65 (RelA) in non-treated (mock-infected), *Salmonella* infected or TNFα (10 ng/ml) stimulated cells and found that p65 (RelA) was localized to the cytoplasm in non-treated cells whereas, in *Salmonella* infected cells or in TNFα treated cells p65 (RelA) had localized to the nucleus (**Fig. 5.1b**). These results demonstrate that *Salmonella* infection activates NF-κB in virtually all of the cells even though only a minority of them become infected and is consistent

with and aids in explanation of our previous results examining *Salmonella* infection and NF-κB activation (Elewaut et al., 1999).

FIGURE 5.1

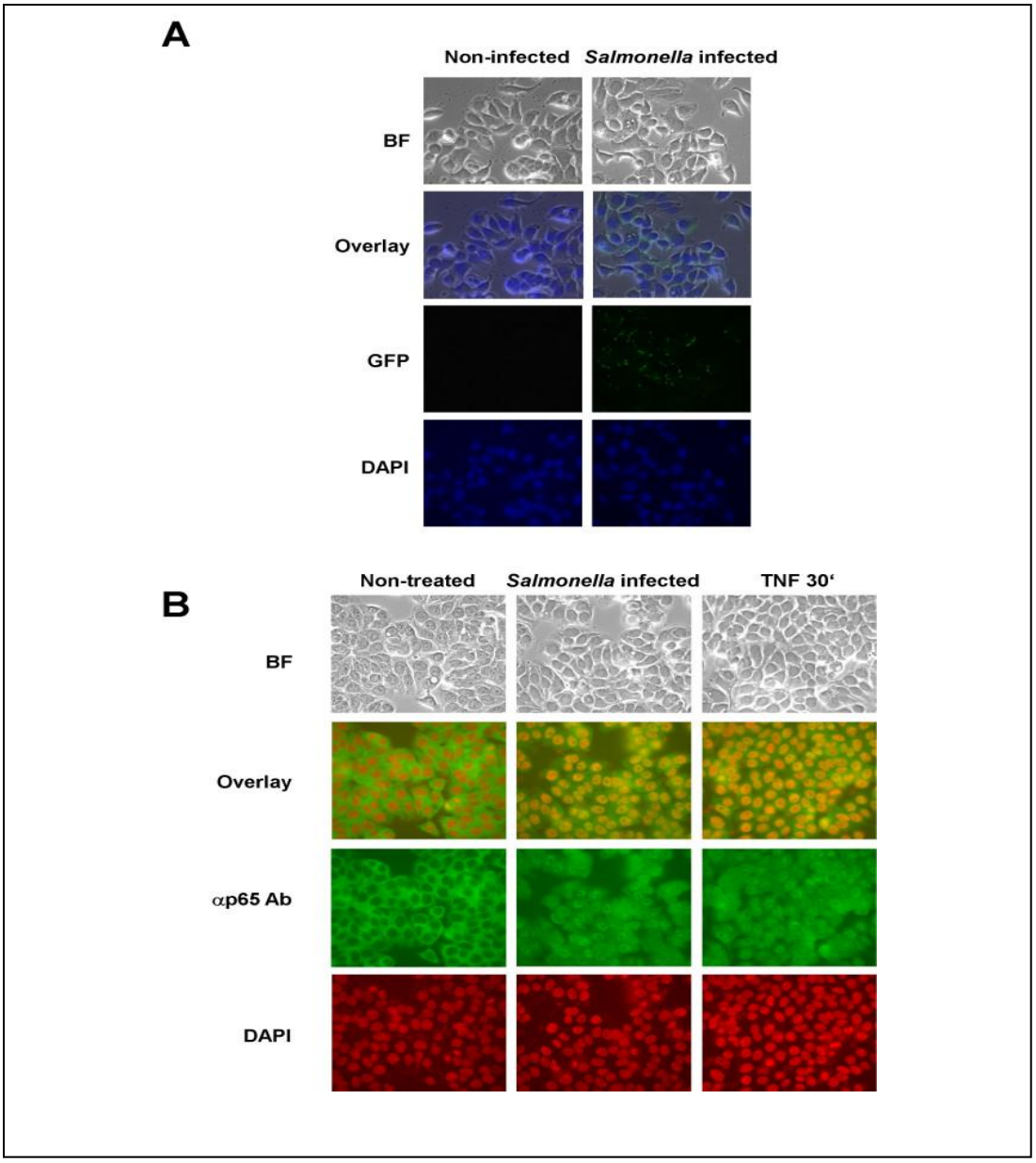
A
Non-infected
Salmonella infected
BF
Overlay
GFP
DAPI
B
Non-treated
Salmonella infected
TNF 30'
BF
Overlay
αp65 Ab
DAPI

Figure 5.1: *Salmonella* infection leads to NF-κB nuclear localization even in non-infected cells.

HT29 cells were grown on glass coverslips and either mock-infected, left untreated, infected with *Salmonella typhimurium*, or treated with TNFα (10 ng/ml). Cells fixed after 30 min (TNF) and 1 h (*Salmonella*) as described in Experimental Procedures and *Salmonella* that had invaded HT29 cells were detected by direct fluorescence microscopy of GFP expression, p65(RelA) localization was monitored by indirect immunoflourescence of rabbit anti-p65 antibody detected with FITC-conjugated donkey anti-rabbit antibody. DAPI was used to stain nuclei. **a**, HT29 cells were mock-infected or infected at an MOI of 50 with *Salmonella typhimurium* strain SJW1103G which expresses GFP from the ssaH promoter that is only active inside infected host cells (Valdivia and Falkow, 1997; Valdivia et al., 1996). Cells were photographed using bright field microscopy (BF), and immunoflourescence to detect GFP or DAPI staining as indicated. Images were merged (overlay)to reveal cells that were infected. **b**, HT29 cells were left untreated, infected with *Salmonella typhimurium* strain 1103 or treated with TNFα. NF-κB p65(RelA) localization under various conditions as indicated was monitored by indirect immunofluorescence. Cells were visualized by bright field microscopy (BF), cell nuclei were stained with DAPI and p65(RelA) was visualized with FITC. DAPI staining was falsely colored red to make visualization of the merge (overlay) easier to distinguish.

5.4.2 Soluble bacterial product identified as flagellin can activate NF-κB in intestinal epithelial cells

Since *Salmonella sp*. infection of intestinal epithelial cells in culture led to only roughly thirty percent infection but activation of NF-κB in nearly all of the cells, we anticipated that NF-κB activation was in response to host cell recognition of bacteria structural components or products produced by the bacteria and not by the invasion process. Invasion itself has been demonstrated not to be required for activation of the proinflammatory gene program as had previously been thought (Eaves-Pyles et al., 1999). To investigate this possibility sterile-filtered *S. dublin* culture broth left either untreated or boiled for twenty minutes was used to challenge HT29 intestinal epithelial cells and NF-κB DNA binding activity was monitored by electromobility shift assays (EMSAs) of whole cell extracts (WCE) prepared forty-five minutes after exposure (DiDonato et al., 1995a; Elewaut et al., 1999). Potent activation of NF-κB in response to the broth under both conditions was observed indicating the activating factor was heat-stable (AD, TT and JD, personal observations) and is not LPS since HT29 cells are not responsive to LPS (DiDonato et al., 1995a; Elewaut et al., 1999).

The native sterile-filtered concentrated broth was subsequently treated with DNase, RNase, proteinase K or crudely size fractionated on 100 kDa centricon filters. The variously treated broths were then used to challenge HT29 intestinal epithelial cells and WCEs were prepared after forty-five minutes and NF-κB DNA binding activity was analyzed by EMSA (**Fig 5.2a**). Direct infection of HT29 cells by *S. typhimurium* 1103 or exposure to the culture broths (supt), as indicated, induced NF-κB DNA binding activity, while the activity-inducing factor was found to be sensitive to protease digestion and was

retained by a 100 kDa filter (**Fig. 5.2a**). To further determine the identity of the NF-κB inducing activity, sterile-filtered concentrated broth culture was fractionated by Superose 12 gel permeation chromatography (**Fig. 5.2b**) and by anion exchange chromatography (**Fig. 5.2c**). Aliquots of chromatography fractions were assayed for their ability to activate NF-κB in HT29 cells and analyzed by EMSA. As can be seen from the Coomassie blue stained gel (Fig. 2b, top panel) increased NF-κB DNA binding activity (**Fig. 5.2b, lower panel lanes 4–6**) corresponded to the increased abundance of an approximately 55 kDa protein. Anion exchange chromatography on POROS HQ matrix and elution of bound proteins with an increasing salt gradient as indicated (**Fig. 5.2c**) demonstrated that NF-κB DNA binding-inducing activity corresponded to chromatographic fractions containing an increased abundance of the 55 kDa protein (**Fig. 5.2c top panel, and data not shown**). Eluted fractions observed in **Fig. 5.2c** were concentrated and fractionated on preparative 12% SDS-PAGE gels and bands corresponding to B1-B6 were cut from the gels and the proteins eluted, precipitated and renatured as described in Experimental Procedures and used to stimulate HT29 cells. Whole cell extracts from these cells were assayed for NF-κB DNA binding-inducing activity by EMSA and only band 2 (B2) corresponding to the 55 kDa protein (**Fig. 5.2c lower panel**) was able to elicit NF-κB DNA binding activity while buffer from the beginning or end of the salt gradient failed to activate NF-κB DNA binding activity.

Proteins corresponding to protein bands B1-B6 and blank areas of the gel were further processed for peptide sequencing as described in Experimental Procedures. Trypsin digestion of the protein corresponding to B2 and analysis by electrospray ion trap LC/MS identified the amino acid sequence of twenty-one peptides. Flagellin (seventy-

five percent coverage by the twenty-one peptides) was unambiguously identified as the protein consistent with inducing NF-κB DNA binding activity (**Fig 5.3**).

FIGURE 5.2

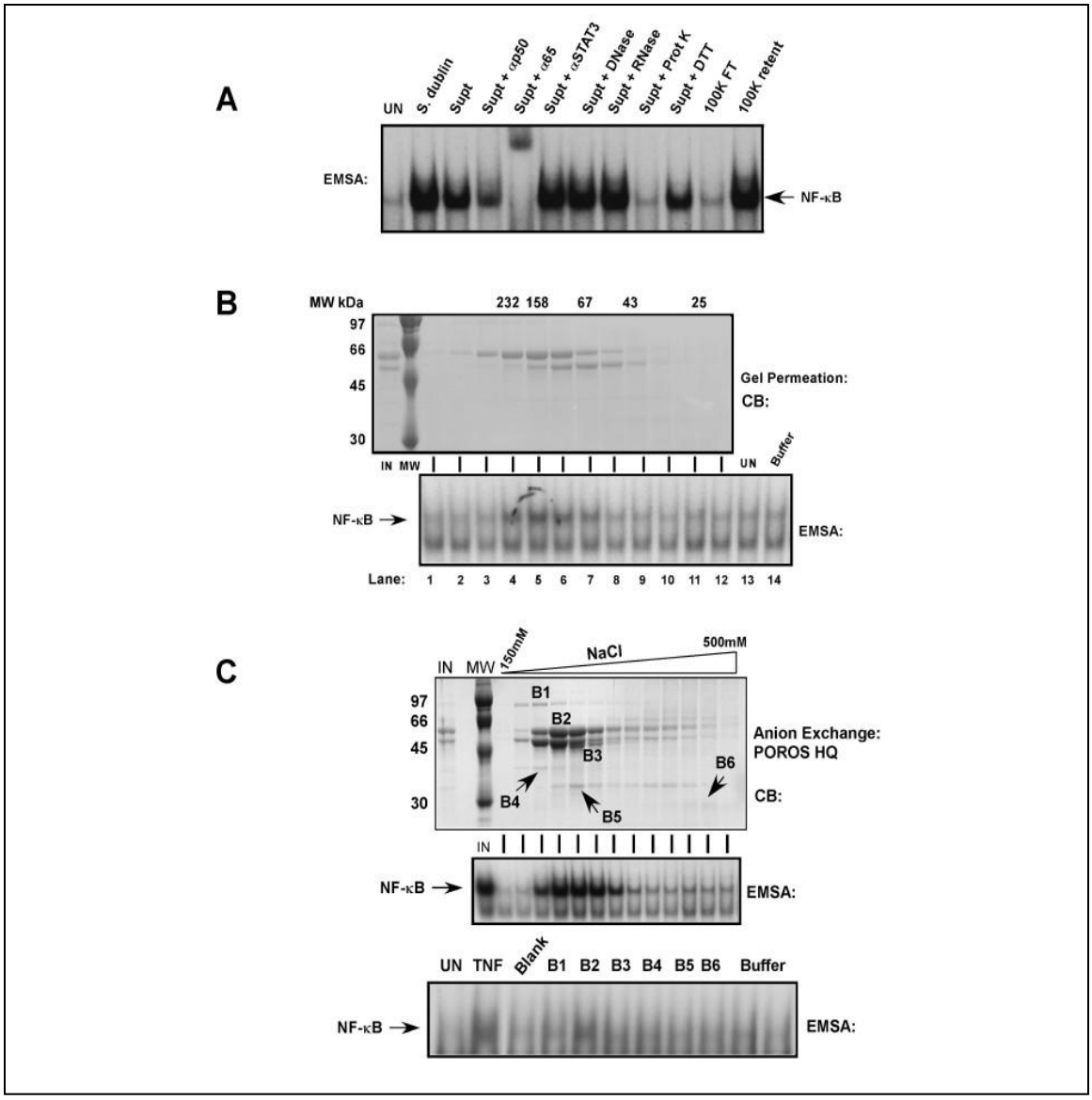
A
UN
S. dublin
Supt
Supt + αp50
Supt + α65
Supt + αSTAT3
Supt + DNase
Supt + RNase
Supt + Prot K
Supt + DTT
100K FT
100K retent
EMSA:
NF-κB
B
MW kDa
97
66
45
30
232 158 67 43 25
Gel Permeation:
CB:
IN MW
UN
Buffer
NF-κB
EMSA:
Lane: 1 2 3 4 5 6 7 8 9 10 11 12 13 14
C
IN MW
150mM
NaCl
500mM
B1
B2
B3
B4
B5
B6
Anion Exchange:
POROS HQ
CB:
IN
NF-κB
EMSA:
UN TNF Blank B1 B2 B3 B4 B5 B6 Buffer
NF-κB
EMSA:

Figure 5.2: Protein factor in *Salmonella* culture broth leads to NF-κB activation.

a, *Salmonella dublin* culture broth concentrated 100-fold was treated as indicated or infectious bacteria, as indicated was used to challenge HT29 cells. NF-κB DNA binding activity was assayed by EMSA from whole cell extracts prepared 45 min after treatment. Authenticity of the NF-κB DNA:protein complex was determined using p65(RelA)-specific and p50-specific antibody supershifts. **b**, Concentrated *Salmonella dublin* culture broth (IN) was chromatographed by gel permeation on a Superose 12 column. Eluted protein fractions were analyzed by fractionation on 10% SDS-PAGE and visualized by Coomassie blue (CB) staining. Molecular weight markers for chromatography and on the gels are indicated. Aliquots of each fraction as indicated was used to stimulate HT29 cells and resultant WCEs were analyzed by EMSA for NF-κB DNA binding activity. **c**, Concentrated *Salmonella dublin* culture broth (IN) was chromatographed by anion exchange chromatography on POROS HQ matrix. Proteins were eluted with an increasing NaCl gradient as indicated and analyzed on 10% SDS-PAGE and visualized by Coomassie blue (CB) staining. Input and aliquots of each fraction as indicated was used to stimulate HT29 cells and resultant WCEs were analyzed by EMSA for NF-κB DNA binding activity. Eluted material corresponding to protein bands B1-B6, a blank portion of the gel was isolated from a duplicate 10% SDS-PAGE gel as described in Experimental Procedures along with buffer samples from the beginning and end NaCl buffer gradient and used to stimulate HT29 cells and resultant WCEs were analyzed by EMSA for NF-κB DNA binding activity.

FIGURE 5.3

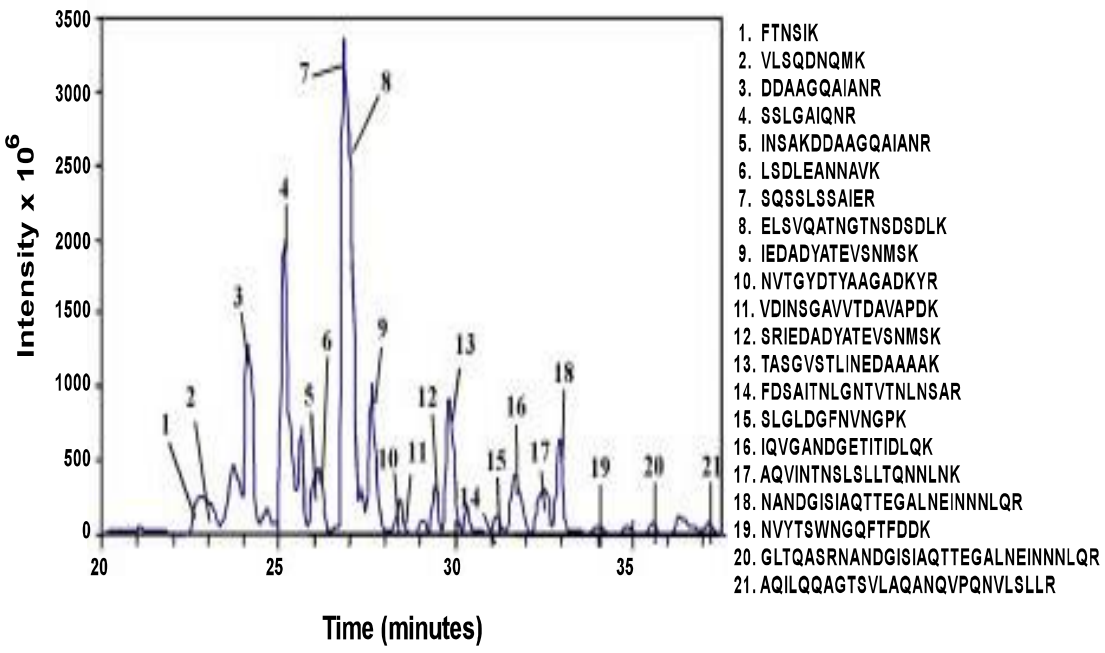

Figure 5.3: Identification by mass spectrometry of flagellin as the NF-κB activating factor in *Salmonella* culture broth.

Microcapillary HPLC tandem mass spectrometry of Band 2 digested by trypsin. Peaks corresponding to *Salmonella* peptides are numbered and identified with the corresponding numbered peptide sequence to the Right

5.4.3 Flagellin is required to activate NF-κB in intestinal epithelial cells

To determine if flagellin was indeed the factor that was responsible for triggering activation of NF-κB after exposure of intestinal epithelial cells to direct bacterial infection or to filtered culture broths of pathogenic *Salmonella sp*. we prepared infectious bacteria and boiled and filtered culture broths from the non-flagellated E. Coli DH5α, pathogenic *S. dublin* strain 2229, an isogenic *S. dublin* 2229 SopE$^-$ mutant, isogenic *S. dublin* 2229 SopB$^-$ mutant, isogenic *S. dublin* 2229 double SopE$^-$/SopB$^-$ mutant (strain SE1SB2), *S. typhimurium* strain 1103, and isogenic *S. typhimurium* fliC$^{::}$Tn*10* insertion mutant (strain 86) and a *S. typhimurium* 1103 isogenic double mutant fliC$^-$/fljB$^-$ and were used to challenge HT29 cells. Bacteria and culture broths were used to challenge HT29 intestinal epithelial cells and WCE extracts were prepared after forty-five minutes and analyzed for NF-κB DNA binding activity by EMSA. *Salmonella* strains could activate NF-κB, while *Salmonella* strains failing to produce flagellin (fliC and fliC$^-$/fljB$^-$ mutants as indicated) also failed to activate NF-κB (**Fig. 5.4a & 5.4b**). *E. Coli* DH5α is non-flagellated and does not produce flagellin failed to activate NF-κB. We also noticed through numerous experiments that *S. dublin* direct infections always activated NF-κB to a greater extent than *S. typhimurium* as observed in **Fig. 5.4a** while culture broths from both species activated NF-κB almost equally well (**Fig. 5.4b**). We believe this difference is due perhaps to *S. dublin* releasing more flagellin into the cell culture media than *S. typhimurium* during infection since purification of flagellin from both *S. dublin* and *S. typhimurium* and addition of equivalent amounts of chromatographically purified flagellin gave similar NF-κB activation profiles (TT & JD, unpublished observations).

Of note is the total failure of the double flagellin gene mutants to activate NF-κB as compared to the very minor activation observed in the single Phase I flagellin fliC::Tn*10* insertion mutant (**next to last lanes in Fig. 5.4a & 5.4b**) which likely is due to the extremely limited expression of the phase II flagellin (from fljB), although the strains of *Salmonella* used here genetically are unable or rarely shift phases of flagellin production. These results are consistent with previous reports identifying flagellin as a potent inducer of the proinflammatory response and IL-8 production (Eaves-Pyles et al., 1999; Gewirtz et al., 2000; Gewirtz et al., 2001b; McDermott et al., 2000). Since flagellin appears required for activation of the NF-κB pathway upon direct infection of intestinal epithelial cells it appeared possible that flagellin may also be the major determinant of other major mitogenic and stress activated signaling pathways activated upon pathogenic *Salmonella* infection of intestinal epithelial cells. Previously others and we have demonstrated that direct *Salmonella* infection of intestinal epithelial cells results in JNK activation (Hobbie et al., 1997) and also the activation of NF-κB via IKK (Elewaut et al., 1999). The identification of flagellin as a potent NF-κB activator is significant since SopE had previously been shown to be a pathogenic *Salmonella* bacteriophage encoded protein that is injected into the host cell and acts as an exchange factor for the small Rho GTPases Rac1 and CdC42 initiating cytoskeleton rearrangements and eventual activation of the MAPK, SAPK and NF-κB pathways (Hardt et al., 1998; Wood et al., 1996), while SopB is a *Salmonella* protein that functions as an inositol phosphate phosphatase and participates in cytoskeletal rearrangements and stimulates host cell chloride secretion (Norris et al., 1998).

FIGURE 5.4

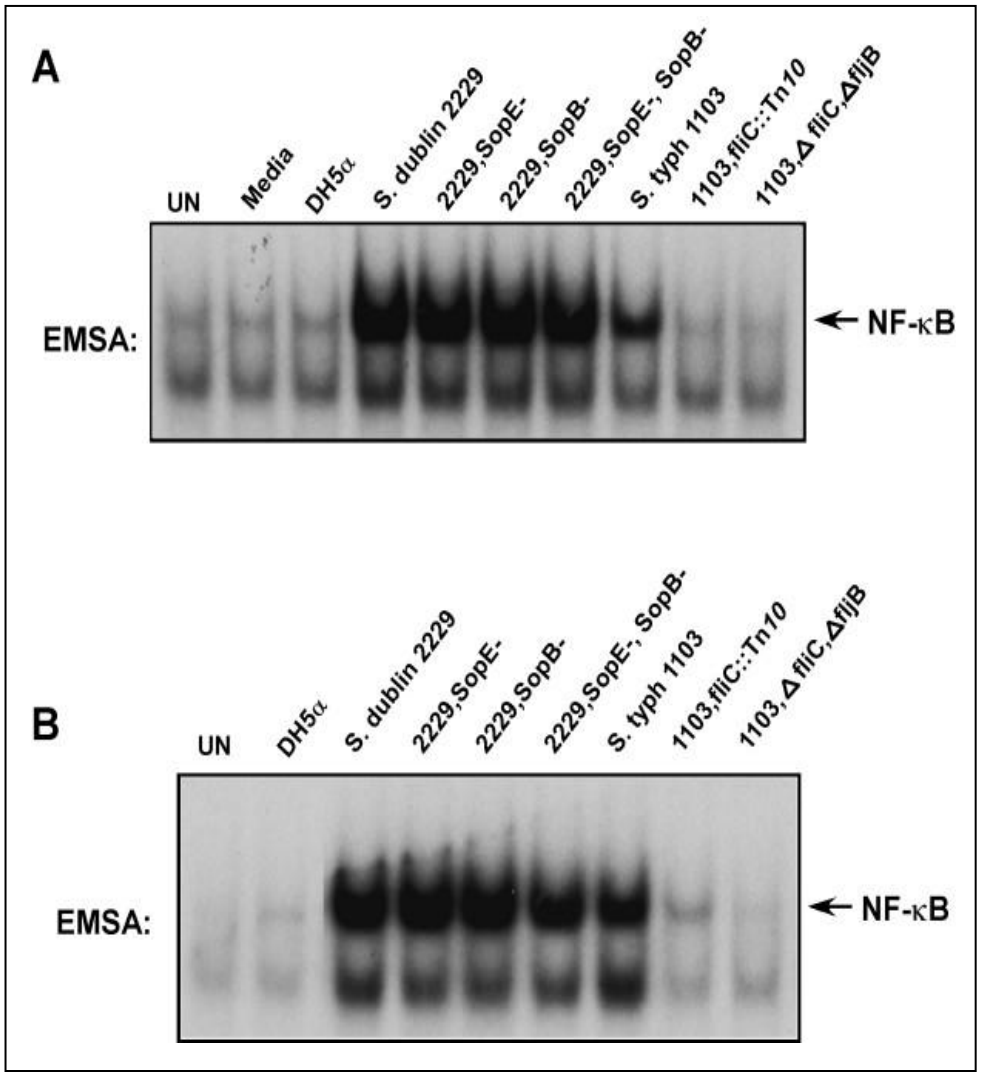

Figure 5.4: Flagellin mutants fail to activate NF-κB.

EMSAs assaying for NF-κB DNA binding activity in WCEs prepared 45 min from non-infected cells (UN) and after direct infection of HT29 cells with wild-type *E. coli* DH5α, wild-type *Salmonella dublin* or SopE mutant, SopB- mutant, the SopE-/SopB- double mutant, wild-type *Salmonella typhimurium* strain 1103, the fliC- mutant (fliC::Tn*10*), the fliC-/fljB- double mutant as indicated at an MOI of 50. B, EMSAs assaying for NF-κB DNA binding activity in WCEs prepared 45 min after challenge of HT29 cells from non-infected cells (UN) or with sterile-filtered concentrated culture broths from wild-type and mutant bacteria as indicated.

5.4.4 Flagellin triggers activation of the mitogen activated protein kinase, stress activated protein kinase and IKK signaling pathways

Intestinal epithelial cells act as sentinels for invasion of luminal surfaces and orchestrate the attraction of effector immune cells to the area by production of chemokine genes like IL-8 and macrophage chemoattractant protein 1 (MCP1) proinflammatory cytokine genes such as TNFα, IL-1 and IL-6 (Eckmann et al., 1997; Jung et al., 1995; Kagnoff and Eckmann, 1997; Witthoft et al., 1998). Expression of these genes primarily depends upon the action of transcription factors that are activated in response to the transmission of signals via the MAPK, SAPK and IKK signaling pathways. Since NF-κB is considered a central regulator/activator of the proinflammatory gene program we decided to examine the effect that non-flagellin producing mutant strains of *Salmonella* had on activation of the MAPK, SAPK and IKK signaling pathways compared to infection of intestinal epithelial cells with wild-type *Salmonella* or by exposure of the intestinal epithelial cells to purified flagellin. Infection of HT29 cells with wild-type *S. typhimurium* resulted in activation of MAPKs ERK1&2, the SAPKs p38, JNK and IKK (**Fig. 5.5**) as determined by use of activation-indicating phospho-specific antibodies in immunoblot (IB) analysis or antibody-specific immuno-kinase assays (KA) for JNK and IKK using their respective substrates GST-cJun 1–79 and GST-IκBα1–54 (DiDonato et al., 1997a; DiDonato and John, 2000; Hibi et al., 1993). Interestingly, MAPK stimulation is transient in nature as activation declines beginning at forty-five minutes while p38, JNK and IKK activity increases with time through one hour. As seen in **Fig. 5.4**, the fliC$^-$/fljB$^-$ double mutant *Salmonella* also failed to induce IKK and NF-κB activity (**Fig. 5.5 as indicated**). Surprisingly, the fliC$^-$/fljB$^-$ double mutant *Salmonella* failed to induce the

SAPKs p38 and JNK and only briefly (fifteen minutes) activated MAPK. This result is puzzling since other *Salmonella* proteins such as SopE and SopE2 can activate the small GTPases Rac and CdC42, and these Rho family GTPases have been linked to JNK and p38 activation (Bakshi et al., 2000; Hardt et al., 1998; Hobbie et al., 1997; Wood et al., 1996) yet appear not to function in the flagellin minus strain.

The fliC$^-$/fljB$^-$ double mutant *Salmonella* failed to invade HT29 cells compared to the wild-type *Salmonella* strain as determined by gentamycin protection/invasion assay (see Experimental Procedures). The flagellin fliC$^-$/fljB$^-$ double mutant displayed a four orders of magnitude difference in its ability to invade HT29 cells (TT & JD, unpublished observations). To demonstrate this point further, we infected HT29 cells with either wild-type *Salmonella* or the fliC$^-$/fljB$^-$ double mutant *Salmonella* (strain 134), both strains were transformed with the plasmid pFM10.1 that encodes GFP under the control of the Salmonella ssaH promoter and only functions once the bacteria has invaded the host cell (Valdivia and Falkow, 1997; Valdivia et al., 1996). The wild-type *Salmonella* clearly was able to infect HT29 cells (**GFP, Fig. 5.5b**) while the flagellin mutant bacteria failed to invade HT29 cells as evidenced by the lack of GFP expression (**Fig. 5.5b**). To determine if flagellin is sufficient or that other bacterially produced proteins are required for invasion, we added either purified flagellin or sterile-filtered culture broths or a combination of both to HT29 cells that were challenged with the *Salmonella* fliC$^-$/fljB$^-$ double mutant and assayed for invasion. Intestinal epithelial cells failed to be invaded using all tested combinations of purified flagellin and/or culture broths with the fliC$^-$/fljB$^-$ double mutant strain (TT & JD, unpublished observations). To our knowledge there is no known direct connection between expression of flagellin genes and the effectiveness of

the type III secretion system to deliver bacterially produced proteins such as SopE, SopE2 and SipA or other Sip or Sop proteins (Bakshi et al., 2000; Galkin et al., 2002; Hardt et al., 1998; Wallis et al., 1999; Wood et al., 1996) that play important roles in initiating bacterial internalization. Furthermore, to evaluate the effectiveness of flagellin to stimulate p65 (RelA) nuclear localization in intestinal epithelial cells we challenged HT29 cells with purified flagellin and examined p65 (RelA) localization using indirect immunofluorescence and found p65 (RelA) nuclear localization in nearly every cell (**Fig. 5.5b as indicated**).

FIGURE 5.5

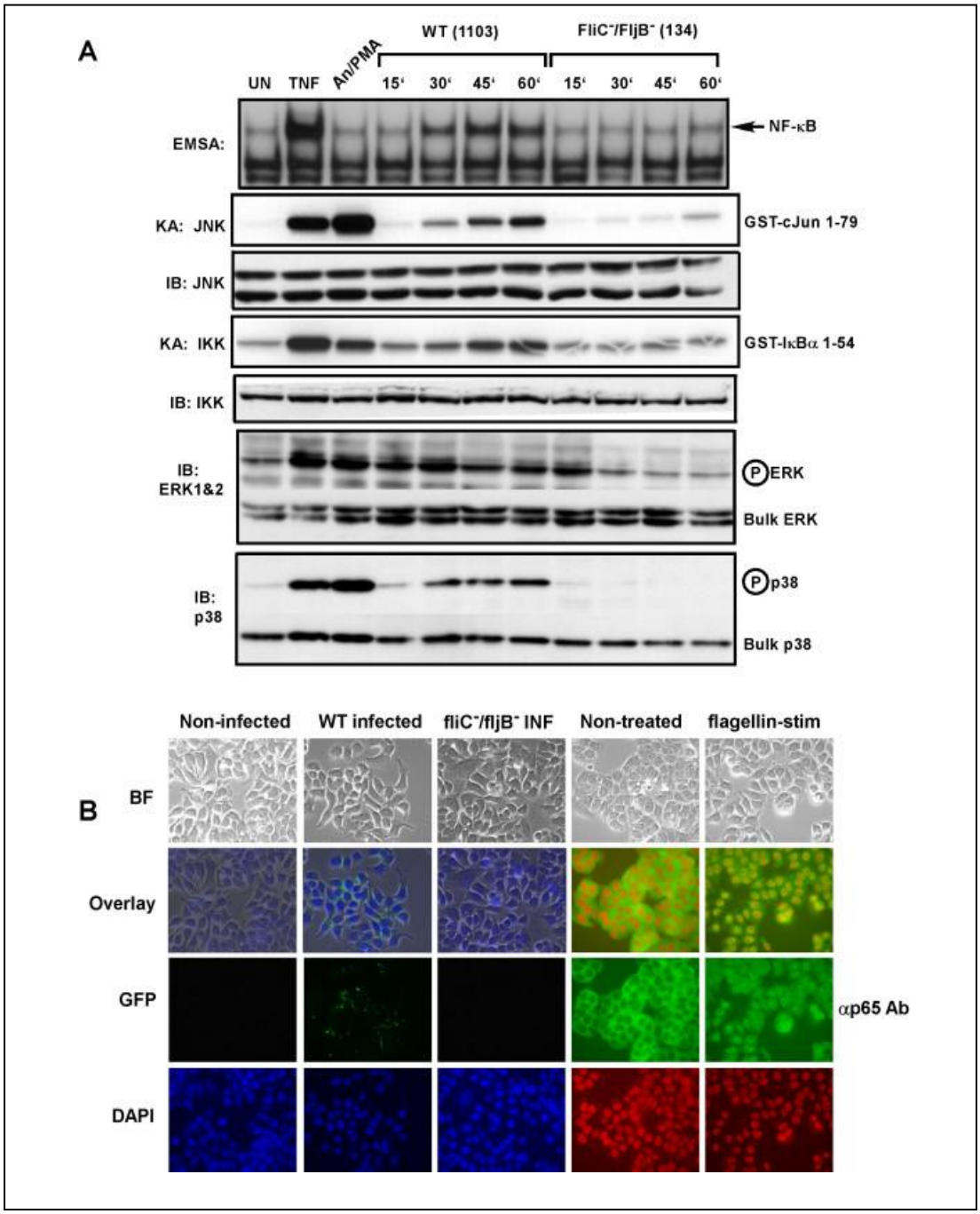
A
WT (1103)
FliC⁻/FljB⁻ (134)
UN
TNF
An/PMA
15'
30'
45'
60'
15'
30'
45'
60'
EMSA:
NF-κB
KA: JNK
GST-cJun 1-79
IB: JNK
KA: IKK
GST-IκBα 1-54
IB: IKK
IB: ERK1&2
PERK
Bulk ERK
IB: p38
Pp38
Bulk p38
B
Non-infected
WT infected
fliC⁻/fljB⁻ INF
Non-treated
flagellin-stim
BF
Overlay
GFP
αp65 Ab
DAPI

Figure 5.5: Flagellin is required for activating multiple signaling pathways during *Salmonella* infection and leads to nuclear localization of NF-κB.

HT29 cells were left untreated, stimulated with TNFα (10 ng/ml) or a cocktail of anisomycin [An] (20 μg/ml)/PMA (12.5 ng/ml) for 15 min, or infected with either wild-type (WT) *Salmonella typhimurium* strain 1103 or the *Salmonella typhimurium* double fliC-/fljB- mutant strain 134 as indicated. WCE were prepared at the indicated times or at 10 min for TNF-treated cells or 15 min for anisomycin/PMA treated cells and used in EMSAs to analyze NF-κB DNA binding activity, or in immuno-kinase assays (KA) using anti-IKK or anti-JNK antibodies to measure IKK and JNK kinase activity on their respective substrates GST-IκBα 1–54 and GST-cJun 1–79 (as indicated). Immunoblot (IB) analysis of equivalent amounts (40 μg) of protein from each extract was fractionated on SDS-PAGE gels and transferred to PVDF membranes and probed with the indicated antibodies to detect bulk IKK, JNK, ERK and p38 as indicated. Immunoblot analysis using phospho-specific antibodies for ERK and p38 to detect activated ERK and p38 are indicated. **b**, Immunofluorescence demonstrating that flagellin mutant Salmonella fail to infect HT29 cells and that purified flagellin stimulation of HT29 cells leads to NF-κB nuclear p65 (RelA) localization as determined by indirect immunofluorescence. Imaging of the treatment indicated HT29 cells

Purified flagellin (0.5 μg/ml) was added to the culture media of HT29 cells and WCE were prepared at various times as indicated after exposure and assayed for NF-κB DNA binding activity in EMSAs (**Fig. 5.6a**). Flagellin potently activated NF-κB in a time dependent manner similar to that observed for TNF (10 ng/ml) treatment of HT29 cells (**Fig. 5.6a**). Analysis of the MAPK, SAPK and IKK signaling pathways (**Fig. 5.6b**) at various times after flagellin treatment of HT29 cells using activation-specific phospho-antibodies to monitor MAPK and p38 kinase activation or antibody-specific immunoprecipitation kinase assays for JNK and IKK activities demonstrated that JNK and IKK activity increased through time to one-hour while p38 and MAPK (ERK1&2) activity peaked at thirty minutes and began to decline to noticeably lower levels by one-hour (**Fig 5.6b as indicated**). The activation profile of the MAPK, SAPK and IKK signaling molecules ERK1&2, p38, JNK and IKK in intestinal epithelial cells in response to purified flagellin exposure remarkably resembled that of intestinal epithelial cells infected with wild-type *Salmonella* (**Fig. 5.5a**). From these observations we conclude that the temporal activation of the signaling pathways examined here (MAPK, SAPK and IKK), which reflect early events in *Salmonella* infection, are determined almost exclusively by recognition and response of intestinal epithelial cells to flagellin.

We wished to further examine the effect of purified flagellin and flagellin present on *Salmonella* on the temporal pattern of proinflammatory cytokine gene expression in intestinal epithelial cells in order to differentiate the effects of flagellin alone vs. flagellated *Salmonella* or non-flagellated *Salmonella* infection. HT29 cells were left untreated, stimulated with TNFα (10 ng/ml), or stimulated with flagellin (0.5 ug/ml), or infected with wild-type *Salmonella* typhimurium or the *Salmonella* fliC/fljB double

mutant (at MOI of 50). Aliquots of the cDNA were used in semi-quantitative RT-PCR reactions using IL1α, IL-1β, IL-8, TNFα, MCP1 and β-actin gene specific primers (sequences available upon request) and the products were fractionated on ethidium bromide containing 1.2% agarose gels. Expression of the known NF-κB target genes IL-1β, IL-8, TNFα and MCP1 was increased in response to TNFα or purified flagellin exposure (**Fig. 5.6c**). Wild-type *Salmonella* infection also led to activation of these same genes although the expression of TNFα and MCP1 was transient in comparison and occurred immediately after infection. The *Salmonella* fliC$^-$/fljB$^-$ double mutant failed to induce IL-1β, IL-8 and TNFα expression, however MCP1 expression was induced, although at lower levels than that induced by wild-type *Salmonella*, and also, the expression of MCP1 was not transient in nature and continued throughout the time course (9 h) (**Fig. 5.6c**). The expression level of β-actin served as an internal standard for comparison. Interestingly, IL-1α, which is not an NF-κB target gene was stimulated in response to HT29 cell challenge by all of the treatments. Obviously, the *Salmonella* fliC$^-$/fljB$^-$ double mutant can activate other signaling pathways leading to IL-1α expression. We presently do not know the identity of these signaling pathways.

FIGURE 5.6

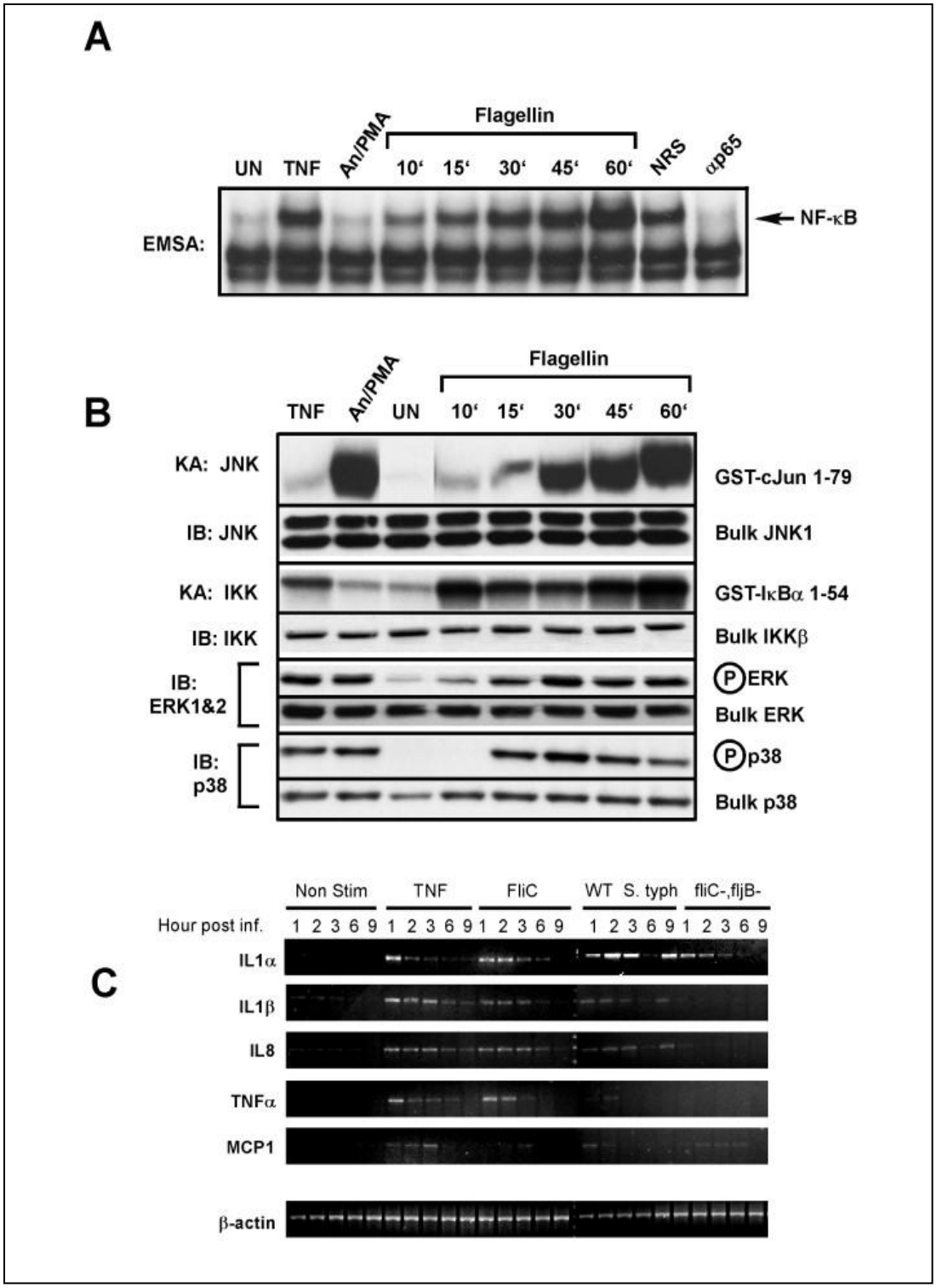
A
Flagellin
UN
TNF
An/PMA
10'
15'
30'
45'
60'
NRS
αp65
EMSA:
NF-κB
B
Flagellin
TNF
An/PMA
UN
10'
15'
30'
45'
60'
KA: JNK
GST-cJun 1-79
IB: JNK
Bulk JNK1
KA: IKK
GST-IκBα 1-54
IB: IKK
Bulk IKKβ
IB: ERK1&2
PERK
Bulk ERK
IB: p38
Pp38
Bulk p38
C
Non Stim
TNF
FliC
WT S. typh
fliC-,fljB-
Hour post inf.
1 2 3 6 9 1 2 3 6 9 1 2 3 6 9 1 2 3 6 9 1 2 3 6 9
IL1α
IL1β
IL8
TNFα
MCP1
β-actin

Figure 5.6: Purified flagellin activates signaling pathways and proinflammatory gene expression in intestinal epithelial cells mimicking that of wildtype a wild-type *Salmonella* infection.

HT29 cells were left untreated or treated with TNFα (10 ng/ml) or a cocktail of anisomycin [An] (20 μg/ml)/PMA (12.5 ng/ml) for 10 min, or with flagellin (1 μg/ml) for the indicated times. WCE were prepared and analyzed by EMSA for NF-κB DNA binding activity, immuno-kinase assays (KA) or immunoblot analysis using phospho-specific antibodies for ERK or p38 to detect activation and with kinase-specific antibodies as described in **Fig. 5a** to detect bulk kinase abundance as indicated. A, EMSA to detect NF-κB DNA binding activity. Authenticity of the NF-κB bandshift was tested with supershift of the complex with p65(RelA)-specific antibody (α p65), normal rabbit serum (NRS) served as an irrelevant antibody control. **b**, immunoblot and kinase assays to detect IKK, JNK, ERK and p38 kinase activities and protein abundance as in **Fig. 5a**. **c**, semi-quantitative RT-PCR of proinflammatory gene expression of non-treated, wild-type and flagellin double mutant Salmonella typhimurium infected, TNFα (10 ng/ml) or flagellin (1 μg/ml) stimulated cells. HT29 cells were harvested at the indicated times after the indicated treatments and isolated RNA was used to make first strand cDNA that subsequently used in RT-PCR reactions (as described in Experimental Procedures) using gene-specific primers for IL1α, IL-1β, IL-8, TNF-α MCP1, and β,Actin was used as a standard for normalizing expression patterns. Resulting PCR products were fractionated on 2% agarose gels and visualized by ethidium bromide staining

5.4.5 Flagellin activates NF-κB DNA binding in a MyD88-dependent manner

Flagellin was capable of activating the requisite signaling pathways consistent with proinflammatory gene activation similar to that of a cytokine like TNFα that activates all cells on which a functional cell surface receptor for it is present (**see p65 [RelA] nuclear localization in Fig. 5.1 and Fig. 5.5c**) we decided to examine the potential of the Toll-like receptors, to activate the NF-κB pathway in response to flagellin exposure. To quickly test this hypothesis we examined the effect that a dominant-negative MyD88 (aa 152–296) (Muzio et al., 1997) expressing adenovirus had on flagellin-mediated NF-κB activation in HT29 cells. MyD88 is an adapter protein utilized by the IL-1 receptor and all of the known TLRs, which share homology to IL-1 through their cytoplasmic signaling domain and is required for immediate activation of the NF-κB pathway (Medzhitov et al., 1998; Takeuchi and Akira, 2002). We found that expression of DN-MyD88 in HT29 cells blocked the activation of NF-κB DNA binding activity assayed by EMSA analysis in response to IL-1 or flagellin exposure, consistent with the action of a TLR-mediated activation of NF-κB (TT & JD, unpublished observations). To examine this possibility further we initially used wild-type, MyD88$^{-/-}$ and TLR2$^{-/-}$/TLR4$^{-/-}$ MEFs (a gift of S. Akira, Univ. of Osaka, JA) to verify the role of MyD88 and to examine the potential role of two of the TLRs to respond to flagellin or to direct wild-type *Salmonella* infection and lead to NF-κB activation (**Fig. 5.7**). Wild-type *Salmonella* infection activates NF-κB potently in both the wild-type and TLR deficient MEFs (**lanes 2 & 15**) but this activation is somewhat defective in the MyD88 deficient MEFs (**lane 10**). Challenge of all three types of cells with concentrated sterile-filtered wild-type *S. dublin* or the double SopE^{-}/SopB^{-} isogenic mutant *S. dublin* strain SE1SB2 culture broths

activated NF-κB in wild-type MEFs and TLR2/4 double deficient cells but failed to activate NF-κB in MyD88 deficient cells (**compare lanes 11 and 12 with lanes 3, 4, 6, 7, 16 and 17**). NF-κB was potently activated in wild-type MEFs by exposure to purified flagellin (0.5 μg/ml) and therefore eliminated the possibility that LPS played a role in NF-κB activation in these experiments. The exclusion of LPS as a major contributor to NF-κB activation is also provided by the potent activation of the TLR2/4 double deficient MEFs (**lanes 16 & 17**). TLRs 2 and 4 respond to bacterial lipopeptides, peptidoglycans, certain LPSs and gram negative LPS respectively (Lien et al., 2000; Lien et al., 1999; Yoshimura et al., 1999). IL-1 stimulation verified the functional requirement of MyD88 in transmission of IL-1 and flagellin-mediated signals.

To further define a possible role for the TLRs in flagellin recognition we assayed for the ability of overexpressed TLRs to activate NF-κB in cells that normally respond poorly to flagellin exposure. Choosing cells that responded slightly to purified flagellin ensured that the signaling components and adapters that flagellin uses were present and functional and that the limiting factor was likely only to be the receptor that responds to flagellin. We found that HeLa cells and HEK293T cells activated NF-κB DNA binding activity in response to IL-1 stimulation but poorly to flagellin exposure (**Fig. 5.9b**) and we chose HEK293T cells to use further because of their greater transfection efficiency. Amino-terminus FLAG epitope-tagged TLRs 1–9 (kind gifts of R. Medzhitov, Yale Univ. and R. Ulevitch, TSRI) (Alexopoulou et al., 2001; Chuang and Ulevitch, 2000) were overexpressed in HEK 293T cells in transient transfections along with the 2×-NF-κB-dependent promoter driven luciferase reporter gene (Devary et al., 1993) and the expression of luciferase in response to no treatment, flagellin (0.5 μg/ml) or TNFα (10

ng/ml) was determined. TLR5 was the only TLR whose expression resulted in a noticeable response to flagellin challenge of the cells (**Table 5.1**).

FIGURE 5.7

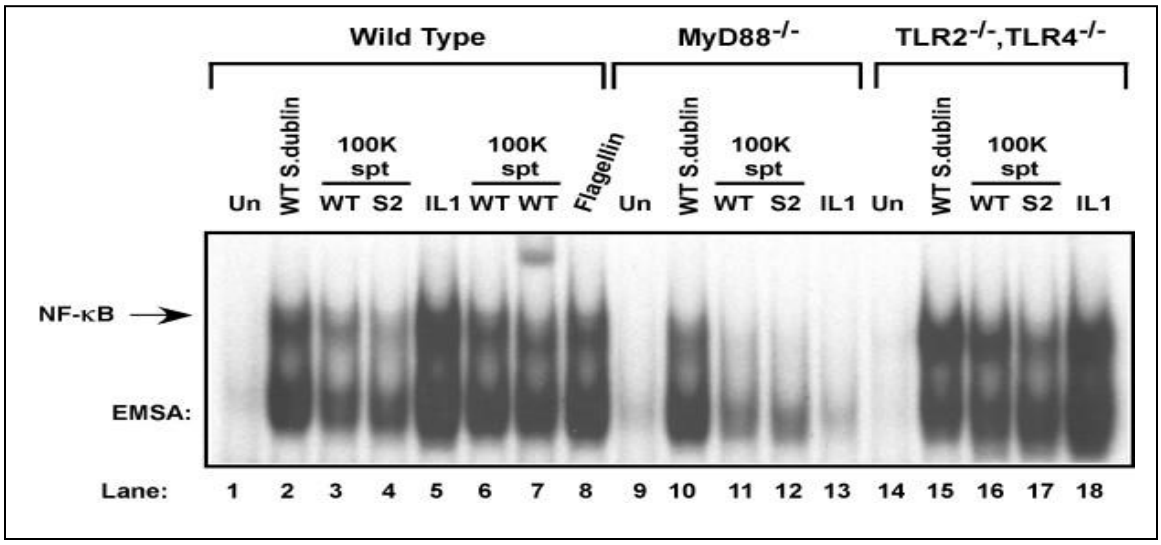

Figure 5.7: Flagellin-mediated activation of NF-κB is MyD88 dependent.

Infectious wild-type *Salmonella Dublin* (MOI of 100), IL-1 (20 ng/ml), purified flagellin (1 μg/ml) (as indicated), sterile-filtered and concentrated 100 kDa filter retentate supernatant (spt) from wild-type *Salmonella dublin* and SopE-/SopB- double mutant *Salmonella dublin* strain SE1SB2 (S2, as indicated) was used to challenge wild-type, MyD88-/- knockout or TLR2-/-/TLR4-/- double knockout MEFs as indicated. WCEs were prepared 45 min after treatments and examined by EMSA to analyze NF-κB DNA binding activity. IL-1 (20 ng/ml) was used as a positive control to monitor MyD88 function.

TABLE 5.1

	No Stim	TNF-α	FliC
Vector	1	13.5	4.9
TLR1	1.7	ND	5.1
TLR2	1.6	ND	5.3
TLR3	1.5	ND	5.0
TLR4	1.8	ND	5.4
TLR5	1.6	ND	9.2*

Table5.1: TLR5 responds to flagellin and activates NF-κB

293T cells were transfected with empty vector (pCDNA3.1) or the individual listed wild-type TLR alleles in triplicate in 6-well dishes. Cells were left untreated (No Stim), TNF-α (10ng/ml) or flagellin (10ug/ml). NF-κB reporter activity was adjusted by normalizing expression to control Renilla luciferase activity and fold induction was calculated as reporter gene activity in treated cells/reporter gene activity in non-stimulated cells. ND is not determined

To further determine the likelihood of TLR5 being the TLR through which flagellin activated NF-κB, we constructed dominant-negative signaling mutations by deletion of the carboxyl portion of each TLR to a conserved tryptophan in the TIR domain (see Materials and Methods). A similar mutation in the IL-1 receptor abrogates its ability to lead to NF-κB activation (Croston et al., 1995; Heguy et al., 1992). Each DN-TLR along with a reverse cloned TLR5 (AS-TLR5) were cloned into the mammalian expression vector pCDNA3.1 (Invitrogen, Carlsbad, CA). All mutant proteins were expressed well (TT & JD unpublished observations). Each DN-TLR mammalian expression vector and empty expression vector along with 2× NF-κB Luc was transfected as previously described (Elewaut et al., 1999) into HT29 cells which respond very well to flagellin. The transfected cells were left untreated, stimulated with TNFα (10 ng/ml) or with purified flagellin (0.5 μg/ml). Reporter gene expression was observed not to be affected by DN-TLR expression in response to TNFα stimulation of transfected cells (**Fig. 5.8a**) however, only expression of either the DN-TLR5 or an antisense TLR5 construct resulted in a nearly fifty percent and twenty-five percent inhibition of flagellin-mediated reporter gene activation respectively (**Fig. 5.8b**), while DN-TLR2 also was found to mildly inhibit flagellin-mediated reporter expression. These results imply that TLR5 takes part in cell surface recognition of flagellin and initiates the signaling pathway leading to NF-κB activation. The effect of DN-TLR2 on NF-κB-dependent reporter gene activation may be non-specific since its expression also inhibited TNFα-mediated reporter activation as compared to the other DN-TLRs. DN-TLR2 may also compete for an unknown adapter protein that both TLR2 and TLR5 might share. In any event, TLR2 and TLR4 were

shown by the results presented in **Fig. 5.7** not to be required for flagellin-mediated activation of NF-κB.

FIGURE 5.8

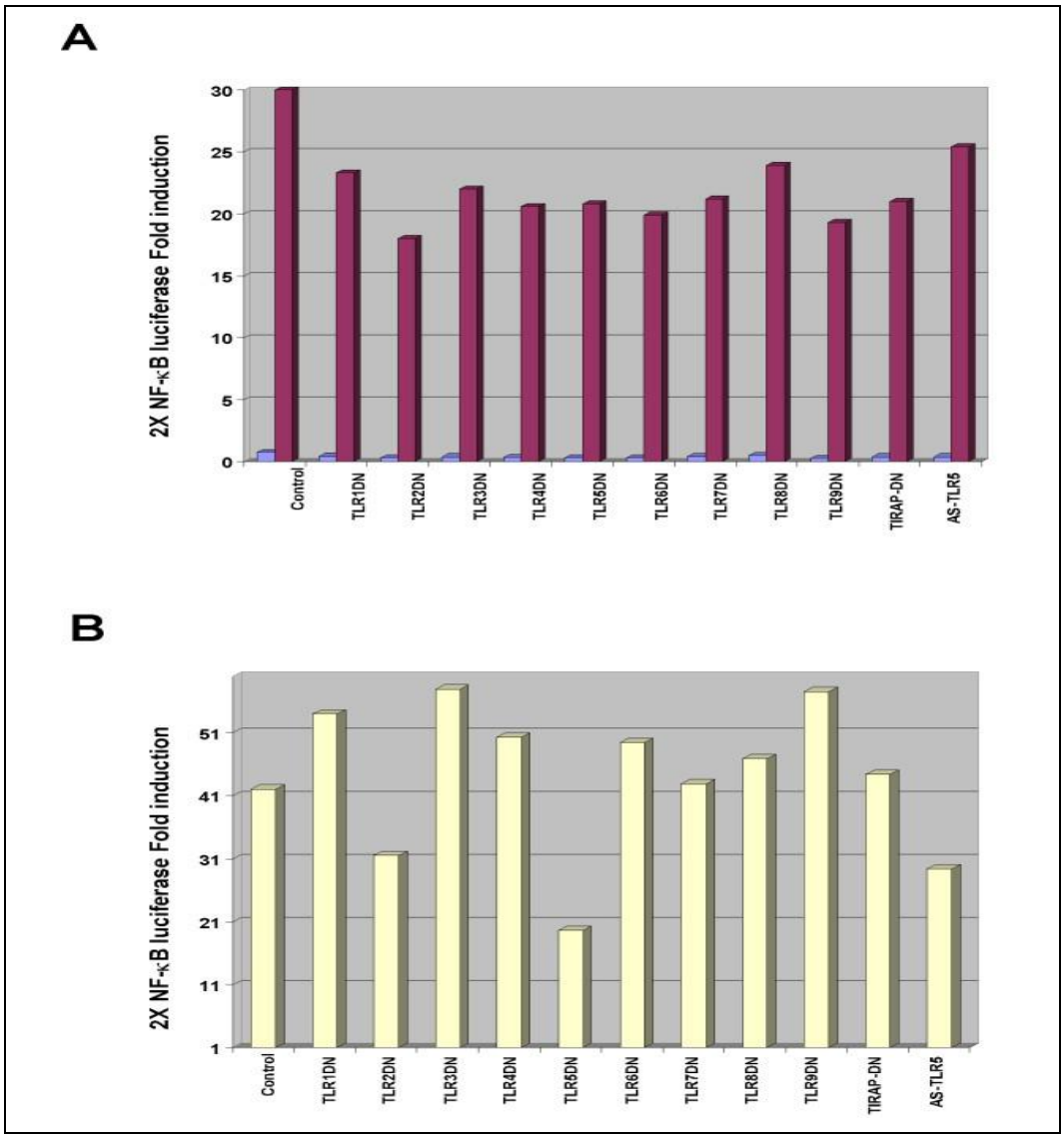

Figure 5.8: TLR5 inhibits flagellin-mediated NF-κB reporter gene activity.

HT29 cells were transfected in triplicate in 6-well dishes using the indicated DN-TLR mammalian expression vectors or antisense TLR5 (AS TLR5) (2 μg/well), 2× NF-κB Luc reporter gene (100 ng/well), pRL-TK Renilla luciferase for normalization (50 ng/well) adjusted to 4 μg total DNA/well with empty vector pCDNA3.1 DNA. A, Fold-induction of 2× NF-κB Luc reporter gene in non-stimulated cells (light shading) and in TNFα (10 ng/ml) treated cells (dark shading). Lysates were prepared 12 h after stimulation. Results of a representative experiment are shown. **b**, HT29 cells transfected as in A were treated with flagellin (1 μg/ml) and cell lysates were prepared and analyzed as in Fig. 8A. Results of a representative experiment are shown.

5.4.6 Flagellin-mediated activation of NF-κB in intestinal epithelial cells leads to increased and decreased expression of a subset of TLRs

Stimulation of intestinal epithelial cells with *S. typhimurium* or with purified flagellin led to activation of the proinflammatory gene program (**Fig. 5.6c**). We wished to examine whether or not expression of TLR genes would also be altered in flagellin stimulated cells. HT29 cells were treated or not with purified flagellin (0.5 μg/ml) or with TNFα (10 μg/ml) and total RNA was isolated from non-treated and treated cells three hours after stimulation and used to make first-strand cDNA. Real-time RT-PCR using gene-specific primers for each of the TLRs (Superarray, Frederick, MD) and first-strand cDNA prepared from non-stimulated or flagellin stimulated cells was used to generate SYBR-green (Perkin-Elmer) labeled DNA products that were detected in an iCycler™ (Bio-Rad). Interestingly, flagellin only mildly activated the expression of TLR2, while expression levels of TLRs 5, 6, 9 and 10 were decreased by 2-fold (**Table 5.2**). Contrastingly, TNF stimulation led to increased expression of TLRs 3 and 4 (1.6- and 3.5-fold respectively), while TLRs 2, 9 and 10 were decreased by approximately 2-, 5- and 3-fold respectively. GAPDH expression served as comparative standard.

TABLE 5.2

Gene	Fold Change TNF-α stimulation	Fold change FliC stimulation
TLR1	ND	ND
TLR2	0.6	1.3
TLR3	1.6	0.6
TLR4	3.5	1.1
TLR5	0.9	0.5
TLR6	0.9	0.6
TLR7	M	M
TLR8	ND	ND

Table 5.2: Change in TLR mRNA levels following TNF-α or FliC stimulation.

ND- Non detected by RT^2 PCR

M -None detected above level of minus RT control.

Reverse Transcription and Real Time PCR (RT^2PCR)-RNA was prepared from cells left untreated, stimulated with TNF-α (10ng/ml) or flagellin (1ug/ml) for 3h. RT^2PCR was performed with an iCycler (Bio-Rad) to quantify SYBR-green labeled products generated from PCR products of 1^{st} strand cDNA prepared from TLR1 through TLR10 mRNA, 18s rRNA, and GAPDH mRNA. RT^2PCR (25ul reaction volume) was performed with the appropriate primers (Super Array) in triplicate with HotStart Taq DNA polymerase (SuperArray) at 95^0 C for 5 min. to activate Taq and amplified for 40 cycles (95^0 C, 30sec., 55^0 C, 30sec., 72^0 C, 30sec.). RT^2PCR was performed on the minus RT controls with TLR5 primers to detect DNA contamination. Fold Change in mRNA expression was expressed as $2^{\Delta\Delta Ct}$. ΔCt is the difference in threshold cycles for the TLR mRNAs and 18S rRNA, Δ ΔCt is the difference between ΔCt non-stimulated control and ΔCt stimulated sample.

5.4.7 TLR5 is expressed in cells that don't respond well to flagellin

This study and others (Akira, 2001; Gewirtz et al., 2001a) have identified TLR5 as the likely TLR through which flagellin activates NF-κB. Previous reports made no determination on the presence or abundance of TLR5 in the cells that they used to ascertain its function (Akira, 2001; Gewirtz et al., 2001a). We wished to determine if TLR5 protein abundance was absent or greatly decreased in cells that failed to respond or responded poorly to challenge by flagellin. TLR5 abundance in a number of cell lines was examined by immunoblot analysis using a TLR5-specific antibody and compared with the ability of purified flagellin to induce NF-κB DNA binding activity of WCEs prepared from them. Intestinal epithelial cell lines T84 and HT29 were used as was the lung adenocarcinoma cell line A549, the human cervical adenocarcinoma cell line HeLa, the human embryonic kidney cell line expressing large T antigen HEK293T, and the glioblastoma cell line T98G. TLR5 protein was detected in all cell lines examined by immunoblot with TLR5-specific antibody (**Fig. 5.9a**). T84 cells exhibited the highest abundance while expression levels of the other cell lines were similar and appeared not to differ by more than two-fold (**Fig. 5.9a**). NF-κB DNA binding activity in non-stimulated, TNFα and flagellin stimulated cells was analyzed by EMSA assays of WCEs prepared from each cell type (**Fig 5.9b**). HT29 and A549 cells responded strongly to flagellin and to TNFα stimulation while HeLa, 293T and T98G cells responded poorly (HeLa, 293T) or not at all (T98G) to flagellin stimulation. The authenticity of the NF-κB DNA binding complex was determined using p65-specific antibody to supershift the NF-κB DNA:protein complex. It is of interest that some cells that express TLR5 either do not respond at all or do so very poorly. This may be due to either lack of receptor presence at

the plasma membrane and intracellular localization, inactivating or detrimental mutations in the TLR5 gene in these cell lines or lack of or low abundance of a required co-receptor or adapter protein (as is the case in some cells for TLR4 and its co-receptor/adapter MD2 (Akashi et al., 2001; Nagai et al., 2002; Schromm et al., 2001)). IL-1 can activate NF-κB DNA binding activity in all of the examined cell lines so it appears that the signaling apparatus downstream of MyD88 to NF-κB is intact.

Recently Muc1 a secreted and membrane bound mucin protein was shown to serve as a receptor that bound *Pseudomonas aeruginosa* and its flagellin, leading to activation of the MAPK pathway (Lillehoj et al., 2002; Lillehoj et al., 2004) although NF-κB activity was not examined. We examined the muc1 abundance levels in HT29 (strong flagellin responder), A549 (strong flagellin responder), HeLa, 293T (both weak flagellin responders) and T98G (no flagellin response) to determine if its expression correlated with the activation profile of NF-κB and MAPK in these cells in response to flagellin (Lillehoj et al., 2004). Should this be the case then muc1 might serve as a viable co-receptor for TLR5 in propagating activation signals leading to NF-κB activation. We observed that only HT29 cellular proteins gave a strong signal by immunoblot analysis using an muc1-specific antibody while muc1 was barely detectable in the other cell lines (**Fig. 5.9c**). These results suggest that muc1 does not serve the role of a TLR5 co-receptor that leads to NF-κB activation and likely plays little to no role activating MAPK pathways in A549 cells where we have observed similar temporal MAPK activation in response to flagellin exposure as we do in HT29 cells (TT and JD, unpublished results). Further examination of muc1's role in HT29 cells in regards to NF-κB and MAPK signaling using siRNA is warranted.

FIGURE 5.9

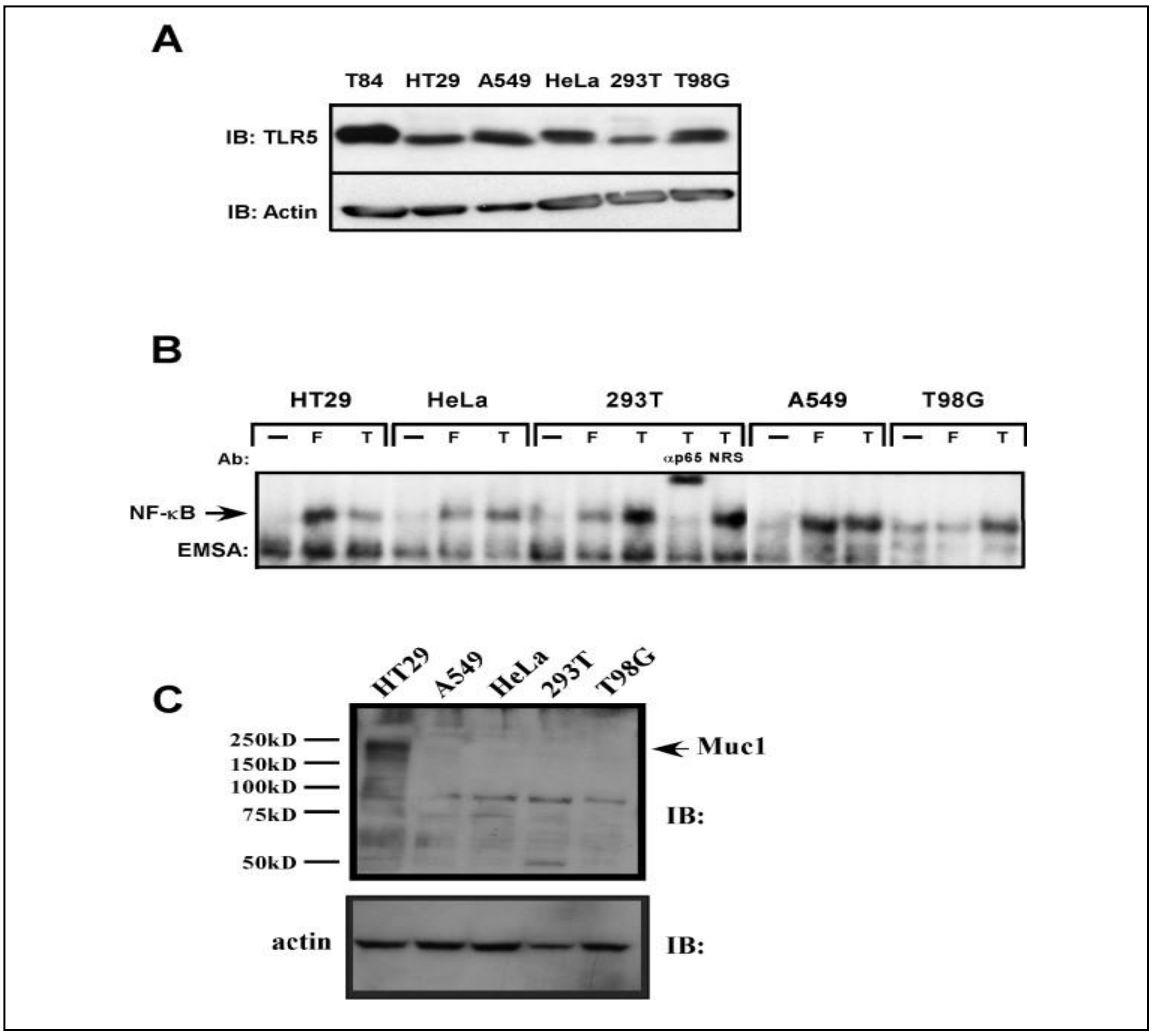

Figure 5.9: TLR5 is expressed in numerous cell types and has variable responses to flagellin.

A, whole cell extracts were prepared from non-stimulated T84, HT29, A549, HeLa, 293T and T98G cells and fractionated on a 8% SDS-PAGE gel, proteins were transferred to PVDF membrane and probed with anti-TLR5 antibody for immunoblot analysis (IB). Protein loading was examined by probing with anti-actin antibody. **b**, HT29, A549, HeLa, 293T and T98G cells were left untreated (--), treated with flagellin (F) or TNFα (T) and WCEs were prepared after 45 min and used in EMSA to monitor NF-κB DNA binding activity. Authenticity of the NF-κB bandshift was tested with supershift of the complex with p65(RelA)-specific antibody (αp65), normal rabbit serum (NRS) served as an irrelevant antibody control. **c**, HT29, A549, HeLa, 293T and T98G cells WCEs (50 μg) were fractionated on a 8% SDS-PAGE gel, proteins transferred to Immobilon P and immunoprobed with anti-muc I (1:450, Santa Cruz). Size markers are listed and muc 1 position is indicated with an arrow.

5.5 DISCUSSION

Intestinal epithelial cells at mucosal surfaces serve as innate immune sentinels controlling the innate host defense instruction to the immune effector cells inside the body in response to the external environment (Eckmann et al., 1995; Kagnoff and Eckmann, 1997). Previous studies examining pathogenic *Salmonella* invasion of intestinal epithelial cells demonstrated activation of the proinflammatory gene program and invasion of only a minor portion of the cells (Valdivia et al., 1996). We previously demonstrated that NF-κB is as potently induced in pathogenic *Salmonella .sp* infected cells similar to those treated with the proinflammatory cytokines that are potent NF-κB activators such as TNFα and IL-1β and that this activity was IKK-mediated (Elewaut et al., 1999). Here we examined how bacterial invasion of only a third of the cells could give rise to NF-κB activity profiles consistent with activation of NF-κB in every cell such as the profile TNFα stimulation provides. We found that bacterial infection activates nuclear translocation of p65 (RelA) in nearly all of the intestinal epithelial cells consistent with the hypothesis that a cell surface receptor was recognizing either a soluble product that bacteria were producing, or a bacterial product on the bacteria, or both. We examined bacterial culture broths and found a bacterial product that was protein in composition and when used to challenge intestinal epithelial cells it potently activated NF-κB DNA binding activity (**Fig. 5.2a**). We further purified this protein by gel permeation and anion exchange chromatography and found the protein to be flagellin by electrospray ion trap mass spectroscopy (**Fig. 5.2b & 5.2c and Fig. 5.3**). While our studies were in progress, flagellin was identified as being a potent proinflammatory mediator leading to IL-8 production and secretion (Eaves-Pyles et al., 1999; Gewirtz et

al., 2000; Gewirtz et al., 2001b). We demonstrate in this study that flagellin appears to be exclusively responsible for activating NF-κB in intestinal epithelial cells since flagellin mutant strains do not activate NF-κB (**Fig. 5.4**) nor lead to their internalization (**Fig. 5.5b**). Furthermore, flagellin challenge of intestinal epithelial cells leads to p65 (RelA) nuclear localization in nearly all of the treated cells (**Fig. 5.5b**). Transcription factors like activator protein 1 (AP-1) and NF-κB, which are key regulators/activators of the proinflammatory gene program (Jobin and Sartor, 2000; Karin et al., 2001) are activated by engagement of the MAPK, SAPK and IKK signaling pathways. We demonstrate that the MAPK, SAPK and IKK signaling pathways activation fails to occur in host cells by infection/exposure to *Salmonella* strains devoid of flagellin or products in the culture broths derived from those mutant *Salmonella* strains (**Figs. 5.5a and 5.6b**). We also demonstrate here that combined mutants of both fliC and fljB exhibit a severe lack of invasion (10^{-4} less than wild-type) and failure to activate stress response signaling, which has not been revealed previously. It is likely that the lack of flagellin production interferes with the functioning of the type III secretion system (TTSS) although flagellin is not known to effect expression of TTSS-required gene products. This hypothesis seems credible since supply of flagellin or bacterial culture components from wild-type *Salmonella* cultures in *trans* to the double $fliC^{-}/fljB^{-}$ mutant bacteria fails to compliment their lack of infectivity in gentamycin invasion assays (TT & JD, unpublished observations and see **Fig. 5.5b**). In fact, we found the abundance of a subset of Sip and Sop proteins (SipA and SopD) released into the bacterial culture media to be drastically reduced in the flagellin mutant strains used here (TT & JD, unpublished observations).

These two proteins have not previously been identified as activators of NF-κB nor are they considered as such here.

The TTSS translocates the *Salmonella* invasion proteins (Sips) and the SopE proteins into the host cell initiating cytoskeletal rearrangements that ultimately lead to bacterial internalization,(Galan, 2001; Galan and Collmer, 1999; Wallis et al., 1999). In any event, it is clear that purified flagellin activates a similar cadre of proinflammatory genes as does infection of intestinal epithelial cells with wild-type flagellated *Salmonella*. The temporal expression pattern of these genes was found to be remarkably similar (**Fig. 5.6c**) indicating that flagellin-mediated temporal activation of the MAPK, SAPK and IKK signaling pathways can suffice for signaling pathways activated by Sips or SopE and SopE2 and largely recapitulates the temporal activation of key proinflammatory genes as does infection of intestinal epithelial cells with wild-type flagellated *Salmonella*.

The rapid, and potent activation of the MAPK, SAPK and IKK signaling pathways by flagellin was consistent with and indicative of the activation of a cell surface receptor. In this study and in other studies TLR5 has been demonstrated to play an integral role in the recognition of flagellin leading to activation of NF-κB and expression of the IL-8 gene (**Fig. 5.6c**) (Gewirtz et al., 2001a; Hayashi et al., 2001). Identification of TLR5 utilized transfection of TLRs 1 – 9 into cell lines which responded poorly to flagellin (this study) or not at all (Gewirtz et al., 2001a; Hayashi et al., 2001) and challenging the transfectants with flagellin to identify which TLR responded to this PAMP. Previous studies that identified TLR5 as the receptor for flagellin did not examine the abundance of TLR5 in these cells or account for the lack of TLR5-mediated signaling in response to flagellin (Gewirtz et al., 2001a; Hayashi et al., 2001). We demonstrate here that cells which

respond poorly (HeLa and HEK293T) or not at all (T98G) contain TLR5 in at least equivalent abundance as HT29 cells which are highly responsive to flagellin. We propose at least three possibilities to account for this discrepancy, first, this may be due to either lack of TLR5 receptor presence at the plasma membrane and intracellular localization; second, inactivating or detrimental mutations in the TLR5 gene in these cell lines; and lastly, lack of or low abundance of a required co-receptor or adapter protein required for either efficient ligand recognition and/or signaling. These possibilities are currently being investigated. We favor the last possibility since surface biotinylation experiments indicate that TLR5 is present on the cell surface in both flagellin responding cells and in non-responders mentioned above (data not shown). Invocation of the second hypothesis would require inactivating mutations be present in three different cell lines, a highly improbable outcome.

How do the findings presented here correlate with events during a "normal" *Salmonella* infection? We have indicated in this study that defective type III secretion system functioning leads to loss of host cell infectivity and underscores the importance of this system in the normal course of infection. In the *in vivo* setting, polarized epithelial cells express TLR5 on the basolateral surface (Alexopoulou et al., 2001) and flagellin can only reach the receptor either after either breaching the tight junction barrier by physical damage or by loosening of the junctions in response to Sips and Sops delivered into the intestinal epithelial cells by the TTSS or by delivery of flagellin across the intestinal epithelial cell by the bacteria itself (Gewirtz et al., 2001b; McCormick, 2003; Sakaguchi et al., 2002; Wood et al., 2000). This scenario would imply the main function of the type III secretion system would be to trigger stress response signaling facilitating invasion and

lead to loosening the tight junctions and result in flagellin/ flagellated bacteria to passing through the junctions and infected cells allowing access the basolateral surface and then systemic dispersion. TLR5 on the basolateral surface of the intestinal epithelial cells, in response to flagellin, could then lead to activation of NF-κB and the proinflammatory gene program and host protection. This model is consistent with activation of the proinflammatory gene program observed in response to flagellated *Salmonella sp*. infection in many reports too numerous to cite here and would allow the innate host defense system a fail-safe way to recognize pathogen exposure. In instances where infection of intestinal epithelial cells by naturally occurring non-flagellated *Salmonella* occurs, a strong proinflammatory response would not initially be presented but the *Salmonella* would instead lead to systemic infection as is the case in chickens with *S. galinarum* and *S. pollorum* and result in typhoid-like disease (Kaiser et al., 2000). Infection of chicken epithelial cells does not lead to proinflammatory gene expression by these non-flagellated pathogens but does when infected with *S. typhimurium* or *S. Dublin* (Kaiser et al., 2000).

Argument for the existence of an additional TLR5 co-receptor/adapter being in limited abundance or absent might be in evidence from the transfection results presented in Table 1 which demonstrated that overexpression of cell surface localized FLAG-tagged TLR5 only resulted in slightly over a two-fold increase in NF-κB reporter gene expression in response to flagellin. If only TLR5 was required for activation of the signaling pathway should not a much more robust response been observed? We have also used DN-TLR5 transfections and NF-κB-dependent reporter gene assays or overexpression of DN-TLR5 using recombinant adenoviruses and analysis of resulting NF-κB DNA binding activity in

response to flagellin to examine its effectiveness to completely inhibit TLR5-mediated flagellin activation of NF-κB. We have found it difficult to gain more than a fifty-percent reduction in either reporter gene activation or NF-κB DNA binding activity in HT29 cells(TT, AD & JD, unpublished observations). These results suggest that the resting TLR5 signaling complex may be quite stable as has recently been suggested (Mizel and Snipes, 2002). Should the endogenous TLR5 signaling complex be extremely stable it would therefore be expected that titration of a required pre-stimulus bound adapter or co-receptor away would be inefficient and this is what we have observed. Expression of a DN-MAL (TIRAP), a MyD88-related TLR adapter (Fitzgerald et al., 2001; Hong et al., 2000) had little to no effect on flagellin-mediated NF-κB activity in transient transfection NF-κB reporter gene assays (TT & JD, unpublished observations). Recently, TLR5 has been shown to bind flagellin (Mizel et al., 2003; Murthy et al., 2004; Smith et al., 2003) and that this is likely a direct interaction due to failure of the human TLR5 to respond to a purified flagellin derived from a mouse-specific *Salmonella* strain (Smith et al., 2003). These observations still do not preclude the existence of a co-receptor or adapter that is critical for signal transmission. Detailed biochemical characterization of the TLR5 signaling complex will resolve this issue. Muc1, a recently described flagellin interacting membrane protein by virtue of its ability to trigger activation of the MAPK pathway in response to flagellin exposure (Lillehoj et al., 2004) was considered a viable candidate for such a co-receptor but our observations suggest that it can not serve as the putative TLR5 co-receptor as it is expressed at similar levels in flagellin non-responding cell lines examined here as it is in A549 cells which respond strongly to flagellin and both cell line types express similar levels of TLR5 (**Fig. 5.9**). In conclusion, our data clearly

demonstrates that flagellin can act as the major determinant in activating key stress response signaling pathways and proinflammatory gene program expression in a temporal and qualitative fashion as observed during infection of intestinal epithelial cells by wild-type *Salmonella sp*. that express flagellin, a point that was not well established until this study. In addition, expression of the *fli C* gene appears to play an important role in the proper functioning of the TTSS since mutants that fail to express *fli C* are defective in expressing a subset of Sip proteins and fail to invade host cells. Flagellin added in *trans* cannot restore the ability of the *fli C* mutant bacteria to invade intestinal epithelial cells. Flagellin is "sensed" by TLR5 and in response propagates signaling pathways culminating in potent proinflammatory gene expression. Interestingly we found that TLR5 is expressed in weakly responding and also in some flagellin non-responding cells, 293T, HeLa and T98G cells respectively at levels similar to cells such as HT29 and A549 cells that respond strongly to flagellin and can be found on the cell surface, raising a strong possibility that productive TLR5 signaling may require an additional factor/adaptor other than those already known to be key in the IL-1 signaling pathway, which shares extensive similarities to the TLRs signaling pathways.

Acknowledgements

We would like to thank Drs.E.Galyor (Compton Laboratory, Berkshire (UK)), Drs. R.M. Macnab (Yale University, New Haven, Conn), S. Mizel (Wake Forest University, Winston-Salem, NC), and M. Kagnoff (UCSD, La Jolla, CA) for bacterial strains. We would also like to thank S. Akira and O. Takeuchi (Osaka University, Osaka, JA) for the gift of MyD88 and TLR 2/4 double knockout cell lines. We also would like to thank S. Falkow (Stanford University, Stanford, CA), M. Karin (UCSD, La Jolla, CA), R.

Medzhitov (Yale University, New Haven, Conn) and R. Ulevitch (TSRI, La Jolla, CA) and V. Dixit (then at Univ. of Michigan, Ann Arbor, MI) for gifts of plasmids. We would also like to thank B. Williams (CCF, Cleveland, OH) for thoughtful discussions and support on this project. This work was supported in part by grants from the National Institutes of Health, CA84406 (to J.A.D.) and the U.S. Army, DAMD 17-01-C-0065 (to B. Williams).

Published in: *BMC Microbiology* 2004 August 23rd ; 4:33
Tallant T., Deb A., Kar N., Lupica J., deVeer M.J., DiDonato J.A.

CHAPTER VI

SUMMARY AND FUTURE DIRECTIONS

6.1 INTRODUCTION

NF-κB activation is a hallmark of the inflammatory response, and is an essential component in both adaptive and innate immunity. It is induced by a number cytokines that propagate not only the inflammatory response but in some instances the induction of the apoptotic pathway, as can a number of chemotherapeutic anti-cancer drugs. NF-κB is also activated by pathogen-manufactured ligands which are by-products of invasion and infection. The function of NF-κB's activation can be varied, however a significant portion of its function is involved in the inhibition of apoptosis, and the promotion of cell survival.

Cancer is a pathological condition that is pseudo-inflammatory in nature. The unchecked growth of cancer cells is a failure in the induction of cell death programs which results in the accumulation of tumor cells. NF-κB has been found to be constitutively active in many cancer cell-types, giving the neoplastic growth a biological survival advantage. Neoplastic cell growth may be attributed to cellular mutations that result in a gain or loss of function in normally highly regulated cellular signal

transduction pathways. A number of chemotherapeutic drugs target the apoptotic pathway for activation. However, these drugs also simultaneously activate NF-κB resulting in increased cell survival and inhibiton of the death pathways.

We hypothesized that if an adjuvant drug that inhibits NF-κB is administered in concert with a chemotherapeutic drug, whose mode of action targets the cellular apoptotic pathway, then the efficacy of the chemotherapeutic drug would be increased. The adjuvant drug we have chosen to study is the Nitric Oxide donor nitrosylcobalamin.

6.2 NF-κB, TRAIL/Apo2L, CHEMOTHERAPEUTIC DRUGS AND NO-Cbl

In chapter II, we began by revealing the synergistic effects that a combination treatment involving NO-Cbl and Apo2L/TRAIL had on A375, WM9 and WM3211 cells. These three melanoma cell lines had previously been shown to be resistant to Apo2L/TRAIL induced apoptosis. Sequential drug treatment resulted in synergistic anti-proliferative activity in all three cell lines, demonstrating that a Nitric Oxide adjuvant enhances the apoptotic effects of TRAIL. In addition, through the use of TUNNEL(IS THIS 1N OR 2?) assays and western blot analysis we made evident that the apoptotic activity in A375 cells treated with NO-Cbl and TRAIL was clearly increased over those that had been treated with TRAIL or NO-Cbl alone.

In support of our hypothesis we demonstrated, by way of EMSA and IKK Kinase Assays that both NF-κB DNA binding activity and IKK kinase activity is repressed, in combination-treated NO-Cbl and TRAIL cells compared to cells treated with either single agent. This phenomenon was demonstrated by western blot assays that exhibited a decrease in IκB degradation, indicating diminished NF-κB activity. Lastly, A375

melanoma xenograft solid tumors in mice, treated with a combination of TRAIL and NO-Cbl exhibited a marked decrease in tumor growth as compared to single drug treated mice or vehicle alone treated controls.

Chapter III explored the effects of combinatorial treatment of NO-Cbl and chemotherapeutic drugs, utilizing 4 dissimilar cancer cell lines, A375 (melanoma), MCF-7 (breast cancer), SW480 (colon cancer) and OVCAR-3 (ovarian cancer). Utilizing 10 different cancer cell lines in combination with 18 chemotherapeutic drugs we confirmed that combined, NO-Cbl and Chemotherapeutic drug treatment, induced a synergistic anti-proliferative effect in approximately 78% of the combinations examined.

Next we showed the effects of NO-Cbl co-treatment on two anti-apoptotic proteins, Akt and XIAP. Overall, the phosphorylated form of Akt was inhibited by NO-Cbl combinatorial treatment and XIAP expression is decreased. NF-κB DNA binding activity and IKK kinase activity exhibited mixed results; however, in general NO-Cbl inhibited IKK kinase and NF-κB transcription factor activity. Ovcar-3 cells treated with a combination treatment of NO-Cbl and Doxorubicin demonstrated an increased apoptotic activity, as indicated by the increase expression of the activated apoptotic biomarkers Caspase 8, PARP and XIAP. Lastly, combination-treated mice in an Ovcar-3 tumor xenograft model exhibited a marked decrease in tumor size, as well as increased animal survival compared to untreated or singularly treated mice. Murine leukemia tumor models resulted in 60% increased survival compared to untreated or singular treated mice.

A major advantage of Nitrosylcobalamin appears to be its tumor-specific accumulation. Cobalamin (Cbl) is avidly taken up by tumor cells relative to most normal cells.(Collins and Hogenkamp, 1997) NO-Cbl is therefore relatively tumor-specifically accumulated due to higher transcobalamin receptor (TCII-R) expression in tumor cells compared with normal tissue. NO-Cbl has a sustained half-life, allowing for a slow NO-release mechanism inside the cell. This results in decreased cellular toxicity as evidenced in **Figure 6.1 A**. There is little Chk2 protein phosphorylation by ATM kinase (an indicator of DNA damage), in cells treated with NO-Cbl alone compared to treatment with DNA damaging agents.

In comparison, the Nitric oxide donor SNP can also inhibit NF-κB, but it lacks tumor specific accumulation and due to its short half- life will release NO spontaneously and indiscriminately. This will induce significant toxicity to normal cells (Volk et al., 1995; Wink et al., 1996). As can be seen in **Figure 6.1 B**, HeLa cells treated with SNP show a considerable amount of ATM activation, as noted by Chk2 phosphorylation, at a level comparable to cells treated with DNA damaging agents.

In conclusion we have accumulated substantial data supporting the hypothesis that, the novel nitric oxide donor NO-Cbl could potentially prove to be an effective adjuvant therapy, to apoptotic-inducing chemotherapy.

FIGURE 6.1

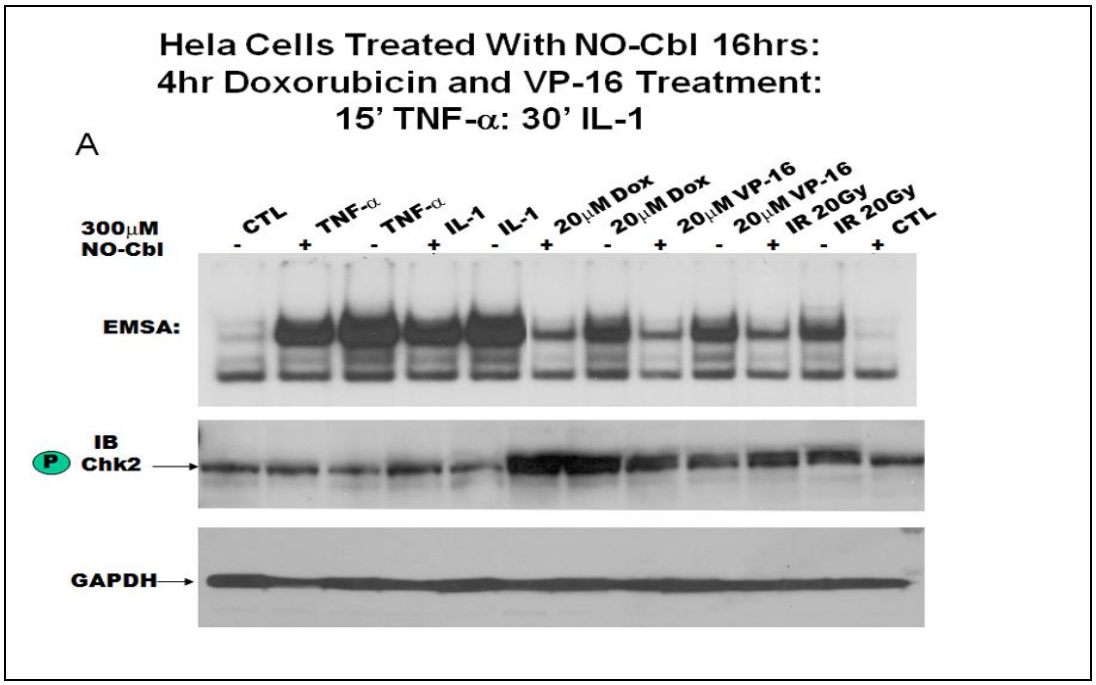
Hela Cells Treated With NO-Cbl 16hrs:
4hr Doxorubicin and VP-16 Treatment:
15' TNF-α: 30' IL-1
A
300μM NO-Cbl
CTL
TNF-α
TNF-α
IL-1
IL-1
20μM Dox
20μM Dox
20μM VP-16
20μM VP-16
IR 20Gy
IR 20Gy
CTL
EMSA:
IB Chk2
P
GAPDH

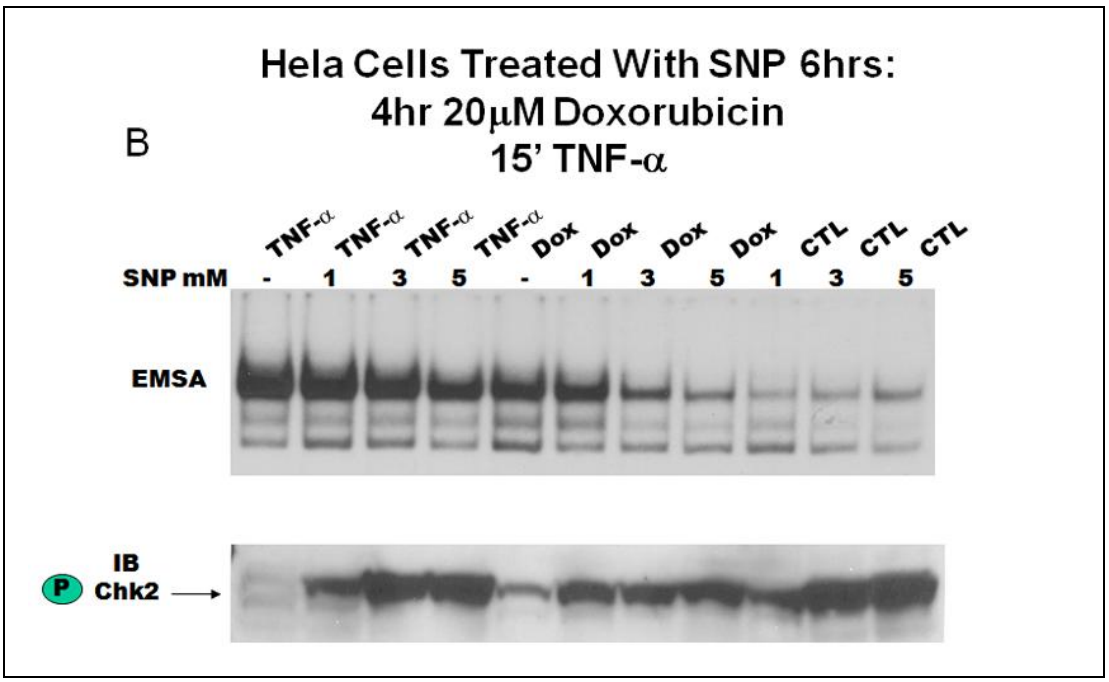
Hela Cells Treated With SNP 6hrs:
4hr 20μM Doxorubicin
15' TNF-α
B
TNF-α
TNF-α
TNF-α
TNF-α
Dox
Dox
Dox
Dox
CTL
CTL
CTL
SNP mM
- 1 3 5 - 1 3 5 1 3 5
EMSA
IB Chk2
P

Figure 6.1: Differential effects of NO-Cbl and SNP Treated HeLa cells on Chk2 activation NF-κB inhibition

HeLa cells were cultured in DMEM supplemented with 10% Fetal bovine serum and 1% antibiotic/antimycotic. Nuclear extracts were prepared as described in (Dignam et al., 1983). EMSA's and western blot analysis were preformed as previously described in (Bauer et al., 2007), p-Chk antibody (Cell Signaling). **a)** HeLa cells were pre-treated with 300μM of NO-Cbl for 16hrs then treated with TNF-α (10ng/mL), IL-1β (10ng/mL) or DNA damaging agent, concentration and time of treatment as noted in figure 6.1.
b) HeLa cells were pre-treated with SNP for 6hrs then treated with TNF-α (10ng/ml) or Doxorubicin DNA damaging agent, time and concentration as noted in figure 6.1.

6.3 PROPOSED MECHANISM OF ACTION FOR NF-κB INHIBITION

Previous studies by others suggested that a critical cysteine residue (C179) in the T-loop of IKKβ, a subunit of IKK and the main catalytic component of the IKK complex resulting in IKB phosphorylation and resultant activation of NF-κB, was nitrosylated interfering with its ability to activate NF-κB. A mutant form of IKKβ was constructed converting the cysteine to alanine (C179A); this mutant was reported to be resistant to the effects of Nitric Oxide. Our repeat of this experiment on two separate occasions (**Fig 6.2) and** data not shown, found little difference between it and wt IKKβ. As can be observed, the NO releasing compound DETA NONOate (Noc-18) can inhibit NF-κB DNA binding activity **(Fig 6.3)** and this inhibition was reflected by the decreased abundance of p65 (as the lower panel in Fig. 6.3 indicates) to translocate to the nucleus and is also an indication of decreased IκB phosphorylation and degradation.

FIGURE 6.2

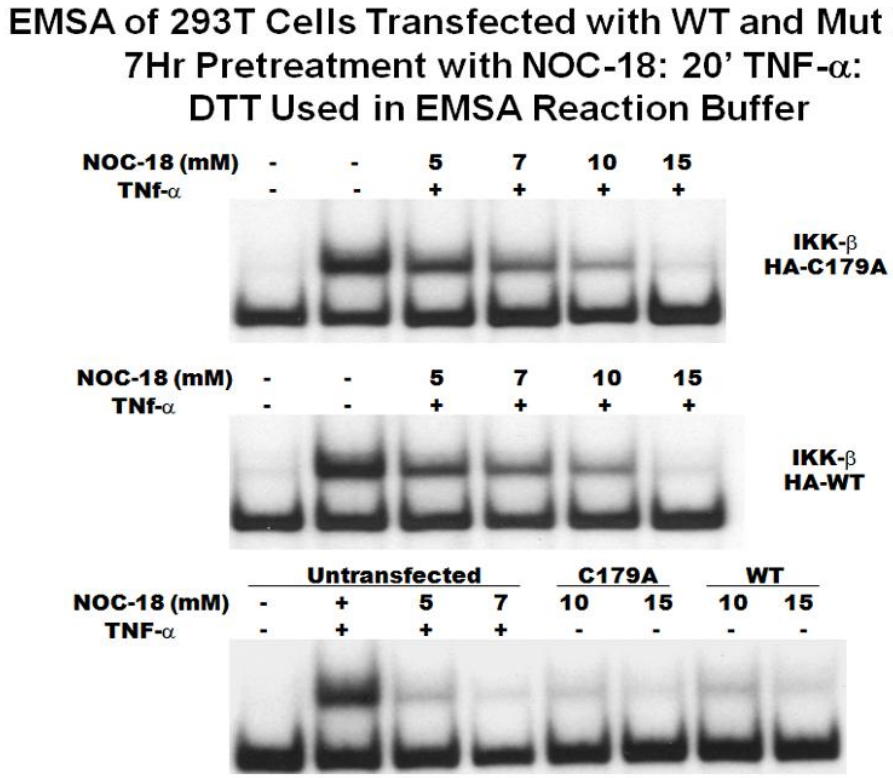

Figure 6.2: C179A Mutated IKKβ does not rescue Cells Treated with the Nitric Oxide Donor NOC-18 from NF-κB inhibition.

293T were cultured in DMEM supplemented with 10% fetal bovine serum and 1% antibiotic/antimycotic. The Constructs (Gift of Michael Karin) were transfected into 293T cells by nucleofection utilizing the Calcium Chloride method as described in (Graham and van der Eb, 1973). After 48 hours the 293T cells were. Transiently expressing wt and mutated IKKβ, as verified by western blot analyses (data not shown). The cells were then pretreated with the indicated concentrations of Noc-18 for 7h prior to stimulation with TNF-α (10ng/mL). Whole cell extracts were prepared as previously described (Chawla-Sarkar et al., 2003), and NF-κB DNA binding activity was monitored utilizing 25μg of whole cell extract with EMSA.

FIGURE 6.3

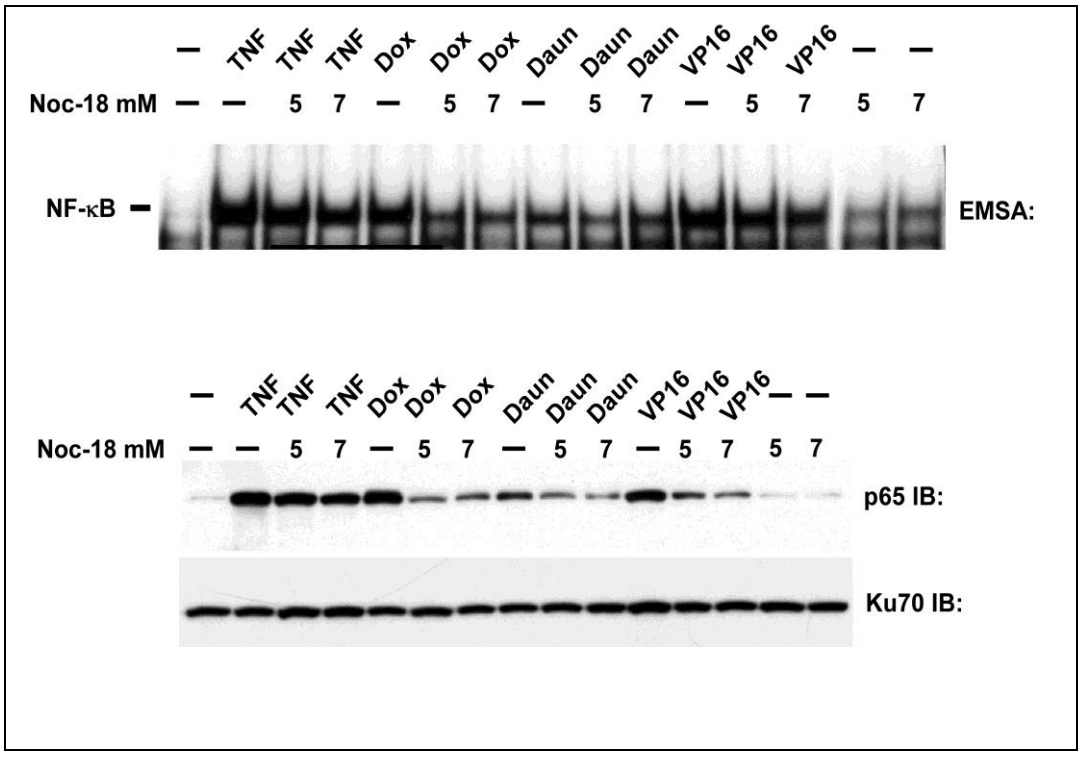

Figure 6.3 The Nitric Oxide Donor Noc-18 inhibits NF-κB

HeLa cells were cultured in DMEM supplemented with 10% Fetal bovine serum and 1% antibiotic/antimycotic. They were pretreated with the indicated concentrations of Noc-18 for 7h prior, at concentrations as noted on figure. Then stimulated with TNF-α (10ng/mL) 15minutes, Doxorubicin (20μM) 4 hrs, Daunorubicin (20μM) 4hrs or Vp-16 (20μM) 4hrs as noted on figure. Nuclear extracts (9μg for EMSA, 27μg for Western blot analysis) were prepared(Dignam et al., 1983) and analyzed by EMSA for DNA binding and by immunoblot analysis for the indicated proteins as previously described(Tallant et al., 2004).

Studies linking chemotherapeutic drugs utilizing the ZN finger of IKKγ to activate NF-κB, led us to postulate that this may be an important target for NO inhibition of IKK activity. To further examine the possibility that IKKγ could be a target for NO-inhibition we concentrated on likely residues in and around the ZN finger of IKKγ.

We focused on tyrosine (Y) 402 in the Zn finger and mutated this to a phenylalanine (F). We produced stably expressing Wt-IKKγ and 402F-expressing IKKγ HeLa cells and examined their sensitivity to NO release by SNP. As can be seen in Fig. 6.4, the 402F IKKγ protein appeared to provide additional protection against IKK and NF-κB inhibition by NO compared to Wt-IKKγ.

We demonstrated conclusively that the NO-releasing compound NO-Cbl can inhibit IKK and NF-κB activity. It appeared most effective against weak inducers of NF-κB or inducers that are known to utilize the ZN finger region of IKKγ. NO-Cbl inhibition of NF-κB is accomplished with little cellular DNA damage, reducing the potential of DNA damage that may done to normal cells. Our preliminary data indicated that the point of inhibition may be upstream of IKKβ or p65, the current purported points of inhibition. The questions still remaining to be answered are: Where is the location of the modification on IKKγ effecting inhibition? For example, it is possible that nitric oxide may nitrosylate one of the cysteines in the zinc finger causing instability and decreased function of IKKγ. What, if any, may this modification have on IKKγ phosphorylation, sumoylation, ubiquitination and nuclear import and export? Does the nitrosylation modification effect the association of IKKγ with ancillary signaling proteins? Secondly, can the expression of iNOS (also called NOS2) in cells increase the

effectiveness of chemotherapeutic drugs to kill cells, if so; can we stimulate high enough endogenous levels of iNOS to increase NO levels high enough to result in sensitizing cells to killing by doxorubicin or VP16? The ability to sensitize cells by triggering increased NO production may provide a key chemotherapeutic benefit

FIGURE 6.4

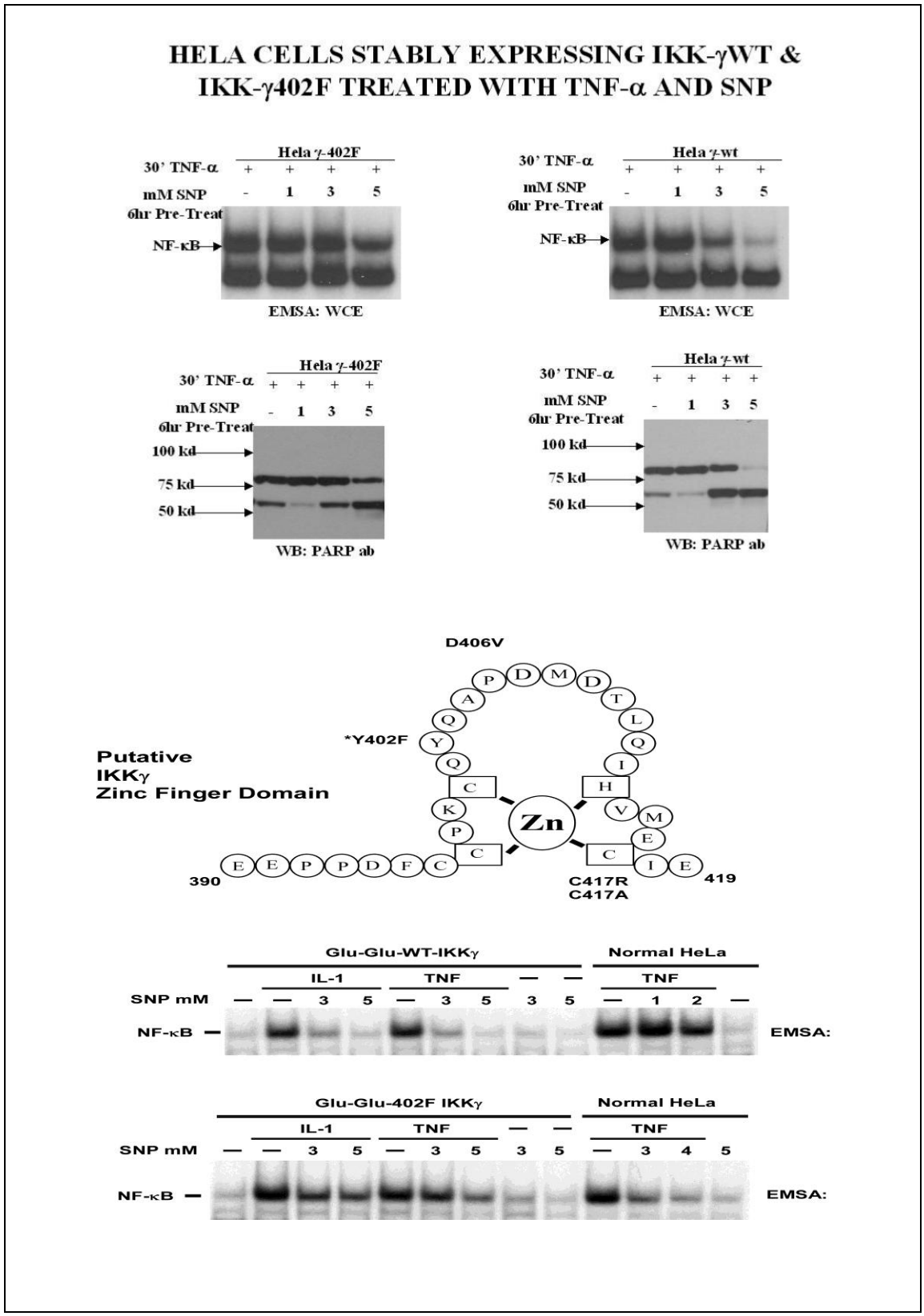
HELA CELLS STABLY EXPRESSING IKK-γWT & IKK-γ402F TREATED WITH TNF-α AND SNP
Hela γ-402F
30' TNF-α + + + +
mM SNP - 1 3 5
6hr Pre-Treat
NF-κB
EMSA: WCE
Hela γ-wt
30' TNF-α + + + +
mM SNP - 1 3 5
6hr Pre-Treat
NF-κB
EMSA: WCE
Hela γ-402F
30' TNF-α + + + +
mM SNP - 1 3 5
6hr Pre-Treat
100 kd
75 kd
50 kd
WB: PARP ab
Hela γ-wt
30' TNF-α + + + +
mM SNP - 1 3 5
6hr Pre-Treat
100 kd
75 kd
50 kd
WB: PARP ab
D406V
Putative
IKKγ
Zinc Finger Domain
*Y402F
Zn
390
419
C417R
C417A
Glu-Glu-WT-IKKγ
Normal HeLa
IL-1
TNF
TNF
SNP mM — — 3 5 — 3 5 3 5 — 1 2 —
NF-κB
EMSA:
Glu-Glu-402F IKKγ
Normal HeLa
IL-1
TNF
TNF
SNP mM — — 3 5 — 3 5 3 5 — 3 4 5
NF-κB
EMSA:

Figure 6.4 Mutated version of IKK-γ protects cells from inhibition of NF-κB by SNP and inhibits apoptotic effects of TNF-α

Protection of IKK and NF-κB activity from NO by IKK-γ 402F. Stably expressing WT or 402F Glu-Glu-epitope tagged IKKγ. HeLa cells were pretreated or not with SNP at the indicated doses for 30 min prior to stimulation with either TNF (10ng/mL) or IL-1 as indicated. Apoptotic effect of TNF-α is inhibited in mutant expressing cells as compared to wild type, as monitored by PARP cleavage. Cell extracts were prepared as previously described (Chawla-Sarkar et al., 2003). NF-κB activity was monitored by EMSA (25ug of Whole cell extract). EMSA and Western blot analyses performed as previously described (Bauer et al., 2007). EMSA's and western blot analysis are the results from 2 independent experiments.

SUPPLEMENTARY MATERIAL

SUPPLEMETAL FIGURE 1

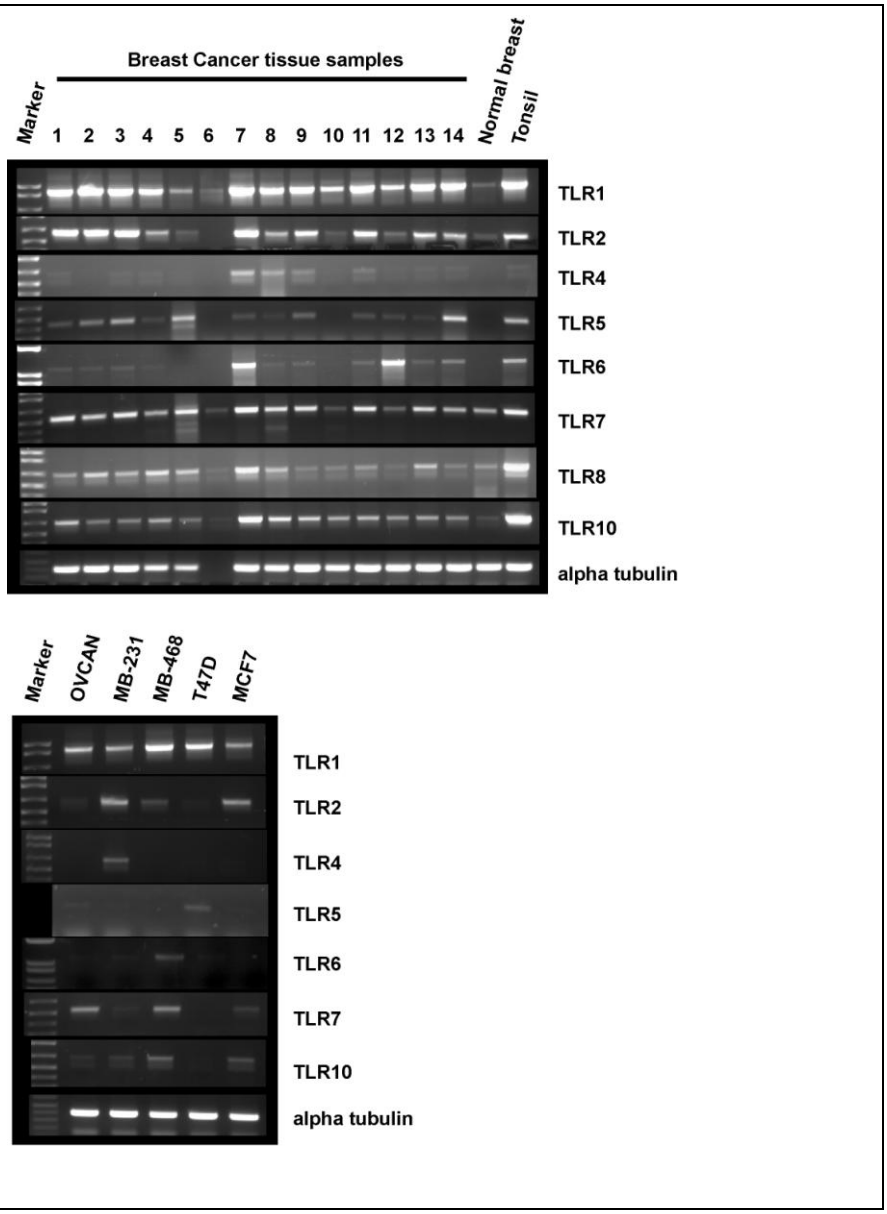

Supplemental Figure 1: RT-PCR examining TLR expression in normal breast tissue and in BC tumor tissue and BC cell line samples.

Total RNA was prepared from the indicated samples and RT-PCR was performed with primer pairs specific to the indicated TLR is indicated on the right side of the panel. Alpha tubulin expression served as the control RNA expression.

Supplemental Data for Supplemental figures 1and 2

Cell Culture-- Human breast cancer cell lines MDA-MB-231, MDA-MB-468, T-47D, MCF-7, SKBR3 Were cultured in Dulbecco's Modified Eagles Medium (DMEM) supplemented with heat inactivated 10% fetal bovine serum and 1% anti-biotic anti-mytotic and Cyprofloxin. The NIH OVCAR-3 cells were cultured in RPMI supplemented with heat inactivated 10% fetal bovine serum and 1%. Antibiotic/Antimycotic and Cyprofloxin. ACHN cells were cultured in Karatinocyte-SFM (GIBCO) media supplemented with L-Glutamate, Epithelial Growth Factor (EGF) and Bovine Pituitary Extract (BPE)

Reverse transcription PCR- Total cellular RNA was extracted from cells, grown in a 10cm plate, with TRIZOL reagent as described in {Chomczynski, 1988 #866}. De-identified discarded frozen pathology sections from human primary tumor breast biopsies, and human tonsil sections, were used as samples. Sections of frozen samples were cut and placed directly in Trizol (50-100mg). The Tissue fragments were homogenized using a microcentrifuge-tube pestle and total RNA extracted using TRIZOL reagent as described in {Chomczynski, 1988 #866}. The first strand cDNA were made using the following reagents.

Amount per 20µL Volume Reaction: 500ng Oligo (dT) $_{12\text{-}15;}$ 1µg total cellular RNA; 1µL 10mM dNTP mix (10mM each dATP, dGTP, dCTP and dTTP); Sterile distilled water 5-9µL; Heat mixture to 65^0C for 5min. and quick chill on ice; 4µL 5x first strand buffer (SuperScript II); 2µL 0.1 M DTT; 1µL RnaseOUT Recombinant Ribonuclease Inhibitor

Mix contents of the tube, incubate at 42^0C for 2minutes. Add 1µL (200 units) SuperScriptII. Incubate 50minutes at 42^0C. Inactivate the reaction by heating at 70^0C for 15 minutes.

PCR product were made utilizing the following reagents: 5µL 10x PCR buffer (200mM Tris, 500mM KCl); 50mM $MgCl_2$; 10mM dNTP mix; 10µM Forward primer; 10µM reverse primer; 10 Units *Taq* DNA polymerase; 200ng cDNA; 35-40µL distilled water.

PCR amplification consists of 1minute initial denaturing at 95^0C, 35 cycles of 30 second denaturing at 95^0C, 30 second annealing at 60^0C and 2 minute extension at 72^0C, then 1 final 10 minute extension at 72^0C. PCR products were fractionated on a 0.8% agarose gel. Refer to Supplemental Table 1 for PCR primer sequence and product BP size. Primers were made by Integrated DNA Technologies, Inc. Coralville, IA 52241.

SUPPLEMENTAL TABLE 1: Oligonucleotide Primers and PCR product sizes.

mRNA Species	5' Primer	3' Primer	Size of PCR Product (bp)
TLR 1	5CGTAAAACTGCAAGCTTTGCAAGA3	5CCTTGGGCCATTCCAAATAAGTCC3	890
TLR 2	5CCAGGTAGGTCTTGGTGTTCA3	5GGCCAGCAAATTACCTGTGTG3	614
TLR 4	5CTGCAATGGATCAAGGACCA3	5TCCCACTCCAGGTAAGTGTT3	622
TLR 5	5CATTGTATGCACTGTGACTC3	5CCACCACCATGATGAGAGCA3	445
TLR 6	5TAGGTCTCATGACGAAGGAT3	5GGCCACTGCAAATAACTCCG3	1107
TLR 7	5-AGTGTCTAAAGAACCTGG3'	5CTTGGCCTTACAGAAATG33	544
α-Tub	5CTGCCATTGCCACCATCAAAACCA3	5ATTCAGGGACCATGACATGCAGCAG3	661

SUPPLEMENTAL FIGURE 2

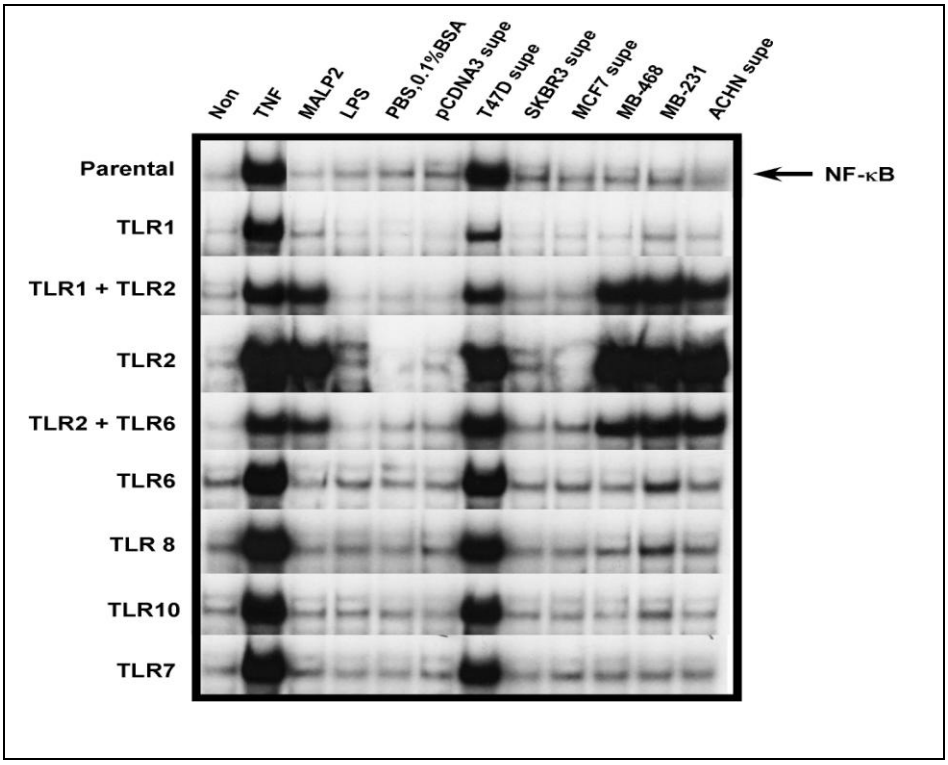

Supplemental Figure 2: Breast cancer cell lines produce factors that activate NF-κB

HEK 293 cells stably expressing individual TLRs or combinations of TLRs (Gift of Kate Fitzgerald, University of Massachusetts) as indicated to the left of each panel were stimulated with TNFα (10ng/ml) or Macrophage activating lipopepeptide [MALP2] (10pg/ml), partially repurified Lipopolysacharide (LPS) [100ng/ml], or with the indicated conditioned medias after preincubation with 20ug/ml neutralizing anti-TNFα antibody. Whole cell extracts (WCE) were prepared 45 min after stimulation and assayed for NF-κB DNA binding activity (indicated to the right of the panel) in EMSAs as previously described (Tallant et al., 2004)

The T47D BC cell line produces a factor(s) that activates NF-κB in all cells tested while MB-231 and MB-468 BC cell as does the ACHN kidney cancer cell line produce factor(s) that activate TLRs 1, 2, 2+1, 2+6, and TLRs 8 and 10. The activation is specific and is not due to contamination of positive cultures by endotoxin or by mycoplasmal contamination as all cells was grown in antibiotics, anti-mycotics and ciprofloxin as stated above and have not tested positive for mycoplasmal infection. It appears as though there may be multiple factors produced by the MB-231 cells as TLRs 8 and 10 show increased NF-κB activity in response to conditioned media from those cells.

BIBLIOGRAPHY

Abraham, R.T. (2001). Cell cycle checkpoint signaling through the ATM and ATR kinases. Genes Dev *15*, 2177-2196.

Aggarwal, B.B. (2003). Signalling pathways of the TNF superfamily: a double-edged sword. Nat Rev Immunol *3*, 745-756.

Aggarwal, B.B., Sethi, G., Nair, A., and Ichikawa, H. (2006). Nuclear Factor-kappaB: A Holy Grail in Cancer Prevention and Therapy. Current Signal Transduction Therapy *1*, 25-52.

Agou, F., Traincard, F., Vinolo, E., Courtois, G., Yamaoka, S., Israel, A., and Veron, M. (2004). The trimerization domain of NEMO is composed of the interacting C-terminal CC2 and LZ coiled-coil subdomains. J Biol Chem *279*, 27861-27869.

Ahn, J., Urist, M., and Prives, C. (2004). The Chk2 protein kinase. DNA Repair (Amst) *3*, 1039-1047.

Akashi, S., Nagai, Y., Ogata, H., Oikawa, M., Fukase, K., Kusumoto, S., Kawasaki, K., Nishijima, M., Hayashi, S., Kimoto, M., and Miyake, K. (2001). Human MD-2 confers on mouse Toll-like receptor 4 species-specific lipopolysaccharide recognition. Int Immunol *13*, 1595-1599.

Akira, S. (2001). Toll-like receptors and innate immunity. Adv Immunol *78*, 1-56.

Akira, S., and Hemmi, H. (2003). Recognition of pathogen-associated molecular patterns by TLR family. Immunol Lett *85*, 85-95.

Alberts, B., Bray, D., Lewis, J., Raff, M., Roberts, K., and Watson, J.D. (1994). Molecular Biology of The Cell, Vol First, Third edn (New York: Garland Publishing Inc.).

Alexopoulou, L., Holt, A.C., Medzhitov, R., and Flavell, R.A. (2001). Recognition of double-stranded RNA and activation of NF-kappaB by Toll-like receptor 3. Nature *413*, 732-738.

Anggard, E. (1994). Nitric oxide: mediator, murderer, and medicine. Lancet *343*, 1199-1206.

Arch, R.H., Gedrich, R.W., and Thompson, C.B. (1998). Tumor necrosis factor receptor-associated factors (TRAFs)--a family of adapter proteins that regulates life and death. Genes Dev *12*, 2821-2830.

Arlt, A., Vorndamm, J., Breitenbroich, M., Folsch, U.R., Kalthoff, H., Schmidt, W.E., and Schafer, H. (2001). Inhibition of NF-kappaB sensitizes human pancreatic carcinoma cells to apoptosis induced by etoposide (VP16) or doxorubicin. Oncogene *20*, 859-868.

Ashkenazi, A. (2002). Targeting death and decoy receptors of the tumour-necrosis factor superfamily. Nature Reviews. Cancer *2*, 420-430.

Ashkenazi, A., Pai, R.C., Fong, S., Leung, S., Lawrence, D.A., Marsters, S.A., Blackie, C., Chang, L., McMurtrey, A.E., Hebert, A., *et al.* (1999). Safety and antitumor activity of recombinant soluble Apo2 ligand. Journal of Clinical Investigation *104*, 155-162.

Auphan, N., DiDonato, J.A., Rosette, C., Helmberg, A., Karin, M., and Department of Pharmacology, S.o.M.U.o.C.S.D.L.J.U.S.A. (1995). Immunosuppression by glucocorticoids: inhibition of NF-kappa B activity through induction of I kappa B synthesis. Science *270(5234)*, 286-290.

Backhed, F., Normark, S., and Richter-Dahlfors, A. (2002). TLR4-dependent lipopolysaccharide signalling in epithelial cells is independent of extracellular protease activity. Cell Microbiol *4*, 297-303.

Baetu, T.M., Kwon, H., Sharma, S., Grandvaux, N., and Hiscott, J. (2001). Disruption of NF-kappaB signaling reveals a novel role for NF-kappaB in the regulation of TNF-related apoptosis-inducing ligand expression. Journal of Immunology *167*, 3164-3173.

Bakkenist, C.J., and Kastan, M.B. (2003). DNA damage activates ATM through intermolecular autophosphorylation and dimer dissociation. Nature *421*, 499-506.

Bakshi, C.S., Singh, V.P., Wood, M.W., Jones, P.W., Wallis, T.S., and Galyov, E.E. (2000). Identification of SopE2, a Salmonella secreted protein which is highly homologous to SopE and involved in bacterial invasion of epithelial cells. J Bacteriol *182*, 2341-2344.

Baldwin, A.S., Jr. (2001). Series introduction: the transcription factor NF-kappaB and human disease. J Clin Invest *107*, 3-6.

Bauer, J.A. (1998). Synthesis, characterization and nitric oxide release profile of nitrosylcobalamin: a potential chemotherapeutic agent. Anticancer Drugs *9*, 239-244.

Bauer, J.A., Lupica, J.A., Schmidt, H., Morrison, B.H., Haney, R.M., Masci, R.K., Lee, R.M., DiDonato, J.A., and Lindner, D.J. (2007). Nitrosylcobalamin Potentiates the Anti-Neoplastic Effects of Chemotherapeutic Agents via Suppression of Survival Signaling. PLoS ONE *2*, e1313.

Bauer, J.A., Morrison, B.H., Grane, R.W., Jacobs, B.S., Dabney, S., Gamero, A.M., Carnevale, K.A., Smith, D.J., Drazba, J., Seetharam, B., and Lindner, D.J. (2002). Effects of interferon beta on transcobalamin II-receptor expression and antitumor activity of nitrosylcobalamin. J Natl Cancer Inst *94*, 1010-1019.

Bava, S.V., Puliappadamba, V.T., Deepti, A., Nair, A., Karunagaran, D., and Anto, R.J. (2005). Sensitization of taxol-induced apoptosis by curcumin involves down-regulation of nuclear factor-kappaB and the serine/threonine kinase Akt and is independent of tubulin polymerization. J Biol Chem *280*, 6301-6308.

Beckman, J.S., and Koppenol, W.H. (1996). Nitric oxide, superoxide, and peroxynitrite: the good, the bad, and ugly. Am J Physiol *271*, C1424-1437.

Bender, K., Gottlicher, M., Whiteside, S., Rahmsdorf, H.J., and Herrlich, P. (1998). Sequential DNA damage-independent and -dependent activation of NF-kappaB by UV. Embo J *17*, 5170-5181.

Beutler, B. (2004). Innate immunity: an overview. Mol Immunol *40*, 845-859.

Bharti, A.C., and Aggarwal, B.B. (2002). Nuclear factor-kappa B and cancer: its role in prevention and therapy. Biochemical Pharmacology *64*, 883-888.

Bours, V., Bentires-Alj, M., Hellin, A.C., Viatour, P., Robe, P., Delhalle, S., Benoit, V., and Merville, M.P. (2000). Nuclear factor-kappa B, cancer, and apoptosis. Biochemical Pharmacology *60*, 1085-1089.

Brasier, A.R. (2006). The NF-kappaB regulatory network. Cardiovasc Toxicol *6*, 111-130.

Buchholz, T.A., Garg, A.K., Chakravarti, N., Aggarwal, B.B., Esteva, F.J., Kuerer, H.M., Singletary, S.E., Hortobagyi, G.N., Pusztai, L., Cristofanilli, M., and Sahin, A.A. (2005). The nuclear transcription factor kappaB/bcl-2 pathway correlates with pathologic complete response to doxorubicin-based neoadjuvant chemotherapy in human breast cancer. Clin Cancer Res *11*, 8398-8402.

Byrd-Leifer, C.A., Block, E.F., Takeda, K., Akira, S., Ding, A., Department of, M., and Immunology, W.M.C.o.C.U.N.Y.N.Y.U.S.A. (2001). The role of MyD88 and TLR4 in the LPS-mimetic activity of Taxol. Eur J Immunol *31(8)*, 2448-2457.

Chawla-Sarkar, M., Bauer, J.A., Lupica, J.A., Morrison, B.H., Tang, Z., Oates, R.K., Almasan, A., DiDonato, J.A., Borden, E.C., Lindner, D.J., *et al.* (2003). Suppression of NF-kappa B survival signaling by nitrosylcobalamin sensitizes neoplasms to the anti-tumor effects of Apo2L/TRAIL. The Journal of biological chemistry. *278(41)*, 39461-39469.

Chawla-Sarkar, M., Leaman, D.W., and Borden, E.C. (2001). Preferential induction of apoptosis by interferon (IFN)-beta compared with IFN-alpha2: correlation with TRAIL/Apo2L induction in melanoma cell lines. Clinical Cancer Research *7*, 1821-1831.

Chawla-Sarkar, M., Leaman, D.W., Jacobs, B.S., and Borden, E.C. (2002). IFN-beta pretreatment sensitizes human melanoma cells to TRAIL/Apo2 ligand-induced apoptosis. J Immunol *169*, 847-855.

Chen, C., Edelstein, L.C., and Gelinas, C. (2000). The Rel/NF-kappaB family directly activates expression of the apoptosis inhibitor Bcl-x(L). Molecular & Cellular Biology *20*, 2687-2695.

Chen, G., Cao, P., and Goeddel, D.V. (2002). TNF-induced recruitment and activation of the IKK complex require Cdc37 and Hsp90. Mol Cell *9*, 401-410.

Chen, L.M., Hobbie, S., and Galan, J.E. (1996). Requirement of CDC42 for Salmonella-induced cytoskeletal and nuclear responses. Science *274*, 2115-2118.

Cheng, J.Q., Godwin, A.K., Bellacosa, A., Taguchi, T., Franke, T.F., Hamilton, T.C., Tsichlis, P.N., and Testa, J.R. (1992). AKT2, a putative oncogene encoding a member of a subfamily of protein-serine/threonine kinases, is amplified in human ovarian carcinomas. Proc Natl Acad Sci U S A *89*, 9267-9271.

Chinnaiyan, A.M., Prasad, U., Shankar, S., Hamstra, D.A., Shanaiah, M., Chenevert, T.L., Ross, B.D., and Rehemtulla, A. (2000). Combined effect of tumor necrosis factor-related apoptosis-inducing ligand and ionizing radiation in breast cancer therapy. Proceedings of the National Academy of Sciences of the United States of America *97*, 1754-1759.

Chlichlia, K., Peter, M.E., Rocha, M., Scaffidi, C., Bucur, M., Krammer, P.H., Schirrmacher, V., and Umansky, V. (1998). Caspase activation is required for nitric oxide-mediated, CD95(APO- 1/Fas)-dependent and independent apoptosis in human neoplastic lymphoid cells. Blood *91*, 4311-4320.

Chou, T.C., and Talalay, P. (1984). Quantitative analysis of dose-effect relationships: The combined effects of multiple drugs or enzyme inhibitors. Advances in Enzyme Regulation *22*, 27-55.

Chuang, T.H., and Ulevitch, R.J. (2000). Cloning and characterization of a sub-family of human toll-like receptors: hTLR7, hTLR8 and hTLR9. Eur Cytokine Netw *11*, 372-378.

Ciacci-Woolwine, F., Blomfield, I.C., Richardson, S.H., and Mizel, S.B. (1998). Salmonella flagellin induces tumor necrosis factor alpha in a human promonocytic cell line. Infect Immun *66*, 1127-1134.

Collins, D.A., and Hogenkamp, H.P. (1997). Transcobalamin II receptor imaging via radiolabeled diethylene- triaminepentaacetate cobalamin analogs. J Nucl Med *38*, 717-723.

Collins, D.A., Hogenkamp, H.P., O'Connor, M.K., Naylor, S., Benson, L.M., Hardyman, T.J., and Thorson, L.M. (2000). Biodistribution of radiolabeled adenosylcobalamin in patients diagnosed with various malignancies. Mayo Clin Proc *75*, 568-580.

Contassot, E., Gaide, O., and French, L.E. (2007). Death receptors and apoptosis. Dermatol Clin *25*, 487-501, vii.

Cooperman, J.e.a. (1960). Distribution of radioactive and nonradioactive vitamin B12 in the dog. Journal of Biological Chemistry *235*, 191-194.

Cordon-Cardo, C., and Prives, C. (1999). At the crossroads of inflammation and tumorigenesis. J Exp Med *190*, 1367-1370.

Coussens, L.M., and Werb, Z. (2002). Inflammation and cancer. Nature *420*, 860.

Croston, G.E., Cao, Z., and Goeddel, D.V. (1995). NF-kappa B activation by interleukin-1 (IL-1) requires an IL-1 receptor-associated protein kinase activity. J Biol Chem *270*, 16514-16517.

D'Acquisto, F., Maiuri, M.C., de Cristofaro, F., and Carnuccio, R. (2001). Nitric oxide prevents inducible cyclooxygenase expression by inhibiting nuclear factor-kappa B and nuclear factor-interleukin-6 activation. Naunyn-Schmiedebergs Archives of Pharmacology *364*, 157-165.

da Silva Correia, J., Soldau, K., Christen, U., Tobias, P.S., and Ulevitch, R.J. (2001). Lipopolysaccharide is in close proximity to each of the proteins in its membrane receptor complex. transfer from CD14 to TLR4 and MD-2. J Biol Chem *276*, 21129-21135.

Dan, H.C., Sun, M., Kaneko, S., Feldman, R.I., Nicosia, S.V., Wang, H.G., Tsang, B.K., and Cheng, J.Q. (2004). Akt phosphorylation and stabilization of X-linked inhibitor of apoptosis protein (XIAP). J Biol Chem *279*, 5405-5412.

Das, K.C., and White, C.W. (1997). Activation of NF-kappaB by antineoplastic agents. Role of protein kinase C. J Biol Chem *272*, 14914-14920.

Datta, S.R., Brunet, A., and Greenberg, M.E. (1999). Cellular survival: a play in three Akts. Genes Dev *13*, 2905-2927.

Davies, C.C., Mak, T.W., Young, L.S., and Eliopoulos, A.G. (2005). TRAF6 is required for TRAF2-dependent CD40 signal transduction in nonhemopoietic cells. Mol Cell Biol *25*, 9806-9819.

Davis, K.L., Martin, E., Turko, I.V., and Murad, F. (2001). Novel effects of nitric oxide. Annu Rev Pharmacol Toxicol *41*, 203-236.

Debatin, K.M. (2004). Apoptosis pathways in cancer and cancer therapy. Cancer Immunol Immunother *53*, 153-159.

DelaTorre, A., Schroeder, R.A., and Kuo, P.C. (1997). Alteration of NF-kappa B p50 DNA binding kinetics by S-nitrosylation. Biochemical & Biophysical Research Communications *238*, 703-706.

Devary, Y., Rosette, C., DiDonato, J.A., and Karin, M. (1993). NF-kappa B activation by ultraviolet light not dependent on a nuclear signal. Science *261*, 1442-1445.

Devin, A., Cook, A., Lin, Y., Rodriguez, Y., Kelliher, M., and Liu, Z. (2000). The distinct roles of TRAF2 and RIP in IKK activation by TNF-R1: TRAF2 recruits IKK to TNF-R1 while RIP mediates IKK activation. Immunity *12*, 419-429.

Devin, A., Lin, Y., Yamaoka, S., Li, Z., Karin, M., and Liu, Z. (2001). The alpha and beta subunits of IkappaB kinase (IKK) mediate TRAF2-dependent IKK recruitment to tumor necrosis factor (TNF) receptor 1 in response to TNF. Mol Cell Biol *21*, 3986-3994.

Dhawan, P., and Richmond, A. (2002). A novel NF-kappa B-inducing kinase-MAPK signaling pathway up-regulates NF-kappa B activity in melanoma cells. J Biol Chem *277*, 7920-7928.

Dhawan, P., Singh, A.B., Ellis, D.L., Richmond, A., and Department of Cancer Biology, V.U.S.o.M.N.T.U.S.A. (2002). Constitutive activation of Akt/protein kinase B in melanoma leads to up-regulation of nuclear factor-kappaB and tumor progression. Cancer research. *62(24)*, 7335-7342.

Di Pietro, R., Secchiero, P., Rana, R., Gibellini, D., Visani, G., Bemis, K., Zamai, L., Miscia, S., and Zauli, G. (2001). Ionizing radiation sensitizes erythroleukemic cells but not normal erythroblasts to tumor necrosis factor-related apoptosis-inducing ligand (TRAIL)--mediated cytotoxicity by selective up-regulation of TRAIL-R1. Blood *97*, 2596-2603.

DiDonato, J., Mercurio, F., Rosette, C., Wu-Li, J., Suyang, H., Ghosh, S., and Karin, M. (1996). Mapping of the inducible IkappaB phosphorylation sites that signal its ubiquitination and degradation. Molecular and Cellular Biology. *16(4)*, 1295-1304.

DiDonato, J.A. (2000). Assaying for I kappa B kinase activity. Methods in Enzymology *322*, 393-400.

DiDonato, J.A., Hayakawa, M., Rothwarf, D.M., Zandi, E., and Karin, M. (1997a). A cytokine-responsive I[kappa]B kinase that activates the transcription factor NF-[kappa]B. Nature *388*, 548.

DiDonato, J.A., Hayakawa, M., Rothwarf, D.M., Zandi, E., Karin, M., Laboratory of Gene, R., and Signal Transduction, D.o.P.U.o.C.a.S.D.L.J.U.S.A. (1997b). A cytokine-responsive IkappaB kinase that activates the transcription factor NF-kappaB. Nature *388(6642)*, 548-554.

DiDonato, J.A., and John, C.R. (2000). [36] Assaying for I[kappa]B kinase activity. In Methods in Enzymology (Academic Press), p. 393.

DiDonato, J.A., Mercurio, F., and Karin, M. (1995a). Phosphorylation of I kappa B alpha precedes but is not sufficient for its dissociation from NF-kappa B. Molecular & Cellular Biology *15*, 1302-1311.

DiDonato, J.A., Mercurio, F., Karin, M., and Department of Pharmacology, U.o.C.S.D.S.o.M.L.J. (1995b). Phosphorylation of I kappa B alpha precedes but is not sufficient for its dissociation from NF-kappa B. Mol Cell Biol *15(3)*, 1302-1311.

Dignam, J.D., Lebovitz, R.M., and Roeder, R.G. (1983). Accurate transcription initiation by RNA polymerase II in a soluble extract from isolated mammalian nuclei. Nucleic Acids Res *11*, 1475-1489.

Dong, Q.G., Sclabas, G.M., Fujioka, S., Schmidt, C., Peng, B., Wu, T., Tsao, M.S., Evans, D.B., Abbruzzese, J.L., McDonnell, T.J., and Chiao, P.J. (2002). The function of multiple IkappaB : NF-kappaB complexes in the resistance of cancer cells to Taxol-induced apoptosis. Oncogene *21*, 6510-6519.

Dunne, A., and O'Neill, L.A. (2005). Adaptor usage and Toll-like receptor signaling specificity. FEBS Lett *579*, 3330-3335.

Eaves-Pyles, T., Szabo, C., and Salzman, A.L. (1999). Bacterial invasion is not required for activation of NF-kappaB in enterocytes. Infect Immun *67*, 800-804.

Eckelman, B.P., Salvesen, G.S., and Scott, F.L. (2006). Human inhibitor of apoptosis proteins: why XIAP is the black sheep of the family. EMBO Rep *7*, 988-994.

Eckmann, L., Kagnoff, M.F., and Fierer, J. (1995). Intestinal epithelial cells as watchdogs for the natural immune system. Trends Microbiol *3*, 118-120.

Eckmann, L., Stenson, W.F., Savidge, T.C., Lowe, D.C., Barrett, K.E., Fierer, J., Smith, J.R., and Kagnoff, M.F. (1997). Role of intestinal epithelial cells in the host secretory response to infection by invasive bacteria. Bacterial entry induces epithelial prostaglandin h synthase-2 expression and prostaglandin E2 and F2alpha production. J Clin Invest *100*, 296-309.

Eid, M.A., Lewis, R.W., Abdel-Mageed, A.B., and Kumar, M.V. (2002). Reduced response of prostate cancer cells to TRAIL is modulated by NFkappaB-mediated inhibition of caspases and Bid activation. Int J Oncol *21*, 111-117.

Elewaut, D., DiDonato, J.A., Kim, J.M., Truong, F., Eckmann, L., and Kagnoff, M.F. (1999). NF-kappa B is a central regulator of the intestinal epithelial cell innate immune response induced by infection with enteroinvasive bacteria. Journal of Immunology *163*, 1457-1466.

Fahy, B.N., Schlieman, M.G., Virudachalam, S., and Bold, R.J. (2004). Inhibition of AKT abrogates chemotherapy-induced NF-kappaB survival mechanisms: implications for therapy in pancreatic cancer. J Am Coll Surg *198*, 591-599.

Falschlehner, C., Emmerich, C.H., Gerlach, B., and Walczak, H. (2007). TRAIL signalling: decisions between life and death. Int J Biochem Cell Biol *39*, 1462-1475.

Fitzgerald, K.A., Palsson-McDermott, E.M., Bowie, A.G., Jefferies, C.A., Mansell, A.S., Brady, G., Brint, E., Dunne, A., Gray, P., Harte, M.T., *et al.* (2001). Mal (MyD88-adapter-like) is required for Toll-like receptor-4 signal transduction. Nature *413*, 78-83.

Flodh, H., and Ullberg, S. (1968). Accumulation of labelled vitamin B12 in some transplanted tumours. Int J Cancer *3*, 694-699.

Frese, S., Brunner, T., Gugger, M., Uduehi, A., and Schmid, R.A. (2002). Enhancement of Apo2L/TRAIL (tumor necrosis factor-related apoptosis-inducing ligand)-induced apoptosis in non-small cell lung cancer cell lines by chemotherapeutic agents without correlation to the expression level of cellular protease caspase-8 inhibitory protein. Journal of Thoracic & Cardiovascular Surgery *123*, 168-174.

Galan, J.E. (2001). Salmonella interactions with host cells: type III secretion at work. Annu Rev Cell Dev Biol *17*, 53-86.

Galan, J.E., and Collmer, A. (1999). Type III secretion machines: bacterial devices for protein delivery into host cells. Science *284*, 1322-1328.

Galkin, V.E., Orlova, A., VanLoock, M.S., Zhou, D., Galan, J.E., and Egelman, E.H. (2002). The bacterial protein SipA polymerizes G-actin and mimics muscle nebulin. Nat Struct Biol *9*, 518-521.

Gasparian, A.V., Yao, Y.J., Kowalczyk, D., Lyakh, L.A., Karseladze, A., Slaga, T.J., and Budunova, I.V. (2002). The role of IKK in constitutive activation of NF-kappaB transcription factor in prostate carcinoma cells. J Cell Sci *115*, 141-151.

Gewirtz, A.T., Navas, T.A., Lyons, S., Godowski, P.J., and Madara, J.L. (2001a). Cutting edge: bacterial flagellin activates basolaterally expressed TLR5 to induce epithelial proinflammatory gene expression. J Immunol *167*, 1882-1885.

Gewirtz, A.T., Rao, A.S., Simon, P.O., Jr., Merlin, D., Carnes, D., Madara, J.L., and Neish, A.S. (2000). Salmonella typhimurium induces epithelial IL-8 expression via Ca(2+)-mediated activation of the NF-kappaB pathway. J Clin Invest *105*, 79-92.

Gewirtz, A.T., Simon, P.O., Jr., Schmitt, C.K., Taylor, L.J., Hagedorn, C.H., O'Brien, A.D., Neish, A.S., and Madara, J.L. (2001b). Salmonella typhimurium translocates flagellin across intestinal epithelia, inducing a proinflammatory response. J Clin Invest *107*, 99-109.

Ghobrial, I.M., Witzig, T.E., and Adjei, A.A. (2005). Targeting apoptosis pathways in cancer therapy. CA Cancer J Clin *55*, 178-194.

Gibson, S.B., Oyer, R., Spalding, A.C., Anderson, S.M., and Johnson, G.L. (2000). Increased expression of death receptors 4 and 5 synergizes the apoptosis response to combined treatment with etoposide and TRAIL. Molecular & Cellular Biology *20*, 205-212.

Gliniak, B., and Le, T. (1999). Tumor necrosis factor-related apoptosis-inducing ligand's antitumor activity in vivo is enhanced by the chemotherapeutic agent CPT-11. Cancer Research *59*, 6153-6158.

Goke, R., Goke, A., Goke, B., and Chen, Y. (2000). Regulation of TRAIL-induced apoptosis by transcription factors. Cellular Immunology *201*, 77-82.

Gong, B., and Almasan, A. (2000). Apo2 ligand/TNF-related apoptosis-inducing ligand and death receptor 5 mediate the apoptotic signaling induced by ionizing radiation in leukemic cells. Cancer Research *60*, 5754-5760.

Graham, F.L., and van der Eb, A.J. (1973). A new technique for the assay of infectivity of human adenovirus 5 DNA. Virology *52*, 456-467.

Gross, S.S., and Wolin, M.S. (1995). Nitric oxide: pathophysiological mechanisms. Annu Rev Physiol *57*, 737-769.

Habraken, Y., and Piette, J. (2006). NF-kappaB activation by double-strand breaks. Biochem Pharmacol *72*, 1132-1141.

Hacker, H., and Karin, M. (2006). Regulation and function of IKK and IKK-related kinases. Sci STKE *2006*, re13.

Hajjar, A.M., O'Mahony, D.S., Ozinsky, A., Underhill, D.M., Aderem, A., Klebanoff, S.J., and Wilson, C.B. (2001). Cutting edge: functional interactions between toll-like receptor (TLR) 2 and TLR1 or TLR6 in response to phenol-soluble modulin. J Immunol *166*, 15-19.

Hanakahi, L.A., Bartlet-Jones, M., Chappell, C., Pappin, D., and West, S.C. (2000). Binding of Inositol Phosphate to DNA-PK and Stimulation of Double-Strand Break Repair. Cell *102*, 721.

Hardt, W.D., Chen, L.M., Schuebel, K.E., Bustelo, X.R., and Galan, J.E. (1998). S. typhimurium encodes an activator of Rho GTPases that induces membrane ruffling and nuclear responses in host cells. Cell *93*, 815-826.

Hayashi, F., Smith, K.D., Ozinsky, A., Hawn, T.R., Yi, E.C., Goodlett, D.R., Eng, J.K., Akira, S., Underhill, D.M., and Aderem, A. (2001). The innate immune response to bacterial flagellin is mediated by Toll-like receptor 5. Nature *410*, 1099-1103.

Hayden, M.S., and Ghosh, S. (2004). Signaling to NF-kappaB. Genes Dev *18*, 2195-2224.

Heguy, A., Baldari, C.T., Macchia, G., Telford, J.L., and Melli, M. (1992). Amino acids conserved in interleukin-1 receptors (IL-1Rs) and the Drosophila toll protein are essential for IL-1R signal transduction. J Biol Chem *267*, 2605-2609.

Herr, I., Posovszky, C., Di Marzio, L.D., Cifone, M.G., Boehler, T., and Debatin, K.M. (2000). Autoamplification of apoptosis following ligation of CD95-L, TRAIL and TNF-alpha. Oncogene *19*, 4255-4262.

Hess, D.T., Matsumoto, A., Kim, S.O., Marshall, H.E., and Stamler, J.S. (2005). Protein S-nitrosylation: purview and parameters. Nat Rev Mol Cell Biol *6*, 150-166.

Hibi, M., Lin, A., Smeal, T., Minden, A., and Karin, M. (1993). Identification of an oncoprotein- and UV-responsive protein kinase that binds and potentiates the c-Jun activation domain. Genes Dev *7*, 2135-2148.

Hobbie, S., Chen, L.M., Davis, R.J., and Galan, J.E. (1997). Involvement of mitogen-activated protein kinase pathways in the nuclear responses and cytokine production induced by Salmonella typhimurium in cultured intestinal epithelial cells. J Immunol *159*, 5550-5559.

Hochwald, S.N., Lind, D.S., Malaty, J., Copeland, E.M., 3rd, Moldawer, L.L., and MacKay, S.L. (2003). Antineoplastic therapy in colorectal cancer through proteasome inhibition. Am Surg *69*, 15-23.

Hong, Y.K., Chung, D.S., Joe, Y.A., Yang, Y.J., Kim, K.M., Park, Y.S., Yung, W.K., and Kang, J.K. (2000). Efficient inhibition of in vivo human malignant glioma growth and angiogenesis by interferon-beta treatment at early stage of tumor development. Clin Cancer Res *6*, 3354-3360.

Huang, T.T., Feinberg, S.L., Suryanarayanan, S., and Miyamoto, S. (2002). The zinc finger domain of NEMO is selectively required for NF-kappa B activation by UV radiation and topoisomerase inhibitors. Mol Cell Biol *22*, 5813-5825.

Huang, T.T., Wuerzberger-Davis, S.M., Wu, Z.H., and Miyamoto, S. (2003). Sequential modification of NEMO/IKKgamma by SUMO-1 and ubiquitin mediates NF-kappaB activation by genotoxic stress. Cell *115*, 565-576.

Huang, Y., and Fan, W. (2002). IkappaB kinase activation is involved in regulation of paclitaxel-induced apoptosis in human tumor cell lines. Mol Pharmacol *61*, 105-113.

Israel, A. (2006). NF-kappaB activation: Nondegradative ubiquitination implicates NEMO. Trends Immunol *27*, 395-397.

Jackson-Bernitsas, D.G., Ichikawa, H., Takada, Y., Myers, J.N., Lin, X.L., Darnay, B.G., Chaturvedi, M.M., and Aggarwal, B.B. (2007). Evidence that TNF-TNFR1-TRADD-TRAF2-RIP-TAK1-IKK pathway mediates constitutive NF-kappaB activation and proliferation in human head and neck squamous cell carcinoma. Oncogene *26*, 1385-1397.

Jain, A., Ma, C.A., Liu, S., Brown, M., Cohen, J., and Strober, W. (2001). Specific missense mutations in NEMO result in hyper-IgM syndrome with hypohydrotic ectodermal dysplasia. Nat Immunol *2*, 223-228.

Jin, Z., and El-Deiry, W.S. (2005). Overview of cell death signaling pathways. Cancer Biol Ther *4*, 139-163.

Jobin, C., and Sartor, R.B. (2000). The I kappa B/NF-kappa B system: a key determinant of mucosalinflammation and protection. Am J Physiol Cell Physiol *278*, C451-462.

Jung, H.C., Eckmann, L., Yang, S.K., Panja, A., Fierer, J., Morzycka-Wroblewska, E., and Kagnoff, M.F. (1995). A distinct array of proinflammatory cytokines is expressed in human colon epithelial cells in response to bacterial invasion. J Clin Invest *95*, 55-65.

Kagnoff, M.F., and Eckmann, L. (1997). Epithelial cells as sensors for microbial infection. J Clin Invest *100*, 6-10.

Kaiser, P., Rothwell, L., Galyov, E.E., Barrow, P.A., Burnside, J., and Wigley, P. (2000). Differential cytokine expression in avian cells in response to invasion by Salmonella typhimurium, Salmonella enteritidis and Salmonella gallinarum. Microbiology *146 Pt 12*, 3217-3226.

Kang, J.L., Park, W., Pack, I.S., Lee, H.S., Kim, M.J., Lim, C.M., and Koh, Y. (2002). Inhaled nitric oxide attenuates acute lung injury via inhibition of nuclear factor-kappa B and inflammation. Journal of Applied Physiology *92*, 795-801.

Karin, M. (1999). How NF-kappaB is activated: the role of the IkappaB kinase (IKK) complex. Oncogene *18*, 6867-6874.

Karin, M., and Ben-Neriah, Y. (2000). Phosphorylation meets ubiquitination: the control of NF-[kappa]B activity. Annu Rev Immunol *18*, 621-663.

Karin, M., Laboratory of Gene, R., and Signal Transduction, D.o.P.U.o.C.S.D.G.D.L.J.C.C.A.U.S.A. (1999a). How NF-kappaB is activated: the role of the IkappaB kinase (IKK) complex. Oncogene *18(49)*, 6867-6874.

Karin, M., Laboratory of Gene, R., and Signal Transduction, D.o.P.U.o.C.S.D.L.J.C.U.S.A.k.u.e. (1999b). The beginning of the end: IkappaB kinase (IKK) and NF-kappaB activation. J Biol Chem *274(39)*, 27339-27342.

Karin, M., and Lin, A. (2002). NF-kappaB at the crossroads of life and death. Nat Immunol *3*, 221-227.

Karin, M., Takahashi, T., Kapahi, P., Delhase, M., Chen, Y., Makris, C., Rothwarf, D., Baud, V., Natoli, G., Guido, F., and Li, N. (2001). Oxidative stress and gene expression: the AP-1 and NF-kappaB connections. Biofactors *15*, 87-89.

Kastan, M.B., and Lim, D.S. (2000). The many substrates and functions of ATM. Nat Rev Mol Cell Biol *1*, 179-186.

Kaufmann, S.H. (1998). Cell death induced by topoisomerase-targeted drugs: more questions than answers. Biochimica et Biophysica Acta *1400*, 195-211.

Kawasaki, K., Akashi, S., Shimazu, R., Yoshida, T., Miyake, K., and Nishijima, M. (2001). Involvement of TLR4/MD-2 complex in species-specific lipopolysaccharide-mimetic signal transduction by Taxol. J Endotoxin Res *7*, 232-236.

Khwaja, A. (1999). Akt is more than just a Bad kinase. Nature *401*, 33-34.

Killeen, S.D., Wang, J.H., Andrews, E.J., and Redmond, H.P. (2006). Exploitation of the Toll-like receptor system in cancer: a doubled-edged sword? Br J Cancer *95*, 247-252.

Kim, D., and Chung, J. (2002). Akt: versatile mediator of cell survival and beyond. J Biochem Mol Biol *35*, 106-115.

Kim, M.R., Lee, J.Y., Park, M.T., Chun, Y.J., Jang, Y.J., Kang, C.M., Kim, H.S., Cho, C.K., Lee, Y.S., Jeong, H.Y., and Lee, S.J. (2001). Ionizing radiation can overcome resistance to TRAIL in TRAIL-resistant cancer cells. FEBS Letters *505*, 179-184.

Kim, S.H., Juhnn, Y.S., and Song, Y.S. (2007). Akt involvement in paclitaxel chemoresistance of human ovarian cancer cells. Ann N Y Acad Sci *1095*, 82-89.

Kinoshita, S., Suzuki, H., Ito, K., Kume, K., Shimizu, T., and Sugiyama, Y. (1998). Transfected rat cMOAT is functionally expressed on the apical membrane in Madin-Darby canine kidney (MDCK) cells. Pharm Res *15*, 1851-1856.

Kopp, E.B., and Medzhitov, R. (1999). The Toll-receptor family and control of innate immunity. Curr Opin Immunol *11*, 13-18.

Korhonen, R., Lahti, A., Kankaanranta, H., and Moilanen, E. (2005). Nitric oxide production and signaling in inflammation. Curr Drug Targets Inflamm Allergy *4*, 471-479.

Krishnan, J., Selvarajoo, K., Tsuchiya, M., Lee, G., and Choi, S. (2007). Toll-like receptor signal transduction. Exp Mol Med *39*, 421-438.

Kroncke, K.-D. (2003). Nitrosative stress and transcription. Biological Chemistry *384*, 1365.

Kroncke, K.D. (2001). Cysteine-Zn2+ complexes: unique molecular switches for inducible nitric oxide synthase-derived NO. Faseb J *15*, 2503-2507.

Kroncke, K.D., and Carlberg, C. (2000). Inactivation of zinc finger transcription factors provides a mechanism for a gene regulatory role of nitric oxide. Faseb J *14*, 166-173.

Kubori, T., and Galan, J.E. (2002). Salmonella type III secretion-associated protein InvE controls translocation of effector proteins into host cells. J Bacteriol *184*, 4699-4708.

Kwak, Y.T., Guo, J., Shen, J., and Gaynor, R.B. (2000). Analysis of domains in the IKKalpha and IKKbeta proteins that regulate their kinase activity. J Biol Chem *275*, 14752-14759.

LaCasse, E.C., Baird, S., Korneluk, R.G., and MacKenzie, A.E. (1998). The inhibitors of apoptosis (IAPs) and their emerging role in cancer. Oncogene *17*, 3247-3259.

Lawrence, D., Shahrokh, Z., Marsters, S., Achilles, K., Shih, D., Mounho, B., Hillan, K., Totpal, K., DeForge, L., Schow, P., *et al.* (2001). Differential hepatocyte toxicity of recombinant Apo2L/TRAIL versions. Nat Med *7*, 383-385.

LeBlanc, H.N., and Ashkenazi, A. (2003). Apo2L/TRAIL and its death and decoy receptors. Cell Death Differ *10*, 66-75.

Lee, S.Y., Reichlin, A., Santana, A., Sokol, K.A., Nussenzweig, M.C., and Choi, Y. (1997). TRAF2 is essential for JNK but not NF-kappaB activation and regulates lymphocyte proliferation and survival. Immunity *7*, 703-713.

Lee, Y.J., Lee, K.H., Kim, H.R., Jessup, J.M., Seol, D.W., Kim, T.H., Billiar, T.R., and Song, Y.K. (2001). Sodium nitroprusside enhances TRAIL-induced apoptosis via a mitochondria-dependent pathway in human colorectal carcinoma CX-1 cells. Oncogene *20*, 1476-1485.

Li, T.K., and Liu, L.F. (2001). Tumor cell death induced by topoisomerase-targeting drugs. Annu Rev Pharmacol Toxicol *41*, 53-77.

Li, X., Commane, M., Nie, H., Hua, X., Chatterjee-Kishore, M., Wald, D., Haag, M., and Stark, G.R. (2000). Act1, an NF-kappa B-activating protein. Proc Natl Acad Sci U S A *97*, 10489-10493.

Li, X., and Stark, G.R. (2002). NFkappaB-dependent signaling pathways. Exp Hematol *30*, 285-296.

Lien, E., Means, T.K., Heine, H., Yoshimura, A., Kusumoto, S., Fukase, K., Fenton, M.J., Oikawa, M., Qureshi, N., Monks, B., *et al.* (2000). Toll-like receptor 4 imparts ligand-specific recognition of bacterial lipopolysaccharide. J Clin Invest *105*, 497-504.

Lien, E., Sellati, T.J., Yoshimura, A., Flo, T.H., Rawadi, G., Finberg, R.W., Carroll, J.D., Espevik, T., Ingalls, R.R., Radolf, J.D., and Golenbock, D.T. (1999). Toll-like receptor 2 functions as a pattern recognition receptor for diverse bacterial products. J Biol Chem *274*, 33419-33425.

Lillehoj, E.P., Kim, B.T., and Kim, K.C. (2002). Identification of Pseudomonas aeruginosa flagellin as an adhesin for Muc1 mucin. Am J Physiol Lung Cell Mol Physiol *282*, L751-756.

Lillehoj, E.P., Kim, H., Chun, E.Y., and Kim, K.C. (2004). Pseudomonas aeruginosa stimulates phosphorylation of the airway epithelial membrane glycoprotein Muc1 and activates MAP kinase. Am J Physiol Lung Cell Mol Physiol *287*, L809-815.

Lind, D.S., Hochwald, S.N., Malaty, J., Rekkas, S., Hebig, P., Mishra, G., Moldawer, L.L., Copeland, E.M., 3rd, and Mackay, S. (2001). Nuclear factor-kappa B is upregulated in colorectal cancer. Surgery *130*, 363-369.

Luo, H.R., Huang, Y.E., Chen, J.C., Saiardi, A., Iijima, M., Ye, K., Huang, Y., Nagata, E., Devreotes, P., and Snyder, S.H. (2003). Inositol Pyrophosphates Mediate Chemotaxis in Dictyostelium via Pleckstrin Homology Domain-PtdIns(3,4,5)P3 Interactions. Cell *114*, 559.

Ma, Y., and Lieber, M.R. (2002). Binding of Inositol Hexakisphosphate (IP6) to Ku but Not to DNA-PKcs. J. Biol. Chem. *277*, 10756-10759.

Mabb, A.M., and Miyamoto, S. (2007). SUMO and NF-kappaB ties. Cell Mol Life Sci *64*, 1979-1996.

Mabuchi, S., Ohmichi, M., Nishio, Y., Hayasaka, T., Kimura, A., Ohta, T., Kawagoe, J., Takahashi, K., Yada-Hashimoto, N., Seino-Noda, H., *et al.* (2004a). Inhibition of inhibitor of nuclear factor-kappaB phosphorylation increases the efficacy of paclitaxel in in vitro and in vivo ovarian cancer models. Clin Cancer Res *10*, 7645-7654.

Mabuchi, S., Ohmichi, M., Nishio, Y., Hayasaka, T., Kimura, A., Ohta, T., Saito, M., Kawagoe, J., Takahashi, K., Yada-Hashimoto, N., *et al.* (2004b). Inhibition of NFkappaB increases the efficacy of cisplatin in in vitro and in vivo ovarian cancer models. J Biol Chem *279*, 23477-23485.

Madrid, L.V., Mayo, M.W., Reuther, J.Y., and Baldwin, A.S., Jr. (2001). Akt stimulates the transactivation potential of the RelA/p65 Subunit of NF-kappa B through utilization of the Ikappa B kinase and activation of the mitogen-activated protein kinase p38. J Biol Chem *276*, 18934-18940.

Madrid, L.V., Wang, C.Y., Guttridge, D.C., Schottelius, A.J., Baldwin, A.S., Jr., and Mayo, M.W. (2000). Akt suppresses apoptosis by stimulating the transactivation potential of the RelA/p65 subunit of NF-kappaB. Mol Cell Biol *20*, 1626-1638.

Makris, C., Roberts, J.L., and Karin, M. (2002). The carboxyl-terminal region of IkappaB kinase gamma (IKKgamma) is required for full IKK activation. Mol Cell Biol *22*, 6573-6581.

Manderscheid, M., Messmer, U.K., Franzen, R., and Pfeilschifter, J. (2001). Regulation of inhibitor of apoptosis expression by nitric oxide and cytokines: relation to apoptosis induction in rat mesangial cells and raw 264.7 macrophages. J Am Soc Nephrol *12*, 1151-1163.

Mani, A., and Gelmann, E.P. (2005). The ubiquitin-proteasome pathway and its role in cancer. J Clin Oncol *23*, 4776-4789.

Mannick, J.B., and Schonhoff, C.M. (2004). NO means no and yes: regulation of cell signaling by protein nitrosylation. Free Radic Res *38*, 1-7.

Marshall, H.E., Merchant, K., and Stamler, J.S. (2000). Nitrosation and oxidation in the regulation of gene expression. Faseb J *14*, 1889-1900.

Marshall, H.E., and Stamler, J.S. (2001). Inhibition of NF-kappa B by S-nitrosylation. Biochemistry *40*, 1688-1693.

Matthews, J.R., Botting, C.H., Panico, M., Morris, H.R., and Hay, R.T. (1996). Inhibition of NF-kappaB DNA binding by nitric oxide. Nucleic Acids Research *24*, 2236-2242.

McClendon, A.K., and Osheroff, N. (2007). DNA topoisomerase II, genotoxicity, and cancer. Mutat Res *623*, 83-97.

McCormick, B.A. (2003). The use of transepithelial models to examine host-pathogen interactions. Curr Opin Microbiol *6*, 77-81.

McDermott, P.F., Ciacci-Woolwine, F., Snipes, J.A., and Mizel, S.B. (2000). High-affinity interaction between gram-negative flagellin and a cell surface polypeptide results in human monocyte activation. Infect Immun *68*, 5525-5529.

Medzhitov, R., and Janeway, C., Jr. (2000). The Toll receptor family and microbial recognition. Trends Microbiol *8*, 452-456.

Medzhitov, R., Preston-Hurlburt, P., Kopp, E., Stadlen, A., Chen, C., Ghosh, S., and Janeway, C.A., Jr. (1998). MyD88 is an adaptor protein in the hToll/IL-1 receptor family signaling pathways. Mol Cell *2*, 253-258.

Mikkelsen, R.B., and Wardman, P. (2003). Biological chemistry of reactive oxygen and nitrogen and radiation-induced signal transduction mechanisms. Oncogene *22*, 5734-5754.

Mizel, S.B., and Snipes, J.A. (2002). Gram-negative flagellin-induced self-tolerance is associated with a block in interleukin-1 receptor-associated kinase release from toll-like receptor 5. J Biol Chem *277*, 22414-22420.

Mizel, S.B., West, A.P., and Hantgan, R.R. (2003). Identification of a sequence in human toll-like receptor 5 required for the binding of Gram-negative flagellin. J Biol Chem *278*, 23624-23629.

Mizutani, Y., Nakanishi, H., Yoshida, O., Fukushima, M., Bonavida, B., and Miki, T. (2002). Potentiation of the sensitivity of renal cell carcinoma cells to TRAIL-mediated apoptosis by subtoxic concentrations of 5-fluorouracil. European Journal of Cancer *38*, 167-176.

Mocellin, S., Bronte, V., and Nitti, D. (2007). Nitric oxide, a double edged sword in cancer biology: searching for therapeutic opportunities. Med Res Rev *27*, 317-352.

Moors, M.A., Li, L., and Mizel, S.B. (2001). Activation of interleukin-1 receptor-associated kinase by gram-negative flagellin. Infect Immun *69*, 4424-4429.

Morrison, B.H., Bauer, J.A., Hu, J., Grane, R.W., Ozdemir, A., Chawla-Sarkar, M., Gong, B., Almasan, A., Kalvakolanu, D.V., and Lindner, D.J. (2002). Inositol hexakisphosphate kinase 2 sensitizes ovarian carcinoma cells to multiple cancer therapeutics. Oncogene *in press*.

Morrison, B.H., Bauer, J.A., Kalvakolanu, D.V., and Lindner, D.J. (2001). Inositol hexakisphosphate kinase 2 mediates growth suppressive and apoptotic effects of interferon-beta in ovarian carcinoma cells. J Biol Chem *276*, 24965-24970.

Murphy, M.P. (1999). Nitric oxide and cell death. Biochim Biophys Acta *1411*, 401-414.

Murthy, K.G., Deb, A., Goonesekera, S., Szabo, C., and Salzman, A.L. (2004). Identification of conserved domains in Salmonella muenchen flagellin that are essential for its ability to activate TLR5 and to induce an inflammatory response in vitro. J Biol Chem *279*, 5667-5675.

Muzio, M., Ni, J., Feng, P., and Dixit, V.M. (1997). IRAK (Pelle) family member IRAK-2 and MyD88 as proximal mediators of IL-1 signaling. Science *278*, 1612-1615.

Nagai, Y., Akashi, S., Nagafuku, M., Ogata, M., Iwakura, Y., Akira, S., Kitamura, T., Kosugi, A., Kimoto, M., and Miyake, K. (2002). Essential role of MD-2 in LPS responsiveness and TLR4 distribution. Nat Immunol *3*, 667-672.

Nagata, E., Luo, H.R., Saiardi, A., Bae, B.-I., Suzuki, N., and Snyder, S.H. (2005). Inositol Hexakisphosphate Kinase-2, a Physiologic Mediator of Cell Death. J. Biol. Chem. *280*, 1634-1640.

Nakanishi, C., and Toi, M. (2005). Nuclear factor-kappaB inhibitors as sensitizers to anticancer drugs. Nat Rev Cancer *5*, 297-309.

Nakano, H., Sakon, S., Koseki, H., Takemori, T., Tada, K., Matsumoto, M., Munechika, E., Sakai, T., Shirasawa, T., Akiba, H., *et al.* (1999). Targeted disruption of Traf5 gene causes defects in CD40- and CD27-mediated lymphocyte activation. Proc Natl Acad Sci U S A *96*, 9803-9808.

Norris, F.A., Wilson, M.P., Wallis, T.S., Galyov, E.E., and Majerus, P.W. (1998). SopB, a protein required for virulence of Salmonella dublin, is an inositol phosphate phosphatase. Proc Natl Acad Sci U S A *95*, 14057-14059.

O'Neill, L. (2001). Specificity in the innate response: pathogen recognition by Toll-like receptor combinations. Trends Immunol *22*, 70.

Oya, M., Ohtsubo, M., Takayanagi, A., Tachibana, M., Shimizu, N., and Murai, M. (2001). Constitutive activation of nuclear factor-kappaB prevents TRAIL-induced apoptosis in renal cancer cells. Oncogene *20*, 3888-3896.

Ozes, O.N., Mayo, L.D., Gustin, J.A., Pfeffer, S.R., Pfeffer, L.M., Donner, D.B., Department of, M., and Immunology, I.U.S.o.M.t.W.O.C.I.U.S.A. (1999). NF-kappaB activation by tumour necrosis factor requires the Akt serine-threonine kinase. Nature *401(6748)*, 82-85.

Ozinsky, A., Underhill, D.M., Fontenot, J.D., Hajjar, A.M., Smith, K.D., Wilson, C.B., Schroeder, L., and Aderem, A. (2000). The repertoire for pattern recognition of pathogens by the innate immune system is defined by cooperation between toll-like receptors. Proc Natl Acad Sci U S A *97*, 13766-13771.

Ozoren, N., Fisher, M.J., Kim, K., Liu, C.X., Genin, A., Shifman, Y., Dicker, D.T., Spinner, N.B., Lisitsyn, N.A., and El-Deiry, W.S. (2000). Homozygous deletion of the death receptor DR4 gene in a nasopharyngeal cancer cell line is associated with TRAIL resistance. International Journal of Oncology *16*, 917-925.

Pahl, H.L. (1999). Activators and target genes of Rel/NF-kappaB transcription factors. Oncogene *18*, 6853-6866.

Pan, G., O'Rourke, K., Chinnaiyan, A.M., Gentz, R., Ebner, R., Ni, J., and Dixit, V.M. (1997). The receptor for the cytotoxic ligand TRAIL. Science *276*, 111-113.

Park, S.W., Huq, M.D., Hu, X., and Wei, L.N. (2005). Tyrosine nitration on p65: a novel mechanism to rapidly inactivate nuclear factor-kappaB. Mol Cell Proteomics *4*, 300-309.

Park, Y.C., Burkitt, V., Villa, A.R., Tong, L., and Wu, H. (1999). Structural basis for self-association and receptor recognition of human TRAF2. Nature *398*, 533.

Pitti, R.M., Marsters, S.A., Ruppert, S., Donahue, C.J., Moore, A., and Ashkenazi, A. (1996). Induction of apoptosis by Apo-2 ligand, a new member of the tumor necrosis factor cytokine family. Journal of Biological Chemistry *271*, 12687-12690.

Radi, R. (2004). Nitric oxide, oxidants, and protein tyrosine nitration. Proc Natl Acad Sci U S A *101*, 4003-4008.

Ray, A., Chakraborti, A., and Gulati, K. (2007). Current trends in nitric oxide research. Cell Mol Biol (Noisy-le-grand) *53*, 3-14.

Reed, J.C. (2003). Apoptosis-targeted therapies for cancer. Cancer Cell *3*, 17-22.

Reynaert, N.L., Ckless, K., Korn, S.H., Vos, N., Guala, A.S., Wouters, E.F., van der Vliet, A., and Janssen-Heininger, Y.M. (2004). Nitric oxide represses inhibitory kappaB kinase through S-nitrosylation. Proc Natl Acad Sci U S A *101*, 8945-8950.

Rock, F.L., Hardiman, G., Timans, J.C., Kastelein, R.A., and Bazan, J.F. (1998). A family of human receptors structurally related to Drosophila Toll. Proc Natl Acad Sci U S A *95*, 588-593.

Romashkova, J.A., and Makarov, S.S. (1999). NF-kappaB is a target of AKT in anti-apoptotic PDGF signalling. Nature *401*, 86-90.

Rossi, A., Kapahi, P., Natoli, G., Takahashi, T., Chen, Y., Karin, M., and Santoro, M.G. (2000). Anti-inflammatory cyclopentenone prostaglandins are direct inhibitors of IkappaB kinase. Nature *403*, 103-108.

Rothwarf, D.M., and Karin, M. (1999). The NF-kappa B activation pathway: a paradigm in information transfer from membrane to nucleus. Sci STKE *1999*, RE1.

Rubinstein, L.V., Shoemaker, R.H., Paull, K.D., Simon, R.M., Tosini, S., Skehan, P., Scudiero, D.A., Monks, A., and Boyd, M.R. (1990). Comparison of in vitro anticancer-drug-screening data generated with a tetrazolium assay versus a protein assay against a diverse panel of human tumor cell lines. J Natl Cancer Inst *82*, 1113-1118.

Saiardi, A., Bhandari, R., Resnick, A.C., Snowman, A.M., and Snyder, S.H. (2004). Phosphorylation of proteins by inositol pyrophosphates. Science *306*, 2101-2105.

Saiardi, A., Sciambi, C., McCaffery, J.M., Wendland, B., and Snyder, S.H. (2002). Inositol pyrophosphates regulate endocytic trafficking. Proc Natl Acad Sci U S A *99*, 14206-14211.

Sakaguchi, T., Kohler, H., Gu, X., McCormick, B.A., and Reinecker, H.C. (2002). Shigella flexneri regulates tight junction-associated proteins in human intestinal epithelial cells. Cell Microbiol *4*, 367-381.

Salvesen, G.S., and Duckett, C.S. (2002). IAP proteins: blocking the road to death's door. Nat Rev Mol Cell Biol *3*, 401-410.

Sato, K., Hida, S., Takayanagi, H., Yokochi, T., Kayagaki, N., Takeda, K., Yagita, H., Okumura, K., Tanaka, N., Taniguchi, T., and Ogasawara, K. (2001). Antiviral response by natural killer cells through TRAIL gene induction by IFN-alpha/beta. European journal of immunology. *31(11)*, 3138-3146.

Schimmer, A.D., Dalili, S., Batey, R.A., and Riedl, S.J. (2006). Targeting XIAP for the treatment of malignancy. Cell Death Differ *13*, 179-188.

Schromm, A.B., Lien, E., Henneke, P., Chow, J.C., Yoshimura, A., Heine, H., Latz, E., Monks, B.G., Schwartz, D.A., Miyake, K., and Golenbock, D.T. (2001). Molecular genetic analysis of an endotoxin nonresponder mutant cell line: a point mutation in a conserved region of MD-2 abolishes endotoxin-induced signaling. J Exp Med *194*, 79-88.

Sebban, H., Yamaoka, S., and Courtois, G. (2006). Posttranslational modifications of NEMO and its partners in NF-kappaB signaling. Trends Cell Biol *16*, 569-577.

Secchiero, P., Gonelli, A., Celeghini, C., Mirandola, P., Guidotti, L., Visani, G., Capitani, S., and Zauli, G. (2001). Activation of the nitric oxide synthase pathway represents a key component of tumor necrosis factor-related apoptosis-inducing ligand-mediated cytotoxicity on hematologic malignancies. Blood *98*, 2220-2228.

Seeler, J.S., and Dejean, A. (2001). SUMO: of branched proteins and nuclear bodies. Oncogene *20*, 7243-7249.

Seetharam, B., Bose, S., and Li, N. (1999). Cellular import of cobalamin (Vitamin B-12). J Nutr *129*, 1761-1764.

Seetharam, B., and Li, N. (2000). Transcobalamin II and its cell surface receptor. Vitam Horm *59*, 337-366.

Senftleben, U., Cao, Y., Xiao, G., Greten, F.R., Krahn, G., Bonizzi, G., Chen, Y., Hu, Y., Fong, A., Sun, S.C., and Karin, M. (2001). Activation by IKKalpha of a second, evolutionary conserved, NF-kappa B signaling pathway. Science *293*, 1495-1499.

Shim, J.H., Xiao, C., Paschal, A.E., Bailey, S.T., Rao, P., Hayden, M.S., Lee, K.Y., Bussey, C., Steckel, M., Tanaka, N., *et al.* (2005). TAK1, but not TAB1 or TAB2, plays an essential role in multiple signaling pathways in vivo. Genes Dev *19*, 2668-2681.

Silverman, N., and Maniatis, T. (2001). NF-kappaB signaling pathways in mammalian and insect innate immunity. Genes Dev *15*, 2321-2342.

Skehan, P., Storeng, R., Scudiero, D., Monks, A., McMahon, J., Vistica, D., Warren, J.T., Bokesch, H., Kenney, S., and Boyd, M.R. (1990). New colorimetric cytotoxicity assay for anticancer-drug screening. J Natl Cancer Inst *82*, 1107-1112.

Smith, K.D., Andersen-Nissen, E., Hayashi, F., Strobe, K., Bergman, M.A., Barrett, S.L., Cookson, B.T., and Aderem, A. (2003). Toll-like receptor 5 recognizes a conserved site on flagellin required for protofilament formation and bacterial motility. Nat Immunol *4*, 1247-1253.

Song, H.Y., Regnier, C.H., Kirschning, C.J., Goeddel, D.V., and Rothe, M. (1997). Tumor necrosis factor (TNF)-mediated kinase cascades: bifurcation of nuclear factor-kappaB and c-jun N-terminal kinase (JNK/SAPK) pathways at TNF receptor-associated factor 2. Proc Natl Acad Sci U S A *94*, 9792-9796.

Sovak, M.A., Bellas, R.E., Kim, D.W., Zanieski, G.J., Rogers, A.E., Traish, A.M., and Sonenshein, G.E. (1997). Aberrant nuclear factor-kappaB/Rel expression and the pathogenesis of breast cancer. J Clin Invest *100*, 2952-2960.

Squadrito, G.L., and Pryor, W.A. (1998). Oxidative chemistry of nitric oxide: the roles of superoxide, peroxynitrite, and carbon dioxide. Free Radic Biol Med *25*, 392-403.

Stamler, J.S., Lamas, S., and Fang, F.C. (2001). Nitrosylation. the prototypic redox-based signaling mechanism. Cell *106*, 675-683.

Storling, J., Binzer, J., Andersson, A.K., Zullig, R.A., Tonnesen, M., Lehmann, R., Spinas, G.A., Sandler, S., Billestrup, N., and Mandrup-Poulsen, T. (2005). Nitric oxide contributes to cytokine-induced apoptosis in pancreatic beta cells via potentiation of JNK activity and inhibition of Akt. Diabetologia *48*, 2039-2050.

Sun, M., Wang, G., Paciga, J.E., Feldman, R.I., Yuan, Z.Q., Ma, X.L., Shelley, S.A., Jove, R., Tsichlis, P.N., Nicosia, S.V., and Cheng, J.Q. (2001). AKT1/PKBalpha kinase is frequently elevated in human cancers and its constitutive activation is required for oncogenic transformation in NIH3T3 cells. Am J Pathol *159*, 431-437.

Sun, Y. (2006). E3 ubiquitin ligases as cancer targets and biomarkers. Neoplasia *8*, 645-654.

Tada, K., Okazaki, T., Sakon, S., Kobarai, T., Kurosawa, K., Yamaoka, S., Hashimoto, H., Mak, T.W., Yagita, H., Okumura, K., *et al.* (2001). Critical roles of TRAF2 and TRAF5 in tumor necrosis factor-induced NF-kappa B activation and protection from cell death. J Biol Chem *276*, 36530-36534.

Takeda, K., Kaisho, T., and Akira, S. (2003). Toll-like receptors. Annu Rev Immunol *21*, 335-376.

Takeuchi, O., and Akira, S. (2002). MyD88 as a bottle neck in Toll/IL-1 signaling. Curr Top Microbiol Immunol *270*, 155-167.

Tallant, T., Deb, A., Kar, N., Lupica, J., de Veer, M.J., and DiDonato, J.A. (2004). Flagellin acting via TLR5 is the major activator of key signaling pathways leading to NF-kappa B and proinflammatory gene program activation in intestinal epithelial cells. BMC Microbiol *4*, 33.

Tang, Z., Bauer, J.A., Morrison, B., and Lindner, D.J. (2006). Nitrosylcobalamin promotes cell death via S nitrosylation of Apo2L/TRAIL receptor DR4. Mol Cell Biol *26*, 5588-5594.

Tergaonkar, V., Bottero, V., Ikawa, M., Li, Q., and Verma, I.M. (2003). IkappaB kinase-independent IkappaBalpha degradation pathway: functional NF-kappaB activity and implications for cancer therapy. Mol Cell Biol *23*, 8070-8083.

Uetsuka, H., Haisa, M., Kimura, M., Gunduz, M., Kaneda, Y., Ohkawa, T., Takaoka, M., Murata, T., Nobuhisa, T., Yamatsuji, T., *et al.* (2003). Inhibition of inducible NF-kappaB activity reduces chemoresistance to 5-fluorouracil in human stomach cancer cell line. Exp Cell Res *289*, 27-35.

Ulrich, H.D. (2005). Mutual interactions between the SUMO and ubiquitin systems: a plea of no contest. Trends Cell Biol *15*, 525-532.

Valdivia, R.H., and Falkow, S. (1997). Fluorescence-based isolation of bacterial genes expressed within host cells. Science *277*, 2007-2011.

Valdivia, R.H., Hromockyj, A.E., Monack, D., Ramakrishnan, L., and Falkow, S. (1996). Applications for green fluorescent protein (GFP) in the study of host-pathogen interactions. Gene *173*, 47-52.

Vivanco, I., and Sawyers, C.L. (2002). The phosphatidylinositol 3-Kinase AKT pathway in human cancer. Nat Rev Cancer *2*, 489-501.

Volk, T., Ioannidis, I., Hensel, M., deGroot, H., and Kox, W.J. (1995). Endothelial damage induced by nitric oxide: synergism with reactive oxygen species. Biochemical & Biophysical Research Communications *213*, 196-203.

Walczak, H., Bouchon, A., Stahl, H., and Krammer, P.H. (2000). Tumor necrosis factor-related apoptosis-inducing ligand retains its apoptosis-inducing capacity on Bcl-2- or Bcl-xL-overexpressing chemotherapy-resistant tumor cells. Cancer Research *60*, 3051-3057.

Walczak, H., Miller, R.E., Ariail, K., Gliniak, B., Griffith, T.S., Kubin, M., Chin, W., Jones, J., Woodward, A., Le, T., *et al.* (1999). Tumoricidal activity of tumor necrosis factor-related apoptosis-inducing ligand in vivo. Nature Medicine *5*, 157-163.

Waldow, T., Witt, W., Weber, E., and Matschke, K. (2006). Nitric oxide donor-induced persistent inhibition of cell adhesion protein expression and NFkappaB activation in endothelial cells. Nitric Oxide *15*, 103-113.

Wallis, T.S., Wood, M., Watson, P., Paulin, S., Jones, M., and Galyov, E. (1999). Sips, Sops, and SPIs but not stn influence Salmonella enteropathogenesis. Adv Exp Med Biol *473*, 275-280.

Wang, C.Y., Cusack, J.C., Jr., Liu, R., and Baldwin, A.S., Jr. (1999). Control of inducible chemoresistance: enhanced anti-tumor therapy through increased apoptosis by inhibition of NF-kappaB. Nat Med *5*, 412-417.

Wang, J.C. (2002). Cellular roles of DNA topoisomerases: a molecular perspective. Nat Rev Mol Cell Biol *3*, 430-440.

Weldon, C.B., Burow, M.E., Rolfe, K.W., Clayton, J.L., Jaffe, B.M., and Beckman, B.S. (2001). NF-kappa B-mediated chemoresistance in breast cancer cells. Surgery *130*, 143-150.

Wiley, S.R., Schooley, K., Smolak, P.J., Din, W.S., Huang, C.P., Nicholl, J.K., Sutherland, G.R., Smith, T.D., Rauch, C., and Smith, C.A. (1995). Identification and characterization of a new member of the TNF family that induces apoptosis. Immunity *3*, 673-682.

Williams, A.W., Yamaguchi, S., Togashi, F., Aizawa, S.I., Kawagishi, I., and Macnab, R.M. (1996). Mutations in fliK and flhB affecting flagellar hook and filament assembly in Salmonella typhimurium. J Bacteriol *178*, 2960-2970.

Wink, D.A., Cook, J.A., Pacelli, R., DeGraff, W., Gamson, J., Liebmann, J., Krishna, M.C., and Mitchell, J.B. (1996). The effect of various nitric oxide-donor agents on hydrogen peroxide-mediated toxicity: a direct correlation between nitric oxide formation and protection. Archives of Biochemistry & Biophysics *331*, 241-248.

Wink, D.A., and Mitchell, J.B. (1998). Chemical Biology of Nitric Oxide: Insights into Regulatory, Cytotoxic, and Cytoprotective Mechanisms of Nitric Oxide. Free Radical Biology & Medicine *25*, 434-456.

Witthoft, T., Eckmann, L., Kim, J.M., and Kagnoff, M.F. (1998). Enteroinvasive bacteria directly activate expression of iNOS and NO production in human colon epithelial cells. Am J Physiol *275*, G564-571.

Wood, M.W., Jones, M.A., Watson, P.R., Siber, A.M., McCormick, B.A., Hedges, S., Rosqvist, R., Wallis, T.S., and Galyov, E.E. (2000). The secreted effector protein of Salmonella dublin, SopA, is translocated into eukaryotic cells and influences the induction of enteritis. Cell Microbiol *2*, 293-303.

Wood, M.W., Rosqvist, R., Mullan, P.B., Edwards, M.H., and Galyov, E.E. (1996). SopE, a secreted protein of Salmonella dublin, is translocated into the target eukaryotic cell via a sip-dependent mechanism and promotes bacterial entry. Mol Microbiol *22*, 327-338.

Wu, Z.H., Shi, Y., Tibbetts, R.S., and Miyamoto, S. (2006). Molecular linkage between the kinase ATM and NF-kappaB signaling in response to genotoxic stimuli. Science *311*, 1141-1146.

Xiao-Ming Yin, M.D., PhD, and Zheng Dong, P. (2003). Essentials of Apoptosis First edn (Totowa New Jersy: Humana Press Inc).

Yakovlev, V.A., Barani, I.J., Rabender, C.S., Black, S.M., Leach, J.K., Graves, P.R., Kellogg, G.E., and Mikkelsen, R.B. (2007). Tyrosine Nitration of IκBα: A Novel Mechanism for NF-κB Activation. Biochemistry *46*, 11671-11683.

Yamaguchi, S., Fujita, H., Sugata, K., Taira, T., and Iino, T. (1984). Genetic analysis of H2, the structural gene for phase-2 flagellin in Salmonella. J Gen Microbiol *130*, 255-265.

Yamanaka, T., Shiraki, K., Sugimoto, K., Ito, T., Fujikawa, K., Ito, M., Takase, K., Moriyama, M., Nakano, T., and Suzuki, A. (2000). Chemotherapeutic agents augment TRAIL-induced apoptosis in human hepatocellular carcinoma cell lines. Hepatology *32*, 482-490.

Yasukawa, T., Tokunaga, E., Ota, H., Sugita, H., Martyn, J.A., and Kaneki, M. (2005). S-nitrosylation-dependent inactivation of Akt/protein kinase B in insulin resistance. J Biol Chem *280*, 7511-7518.

Yeh, P.Y., Chuang, S.E., Yeh, K.H., Song, Y.C., and Cheng, A.L. (2003). Involvement of nuclear transcription factor-kappa B in low-dose doxorubicin-induced drug resistance of cervical carcinoma cells. Biochem Pharmacol *66*, 25-33.

Yeh, W.C., Shahinian, A., Speiser, D., Kraunus, J., Billia, F., Wakeham, A., de la Pompa, J.L., Ferrick, D., Hum, B., Iscove, N., *et al.* (1997). Early lethality, functional NF-kappaB activation, and increased sensitivity to TNF-induced cell death in TRAF2-deficient mice. Immunity *7*, 715-725.

Yoshimura, A., Lien, E., Ingalls, R.R., Tuomanen, E., Dziarski, R., and Golenbock, D. (1999). Cutting edge: recognition of Gram-positive bacterial cell wall components by the innate immune system occurs via Toll-like receptor 2. J Immunol *163*, 1-5.

Yuan, Z.Q., Feldman, R.I., Sussman, G.E., Coppola, D., Nicosia, S.V., and Cheng, J.Q. (2003). AKT2 inhibition of cisplatin-induced JNK/p38 and Bax activation by phosphorylation of ASK1: implication of AKT2 in chemoresistance. J Biol Chem *278*, 23432-23440.

Yuan, Z.Q., Sun, M., Feldman, R.I., Wang, G., Ma, X., Jiang, C., Coppola, D., Nicosia, S.V., and Cheng, J.Q. (2000). Frequent activation of AKT2 and induction of apoptosis by inhibition of phosphoinositide-3-OH kinase/Akt pathway in human ovarian cancer. Oncogene *19*, 2324-2330.

Zandi, E., Chen, Y., and Karin, M. (1998). Direct phosphorylation of IkappaB by IKKalpha and IKKbeta: discrimination between free and NF-kappaB-bound substrate. Science *281*, 1360-1363.

Zhang, X.D., Franco, A., Myers, K., Gray, C., Nguyen, T., and Hersey, P. (1999). Relation of TNF-related apoptosis-inducing ligand (TRAIL) receptor and FLICE-inhibitory protein expression to TRAIL-induced apoptosis of melanoma. Cancer Research *59*, 2747-2753.

Ziegler, D.S., and Kung, A.L. (2008). Therapeutic targeting of apoptosis pathways in cancer. Curr Opin Oncol *20*, 97-103.